TECHNISCHE UNIVERSITÄT MÜNCHEN

Robust Design Optimization Based on Metamodeling Techniques

Florian Jurecka

Technische Universität München
Fakultät Bauingenieur- und Vermessungswesen

Lehrstuhl für Statik
Univ.-Prof. Dr.-Ing. Kai-Uwe Bletzinger
Arcisstr. 21
80333 München

Tel.: (+49 89) 289 - 22422
Fax: (+49 89) 289 - 22421

http://www.st.bv.tum.de

Statik

Lehrstuhl für Statik
der Technischen Universität München

Robust Design Optimization Based on Metamodeling Techniques

Florian Jurecka

Vollständiger Abdruck der von der Fakultät für Bauingenieur– und Vermessungswesen der Technischen Universität München zur Erlangung des akademischen Grades eines

Doktor–Ingenieurs

genehmigten Dissertation.

Vorsitzender: Univ.–Prof. Dr. rer.nat. Ernst Rank

Prüfer der Dissertation:

1. Univ.–Prof. Dr.–Ing. Kai–Uwe Bletzinger
2. Prof. Vassili Toropov, Ph.D.,
   University of Leeds / UK

Die Dissertation wurde am 01.03.2007 bei der Technischen Universität München eingereicht und durch die Fakultät für Bauingenieur– und Vermessungswesen am 23.04.2007 angenommen.

Robust Design Optimization Based on Metamodeling Techniques

Abstract. In this thesis, the idea of robust design optimization is adopted to improve the quality of a product or process by minimizing the deteriorating effects of variable or not exactly quantifiable parameters. Robustness can be achieved via different formulations, which are compiled and discussed in the present work. All of these formulations have in common that they require many function evaluations throughout the optimization process. Especially in the growing field of computational engineering, the governing equations are typically not explicit functions but rather a nonlinear system of equations – for instance, derived from a nonlinear finite element discretization. In this case, even pointwise solutions can be quite expensive to evaluate. To reduce the tremendous numerical effort related to the described robustness analyses, metamodeling techniques are used replacing the actual numerical analysis codes by a simpler formulation. In this thesis, a method is proposed to sequentially augment the significance of metamodels for robust design optimization through additional sampling at infill points. As a result, a robust design optimization can be applied efficiently to engineering tasks that involve complex computer simulations. Even though the suggested approach is applicable to many engineering disciplines, the present work is focused on problems in the field of structural mechanics.

Robust Design Optimierung mit Hilfe von Metamodellierungstechniken

Zusammenfassung. In dieser Arbeit wird die Idee der Robust-Design-Optimierung aufgegriffen, deren Ziel es ist, die Qualität eines Produktes oder Prozesses dadurch zu verbessern, dass die störenden Auswirkungen von variablen oder nicht genau quantifizierbaren Parametern reduziert werden. Robustheit kann durch verschiedene Formulierungen erreicht werden, die in dieser Arbeit zusammengetragen und diskutiert werden. Alle diese Ansätze haben gemein, dass sie im Laufe der Optimierung viele Auswertungen der Systemgleichungen erfordern. Insbesondere für das aufstrebende Gebiet des *Computational Engineering* ist es typisch, dass das betrachtete System nicht durch geschlossen darstellbare Formeln beschrieben wird, sondern vielmehr durch ein nichtlineares Gleichungssystem, wie es z.B. aus einer nichtlinearen Finite-Elemente-Diskretisierung entsteht. In einem solchen Fall sind meist selbst punktweise Auswertungen der Systemgleichungen recht zeitaufwändig und damit teuer. Um den numerischen Aufwand von Robustheitsanalysen dennoch überschaubar zu halten, werden hier Metamodelltechniken verwendet, mit deren Hilfe das teure Originalproblem durch eine simplere Formulierung ersetzt wird. In dieser Arbeit wird eine Methode vorgeschlagen, mit der die Aussagekraft von Metamodellen in Bezug auf die Robustheit des Systems durch Hinzunahme von neuen Stützstellen sequentiell verbessert wird. Auf diese Weise kann eine Robust-Design-Optimierung auch auf Ingenieurprobleme angewendet werden, die durch aufwändige Computersimulationen beschrieben werden. Das hier vorgestellte Verfahren kann in vielen Feldern des Ingenieurwesens eingesetzt werden, im Fokus der vorliegenden Arbeit sind jedoch strukturmechanische Problemstellungen.

Acknowledgements

The present dissertation was written between 2001 and 2007 while I was research associate at the Chair of Structural Analysis (Lehrstuhl für Statik), Technische Universität München.

First of all I would like to express my gratitude to my supervisor and examiner Professor Dr.-Ing. Kai-Uwe Bletzinger for his remarkable support and guidance during my time at his chair. He initiated this research in the fascinating field of robust design and gave me the opportunity to work as course director for the master course Computational Mechanics. His permanent willingness to spare precious time for me – even when a short question turned into a lengthy discussion – and his valuable contributions to this thesis are highly respected.

Sincere thanks go to Professor Dr. Vassili Toropov, who acted as co-examiner of this thesis. His thorough and constructive review has contributed significantly to my dissertation. Furthermore, I owe many thanks to Professor Dr. Ernst Rank, who not only presided the examining commission for my doctorate but also supported me throughout the management of the master course. Special thanks go to Professor Dr.-Ing. Manfred Bischoff for taking the time to proof-read the following text. I also enjoyed the proficient counseling he provided by many invaluable advices while he was engaged in Munich.

I was always fond of working at TUM and this is due to the cordial and motivating atmosphere amongst all colleagues at the institute. I am deeply grateful to all current and former staff members for contributing to this unique work environment. I will always love to reminisce not only about our close and amicable collaboration but also about all common leisure activities. I am much obliged to my 'room mates' Dr.-Ing. Bernhard Thomée and Dipl.-Ing. Johannes Linhard as well as to my 'fellow passenger' Matthias Firl, M.Sc. for enduring my nature with great patience. Furthermore, I would like to thank Dipl.-Ing. Kathrin Grossenbacher and Dipl.-Math. Markus Ganser for their assistance in setting up the application example.

I would like to thank my family and especially my parents Ulrike and Harald for all their love and support. Above all, I am deeply indebted to my dear wife Britta who was bearing the brunt of work while I was released to compile my dissertation. Thank you for everything – most notably for being such a caring mother to our children.

Munich, May 2007 Florian Jurecka

Contents

List of Figures

List of Tables

Chapter 1

Introduction

1.1 Motivation and Thematic Framework

In today's engineering world, product development processes are strongly influenced by computer simulations. These numerical simulations offer the possibility to study the characteristics of engineering problems thoroughly before the actual product or a prototype is manufactured. The importance of this process, which is typically referred to as *virtual prototyping*, is constantly growing – driven by the demand for continually shortened development cycles. A shrinking time span from conception to market maturity can result in significant cost reduction due to the competitive edge conferred by up-to-date products. Computer simulations allow for fast investigation of a large number of alternative designs, thus reducing the time required for product development. Additionally, the more development is made based on numerical analysis, the fewer "physical" prototypes are generally required – a fact that may for itself considerably reduce development costs. Moreover, numerical analyses of engineering problems (e.g. finite element analyses) provide a way to process the data which is well-suited for the use of optimization techniques called *mathematical programming* [Sch60].

As a result of the optimization process, a product is obtained that exhibits optimal properties with respect to the performance measure which has been utilized to assess the quality of the design. Obviously, two key factors govern the usefulness of the attained result. First, the numerical model used to describe the real physical behavior has to be adequate. In other words, the main characteristics of the physical behavior have to be captured by the numerical model. Poor approximations can lead to severe mistakes and wrong decisions. Second, the optimization problem has to be formulated carefully. This means that the formulation of the objective and – even more important – the constraints can have a tremendous impact on the resulting design.

The optimized designs typically appear to be highly sensitive even to small changes in the problem formulation. This effect directly results from the removal of all possible redundancies and is hence an inherent character of optimized designs – in particular of constrained solutions. In this case, the optimum design is controlled by some restrictions (e.g. maximum allowable stress or displacements) which constitute sharp borders between admissible design and waste. In practice, however, variations and uncertainties inhere almost all quantities that show up in engineering problems e.g. in form of dimensions of structural

members, material properties, or loadings. If the optimized product shows high sensitivities concerning such inevitable imperfections or environmental variations, the product performance in everyday use may be far from optimal.

In most of today's engineering practice, the true effects of variations are typically neglected for reasons of simplification and reduced numerical effort. Calculations are in general performed based on deterministic values (statistical measures such as the mean or fractiles) multiplied by some safety factors. In contrast to this approach, *robust design* methods attempt to make a product or process insensitive to changes in the noise factors (representing the source of variation) by choosing qualified levels of the controllable factors [FC95, Par96]. The concept of robust design, which is also referred to as *quality engineering*, is not addressing the possibilities to reduce the variance of the noise variables itself, it focuses on reducing the effects of variations and uncertainties on the product (or process) performance [Pha89]. To achieve this goal, both mean value and variation of the performance measure have to be considered in the formulation of the optimization problem.

The stochastic analyses, which are necessary to quantify the effects of varying parameters on the observed performance measure, are quite time consuming. Typically, several analyses have to be completed before one design can be assessed. Furthermore, the desire to produce high-fidelity approximations to the true physical behavior, the numerical analyses themselves become more and more detailed and complex. During the last decades, the remarkable gain in computing power was steadily compensated by the complexity of features newly added to the *computational engineering* software. As a consequence, stochastic analyses and optimization of stochastic problems are only viable if the extra effort compared to a single (deterministic) evaluation can be reduced to a minimum. In this work, a metamodel-based approach is presented to economize on necessary numerical analyses. Here, a so-called *metamodel* is established based on selected computer simulations. During the stochastic analyses, this approximation model can serve as a convenient surrogate for the original (complex) computer software.

The range of possible applications for numerical analysis and optimization is enormous. In classical engineering fields such as civil or mechanical engineering (including the automotive and aerospace branches), various problems have been tackled effectively. But also in the area of electrical engineering or biomechanics, successful applications have been reported in many publications. In the present work, the focus will be on the solution of problems in structural mechanics, typically based on finite element analyses [ZT05].

1.2 Literature Review

In this section, previous developments in the two fields which are of utmost importance for this work will be described: *robust design* and *metamodeling approaches*. The list of references herein is chosen to give an adequate picture of the respective advances and applications. This section tries to offer a representative overview but due to the diversity within the individual fields of research, the list cannot be complete.

1.2.1 Robust Design

In the 1920s, SIR RONALD A. FISHER made some efforts to grow larger crops despite varying weather and soil conditions [Fis66]. Founding on this research, he elaborated the basic techniques of design of experiments (DoE) and analysis of variance (ANOVA) [Yat64, Box80], which were enhanced afterwards by many statisticians. Based on this previous work, the Japanese engineer GENICHI TAGUCHI worked on different techniques for quality improvement of industrial products or processes in the 1950s and early 1960s. However, before the 1980s, his concept, which he called *robust parameter design*, was virtually unknown outside Japan. This changed rapidly after Taguchi's journey through the USA, where he visited many companies such as Ford and AT&T [Kac85, Tag86, Pha89, Roy90].

In the framework of robust (parameter) design, a distinction is made between three types of parameters. The controllable variables (also called *control parameters*) can be chosen or controlled by the designer during the design process and the optimization. *Noise parameters* represent the source of variation in the system. The variations cannot be controlled but might be known to the designer and describable as by probability density functions. Finally, the fixed parameters or process constants describe deterministic characteristics of the system. Accordingly, the robust design task is to determine control variable settings such that the resulting process (or product performance) is robust (or insensitive) to the variation originating from the noise parameters.

The robust design concept is based on classical DoE techniques with all design variables being varied according to an orthogonal array (termed *inner array*). At each design variable setting the noise variables are varied according to a second orthogonal array (*outer array*), thus generating a *crossed array*. The response data gained at the different replications are used to estimate the process mean and variance. Both statistics are then combined to a single performance measure, the *signal-to-noise-ratio (SNR)*. The resulting array of estimated SNRs is used to perform a standard analysis of variance and those design variable settings are identified that yield the most robust performance. More details are given e.g. in [Pha89].

TAGUCHI's contributions started a process which made aware the importance of parameter variations to many design engineers and statisticians. His approach was reviewed, criticized, and enhanced throughout the years. NAIR initiated a panel discussion and summarized the main contributions with references to the original sources [Nai92]. The bone of contention was the inefficiency of the approach, especially with respect to the number of required experiments. In consequence, several publications introduced response surface approaches for robust design optimization based on combined arrays [VM90, RSSH91, MKV92, Kha96]. In [RBM04], the different approaches for solving robust design problems based on polynomial response surface models have been reviewed.

The original robust design concept was developed for the experimental analysis of physical problems. Due to the enormous effort related to conducting physical experiments, the approach disregarded any sequential layout. Additionally, for reasons of costs, the number of levels is typically limited in physical experimentation. However, modern computer simulations can easily be used in a sequential manner and also the restrictions concerning

the number of variable settings do not apply to computer simulations. By means of numerical simulations, the stochastic properties of noise variables can be mapped onto the response value, which also becomes a random variable. Commonly, sampling methods or TAYLOR expansion approaches are used to determine the mean and variance of the response. These statistics can then be used to formulate a robustness criterion, which serves as objective function in a nonlinear optimization process. As a result, a robust design optimization can be performed analogously to the well-known numerical optimization methods [Vie94, RR96, Das97, Mar02].

For the definition of the *stochastic optimization problem*, the effects of noise variables on both the objective function and the constraints have to be considered [PSP93, DC00, JL02]. Robust design optimization regarding the objective function makes the system performance least sensitive to variation of noise variables. The fulfillment of the constraints subject to noise governs the *reliability* of the process (sometimes called feasibility robustness). Reliability analysis i.e. the question on the probability of failure developed as a separate field of research and is not in the focus of this work.

The major drawback related to numerical optimization of stochastic problems is that they need substantially more response evaluations compared to standard deterministic optimization problems. Hence, the numerical effort is significantly higher. In many cases, this leads to the need for simpler approximation models (also called *metamodels*) to considerably reduce computing time [TAW03]. The developments in the field of metamodels will be discussed in the next section.

Over the past years, robust design methods have been successfully applied in many fields of engineering. Industrial applications have been reported amongst others for router bit life improvement [KS86], optimization of a rocket propulsion system [USJ93], shape optimization of rotating disks for energy storage [Lau00], vibration reduction for an automobile rear-view mirror [HLP01], airfoil shape optimization [LHP02], vehicle side impact crash simulation [KYG04], structural optimization of micro-electro-mechanical systems (MEMS) [HK04], fatigue-life extension for notches [MH04], and tuning of vibration absorbers [ZFM05].

1.2.2 Metamodeling Techniques

The fundamental idea of the metamodeling concept is to find an empirical approximation model, which can be used to describe the typically unknown relation between input variables and response values of a process or product. To adjust the chosen analytical formulation to the problem under investigation, the original response values are evaluated at some selected input variable settings, the so-called *sampling points*. Based on these input-output pairs, free parameters in the model formulation are fit to approximate the original (training) data in a best possible way. The approximation models can then be used to predict the behavior of the original system at "untried" input variable settings. Originally, the primary application for this technique was the analysis of physical experiments.

The strength of the approximation concept and its straightforward applicability in optimization procedures was soon recognized [SF74]. In the following years, approximation

concepts have proved to be an efficient tool for saving computation time in structural optimization [Sva87, TFP93, RSH98]. In the optimization context, approximations either allow for the analytical determination of the approximate optimum or they replace the original functions within one or in the course of several iteration steps. In general, three different categories of approximations can be distinguished dependent on their region of validity: *local*, *mid-range*, and *global approximations* [BH93]. While local approximations are only valid in the immediate vicinity of the observed point, mid-range approximations try to predict the original functional response in a well-defined subregion of the design space. In contrast to this, global approximations aim at predicting the characteristics of the functions over the entire design space.

Local approximations are based on local information obtained at a single point only. Hence, they are also called *single point approximations*. The more information is available (e.g. by means of sensitivity analysis [Kim90, SCS00]) the better the fit will possibly be. Mid-range approximations rely on information gathered from multiple points. Both local and mid-range approximations form explicit subproblems (defined on a subregion of the design space) that can be solved analytically. Accordingly, an iterative optimization technique is commonly applied where the area of model validity successively moves around in the design space. For the present work, however, the emphasis is placed on global approximations.

In virtually all engineering fields, complex computer simulations are used to study behavior and properties of the engineered product or process. In many applications, a single computational analysis can take up to several hours or even days. As a consequence, an application of sequential optimization algorithms or stochastic analyses is practically impossible. In these cases, global approximation models are constructed to serve as a surrogate for the original system under investigation. The resulting surrogate model is often called metamodel indicating that a model of a model is determined. The main advantage of the metamodeling approach is that the training data to fit the surrogate model can be determined in advance and in parallel, thus resulting in shorter analysis times. The response values for untried designs which are actually required during the optimization process (or a stochastic analysis) can then be predicted by the metamodel which is inexpensive to evaluate.

The probably most famous and best-established approximation model approach is the *response surface method (RSM)* [BD87, MM02]. Here, user-determined polynomials are fit to the training data by means of linear regression i.e. by choosing the free parameters such that the sum of squared residuals becomes minimal [MPV01]. Usually, low order polynomials are chosen to keep the number of free model parameters and hence the required training data set as small as possible. To enhance the approximation quality, several variable transformation techniques have been proposed, for instance logarithmic or reciprocal transformations.

Computer simulations (sometimes also referred to as *computer experiments*) exhibit a major difference compared to typical physical experiments: they have no random error associated with the evaluated response values. In physical experiments, measurement errors and environmental variances substantiate the assumption of a random error. The presence of a random error, however, is a central point in the foundation of least-squares regression.

Accordingly, the use of response surface models to approximate results of computer simulations is questionable [SSW89, SPKA97]. As a consequence, a metamodel, which is intended to replace a deterministic computer simulation, is expected to interpolate exactly all original response values observed at the sampling points. This insight was the motivation for the development of a metamodel formulation which is commonly termed *DACE*, derived from the title of the original paper by SACKS et al. [SWMW89]. Often, the resulting metamodel type is also called *kriging*, named after DANIEL G. KRIGE, who introduced the approach for geostatistical analyses [Kri51].

Other metamodeling techniques have been developed to attain the desired interpolating feature, for instance *radial basis function models (RBF)* [Pow92, Gut01, Kri03]. The weighted polynomial regression technique [LS86, MPV01, TSS+05], which is also called *moving least-squares (MLS)*, can yield a better local approximation of the original observations or even an interpolative behavior depending on the chosen weighting formulation. Furthermore, *artificial neural networks (ANN)*, a technique originating from machine learning and "artificial intelligence", have been used as metamodels in optimization procedures [CB93, CU93, PLT98]. Several survey papers have been published comparing accuracy and computational efficiency of the different approaches for some selected examples, for instance [Etm94, SMKM98, JCS01, SPKA01, SBG+04].

A crucial factor for the performance of the respective metamodel types is the proper selection of sampling points. These points should be chosen carefully, namely by means of *design of experiments (DoE)* techniques, to get the maximum information with a minimum effort. To match the individual structure of the different metamodel formulations, customized DoE methods have to be developed [SSW89, Mon01, SWN03].

Finally, the designing engineer should be aware of the fact that the solution of the approximated problem is only a estimate for the true optimum of the original system. To obtain an accurate and reliable solution, the metamodels have to be validated and – if necessary – updated successively. The update procedures again have to take into account the special traits of each metamodel formulation. The validation and update process is currently an area of active research – with many recent publications e.g. [SLK04, JGB04, JHN05, RS05, GRMS06]. However, in the literature, no update procedure is described so far that accommodates for the peculiarities of stochastic optimization problems. For this purpose, an adapted approach to fit for robust design problems is presented in this work. Here, the update procedure is split into two parts: During the first part, the variety of possible designs is explored to find promising candidates for a robust design. The second part investigates the noise space to yield a more reliable estimation of the robustness criterion.

Metamodeling techniques have expanded into many industrial applications. According to an extract of recent publications, they have been successfully applied to combined aerodynamic-structural optimization of a supersonic passenger aircraft [GDN+94], helicopter rotor blade design [BDF+99], aerospike nozzle design (rocket engine) [SMKM98, SMKM01], vehicle crashworthiness studies [KEMB02, RGN04, FN05], internal combustion engine design [GRMS06], conceptual ship design [KWGS02], embedded electronic chip design [OA96], underwater vehicle design [MS02], roll-over analysis of a semi-tractor trailer [SLC01], and the robust design of a welded joint [Koc02].

1.3 Organization of this Thesis

The introductory Chapter 1, which presented the motivation for this work and a selective overview over relevant and representative publications in the field of robust design and metamodeling techniques, now concludes with an outline of this thesis.

Chapter 2 presents the field of structural optimization. This includes an introduction to the terms and definitions commonly used in the optimization context. Furthermore, the mathematical fundamentals are given to describe structural optimization problems and suitable solution techniques. Subsequently, a general overview of numerical optimization algorithms is given. The classification of algorithms is followed by a detailed description of those optimization methods that have been used for the work described in this thesis. In this chapter, only the case of deterministic optimization problems is considered, i.e. all decisive quantities are regarded as deterministic.

Chapter 3 generalizes the view to the case where the investigated problem has stochastic properties – more precisely, where the input variables may include random variables. The chapter starts with an introduction to the basic statistical concepts and measures used to characterize the problem. Hereafter, a general formulation for optimization problems including random variables is presented. The core of this chapter is a detailed discussion of different robustness criteria, which transform the stochastic optimization problem into a deterministic surrogate problem. In the remainder of this chapter, different methods to solve stochastic optimization problems are detailed. At this point, reliability and robustness problems – two special cases of stochastic optimization problems – are distinguished and special emphasis is placed on the solution of robust design problems.

In Chapter 4, metamodeling techniques are presented. Metamodels can be used to reduce the computational costs associated with the solution of stochastic optimization problems. After a general introduction to the metamodeling concept, the commonly used metamodel formulations including polynomial regression models, moving-least-squares approximations, kriging models, radial basis functions and artificial neural networks are detailed. The chapter concludes with a comparison of the presented techniques with respect to approximation quality and computational issues.

Chapter 5 provides a review of the field “design of experiments”. To fit metamodels to a specific problem, training data has to be provided. This data is gathered from so-called sampling points. The question on how to choose the sampling point coordinates thus ensuring a good and balanced predictive behavior of the approximation models is addressed in this chapter. Here, special characteristics of the respective metamodel types are considered to formulate customized experimental designs, for instance space-filling designs or Latin hypercube designs.

The theoretical part of this thesis ends with Chapter 6. In this chapter, methods are presented which allow for a reliable optimization process based on the metamodeling concept. To assure a good predictive behavior of the metamodel especially in the proximity of the predicted optimum, the metamodels have to be updated sequentially. Well-established update procedures, that have been proposed in the literature, will be sketched first. Since

these methods have been developed to solve deterministic optimization problems, they are in general not suited for the solution of robust design problems. Here, some minor changes are proposed to fit the standard update procedures to the special case of stochastic optimization problems. Furthermore, an approach is suggested which particularly elaborates on the solution of robust design problems by means of interpolating metamodels.

In Chapter 7, the solution of robust design problems based on metamodeling techniques is illustrated by numerical examples. Three different mathematical test problems are studied to prove applicability and efficiency of the proposed method. This chapter concludes with an industrial application example taken from the field of sheet metal forming.

Figure 1.1 on the facing page summarizes the suggested framework for metamodel-based robust design optimization in a flowchart. The internal optimization loop is illustrated in more detail in Figure 1.2 on page 10.

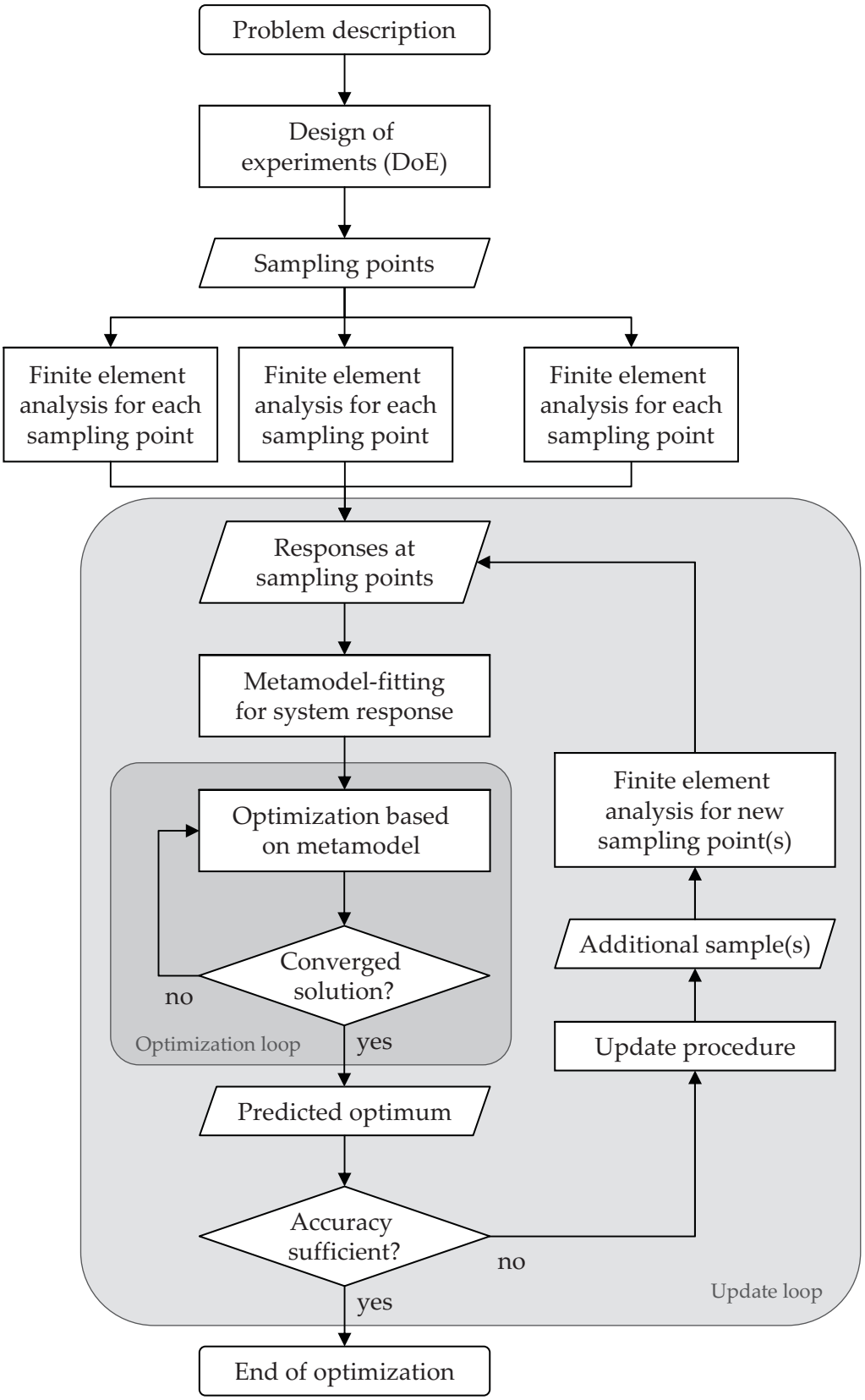

Figure 1.1: Proposed framework for metamodel-based robust design optimization.

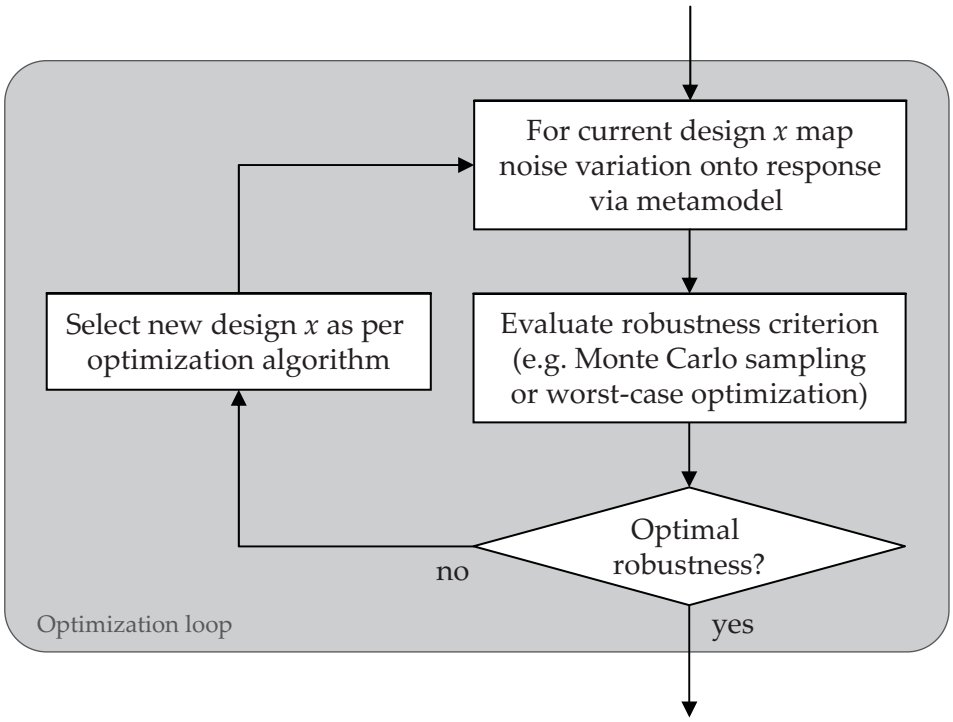

Figure 1.2: Detailing of internal optimization loop performed on the metamodel.

Chapter 2

Structural Optimization

The field of structural optimization and its historical developments have been reviewed in many publications e.g. [Sch81, Van82], or more recently in [Van06]. Furthermore, excellent textbooks [Aro89, HG91, Kir93] exists which present a comprehensive and detailed view on the topic including a broad literature review. On this account, a thorough discussion is omitted here and only a condensed introduction is given to familiarize the terminology and notation used in the remainder of this text.

Accordingly, the theoretical basis, terms, and definitions for the field of structural optimization are summarized in this chapter, and a selection of common optimization algorithms is presented. At this point, only the deterministic case is considered, where all crucial parameters e.g. dimensions, material parameters, and loads can be described by unique values, and the governing functional relationships are inherently deterministic i.e. the same input will cause exactly the same output as structural response. Stochastic aspects will be considered in Chapter 3.

2.1 Terms and Definitions in Structural Optimization

2.1.1 Design Variables

In structural optimization, the aim of the designing engineer is to optimize performance of a structure within certain restrictions set e.g. by the manufacturing process, serviceability, or safety of the structure. The parameters, the engineer can possibly use to alter the structural design, are usually called *design variables* x_i and are assembled into the vector $\mathbf{x} = [x_1, x_2, \ldots, x_n]^T$ for a convenient notation. The solution of the structural optimization problem i.e. the vector of design variables describing the optimal design is denoted by $\mathbf{x}^*$. Common design variables in structural optimization problems are dimensions of structural members (like beam length, plate thickness, and cross sections) or other attributes controlling the geometry and topology of the structure, respectively (e.g. holes, fillets, and stiffeners) as well as material properties of different components (including reinforcement distribution, etc.).

Design variables are either *continuous* or *discrete*. Continuous variables can take on any real value within a given range characterized by so-called *side constraints*. In contrast to this,

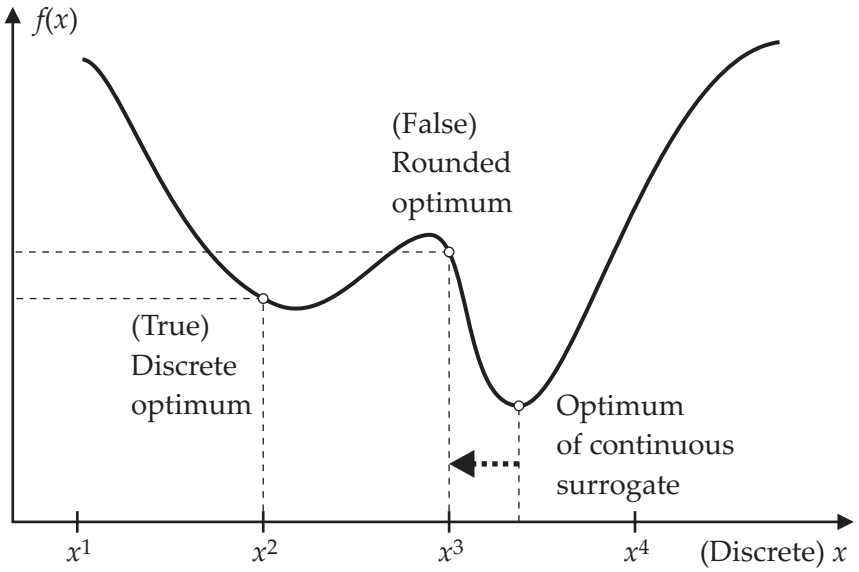

Figure 2.1: Discrete optimization problem and continuous surrogate.

discrete variables are restricted to a certain selection of admissible values or integer values e.g. in-stock cross sections, standardized material classifications, or number of welding spots.

In most engineering problems the discrete features of design variables are neglected during the optimization process and all variables are varied continuously. Based on the continuous optimum design, the values of the inherently discrete variables are then adjusted to the nearest feasible discrete value. This workaround is commonly adopted because solving a continuous surrogate problem is generally easier than accounting for the discrete characteristics during optimization. However, rounding off to the nearest allowable value might introduce significant differences compared to the solution of the original discrete optimization problem. This possible discrepancy has to be considered in particular if the admissible values are located too far away from the continuous solution, or if the variation in the observed quantity is very large (see Figure 2.1). In these cases special optimization techniques have to be employed to find the true optimum e.g. [LD60, LW66, HL92, AHH94, KKB98].

2.1.2 Disciplines in Structural Optimization

Depending on the type of design variables, three different disciplines of optimization tasks are distinguished within the structural optimization community, as depicted in Figure 2.2.

Sizing. An optimization problem with cross-sectional dimensions as design variables is the simplest optimization task. For sizing, topology and geometry of the structure remain fixed. A typical application for sizing is the determination of minimal cross-sectional areas in truss structures.

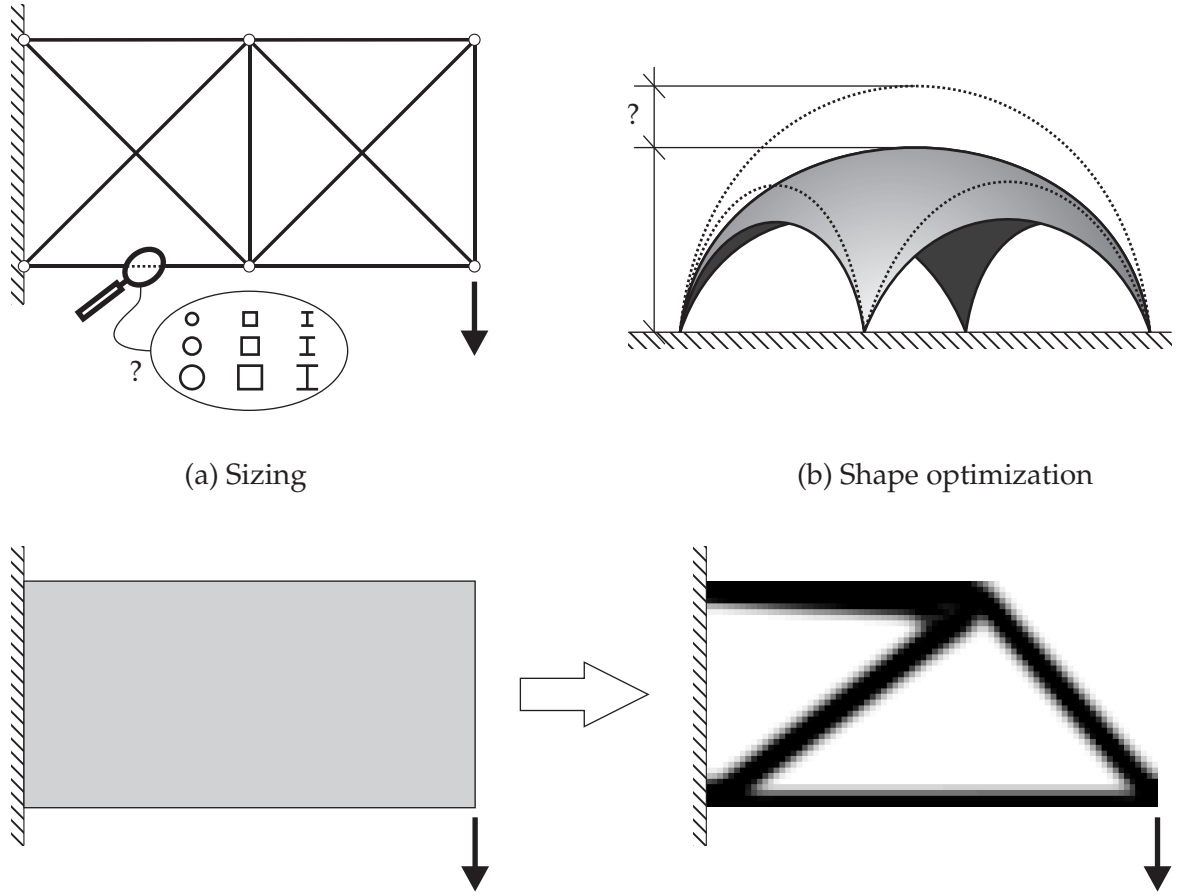

(a) Sizing

(b) Shape optimization

(c) Topology optimization

Figure 2.2: Disciplines in structural optimization.

Shape optimization. In shape optimization, geometrical parameters of the structure are determined to optimize system performance. The topology of the system, e.g. the connectivity, remains unchanged during optimization. As an example, the height of a shell structure can be treated as design variable for shape optimization.

Topology optimization. In contrast to shape optimization, design variables in topology optimization describe the structural configuration. Due to the fact that a broad variety of configurations might be possible, topology optimization is computationally expensive. Hence, the application of topology optimization is often restricted to truss design problems. In this special case, the idea of topology is very clear. The question to answer is: where to add a new or remove an existing truss member in the truss structure.

In general, these three different classes of optimization problems do not appear separately in engineering problems; combinations rather emerge frequently.

2.1.3 Constraints

On top of the side constraints, which may impose lower and upper bounds on each design variable (assembled in the vectors $\mathbf{x}^L$ and $\mathbf{x}^U$, respectively) and thus define the *design space* $\mathcal{D}$, other restrictions to allowable or acceptable designs are possible. If a design complies with all restrictions, it is called a *feasible design*. In the context of structural optimization, these restrictions are called *constraints*. Constraints divide the design space into a *feasible domain* (symbolized by $\mathcal{C}$) and an *infeasible domain*.

Depending on their formulation, *equality* and *inequality constraints* are distinguished. Some optimization algorithms are not able to handle equality constraints; in that case equality constraints are usually transformed into two inequality constraints defining a lower and an upper bound with the same limit value. Throughout this text, equality constraints are assumed to be transformed to the standard form $h(\mathbf{x}) = 0$. Inequality constraints are reformulated to be satisfied if they are less than or equal to zero denoted by $g(\mathbf{x}) \leq 0$. In some other texts, especially in the reliability community, the opposite convention is used i.e. constraints are violated for values smaller than zero and satisfied otherwise. Inequality constraints are commonly depicted by the contour $g(\mathbf{x}) = 0$, which is called *limit state*. An inequality constraint is called *active* if for a specific design $\mathbf{x}'$ the constraint is fulfilled at equality i.e. $g(\mathbf{x}') = 0$. If the strict inequality $g(\mathbf{x}) < 0$ holds, the respective constraint is *inactive*. For values $g(\mathbf{x}) > 0$ a constraint is *violated*. An active constraint is termed *redundant* if the resulting optimum does not change once this constraint is removed from the problem definition.

2.1.4 Objective Function

In order to solve an optimization problem, the different possible designs have to be compared and rated. Performance of each design is assessed by some merit function that is formulated as a scalar valued function. This criterion, defining a ranking of the different designs, has to be a function of the design variables in a way that ensures that different design configurations may lead to different performance values. It is commonly referred to as *objective function* and represented by $f(\mathbf{x})$. Representative examples for objective functions are weight, stiffness, displacements, frequencies, or simply costs. Thus the objective function is frequently termed cost function as well. Without loss of generality, the formulation of the objective function is commonly chosen to define a minimization problem, an arrangement also maintained throughout this text. This does not impose a restriction because a problem description $f_{max}(\mathbf{x})$ that intrinsically requires a maximization can easily be transformed into a minimization formulation by $f(\mathbf{x}) = -f_{max}(\mathbf{x})$.

Optimization tasks where several criteria $\mathbf{f}(\mathbf{x}) = [f_1(\mathbf{x}), f_2(\mathbf{x}), \ldots, f_p(\mathbf{x})]^T$ characterize the performance of a design are termed *multicriteria* or *multiobjective optimization problems*. As the system response is described by a vector of objective functions, the term *vector optimization* is used in some texts. In cases where some criteria are conflicting, there is no general optimal solution. Each possible optimum will only be a compromise of the different objectives. If the different criteria are compatible, consequently all functions are redundant except for one.

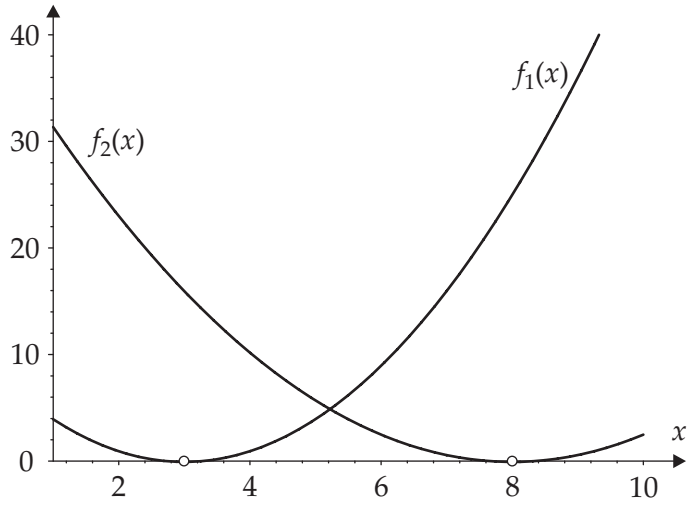

Figure 2.3: Multicriteria optimization with two conflicting objectives $f_1(x)$ and $f_2(x)$.

For the case of multiple conflicting objectives, two intuitive approaches are commonly used to reduce the number of objectives to one. The first approach is to extract the most significant one as the only objective function and to impose an upper bound value on the unconsidered objectives. Hence, except for the so-called *preference function* all other objectives are treated as constraints in the optimization process.

$$\begin{aligned} F(\mathbf{x}) &= f_j(\mathbf{x}) \quad ; && j \in \{1,\ldots,p\} \\ g_i(\mathbf{x}) &= f_i(\mathbf{x}) - c_i \leq 0 \quad ; && i = 1,\ldots,j-1,j+1,\ldots,p \end{aligned} \tag{2.1}$$

To transform an objective function f_i into a constraint g_i, an upper limit c_i must be specified to define the maximum allowable value for each individual objective.

The second straightforward approach to reduce the number of objective functions to a single criterion compiles one *composite function* $F(\mathbf{x})$ consisting of a weighted sum of the different objective functions

$$F(\mathbf{x}) = \sum_{i=1}^{p} w_i f_i(\mathbf{x}) \,. \tag{2.2}$$

The choice of the individual weights w_i should reflect the relative importance of each corresponding objective function $f_i(\mathbf{x})$. Determining the weights of the different objectives can be a difficult task because the choice can severely affect the optimization result.

Example 1. To illustrate the approaches, consider the two conflicting objective functions $f_1(x) = (3-x)^2$ and $f_2(x) = (6.4 - 0.8x)^2$ (cf. Figure 2.3) with their individual minima at $x_1^* = 3$ and $x_2^* = 8$, respectively.

Figure 2.4a depicts $f_2(x)$ as the dominant objective while the other objective $f_1(x)$ is transformed into a constraint with an upper limit $g_1(x) = f_1(x) - 10 \leq 0$. The resulting optimum of this strategy is found to be $x^* = 6.16$.

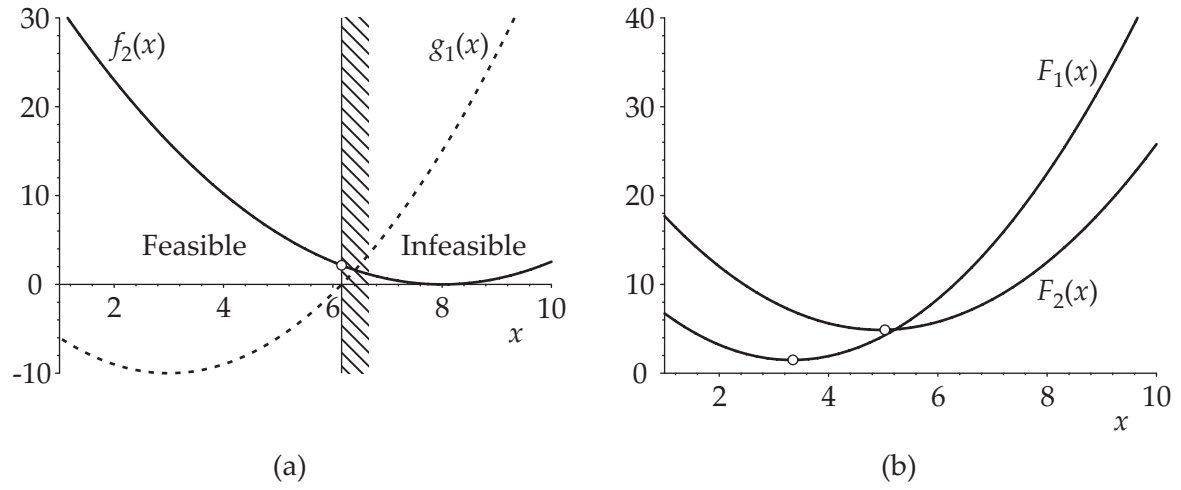

Figure 2.4: Illustration of two approaches to handle conflicting objectives.

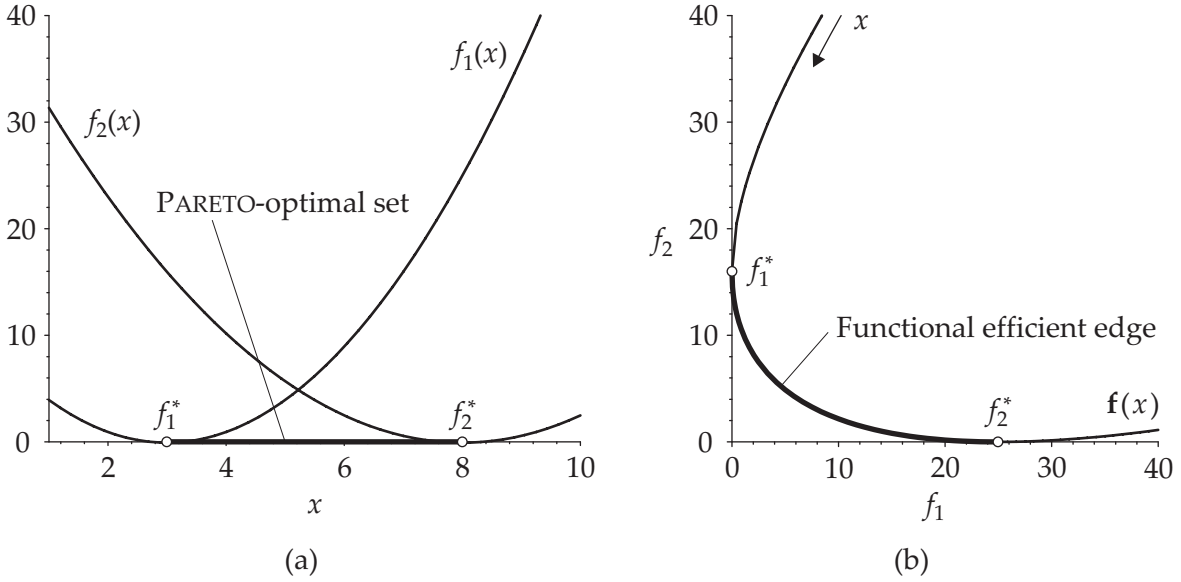

Figure 2.5: PARETO-optimal set plotted (a) in design space and (b) in space of objective functions.

The conflicting objective functions can also be combined to one objective by the weighted sum approach as demonstrated in Figure 2.4b. Different compromises can be found by altering the weighting factors e.g. $F_1(x) = 0.9f_1(x) + 0.1f_2(x)$ or $F_2(x) = 0.5f_1(x) + 0.5f_2(x)$ with their optima at $x_1^* = 3.33$ and $x_2^* = 4.95$, respectively. □

A systematic approach to handle multicriteria optimization is offered by the concept of PARETO-optimality [Par06]. A design $\mathbf{x}^*$ is termed *PARETO-optimal* if for any other choice of $\mathbf{x}$ either the values of all objective functions remain unchanged or at least one of them worsens compared to $\mathbf{x}^*$. This definition covers the set of all possible compromises that can be obtained by varying the weights in Equation (2.2). The set of PARETO-optimal points for the presented example is illustrated in Figure 2.5. The PARETO-optimal part of the plot in

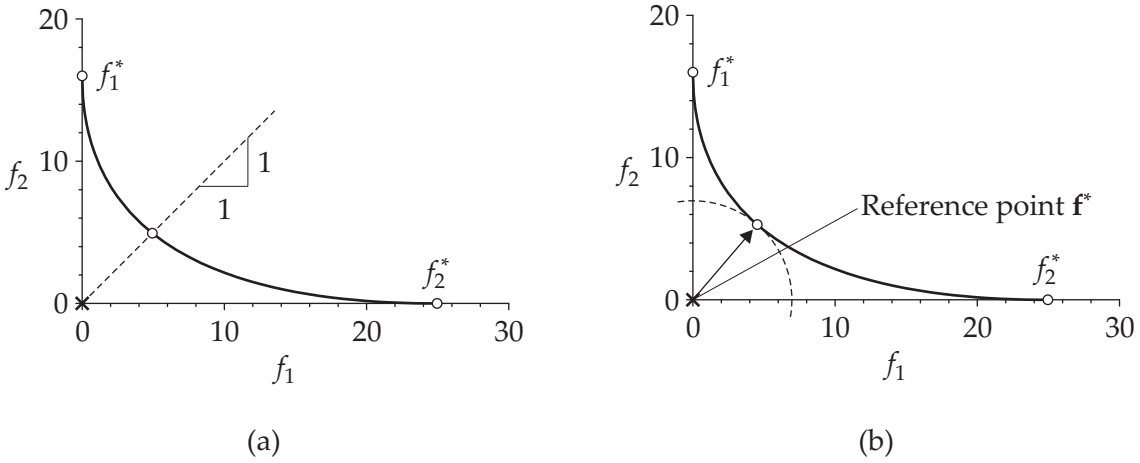

Figure 2.6: Criteria for single optimum from PARETO-optimal set: (a) L_∞ norm and (b) L_2 norm of the normalized distance d_i.

space of objective functions (cf. Figure 2.5b) is often called *functional efficient edge*.

One possible strategy to specify a distinguished point $\mathbf{x}^*$ of the set of PARETO-optimal solutions is based on the deviation from the individual minimum of each objective f_i. Let $f_1^*, f_2^*, \ldots f_p^*$ denote the results of the independent minimization of each individual objective function $f_i(\mathbf{x})$, then the normalized distance d_i of a candidate point $\mathbf{x}$ from the individual optimum f_i^* is defined as

$$d_i(\mathbf{x}) = \frac{f_i(\mathbf{x}) - f_i^*}{f_i^*} \quad ; \qquad i = 1, 2, \ldots, p \,. \tag{2.3}$$

To avoid division by zero, the denominator of Equation (2.3) has to be replaced by a number which represents a characteristic magnitude of the respective objective in case an individual minimum is equal to zero.

Based on the normalized distance, one distinctive compromise setting can be found either as the minimum of the largest deviation (L_∞-norm) of the different objective functions from their individual minima (cf. Figure 2.6a)

$$\text{minimize} \max_{i=1,\ldots,p} \{d_i(\mathbf{x})\} \tag{2.4}$$

or as the minimum distance (L_2 or Euclidean norm) from the reference point $\mathbf{f}^* = [f_1^*, f_2^*, \ldots, f_p^*]^T$

$$\text{minimize} \sum_{i=1}^{p} \left(d_i(\mathbf{x})\right)^2 . \tag{2.5}$$

Further details about solution techniques in multicriteria optimization and some applications can be found in [EKO90].

2.1.5 Standard Formulation of Optimization Problems

The introduced terms and definitions are summarized to form the standard formulation of a structural optimization problem with continuous design variables:

$$\begin{aligned}
&\text{minimize} && f(\mathbf{x}) \quad ; && \mathbf{x} \in \mathbb{R}^n && \text{(2.6a)}\\
&\text{such that} && g_j(\mathbf{x}) \leq 0 \quad ; && j = 1, \ldots, n_g && \text{(2.6b)}\\
& && h_k(\mathbf{x}) = 0 \quad ; && k = 1, \ldots, n_h && \text{(2.6c)}\\
& && x_i^L \leq x_i \leq x_i^U \quad ; && i = 1, \ldots, n\,. && \text{(2.6d)}
\end{aligned}$$

Combining Equations (2.6b-d), the feasible domain $\mathcal{C}$ is characterized by

$$\mathcal{C} = \{\mathbf{x} \in \mathbb{R}^n \mid g_j(\mathbf{x}) \leq 0 \ \wedge \ h_k(\mathbf{x}) = 0 \ \wedge \ x_i^L \leq x_i \leq x_i^U\}\,. \tag{2.7}$$

The set of points defined by Equation (2.6d) constitutes the design space $\mathcal{D}$

$$\mathcal{D} = \{\mathbf{x} \in \mathbb{R}^n \mid x_i^L \leq x_i \leq x_i^U\}\,. \tag{2.8}$$

In this thesis the objective function is always formulated to define a minimization problem. All inequality constraints are transformed to the form given in Equation (2.6b). Multicriteria optimization problems are solved either by forming one composite objective function or by determining a preference function from the set of conflicting objectives. Hence, a unique solution vector $\mathbf{x}^*$, which defines the optimal design, will be obtained. This solution vector may either describe a *local* or a *global* minimum depending on both the characteristics of the objective and constraint functions and on the features of the optimization algorithm.

2.1.6 Special Cases of Optimization Problems

Constrained vs. unconstrained optimization. Optimization formulations containing neither equality nor inequality constraints are called *unconstrained optimization problems*, all others are termed *constrained* optimization problems. For constrained optimization problems, the number of equality constraints n_h has to be less than or equal to the length of the design variable vector n, which quantifies the number of degrees of freedom in the optimization problem. If $n_h > n$ and no equality constraint is redundant, the system of equations is *overdetermined*, and the formulation of the optimization problem becomes *inconsistent* i.e. no solution of the optimization problem exists. There is no limit to the number of inequality constraints in the formulation of the optimization task; the maximum number of active, non-redundant constraints at the optimum, however, is limited to the number of design variables n.

With many optimization algorithms only unconstrained problems can be solved, or unconstrained problems are at least much easier to handle. Hence, the standard formulation in Equations (2.6a-d) for constrained problems is often transformed to the unconstrained case using the *Lagrangian function*. The formulation of a Lagrangian function will be explained in detail in Section 2.2.

Linear and quadratic programming. In cases where the functions $f(\mathbf{x})$, $g_j(\mathbf{x})$ and $h_k(\mathbf{x})$ describing the objective, inequality, and equality constraints, respectively, are linear and/or quadratic functions only, the optimization problem can be solved very efficiently. On this account, a distinction is drawn between *linear programming*

$$\begin{array}{lllll} \text{minimize} & f(\mathbf{x}) & = \mathbf{e}^T\mathbf{x} \quad ; & \mathbf{x} \in \mathbb{R}^n \\ \text{such that} & g_j(\mathbf{x}) & = \mathbf{A}\,\mathbf{x} + \mathbf{b} \leq 0 \quad ; & j = 1, \ldots, n_g \\ & h_k(\mathbf{x}) & = \mathbf{C}\,\mathbf{x} + \mathbf{d} = 0 \quad ; & k = 1, \ldots, n_h \\ & x_i^L \leq x_i \leq x_i^U \quad ; & & i = 1, \ldots, n \end{array} \tag{2.9}$$

and *quadratic programming*

$$\begin{array}{lllll} \text{minimize} & f(\mathbf{x}) & = \dfrac{1}{2}\mathbf{x}^T\mathbf{Q}\,\mathbf{x} + \mathbf{e}^T\mathbf{x} \quad ; & \mathbf{x} \in \mathbb{R}^n \\ \text{such that} & g_j(\mathbf{x}) & = \mathbf{A}\,\mathbf{x} + \mathbf{b} \leq 0 \quad ; & j = 1, \ldots, n_g \\ & h_k(\mathbf{x}) & = \mathbf{C}\,\mathbf{x} + \mathbf{d} = 0 \quad ; & k = 1, \ldots, n_h \\ & x_i^L \leq x_i \leq x_i^U \quad ; & & i = 1, \ldots, n\,. \end{array} \tag{2.10}$$

Because of their beneficial features, linear and quadratic programming schemes are often used as formulations for sub-problems in sequential solution procedures. These solution techniques are called *sequential linear programming (SLP)* or *sequential quadratic programming (SQP)* methods, respectively.

Nonlinear problems. In general, the functions $f(\mathbf{x})$, $g_j(\mathbf{x})$ and $h_k(\mathbf{x})$ are nonlinear in the design variables $\mathbf{x}$. If this is the case for at least one of these functions, the optimization problem is called *nonlinear*.

Convex vs. non-convex problems. To distinguish convex and non-convex problems, the concept of convexity has to be established for the set of feasible designs (feasible domain) and for the objective function. A collection of points $\mathcal{S}$ is called a *convex set* if the line segment joining any two points $\mathbf{x}^1, \mathbf{x}^2 \in \mathcal{S}$ lies entirely in $\mathcal{S}$. This notion can be represented by

$$\mathbf{x}^1, \mathbf{x}^2 \in \mathcal{S} \quad \Rightarrow \quad \{\alpha\,\mathbf{x}^1 + (1-\alpha)\,\mathbf{x}^2 \mid 0 < \alpha < 1\} \subset \mathcal{S} \tag{2.11}$$

or graphically as depicted in Figure 2.7.

A function $f(\mathbf{x})$ is called a *convex function* if first, it is defined on a convex set $\mathbf{x} \in \mathcal{S}$, and second, it lies below the line segment linking any two points on $f(\mathbf{x})$. This geometrical characterization (cf. Figure 2.8) of a convex function can be formulated mathematically as

$$f\big(\alpha\,\mathbf{x}^1 + (1-\alpha)\,\mathbf{x}^2\big) \leq \alpha f(\mathbf{x}^1) + (1-\alpha) f(\mathbf{x}^2) \quad ; \quad 0 < \alpha < 1\,. \tag{2.12}$$

In practice the fulfillment of the inequality in Equation (2.12) will be difficult to prove because an infinite number of combinations of two points has to be analyzed. Alternatively, the convexity of a function can be checked using the *Hessian matrix* (or simply *Hessian*) of

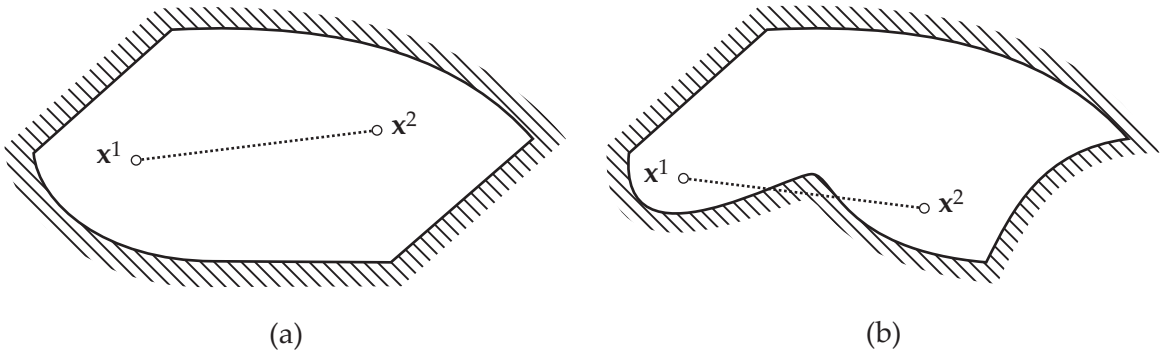

Figure 2.7: (a) Convex set and (b) non-convex set in 2D space.

the function $f(\mathbf{x})$ if $f(\mathbf{x})$ is twice differentiable. The Hessian $\mathbf{H}$ is a symmetric $n \times n$ matrix containing the second derivatives of $f(\mathbf{x})$ with respect to the independent variables x_i. Consequently, it is also denoted by $\boldsymbol{\nabla}^2 f$.

$$\mathbf{H}(\mathbf{x}) = \boldsymbol{\nabla}^2 f(\mathbf{x}) = \begin{bmatrix} \dfrac{\partial^2 f(\mathbf{x})}{\partial x_1 \partial x_1} & \dfrac{\partial^2 f(\mathbf{x})}{\partial x_1 \partial x_2} & \cdots & \dfrac{\partial^2 f(\mathbf{x})}{\partial x_1 \partial x_n} \\ \dfrac{\partial^2 f(\mathbf{x})}{\partial x_2 \partial x_1} & \dfrac{\partial^2 f(\mathbf{x})}{\partial x_2 \partial x_2} & \cdots & \dfrac{\partial^2 f(\mathbf{x})}{\partial x_2 \partial x_n} \\ \vdots & \vdots & & \vdots \\ \dfrac{\partial^2 f(\mathbf{x})}{\partial x_n \partial x_1} & \dfrac{\partial^2 f(\mathbf{x})}{\partial x_n \partial x_2} & \cdots & \dfrac{\partial^2 f(\mathbf{x})}{\partial x_n \partial x_n} \end{bmatrix} \tag{2.13}$$

It can be shown that $f(\mathbf{x})$ is convex if and only if the Hessian is positive semidefinite for every point $\mathbf{x} \in \mathcal{S}$.

The optimization problem in Equations (2.6a-d) is called a *convex problem* if both the objective function and the feasible domain characterized by the constraints are convex. To

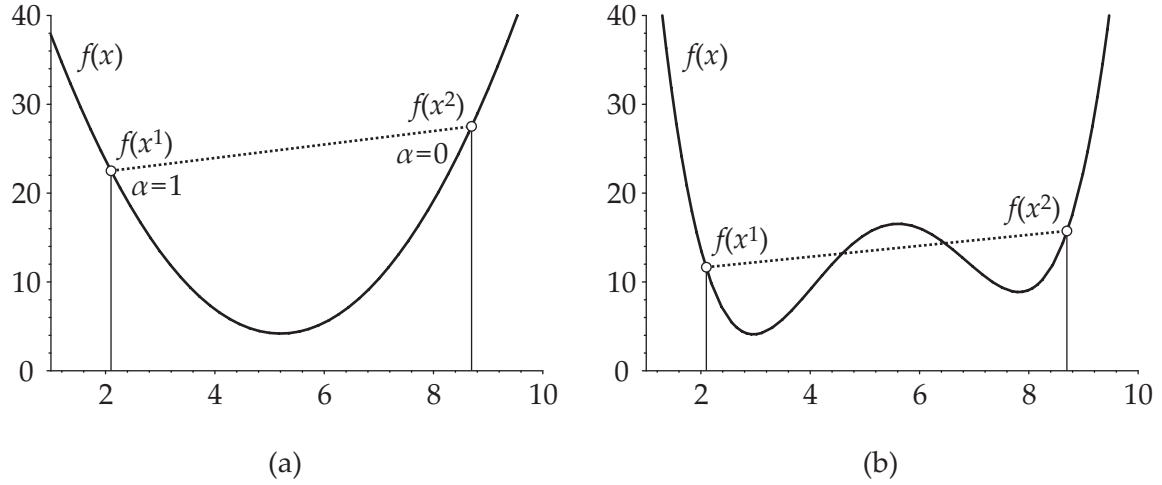

Figure 2.8: (a) Convex and (b) non-convex function $f(x)$ for a 1D problem.

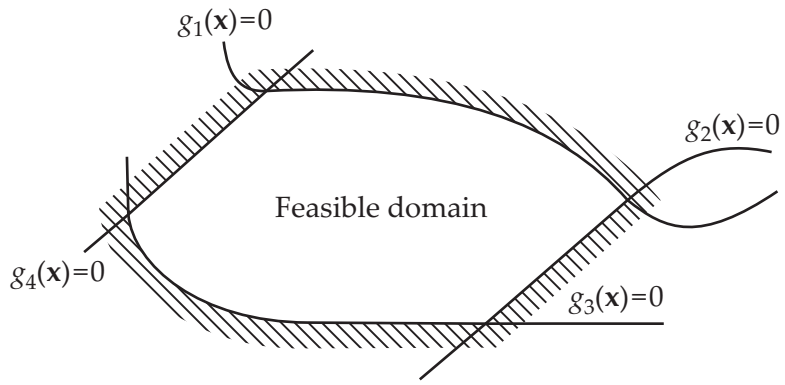

Figure 2.9: Convex feasible domain defined by non-convex inequality constraints.

identify whether the feasible domain is a convex set, the following statements will be helpful:

- ◇ If a function $g(\mathbf{x})$ is convex, then the set $\mathcal{S} = \{\mathbf{x} \in \mathbb{R}^n \mid g(\mathbf{x}) \leq 0\}$ is convex.
- ◇ If an equality is used to delimit a set of points $\mathcal{S} = \{\mathbf{x} \in \mathbb{R}^n \mid h(\mathbf{x}) = 0\}$, then $\mathcal{S}$ is convex if and only if $h(\mathbf{x})$ is linear.
- ◇ A set defined as intersection of several convex sets is always convex.

Relating these statements leads to a possible identification of a convex optimization problem: If a problem has a convex objective function $f(\mathbf{x})$, convex inequality constraint functions $g_j(\mathbf{x})$, and linear equality constraint functions $h_k(\mathbf{x})$, then it is a convex optimization problem. This, however, is not a necessary condition for a convex problem because a feasible domain defined by non-convex inequality constraints (cf. g_1 and g_2 in Figure 2.9) can still be convex.

A convex problem has the important feature that it has only one minimum i.e. a local minimum is also a global minimum. Although convex problems are rarely encountered in engineering practice, this special trait is often used in solution techniques applying sequential (convex) approximations to the true optimization problem e.g. SQP. Further details on optimization algorithms using convex approximations are given in Section 2.3.

2.2 Optimality Conditions

In this section, several criteria are discussed to decide whether an investigated point represents a local or a global minimum for the optimization problem. Apart from the obvious requirement that the solution of the optimization problem $\mathbf{x}^*$ must yield the lowest feasible value for the objective function i.e. there is no other point $\mathbf{x}'$ within the feasible domain $\mathcal{C}$ resulting in a better objective value

$$f(\mathbf{x}^*) \leq f(\mathbf{x}') \quad \forall \quad \mathbf{x}' \in \mathcal{C} \,, \tag{2.14}$$

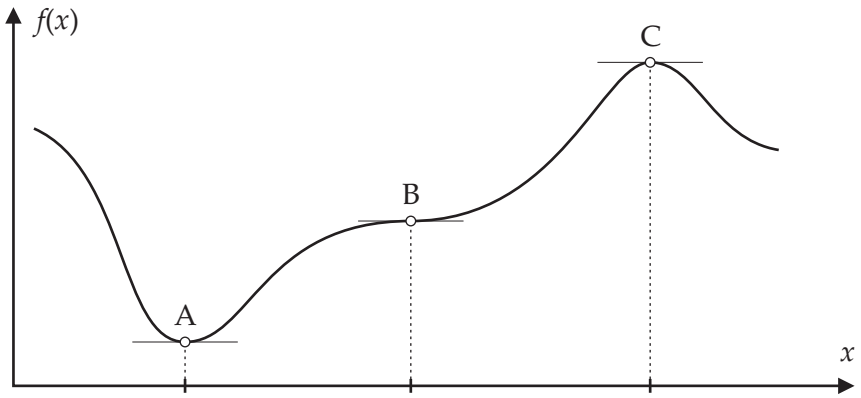

Figure 2.10: Minimum (A), saddle point (B), and maximum (C) for a 1D problem.

further conditions for an optimum point can be identified which prove more helpful for many solution techniques. But before these conditions are introduced, two different types of optimal points are distinguished: *global* and *local* minima. The formulation in Equation (2.14) describes a global optimum since no better solution can be determined within the entire feasible domain $\mathcal{C}$. If the condition only holds in a neighborhood $\mathcal{N}(\mathbf{x}^*)$ of the candidate point $\mathbf{x}^*$

$$f(\mathbf{x}^*) \leq f(\mathbf{x}') \quad \forall \quad \mathbf{x}' \in \mathcal{N}(\mathbf{x}^*) \tag{2.15}$$

$$\text{with} \quad \mathcal{N}(\mathbf{x}^*) = \{\mathbf{x} \in \mathbb{R}^n \mid \|\mathbf{x} - \mathbf{x}^*\| < \varepsilon \ \wedge \ \varepsilon > 0\}\,, \tag{2.16}$$

the point $\mathbf{x}^*$ is a local optimum. If strict inequality holds in Equation (2.14) or (2.15), the respective minimum point is termed *isolated* (global or local) minimum.

In view of the strongly unequal complexity of the formulation of optimality criteria, two different cases are distinguished in the following: unconstrained and constrained optimization.

Unconstrained Problems. As a *necessary* condition for a point to be a candidate for a minimum, it must be a *stationary point* i.e. the gradient of the objective function evaluated at $\mathbf{x}^*$ must vanish.

$$\boldsymbol{\nabla} f(\mathbf{x}^*) = \mathbf{0} \tag{2.17}$$

with

$$\boldsymbol{\nabla} f(\mathbf{x}) = \frac{\partial f(\mathbf{x})}{\partial \mathbf{x}} = \left[\frac{\partial f(\mathbf{x})}{\partial x_1}, \quad \frac{\partial f(\mathbf{x})}{\partial x_2}, \quad \cdots, \quad \frac{\partial f(\mathbf{x})}{\partial x_n}\right]^T \tag{2.18}$$

Yet another condition must be fulfilled to exclude the cases of maxima or saddle points as depicted in Figure 2.10 – points that will also fulfill the necessary condition of Equation (2.17). To identify the case of a minimum, information about the second partial derivatives at the stationary points is used. If the Hessian, as defined in Equation (2.13), is positive definite at a stationary point, this point marks a minimum. This is a *sufficient* condition for a minimum of the unconstrained optimization problem.

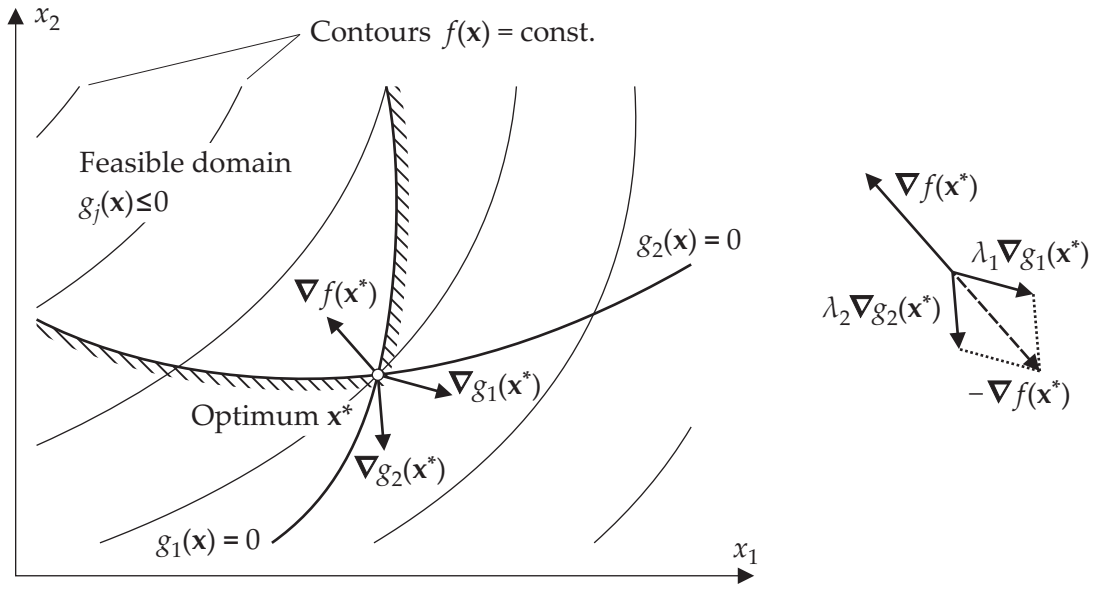

Figure 2.11: Geometrical interpretation of Equation (2.21).

Constrained Problems. For constrained optimization problems, the necessary condition as formulated in Equation (2.17) may not hold if at least one constraint is active at the optimum (cf. Fig 2.4a). Hence, a different necessary condition must be formulated for the constrained optimization case. The following requirements form the so-called *KUHN-TUCKER conditions*, which represent the necessary conditions for a constrained optimum.

$$1. \quad \mathbf{x}^* \in \mathcal{C} \tag{2.19}$$

$$2. \quad \lambda_j^* g_j(\mathbf{x}^*) = 0 \quad ; \quad j = 1, \ldots, n_g \tag{2.20}$$

$$3. \quad \nabla f(\mathbf{x}^*) + \sum_{j=1}^{n_g} \lambda_j^* \nabla g_j(\mathbf{x}^*) + \sum_{k=1}^{n_h} \mu_k^* \nabla h_k(\mathbf{x}^*) = \mathbf{0} \quad ; \quad \lambda_j^* \geq 0 \tag{2.21}$$

As an obvious prerequisite, exclusively feasible designs are allowed as candidate points for the optimum as formulated in Equation (2.19). According to Equation (2.20), the scalar parameters λ_j^* are identically zero if the corresponding inequality constraint is not active i.e. $g_j(\mathbf{x}^*) < 0$. After the following rearrangement

$$-\nabla f(\mathbf{x}^*) = \sum_{j=1}^{n_g} \lambda_j^* \nabla g_j(\mathbf{x}^*) + \sum_{k=1}^{n_h} \mu_k^* \nabla h_k(\mathbf{x}^*)\,, \tag{2.21'}$$

the third condition can be understood geometrically as depicted in Figure 2.11: The gradients of all inequality and equality constraints, evaluated at a stationary point and scaled with factors λ_j^* and μ_k^*, respectively, sum up to the negative gradient of the objective function. Only gradients of active constraints are included in the vector sum since the gradients of inactive constraints are scaled to zero length by their corresponding λ_j as stipulated in Equation (2.20). A closer look at Equation (2.21) reveals that this necessary condition for

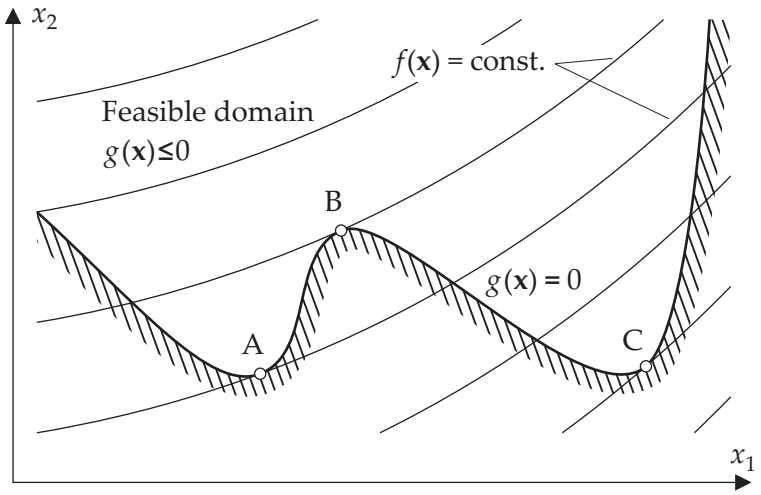

Figure 2.12: Stationary points for a non-convex problem.

stationary points is in fact also the gradient of a yet to determine function similar to Equation (2.17). The function corresponding to the objective $f(\mathbf{x})$ of the unconstrained case is the antigradient of Equation (2.21) with respect to the design variables $\mathbf{x}$, termed the *Lagrangian function L*

$$L(\mathbf{x}, \boldsymbol{\lambda}, \boldsymbol{\mu}) = f(\mathbf{x}) + \sum_{j=1}^{n_g} \lambda_j g_j(\mathbf{x}) + \sum_{k=1}^{n_h} \mu_k h_k(\mathbf{x}) \tag{2.22}$$

with the so-called *Lagrangian multipliers* λ_j and μ_k. The Lagrangian function combines both objective and constraint functions to a single function which has the same solution as the original problem formulation since the terms added to the objective are all equal to zero at the optimum. Furthermore the Lagrangian function transforms the constrained into an unconstrained optimization problem.

The KUHN-TUCKER conditions are necessary conditions only under a certain restriction called *constraint qualification*. The constraint qualification excludes those cases where non-redundant active constraints are linearly dependent. In such cases, constrained minima that do not fulfill the KUHN-TUCKER conditions are also possible. Even when constraint qualification is ensured, the KUHN-TUCKER conditions are necessary, but in general not sufficient for optimality as illustrated in Figure 2.12. Although all three points A, B, and C fulfill the KUHN-TUCKER conditions, only points A and C are minima (a local and a global minimum, respectively). For convex problems however, a point that fulfills Equations (2.19)-(2.21) is a global minimum. Hence, the KUHN-TUCKER conditions are both necessary *and* sufficient for a minimum of convex problems.

For the general case of non-convex problems, an additional criterion is needed as sufficient condition for optimality. This sufficient condition for the constrained case is established by use of the Hessian of the Lagrangian function in analogy to the procedure in un-

constrained optimization.

$$\nabla^2 L(\mathbf{x}, \boldsymbol{\lambda}, \boldsymbol{\mu}) = \nabla^2 f(\mathbf{x}) + \sum_{j=1}^{n_g} \lambda_j \nabla^2 g_j(\mathbf{x}) + \sum_{k=1}^{n_h} \mu_k \nabla^2 h_k(\mathbf{x}) \tag{2.23}$$

A point $\mathbf{x}^*$ that satisfies the KUHN-TUCKER conditions is a minimum if

$$\mathbf{s}^T \left[\nabla^2 L(\mathbf{x}^*, \boldsymbol{\lambda}^*, \boldsymbol{\mu}^*) \right] \mathbf{s} > 0 \tag{2.24}$$

for all $\mathbf{s} \neq \mathbf{0}$ such that

$$\mathbf{s}^T \nabla g_j(\mathbf{x}^*) = 0 \quad \text{for all active constraints with } \lambda_j^* > 0 \tag{2.25}$$

$$\mathbf{s}^T \nabla g_j(\mathbf{x}^*) \leq 0 \quad \text{for all active constraints with } \lambda_j^* = 0 \tag{2.26}$$

$$\mathbf{s}^T \nabla h_k(\mathbf{x}^*) = 0\,. \tag{2.27}$$

Equations (2.25) through (2.27) determine the vectors $\mathbf{s}$ to be tangential to all active constraints at $\mathbf{x}^*$. Hence, Equation (2.24) stipulates that the Hessian of the Lagrangian function must be positive definite for all $\mathbf{s}$ lying in the hyperplane tangent to the active constraints at the candidate point $\mathbf{x}^*$. In this context, two special cases ought to be addressed: First, the fact that Equation (2.24) is not met at a candidate point does not imply that this point is not a minimum (like in case of a plateau at the minimum). However, the case of an isolated minimum is ruled out. Second, if the total number of active constraints (incl. at least one inequality) at a point that complies with the KUHN-TUCKER conditions is equal to the number of design variables n, the only solution to Equations (2.25) through (2.27) is $\mathbf{s} = \mathbf{0}$ and thus Equation (2.24) is not valid. Still, these points are (local or global) minima. An example for this case is depicted in Figure 2.11, where the number of active constraints matches the number of design variables $n = 2$.

2.3 Optimization Algorithms

The solution of optimization problems has been addressed by many contributions from different communities viz. mathematicians, engineers, computer scientists, and economists. Consequently, the range of available algorithms is about as broad as their possible applications [Van84, Evt85, Min86, Fle87, BSS93, BGLS97, NW99]. Due to the conflicting needs depending on the different problem types, there is no "one fits all" method that perfectly suits all possible optimization tasks. The appropriate solution strategy must be chosen on the basis of individual properties in distinctive features e.g. constrained vs. unconstrained, convex vs. non-convex problem, discrete vs. continuous optimization, problem size (number of design variables n), or simply the response values available for the governing functions (objective and constraints). If these functions are known explicitly and they are twice differentiable, the optimum points can be determined analytically using Equations (2.19) through (2.21) and (2.24) through (2.27). If inequality constraints are present in the formulation of the problem, the set of active constraints must be determined by means of a case differentiation.

In most engineering problems, however, the objective and constraints cannot be formulated explicitly and thus can only be evaluated pointwise by solving a linear system of

equations e.g. using the finite element method [ZT05]. In this case, the problem has to be solved by some iterative optimization technique and the most suitable algorithm will depend, amongst other criteria, on whether higher order information can be obtained for the pointwise determined response values, namely first or second derivatives with respect to the design variables (gradient vector and Hessian, respectively). Two fundamentally different concepts can be distinguished:

◇ A *descent algorithm* tries to find the optimum by descending to the lowest point in a "local valley" (i.e. the convex neighborhood around the starting point). This search involves the determination of a search direction $\mathbf{s}^{(l)}$ at each current iterate $\mathbf{x}^{(l)}$ along which a new iterate $\mathbf{x}^{(l+1)}$ is appointed by a *line search* i.e. a one-dimensional optimization with α as independent variable.

$$\mathbf{x}^{(l+1)} = \mathbf{x}^{(l)} + \alpha\, \mathbf{s}^{(l)} \quad ; \quad \alpha > 0 \tag{2.28}$$

This new design point $\mathbf{x}^{(l+1)}$ is then investigated and a new search direction $\mathbf{s}^{(l+1)}$ is established. This iterative procedure is repeated until some stopping criterion is fulfilled (e.g. the change in the design variables becomes very small or the objective does not decrease in search direction). The diverse descent algorithms differ in the way the search direction $\mathbf{s}$ is established and in the technique used to specify the step size parameter α. This category of algorithms is in general very efficient if first, second, or higher order information is available for determination of the search direction.

◇ According to the second concept, algorithms sample a set of points simultaneously. Based on this set of sampling points either the best element is picked to define the optimum or approximation models (e.g. polynomial approximations) for the response values are built. These approximations are used as surrogate for the original functions to solve the optimization problem. Some algorithms of this class also allow for a sequential approach as well where further sets of sampling points are determined using information gained from each previous set until a stopping criterion is met. Using this second category of algorithms, a more global search is conducted – increasing chances to find the global minimum even for non-convex problems.

Unfortunately, the choice of algorithms is often limited for the designing engineer since commercially available program packages usually provide only a small selection of methods if there are any options at all. Additionally, the underlying analysis code (usually a finite element code) will restrict the choice dependent on the available sensitivities as indicated above. Often no more than zero-order information is available for the response values. Hence, gradients would have to be determined through finite differences which significantly increase computational effort (at least $n + 1$ analyses are needed to evaluate one gradient vector).

In this text, a classification of optimization algorithms based on two characteristics is introduced and depicted in the matrix of Table 2.1. On the one hand, the necessary order of information (zero-order, first-order or second-order) allows for a proper categorization of optimization algorithms depending on the code that is used to evaluate the system

Table 2.1: Classification of optimization algorithms.

	Solving unconstrained problems		Solving constrained problems	
	1D problems	*n*D problems	Primal methods	Transformation methods
zero-order	Interval search	Grid search	Grid search	Penalty methods
	Polynomial interpolation	Monte Carlo random search	Monte Carlo random search	Dual methods
		DiRect algorithm	Evolutionary strategy	
		GAUSS/SEIDEL	Genetic algorithm	
		POWELL's method, HOOKE-JEEVES' method	Complex method (BOX)	
		Simplex method (NELDER, MEAD)		
first-order	Polynomial interpolation	Conjugate gradient (FLETCHER, REEVES)	Generalized reduced gradients	LAGRANGE methods (SQP – quasi NEWTON)
	Bisection	Steepest descent	Feasible directions	Penalty methods
			SLP	Dual methods
second-order	NEWTON method	Conjugate gradient (HESTENES, STIEFEL)		LAGRANGE methods (SQP – full NEWTON)
		NEWTON method		Penalty methods
				Dual methods

characteristics. On the other hand, a distinction is drawn between solution techniques for constrained and for unconstrained problems. The algorithms used for unconstrained problems are again subdivided into a class especially suited for 1D problems (i.e. problems with only one unknown) and n-dimensional problems. Unconstrained optimization problems with only one design variable are rarely encountered in engineering practice. However, this special class of algorithms plays an important role in many solution techniques for multidimensional problems using a line search during optimization. The related methods will be particularized in the next section. Within the approaches used to solve constrained optimization tasks, *primal* and *transformation methods* are distinguished. Primal methods solve the original optimization problem with only the design variables as independent variables whereas transformation methods convert the original formulation into another type (usually an unconstrained formulation) which is easier to solve but also introduces additional independent variables to solve for. Details about the different transformations are given later in the respective sections in which the key features of some preferred algorithms presented in Table 2.1 are discussed.

As a consequence of the broad variety of algorithms presented in the literature, Table 2.1 can only present a selection of commonly applied optimization methods for engineering problems. In the remainder of this section a short discussion of some basic features is given. For an in-depth discussion of the algorithms addressed in this text and further numerical optimization techniques, the reader is referred to the cited literature.

2.3.1 Direct Search Methods

Direct search methods use only zero-order information about the governing equations to find the desired minimum. First, algorithms for 1D minimization will be presented followed by search methods that apply to multidimensional problems.

Interval search. One example for the class of direct search methods is the interval search. The basic idea is to gradually reduce the interval in which the minimum lies to a sufficiently low width. If a function $f(\alpha)$ has only one minimum in the interval under investigation (a *unimodal function*), interval search can be applied to reduce the possible range for the minimum without any requirements on continuity or differentiability of the function. If values for the objective function f have been computed at four different points α_1, α_2, α_3, and α_4 of the interval $[\alpha_1, \alpha_4]$, a subinterval can be determined that does not contain the minimum and hence will be left out for subsequent investigations. As a consequence, the interval containing the minimum is repeatedly scaled down by evaluating the function values at the boundaries of each interval.

A very efficient way to choose each interval size can be derived using the *golden section method* because each iteration to reduce the interval size requires only one additional function evaluation. To achieve this favorable behavior the individual subinterval ranges $\Delta_a = \alpha_{a+1} - \alpha_a$ with $a = 1, 2, 3$ must fulfill the condition

$$\frac{\Delta_1}{\Delta_2} = \frac{\Delta_3}{\Delta_2} = \gamma \quad \text{with} \quad \gamma = \frac{\sqrt{5}+1}{2} \approx 1.618\,. \tag{2.29}$$

For each iteration step, one subinterval of the previous segmentation can be "reused" and only one additional intermediate point α_x must be evaluated to regain three (smaller) subintervals. Using this scheme for the subdivision of the intervals, the rate of interval sizes in subsequent steps is $1/\gamma \approx 0.618$. Hence, the remaining range of uncertainty for the minimum after m iteration steps can be computed in advance to be $(1/\gamma)^m$ relative to the initial interval size.

Polynomial Interpolation. Another efficient technique for one-dimensional optimization is to approximate the true objective function $f(\alpha)$ by a polynomial $p(\alpha)$. The minimum of the approximation can be found analytically using the first and second derivative of the polynomial. The procedure begins with evaluating $f(\alpha)$ at several points. The information gained at these points (which can also include higher order information) is then used to fit the polynomial. The optimum of this polynomial, which is used as an estimate for the optimum of $f(\alpha)$, can be determined analytically.

To identify the optimum α^* of the commonly applied quadratic polynomial $p(\alpha)$

$$p(\alpha) = c_0 + c_1\,\alpha + c_2\,\alpha^2 \quad \text{with} \quad \frac{\partial p(\alpha)}{\partial \alpha} = c_1 + 2\,c_2\,\alpha \tag{2.30}$$

$$\left.\frac{\partial p(\alpha)}{\partial \alpha}\right|_{\alpha^*} = 0 \quad \Rightarrow \quad \alpha^* = -\frac{c_1}{2\,c_2}\,, \tag{2.31}$$

the parameters c_1 and c_2 must be determined. This can be realized with three responses of the original function f_1, f_2, and f_3 at α_1, α_2, and α_3, respectively

$$c_2 = \frac{\dfrac{f_3 - f_1}{\alpha_3 - \alpha_1} - \dfrac{f_2 - f_1}{\alpha_2 - \alpha_1}}{\alpha_3 - \alpha_2} \quad , \quad c_1 = \frac{f_2 - f_1}{\alpha_2 - \alpha_1} - c_2\,(\alpha_1 + \alpha_2) \tag{2.32}$$

or two response values f_1, f_2 and one gradient f_1' at α_1 and α_2, respectively

$$c_2 = \frac{\dfrac{f_2 - f_1}{\alpha_2 - \alpha_1} - f_1'}{\alpha_2 - \alpha_1} \quad , \quad c_1 = f_1' - 2\,c_2\,\alpha_1\,. \tag{2.33}$$

For the parameter c_0 no formulas are given because it does not influence the position of the optimum α^* as shown in Equation (2.31).

The polynomial interpolation method has the advantage of requiring only few function evaluations. The quality of the obtained estimate for the minimum, however, strongly depends on the accuracy of the approximation $p(\alpha)$ which can be quite poor especially for highly nonlinear functions $f(\alpha)$. Although the procedure is not restricted to 1D minimization, the number of function evaluations to determine the free parameters of multidimensional polynomials rapidly increases with the number of design variables. While a quadratic polynomial in 1D requires three response values to fit the free parameters, a fully quadratic polynomial in 3D already needs ten function (or gradient) evaluations. For this reason, multidimensional problems are usually solved by other approaches.

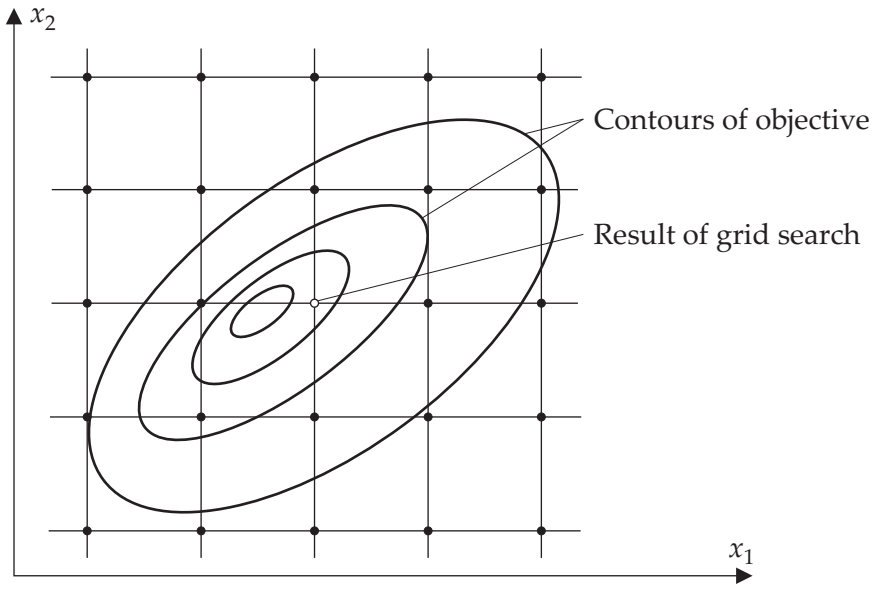

Figure 2.13: Grid search for an unconstrained 2D problem.

Grid search. This method is one of the simplest optimization schemes possible. The design space is examined through evaluations of the objective and constraints at equally spaced grid points. The point with the smallest sampled value for the objective that satisfies all constraints is accepted as the best solution (cf. Figure 2.13). This method is computationally very expensive and the effort required increases exponentially with the number of design variables. If the points are not positioned on a grid but randomly spread over the design space (*Monte Carlo random search*), the computational effort is decoupled from the number of design variables. Despite the costs for both methods, the location of the optimum will only roughly be assessed depending on the grid spacing or the number of Monte Carlo points, respectively. Since these optimization schemes are not bound to a local "valley", there is a chance to find the global minimum – but at a high price.

DiRect algorithm. The name of this method is a shortening of the phrase "dividing rectangles" and already suggests the underlying idea. Similar to the interval search in 1D, the DiRect algorithm of JONES et al. subdivides the n-dimensional design space into hyperrectangles of different sizes [JPS93]. One function evaluation is performed for each hyperrectangle at its center point. Then, the hyperrectangles are sequentially redivided according to the following scheme (cf. Figures 2.14 and 2.15) until the algorithm converges to a solution. In the figures, the current approximation for the minimum f_{min} after each iteration step is marked with a white circle.

1. To start the algorithm, the originally hyperrectangular design space $\mathcal{D}$ as defined in Equation (2.8) is normalized to form a unit hypersquare $\tilde{\mathcal{D}} = \{\tilde{\mathbf{x}} \in \mathbb{R}^n \mid 0 \leq \tilde{x}_i \leq 1 \; ; \; i = 1, \ldots, n\}$ with center point $\tilde{\mathbf{c}}$ as depicted in Figure 2.14.

   The algorithm works in this normalized space, referring to the original space only

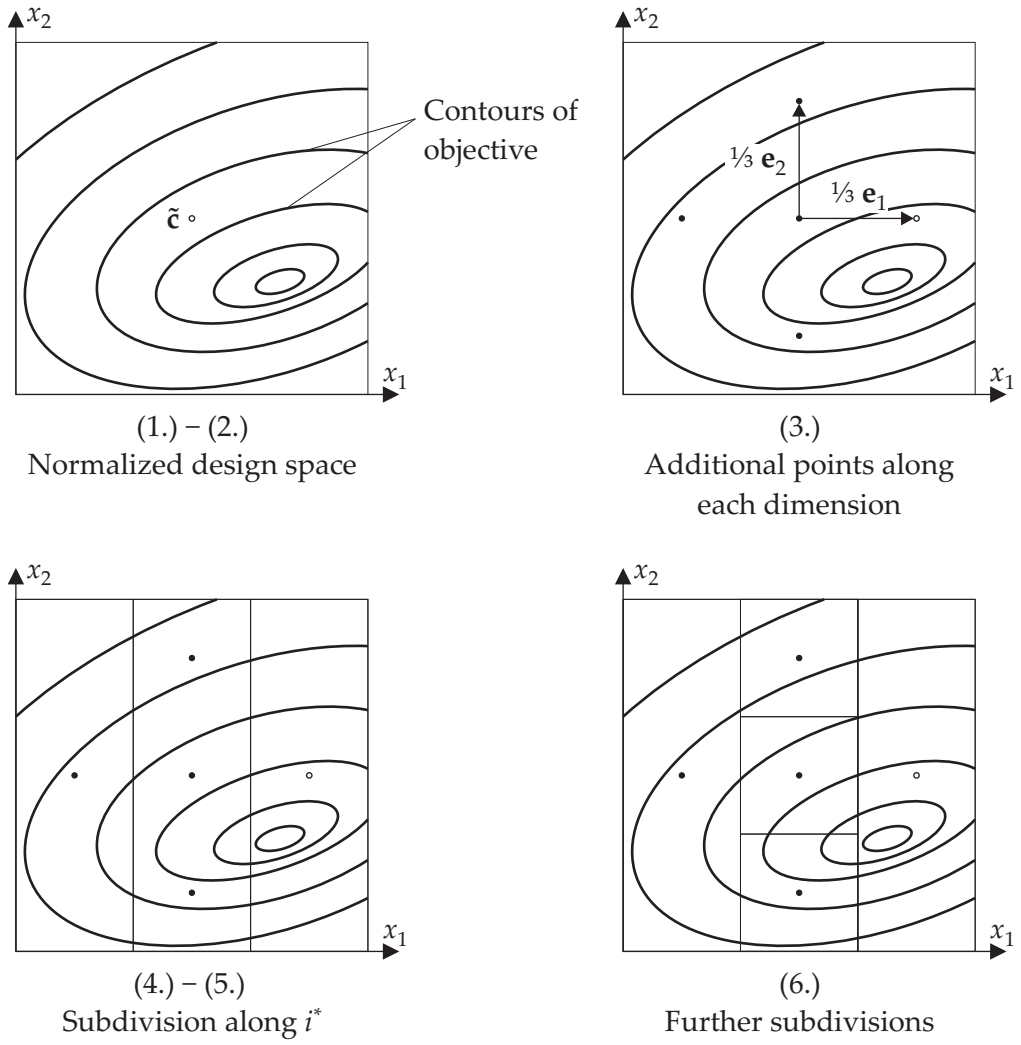

Figure 2.14: Initialization of the DiRect algorithm for a 2D problem.

when evaluating the objective function defined on $\mathcal{D}$. Thus, the function call $f(\mathbf{c})$ denotes the evaluation of $\mathbf{c} \in \mathcal{D}$ that corresponds to $\tilde{\mathbf{c}} \in \tilde{\mathcal{D}}$.

2. Evaluate the objective function at the center point and set current minimum to $f_{\min} = f(\mathbf{c})$.

3. Determine response values of the objective for all points defined by $\tilde{\mathbf{c}} \pm \frac{1}{3}\,\mathbf{e}_i$ where $\mathbf{e}_i$ are the n unit vectors of the normalized design space. As a result, two additional sampled points are obtained along each dimension i. Store the smallest sampled value as new current minimum $f_{\min}$.

4. Based on the smaller value of the two additional functional responses per dimension (Step 3), establish a ranking for the different dimensions, start with dimension i^* that contains the lowest sampled response $f_{\min}$.

5. According to this ranking, subdivide the hypersquare into smaller hyperrectangles starting in dimension i^*. Along this dimension, split the hypersquare into three

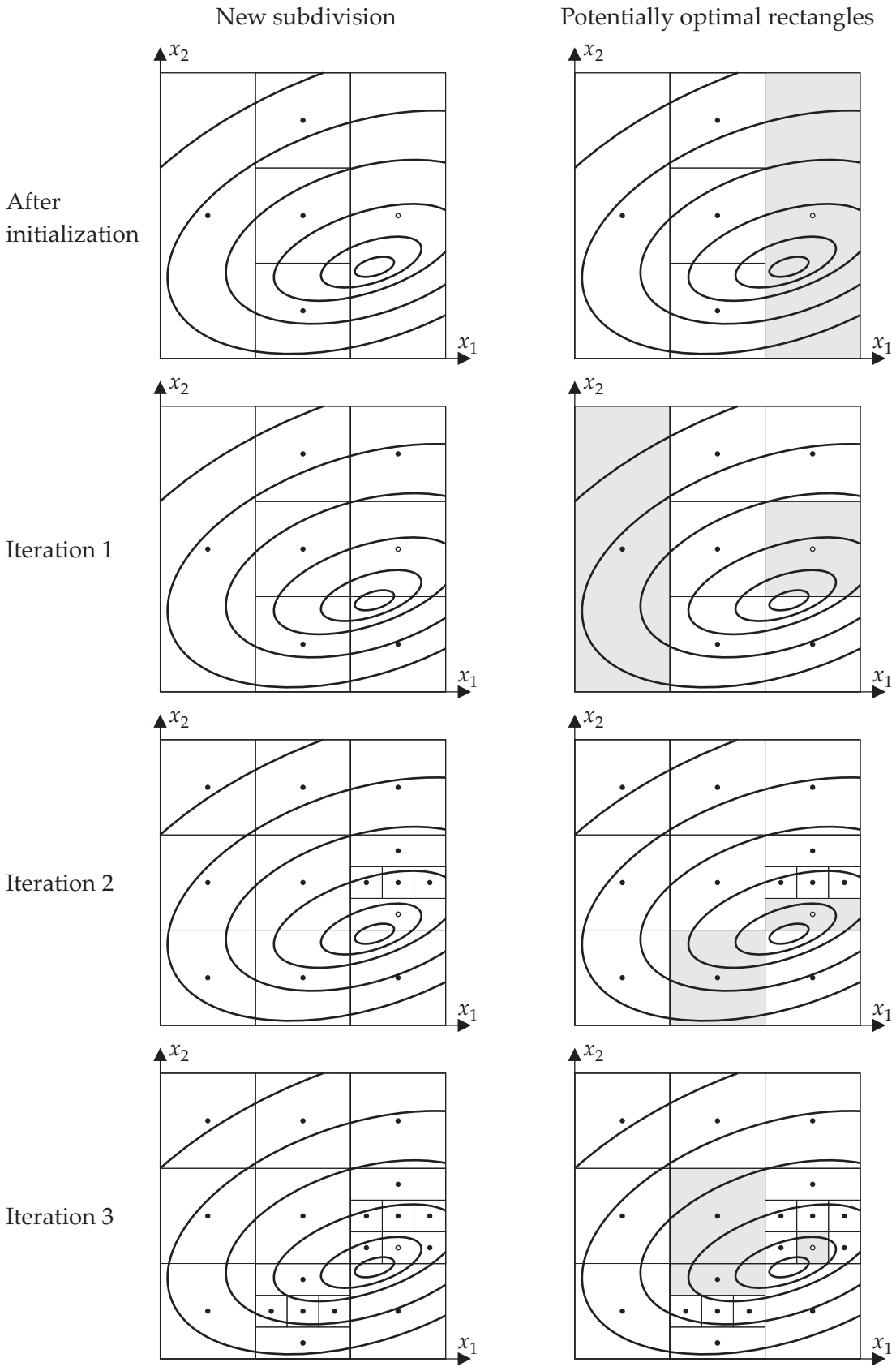

Figure 2.15: Iteration steps (6.) – (8.) of the DiRect algorithm for a 2D problem.

equally sized hyperrectangles such that $\tilde{\mathbf{c}} \pm \frac{1}{3}\,\mathbf{e}_{i^*}$ are the center points of the new hyperrectangles.

6. Continue to subdivide the central hyperrectangle, which still contains more than one point, along the second dimension of the ranking. Repeat this procedure until the center hyperrectangle has been divided along each dimension. Now, each hyperrectangle contains only one point (located at its center point). After this initial segmentation of the hypersquare, start the iteration.

7. For each iteration step, the DiRect algorithm will identify potentially optimal hyperrectangles for further subdivisions.

   A hyperrectangle is potentially optimal if there is no hyperrectangle of the same size or bigger with a smaller response value for its center point. According to [JPS93], the size of a hyperrectangle is measured by the distance of its center point to the vertices.

   Identify all potentially optimal hyperrectangles, and divide each of those into three equally sized hyperrectangles. The division is executed only along the longest dimension(s) of the hyperrectangle. This restriction ensures that the rectangles will shrink in every dimension. If the potentially optimal hyperrectangle is a hypersquare, then divisions must be performed along all sides, as in the initial step.

8. Evaluate the objective function at the center points of all new hyperrectangles and update $f_{\min}$.

9. If the stopping criteria are not met yet, begin the next iteration step with identification of potentially optimal hyperrectangles (Step 7).

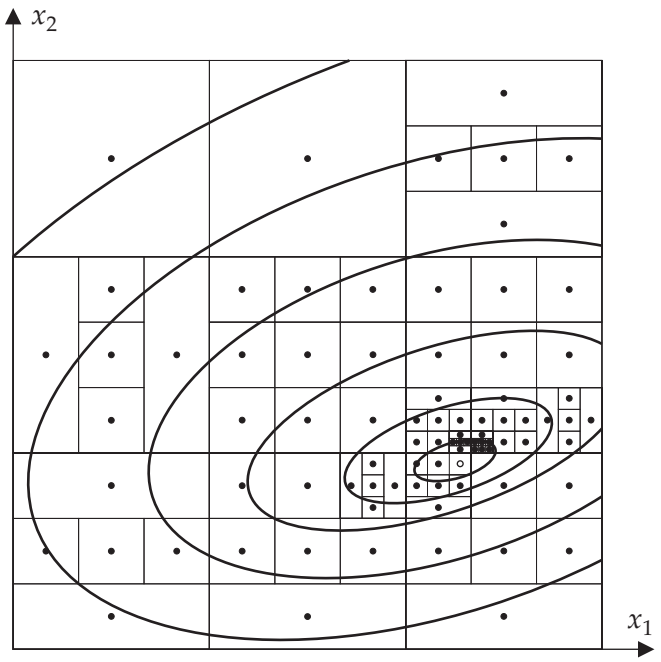

Figure 2.16: DiRect algorithm after eight iterations and 85 function evaluations.

Typical stopping criteria are a maximum number of iterations or function evaluations. To stop the iteration if no change is obtained in $f_{\min}$ or in the corresponding design variables from one iteration to the other, will in general not lead to the desired optimum as the DiRect algorithm might behave "idle" during several iterations before a new optimal point is detected.

Figure 2.16 shows the result after eight iterations of the example introduced in Figure 2.15. To find the approximation for the optimum (marked with a white circle), the objective function was evaluated 85 times.

The set of potentially optimal hyperrectangles always includes the largest hyperrectangle which will be split during the next iteration step. In case several hyperrectangles are concurrently the largest, one of these hyperrectangles belongs to the potentially optimal set. As a consequence, the DiRect algorithm converges to the global optimum at the expense of an exhaustive search requiring many function evaluations. It is suitable for problems with a highly nonlinear objective function for which zero order information is cheap to evaluate. Further details about the DiRect algorithm can be found in [Jon01].

Evolutionary strategies and genetic algorithms. These stochastic optimization methods imitate evolution in the biological sense and hence represent a numerical adoption of DARWIN's principle of "survival of the fittest". The optimal design evolves by means of sequential *selection*, *mutation*, and *recombination* starting with an initial *population* of design points that usually consists of randomly sampled *individuals* (cf. Monte Carlo random search). "Selection" means that from each population a subset of individuals is chosen as archetypes for the next generation. The terms "mutation" and "recombination" denote different methods to form offspring for a selection of individuals.

Mutation diversifies a parent design by changing an arbitrary entry of its numerical description. This means that a randomly selected design information is spoiled. One example for mutation, which is often applied to real-valued design vectors, is a random variation. Typically, a Gaussian normal distribution with mean zero and different standard deviations σ_i for each dimension of the design space is used.

$$x_i^{(l+1)} = x_i^{(l)} + N(0, \sigma_i) \quad ; \quad i = 1 \dots n \tag{2.34}$$

As a consequence of this formulation, small mutations are more likely to occur than greater changes.

For recombination, two selected parents $\mathbf{x}^{(l)}$ and $\mathbf{z}^{(l)}$ are both split at the same position j and reassembled cross-over to form two new individuals $\mathbf{x}^{(l+1)}$ and $\mathbf{z}^{(l+1)}$.

$$\mathbf{x}^{(l+1)} = \begin{bmatrix} x_1^{(l)} \\ \vdots \\ x_j^{(l)} \\ z_{j+1}^{(l)} \\ \vdots \\ z_n^{(l)} \end{bmatrix} \quad ; \quad \mathbf{z}^{(l+1)} = \begin{bmatrix} z_1^{(l)} \\ \vdots \\ z_j^{(l)} \\ x_{j+1}^{(l)} \\ \vdots \\ x_n^{(l)} \end{bmatrix} \tag{2.35}$$

The probability of "survival" of the newly generated individuals depends on their *fitness* which takes into account the objective function and constraints. Accordingly, the fittest are kept with high probability, the worst are rapidly discarded.

The basic difference between genetic algorithms and evolutionary strategies lies in the description of each individual, the so-called *gene*. For genetic algorithms, each design is coded in form of a binary string to allow "genetic" operators like mutation and recombination to apply to any part of the gene without any knowledge of its physical meaning. In contrast, evolutionary strategies constitute their genes as a vector of real-valued parameters which are altered primarily by mutation. This rather slightly perturbs the individual parameters of the genes in a useful way. Hence, evolutionary strategies are mostly applied to continuous problems while genetic algorithms are a preferred tool for discrete optimization.

Many different configurations exist for both methods [BS93, BFM96]. The underlying optimization scheme, however, is basically the same for all procedures:

1. Specify an initial population i.e. a set of n_p individuals $\mathbf{x}_p$ with $p = 1 \dots n_p$ in the design space.

2. Evaluate the objective function and constraints at all points $\mathbf{x}_p$ to assign their fitness value.

3. Select members of the parent population with adequate fitness as archetypes for a child population.

4. Create a child population $\mathbf{x}_c$ with $c = 1 \dots n_c$ by means of reproduction and mutation.

5. Evaluate the fitness for all points $\mathbf{x}_c$.

6. Check stopping criterion. If it is not met, proceed with Step 3 to set up a new generation.

To assess this class of algorithms the following observations can be made. They need only zero order information but require numerous function evaluations. They can easily handle nonlinear problems even with functions of discrete variables and tend to detect the global optimum after sufficient iterations. The problem is to specify a suitable stopping criterion since the optimization might be stalling for several iterations before further improvement is attained. Consequently, the only generally applicable stopping criterion is to limit the number of iterations or evaluations.

When applied to multicriteria problems, evolutionary strategies and genetic algorithms are capable of finding several points of the PARETO-optimal set during one optimization run [Deb01]. These special traits make this class particularly suited for applications with discrete design variables and for highly nonlinear problems. To assure that the computational effort remains within acceptable limits, response values have to be rather cheap to evaluate.

2.3.2 Gradient Methods

With the help of first order information for the objective and constraint functions, more efficient algorithms can usually be formulated to find the solution of the optimization problem. If gradients are readily available, this will in general reduce the number of function evaluations needed to solve the optimization task as already indicated for the polynomial interpolation approach. But even if the first order information must be determined via finite differences, gradient methods still perform better than direct search methods in some applications.

Steepest descent method. The most intuitive approach for descent methods is to use the direction of the steepest descent (i.e. the opposite direction of the gradient of the objective) to search for the optimum. Hence, the search direction $\mathbf{s}^{(l)}$ in Equation (2.28) for each iteration step l is calculated from

$$\mathbf{s}^{(l)} = -\nabla f\left(\mathbf{x}^{(l)}\right) . \tag{2.36}$$

The step size α is determined by a line search method. If the line search found the minimum in the search direction $\mathbf{s}^{(l)}$, the next search direction $\mathbf{s}^{(l+1)}$ will be orthogonal to $\mathbf{s}^{(l)}$. This feature leads to a poor convergence rate of the steepest descent method when the underlying problem is badly scaled (cf. Figure 2.17).

Conjugate gradient method. In order to overcome the aforementioned poor convergence behavior of the steepest descent method, FLETCHER and REEVES developed the conjugate gradient method [FR64] which requires only a minor change in the determination of the search direction. The initial search direction $\mathbf{s}^{(0)}$ is chosen to be the steepest descent direction of Equation (2.36). All subsequent search directions are determined by

$$\mathbf{s}^{(l+1)} = -\nabla f\left(\mathbf{x}^{(l)}\right) + \beta^{(l)}\,\mathbf{s}^{(l)} \quad \text{with} \quad \beta^{(l)} = \left(\frac{\left\| \nabla f\left(\mathbf{x}^{(l)}\right) \right\|}{\left\| \nabla f\left(\mathbf{x}^{(l-1)}\right) \right\|} \right)^2 , \tag{2.37}$$

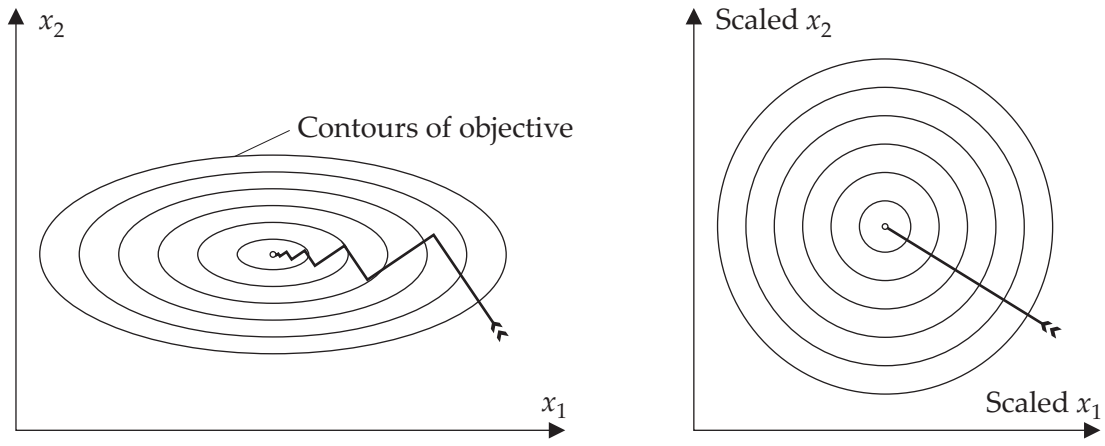

Figure 2.17: Influence of scaling on convergence behavior of the steepest descent method.

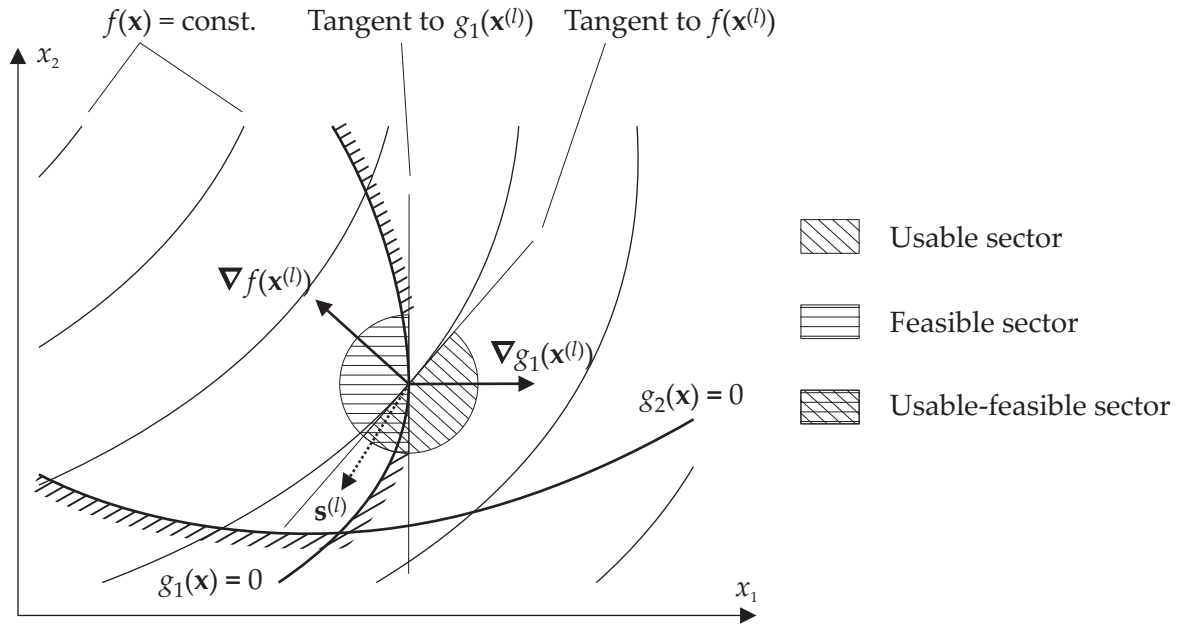

Figure 2.18: Feasible and usable search directions for a 2D problem with one active constraint.

where the direction of the previous step scaled by the factor $\beta^{(l)}$ is added to the current negative gradient. The scaling factor is defined using the L_2 norm of the gradients at the current design point and the gradient from the previous iteration step. By means of this enhancement, the conjugate gradient method finds the optimum of a quadratic function of n design variables in n or fewer iterations.

Method of feasible directions. To allow for solution of constrained problems, an enhancement of descent methods described earlier is presented next: the method of feasible directions. The initial design point is imposed to be a feasible design. As long as the iteration remains inside the feasible domain, the search direction is determined as for the unconstrained case. If during the iteration a constraint j becomes active, the next search direction $\mathbf{s}^{(l)}$ must satisfy two conditions:

1. The search direction must be feasible i.e. it must point into the feasible domain.

$$\nabla g_j\left(\mathbf{x}^{(l)}\right)^T \mathbf{s}^{(l)} \leq 0 \tag{2.38}$$

2. The search direction must be usable i.e. the objective must be reduced in this direction.

$$\nabla f\left(\mathbf{x}^{(l)}\right) \mathbf{s}^{(l)} < 0 \tag{2.39}$$

As a consequence, the new search direction must fall into the cone spanned by the tangents to the active constraint and the contour of the objective as illustrated in Figure 2.18. Search directions close to the constraint tangent are in general not advantageous because for

nonlinear constraints even small steps in this direction would result in infeasible designs. Consequently, a "push-off" factor $\theta > 0$ is introduced to enhance the search direction.

$$\nabla g_j\left(\mathbf{x}^{(l)}\right)^T \mathbf{s}^{(l)} + \theta \leq 0 \tag{2.40}$$

For further details on the choice of θ and its influence on convergence behavior of the method, it is referred to [VM73]. An extension of the method to cope with initially infeasible designs is described in [Van84].

2.3.3 NEWTON and Quasi NEWTON Methods

Newton methods use second order information to find the optimum. They are derived from the linearization of the stationary condition in Equation (2.17). The linearized stationary condition of the unconstrained case at some iterate $\mathbf{x}^{(l)}$ reads

$$\nabla f\left(\mathbf{x}^{(l)}\right) + \nabla^2 f\left(\mathbf{x}^{(l)}\right) \mathbf{d}^{(l)} = 0 \quad \text{with} \quad \mathbf{d}^{(l)} = \mathbf{x}^{(l+1)} - \mathbf{x}^{(l)} \,, \tag{2.41}$$

where $\mathbf{d}^{(l)}$ denotes the vector that describes the next iteration step. Solving Equation (2.41) for the next iteration point $\mathbf{x}^{(l+1)}$ yields

$$\mathbf{x}^{(l+1)} = \mathbf{x}^{(l)} - \left[\nabla^2 f\left(\mathbf{x}^{(l)}\right)\right]^{-1} \nabla f\left(\mathbf{x}^{(l)}\right) \,, \tag{2.42}$$

which represents the update formula for a classical NEWTON-RAPHSON method to find the roots of Equation (2.17). Even if the Hessian for the objective $\nabla^2 f\left(\mathbf{x}^{(l)}\right)$ can be determined, evaluating and inverting it for every iteration step is in general too expensive for practical applications. Hence, an approximation is used in most cases e.g. by updating the Hessian only every few iterations assuming that the second derivatives of the objective do not change as fast as the corresponding zero and first order information. Another possibility to reduce the computational effort in combination with NEWTON methods is the approximation of the Hessian by means of first order information only. Due to the different possibilities of approximating the Hessian or its inverse, this leads to a special class of algorithms, the so-called *quasi NEWTON methods*. Two prominent members of this class are the *DFP method* (named after DAVIDON [Dav59], FLETCHER, and POWELL [FP63]) and the *BFGS method* (named after BROYDEN [Bro70], FLETCHER [Fle70], GOLDFARB [Gol70], and SHANNO) [Sha70]. The DFP method starts with an initial guess $\mathbf{A}^0$ for the inverse of the Hessian (usually the identity matrix $\mathbf{A}^0 = \mathbf{I}$) which is modified after each iteration step using two correction matrices $\mathbf{B}^{(l)}$ and $\mathbf{C}^{(l)}$ such that

$$\mathbf{A}^{(l+1)} = \mathbf{A}^{(l)} + \mathbf{B}^{(l)} + \mathbf{C}^{(l)} \tag{2.43}$$

with

$$\mathbf{B}^{(l)} = \frac{\mathbf{d}^{(l)}\,\mathbf{d}^{(l)^T}}{\mathbf{d}^{(l)^T}\,\mathbf{y}^{(l)}} \quad ; \quad \mathbf{C}^{(l)} = -\frac{\mathbf{A}^{(l)}\,\mathbf{y}^{(l)}\,\mathbf{y}^{(l)^T}\mathbf{A}^{(l)}}{\mathbf{y}^{(l)^T}\mathbf{A}^{(l)}\,\mathbf{y}^{(l)}} \quad ; \quad \mathbf{y}^{(l)} = \nabla f(\mathbf{x}^{(l+1)}) - \nabla f\left(\mathbf{x}^{(l)}\right) \,. \tag{2.44}$$

The BFGS method updates an approximation $\hat{\mathbf{H}}^{(l)}$ for the true Hessian rather than its inverse at every iteration, also starting with an initial guess which, in absence of more information, is often estimated by the identity matrix $\hat{\mathbf{H}}^0 = \mathbf{I}$.

$$\hat{\mathbf{H}}^{(l+1)} = \hat{\mathbf{H}}^{(l)} + \mathbf{D}^{(l)} + \mathbf{E}^{(l)} \tag{2.45}$$

with

$$\mathbf{D}^{(l)} = \frac{\mathbf{y}^{(l)}\,\mathbf{y}^{(l)^T}}{\mathbf{y}^{(l)^T}\mathbf{d}^{(l)}} \quad ; \quad \mathbf{E}^{(l)} = -\frac{\hat{\mathbf{H}}^{(l)}\,\mathbf{d}^{(l)}\,\mathbf{d}^{(l)^T}\hat{\mathbf{H}}^{(l)}}{\mathbf{d}^{(l)^T}\hat{\mathbf{H}}^{(l)}\,\mathbf{d}^{(l)}} \tag{2.46}$$

For both methods the matrices $\mathbf{A}$ and $\hat{\mathbf{H}}$, respectively, must remain positive definite during the iteration process to allow for convergence of the algorithm. Since poor approximations for the Hessian might lead to non-convergent behavior of the algorithm, a line search should always be performed in combination with quasi-NEWTON methods. Derived from the update direction of NEWTON methods

$$\mathbf{s}^{(l)} = \left[\boldsymbol{\nabla}^2 f\left(\mathbf{x}^{(l)}\right)\right]^{-1} \boldsymbol{\nabla} f\left(\mathbf{x}^{(l)}\right) , \tag{2.47}$$

the search direction for a line search during a quasi-NEWTON iteration can be deduced:

$$\mathbf{s}^{(l)}_{\mathrm{DFP}} = \mathbf{A}^{(l)}\,\boldsymbol{\nabla} f\left(\mathbf{x}^{(l)}\right) \quad ; \quad \mathbf{s}^{(l)}_{\mathrm{BFGS}} = \left[\hat{\mathbf{H}}^{(l)}\right]^{-1} \boldsymbol{\nabla} f\left(\mathbf{x}^{(l)}\right) . \tag{2.48}$$

More details about quasi-NEWTON methods can be found e.g. in [Fle87, NW99, Van84].

2.3.4 LAGRANGE Methods

In order to solve constrained optimization problems, the aforementioned NEWTON methods can also be applied to the Lagrangian function instead of the objective function. The Lagrangian function transforms the original constrained problem into an unconstrained problem. The resulting unconstrained problem can then be solved using the techniques described in the previous sections. Assuming that the set of active inequality constraints has already been determined for the current iteration step, all active inequality constraints can be treated as additional equality constraints

$$g_j(\mathbf{x}) = 0 \quad ; \quad j = 1 \ldots n_a \, , \tag{2.49}$$

where n_a denotes the number of active inequality constraints at point $\mathbf{x}$. Constraints that are inactive at the current iterate are neglected for the next step. Using the information about the active set, the Lagrangian function reads

$$L(\mathbf{x}, \boldsymbol{\mu}) = f(\mathbf{x}) + \sum_{k=1}^{n_h+n_a} \mu_k\, h_k(\mathbf{x}) \tag{2.50}$$

The desired minimum must fulfill the stationary condition for the Lagrangian function i.e.

$$\frac{\partial L(\mathbf{x}, \boldsymbol{\mu})}{\partial \mathbf{x}} = 0 \tag{2.51}$$

$$\frac{\partial L(\mathbf{x}, \boldsymbol{\mu})}{\partial \boldsymbol{\mu}} = 0 \tag{2.52}$$

Again, applying the NEWTON-RAPHSON method to find the roots of these equations yields the linearized forms of Equations (2.51) and (2.52) which can be combined to

$$\begin{bmatrix} \boldsymbol{\nabla}^2 f(\mathbf{x}^{(l)}) + \sum_{k=1}^{n_h+n_a} \mu_k^{(l)}\, \boldsymbol{\nabla}^2 h_k(\mathbf{x}^{(l)}) & \boldsymbol{\nabla}\mathbf{h}(\mathbf{x}^{(l)})^T \\ \boldsymbol{\nabla}\mathbf{h}(\mathbf{x}^{(l)}) & 0 \end{bmatrix} \begin{bmatrix} \mathbf{d}^{(l)} \\ \boldsymbol{\delta}^{(l)} \end{bmatrix} = - \begin{bmatrix} \boldsymbol{\nabla} L(\mathbf{x}^{(l)}) \\ \mathbf{h}(\mathbf{x}^{(l)}) \end{bmatrix} \tag{2.53}$$

with

$$\mathbf{d}^{(l)} = \mathbf{x}^{(l+1)} - \mathbf{x}^{(l)} \quad ; \quad \boldsymbol{\delta}^{(l)} = \boldsymbol{\mu}^{(l+1)} - \boldsymbol{\mu}^{(l)} \tag{2.54}$$

In Equation (2.53), the different equality constraints $h_k(\mathbf{x})$ are assembled to the vector $\mathbf{h}(\mathbf{x})$ and $\boldsymbol{\nabla}\mathbf{h}(\mathbf{x}^{(l)})$ denotes the matrix that contains the partial derivatives of each $h_k(\mathbf{x})$ with respect to the design variables $\mathbf{x}$.

$$\boldsymbol{\nabla}\mathbf{h}(\mathbf{x}) = \begin{bmatrix} \dfrac{\partial h_1(\mathbf{x})}{\partial x_1} & \dfrac{\partial h_1(\mathbf{x})}{\partial x_2} & \cdots & \dfrac{\partial h_1(\mathbf{x})}{\partial x_n} \\ \dfrac{\partial h_2(\mathbf{x})}{\partial x_1} & \dfrac{\partial h_2(\mathbf{x})}{\partial x_2} & \cdots & \dfrac{\partial h_2(\mathbf{x})}{\partial x_n} \\ \vdots & \vdots & & \vdots \\ \dfrac{\partial h_{n_h+n_a}(\mathbf{x})}{\partial x_1} & \dfrac{\partial h_{n_h+n_a}(\mathbf{x})}{\partial x_2} & \cdots & \dfrac{\partial h_{n_h+n_a}(\mathbf{x})}{\partial x_n} \end{bmatrix} \tag{2.55}$$

Equations (2.53) and (2.54) characterize an iterative optimization algorithm called *sequential quadratic programming (SQP)* that will iteratively find a stationary point of $L(\mathbf{x}, \boldsymbol{\mu})$, the solution of the constrained optimization problem. After each step, the active set at $\mathbf{x}^{(l)}$ must be redetermined for the next iteration. To reduce the computational effort related to the evaluation of the second derivatives in Equation (2.53), the approximation techniques for the Hessian described in the preceding section can be applied in an analogous manner. The only difference is that a line search on the Lagrangian function will not help to stabilize because its stationary point is not a global minimum, but a saddle point (maximum with respect to $\boldsymbol{\mu}$ and minimum with respect to $\mathbf{x}$). Hence, other techniques must be applied to ensure convergence [NW99].

2.3.5 Penalty and Barrier Methods

Another possibility to solve a constrained optimization problem is to reformulate the objective such that the new objective worsens rapidly where constraints are violated. This can be accomplished by adding a *penalty* or *barrier function* to the original objective

$$\tilde{f}(\mathbf{x}, r) = f(\mathbf{x}) + P(\mathbf{x}, r) \,, \tag{2.56}$$

which is also a function of an additional scalar, called the *penalty parameter* r.

The basic difference between penalty and barrier methods is that the former penalize the objective only if a constraint is violated (i.e. $\tilde{f}(\mathbf{x}, r) = f(\mathbf{x})$ within the whole feasible domain) whereas the latter do not allow for infeasible designs by means of a singularity at the limit state $g_j(\mathbf{x}) = 0$. Consequently, barrier methods are applicable only to inequality constrained problems.

A popular example for a penalty function is the *quadratic loss function* defined as

$$P(\mathbf{x}, r) = r \left(\sum_{j=1}^{n_g} \left\langle g_j^+(\mathbf{x}) \right\rangle^2 + \sum_{k=1}^{n_h} \left(h_k(\mathbf{x}) \right)^2 \right) \tag{2.57}$$

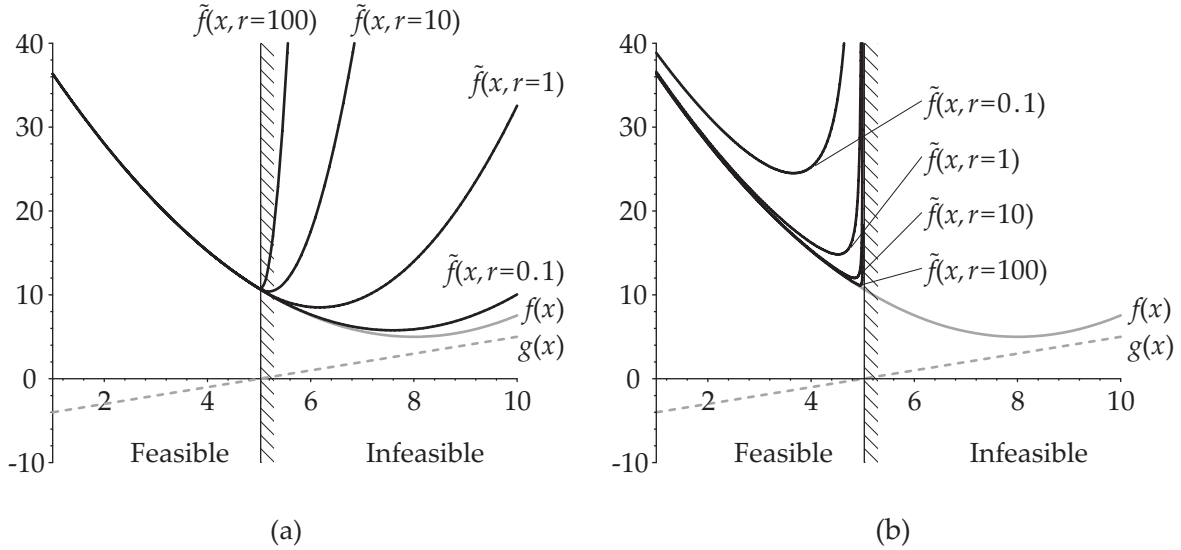

Figure 2.19: Influence of penalty parameter r on approximation quality of (a) penalty and (b) barrier methods.

with

$$g_j^+(\mathbf{x}) = \max\left\{0\,;\, g_j(\mathbf{x})\right\}\ . \tag{2.58}$$

Commonly used barrier functions are the *inverse barrier function*

$$P(\mathbf{x},r) = \frac{1}{r}\sum_{j=1}^{n_g}\left(-\frac{1}{g_j(\mathbf{x})}\right) \tag{2.59}$$

and the *logarithmic barrier function*

$$P(\mathbf{x},r) = -\frac{1}{r}\sum_{j=1}^{n_g}\log\left(-g_j(\mathbf{x})\right)\ . \tag{2.60}$$

Similar to the LAGRANGE formulation, Equation (2.56) transforms the original constrained problem into an unconstrained problem. In contrast to the LAGRANGE method, however, the solution of the penalty formulation in Equation (2.56) is in general not the same as for the original formulation. If the true optimum lies on the boundary of the feasible domain, penalty methods will typically yield "optimal" solutions that are located slightly in the infeasible domain while barrier methods will "back off" into the feasible domain and thus also miss the true optimum. The difference between the found optimum and the true minimum strongly depends on the penalty parameter r. As illustrated in Figure 2.19, the approximation ameliorates for increasing r. Extremely large values for r, however, lead to numerical problems during optimization. A detailed discussion of advantages and disadvantages of both penalty and barrier methods are discussed for instance in [Aro89, BSS93].

2.3.6 Approximation Concepts

Seizing the idea used for the method of polynomial interpolation, other approximations to the original objective function or constraints can be established to find the optimum [BH93]. Dependent on their region of validity, *local*, *mid-range*, and *global approximations* are distinguished. While local approximations are only valid in the immediate vicinity of the observed point, mid-range approximations try to predict the original functional response in a well-defined subregion of the design space. In contrast, global approximations aim at predicting the characteristics of the functions over the entire design space.

Local approximations are fit based on local information obtained at a single point such as the functional value, gradient and curvature, respectively. Hence, they are also called *single point approximations*. The more information is available (e.g. by means of sensitivity analysis [Kim90, SCS00]) the better the possible fit will be. Mid-range approximations rely on information gathered from multiple points. Both local and mid-range approximations form explicit subproblems (defined on a subregion of the design space) that can be solved analytically. Accordingly, an iterative solution technique is commonly applied where the solution of one subproblem provides the expansion point for the next approximation. This iteration is performed until convergence is achieved. Well-known local approximation methods are the *TAYLOR expansion* and the *method of moving asymptotes (MMA)* [Sva87, Ble93]. A prominent member of the mid-range approximation family is the so-called *multipoint approximation* [TFP93].

The simplest local approximation is the linear TAYLOR expansion about current design $\mathbf{x}'$. In this case, the TAYLOR series is truncated after the linear term. Applied to the objective function $f(\mathbf{x})$, the linear approximation reads

$$\hat{f}(\mathbf{x}) = f(\mathbf{x}') + \sum_{i=1}^{n} \left.\frac{\partial f(\mathbf{x})}{\partial x_i}\right|_{\mathbf{x}'} (x_i - x_i') \,. \tag{2.61}$$

If the quadratic terms of the TAYLOR series are included in the expansion, the approximation is improved at the price of requiring curvature information at $\mathbf{x}'$, either determined analytically or by means of finite differences. This additional computational effort makes the quadratic Taylor approximation inapplicable to most structural optimization problems.

$$\hat{f}(\mathbf{x}) = f(\mathbf{x}') + \sum_{i=1}^{n} \left.\frac{\partial f(\mathbf{x})}{\partial x_i}\right|_{\mathbf{x}'} (x_i - x_i') + \frac{1}{2} \sum_{i=1}^{n} \sum_{j=1}^{n} \left.\frac{\partial^2 f(\mathbf{x})}{\partial x_i \, \partial x_j}\right|_{\mathbf{x}'} (x_i - x_i')(x_j - x_j') \tag{2.62}$$

As a more general approach for local approximations, which also includes the linear TAYLOR expansion as a marginal case, the MMA is discussed in brief. A thorough discussion of MMA and enhanced approaches can be found in [Dao05]. The MMA approximation

$$\hat{f}(\mathbf{x}) = r' + \sum_{i=1}^{n} \left(\frac{p_i}{U_i - x_i} + \frac{q_i}{x_i - L_i} \right) \tag{2.63}$$

is convex within the range $[L_i, U_i]$ defined by an upper and lower asymptote L_i and U_i, respectively. The position of the asymptotes can be changed from one iteration step to the

other, a feature motivating the name of this method. The coefficients of Equation (2.63) are defined as

$$r' = f(\mathbf{x}') - \sum_{i=1}^{n} \left(\frac{p_i}{U_i - x_i'} + \frac{q_i}{x_i' - L_i} \right) \tag{2.64}$$

$$p_i = \begin{cases} (U_i - x_i')^2 \left. \dfrac{\partial f(\mathbf{x})}{\partial x_i} \right|_{\mathbf{x}'} & \text{, if } \left. \dfrac{\partial f(\mathbf{x})}{\partial x_i} \right|_{\mathbf{x}'} > 0 \\ 0 & \text{, otherwise} \end{cases} \tag{2.65}$$

$$q_i = \begin{cases} 0 & \text{, if } \left. \dfrac{\partial f(\mathbf{x})}{\partial x_i} \right|_{\mathbf{x}'} \geq 0 \\ -(x_i' - L_i)^2 \left. \dfrac{\partial f(\mathbf{x})}{\partial x_i} \right|_{\mathbf{x}'} & \text{, otherwise.} \end{cases} \tag{2.66}$$

Mid-range and global approximations are based on evaluations of the original functions at a set of points, called *sampling points*. To yield the best possible approximation, the sampling points are carefully chosen according to *design of experiments (DoE)* techniques [Mon01]. The resulting approximations can be used to efficiently study the behavior of the problem replacing expensive evaluations of the original functions. These approximations models (also termed *metamodels*) and related DoE methods are a key issue of the present work. Therefore, they are thoroughly discussed together with aspects related to their use in optimization algorithms in Chapters 4, 5, and 6.

Chapter 3

Stochastic Structural Optimization

The concepts introduced in Chapter 2 imply that all parameters involved are inherently deterministic i.e. known, determined, or produced to exactly the value used in the optimization process. Obviously, this approach is an idealization of real-life processes, products, and materials subject to environmental influences. The natural stochastic character is neglected in most engineering problems for the sake of an easy implementation, reduced numerical effort, or increased clarity in the problem formulation.

In the context of structural optimization, however, this approach may be very critical. During optimization, existing redundancies are typically downsized or even eliminated completely, since any redundancy is a potential source for further improvement. Finally, the optimized design has no redundancies left to cover inherent uncertainties. In particular constrained optima are highly sensitive even to small deviations in the governing parameters because any variation in direction of the active constraint leads to an infeasible layout. In contrast, a *robust design*, the goal of a stochastic optimization, is characterized by minimal impact of variations on the system response.

Bearing the formulation of a stochastic optimization problem in mind, some major statistical measures are introduced first. Subsequently, several formulations for stochastic optimization problems are discussed, followed by a presentation of solution techniques for this class of problems.

3.1 Basic Statistical Concepts

A design variable or system parameter that exhibits stochastic properties is called a *random variable*. Random variables are denoted by uppercase letters, such as X. All statistical quantities and functions that characterize a particular random variable are indexed with the respective uppercase letter. The corresponding lowercase letter x is used to denote a possible value of X. The set of possible outcomes for X are called the *sample space* Ω. Any subset of Ω is called an *event*.

The character of a random variable X is specified by its *probability distribution* $p_X(x)$. If X is a discrete variable, $p_X(x)$ is often called *probability function* or *probability mass function*. In case of a continuous X, it is termed *probability density function*. Examples for possible probability distributions are depicted in Figure 3.1.

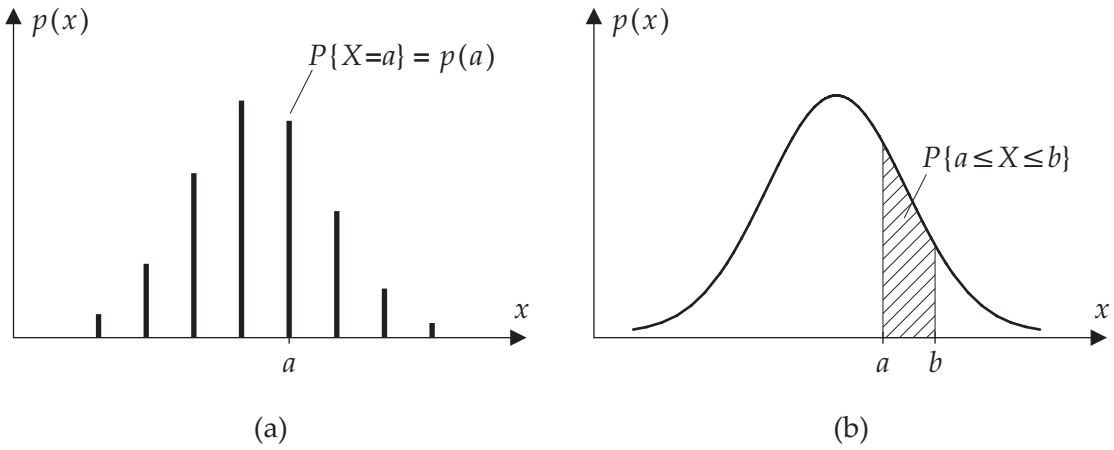

Figure 3.1: Probability distribution p_X for (a) discrete and (b) continuous random variable X.

The probability distribution quantifies the *probability* P of a specific event to occur. It is noteworthy that in the discrete case the value $p_X(a)$ represents the probability of the event $X = a$ whereas for continuous variables the integral over a range of X provides a measure for probability. Consequently, for continuous X, the probability of occurrence of one distinct $X = a$ is zero. Probability distributions must have the following properties:

◇ Discrete x:

$$0 \leq p_X(x_i) \leq 1 \qquad \forall \quad x_i \in \Omega \tag{3.1}$$

$$P\{X = x_i\} = p_X(x_i) \qquad \forall \quad x_i \in \Omega \tag{3.2}$$

$$\sum_i p_X(x_i) = 1 \tag{3.3}$$

◇ Continuous x:

$$p_X(x) \geq 0 \tag{3.4}$$

$$P\{a \leq X \leq b\} = \int_a^b p_X(x)\, dx \tag{3.5}$$

$$\int_\Omega p_X(x)\, dx = 1\,. \tag{3.6}$$

For the purpose of clarity, only the case of continuous random variables is further elaborated, a detailed discussion on discrete random variables can be found e.g. in [MR03].

A fundamental function in statistics is the *cumulative distribution function*

$$C(x) = P\{X \leq x\} = \int_{-\infty}^{x} p_X(u)\, du\,, \tag{3.7}$$

which quantifies the probability of the event that a random realization of X is smaller than the value x. Using the inverse of the cumulative distribution function, *quantiles* of X can be specified i.e. values x_q for which the probability of X being smaller than x_q is equal to a preset probability q

$$x_q = C^{-1}(q)\,. \tag{3.8}$$

Two important statistical measures are *mean* μ and *variance* σ^2, respectively. The mean of a distribution is also termed *expected value* and is a measure of its *location* (or *central tendency*) while the variance is a measure of *dispersion* of a probability distribution.

$$E(X) = \mu_X = \int_\Omega x\, p_X(x)\, dx \tag{3.9}$$

$$V(X) = \sigma_X^2 = \int_\Omega (x-\mu_X)^2\, p_X(x)\, dx = \int_\Omega x^2\, p_X(x)\, dx - \mu_X^2 \tag{3.10}$$

For engineering problems, the positive square root of the variance, called *standard deviation* σ, is often the preferred measure for variability because it has the same dimension as the corresponding random variable X. Additional measures of location and dispersion are discussed in standard literature on statistics, for instance [Ros87, MR03, Sac04].

Only few probability distributions are needed to qualify almost any random variable used in engineering problems. One of the most important distributions is the *normal* (or *Gaussian*) *distribution*

$$p_X(x) = \frac{1}{\sigma_X\sqrt{2\pi}}\, \mathrm{e}^{-\frac{(x-\mu_X)^2}{2\,\sigma_X^2}} \tag{3.11}$$

which describes the statistical behavior of many natural processes. A normal distribution with mean μ and variance σ^2 is commonly abbreviated by $N(\mu, \sigma^2)$. Accordingly, the notation $X \sim N(0,1)$ describes a random variable X that is normally distributed with $\mu_X = 0$ and $\sigma_X^2 = 1$.

The *uniform distribution*

$$p_X(x) = \begin{cases} \dfrac{1}{(b-a)} & , \quad a \le x \le b \\ 0 & , \quad x < a \ \vee \ x > b \end{cases} \tag{3.12}$$

is used to qualify random variables with equally likely occurrence of every $x \in \Omega$ with $\Omega = [a,b]$. A uniform distribution with lower bound a and upper bound b is commonly abbreviated by $U(a,b)$. Its mean and variance are computed according to Equations (3.9) and (3.10) resulting in

$$\mu_X = \frac{a+b}{2} \tag{3.13}$$

$$\sigma_X^2 = \frac{(b-a)^2}{12}\,. \tag{3.14}$$

Other important distributions are *WEIBULL*, *POISSON*, *exponential*, or *lognormal distributions* which can be helpful for many structural problems e.g. characterization of loads, stresses, dimensions, and material parameters [TCB82, Vie94, Rei97]. Details on these distributions can be found in statistical reference books e.g. [Ros87, MR03, Sac04].

In many engineering problems, several random variables occur simultaneously. For the sake of a clear notation, they are commonly assembled into a *random vector* $\mathbf{X}$. Analogously, a vector of mean values $\boldsymbol{\mu}$ for all components of $\mathbf{X}$ can be established:

$$\boldsymbol{\mu}_\mathbf{X} = E(\mathbf{X}) = [E(X_1), E(X_2), \ldots, E(X_n)]^T = [\mu_{X_1}, \mu_{X_2}, \ldots, \mu_{X_n}]^T\,. \tag{3.15}$$

The counterpart of the variance for the multidimensional case is the *covariance matrix* which is defined as

$$\mathbf{C} = \mathrm{Cov}(\mathbf{X}, \mathbf{X}) = E\Big((\mathbf{X} - \boldsymbol{\mu}_{\mathbf{X}}) (\mathbf{X} - \boldsymbol{\mu}_{\mathbf{X}})^T \Big) \ . \tag{3.16}$$

If all n random variables are mutually independent, the n-dimensional *joint probability function* $p_{\mathbf{X}}(\mathbf{x})$ is characterized by the product of the individual probability density functions $p_{X_i}(x_i)$

$$p_{\mathbf{X}}(\mathbf{x}) = \prod_{i=1}^{n} p_{X_i}(x_i) \ . \tag{3.17}$$

For correlated random variables with arbitrary probability distribution, a joint probability density function can be established by means of transformations which are given for instance in [BM04, Vie94]. Because the random variables usually encountered in structural analysis (e.g. dimensions, loads and material parameters) are mutually independent in many cases, a thorough discussion of possible transformations is omitted here.

3.2 Formulation of the Stochastic Optimization Problem

Random variables in optimization problems can either occur as system parameters Z or as part of the design variables X. Examples for random system parameters are variable loads (as for example wind loads) or material parameters. Typical design variables with stochastic properties are dimensions of structural members or material strength. These design variables can be altered during the optimization process but only up to a certain precision with corresponding tolerances or probability distributions. In case of steel, concrete, or timber, the engineer can usually choose a suitable strength class for the design of a structure. The strength class is identified by a nominal value (e.g. 5% quantile) for the underlying distribution. For the solution of stochastic optimization problems such random design variables are split into two parts: the nominal value x which is considered as a deterministic design variable and a residual random part Z which is treated as a random system parameter with corresponding probability distribution shifted by the nominal value x.

$$X = x + Z \tag{3.18}$$

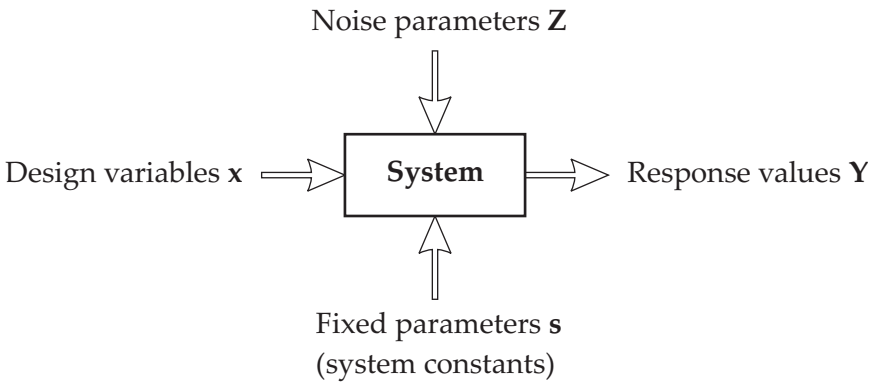

Figure 3.2: Scheme of a typical system including random variables.

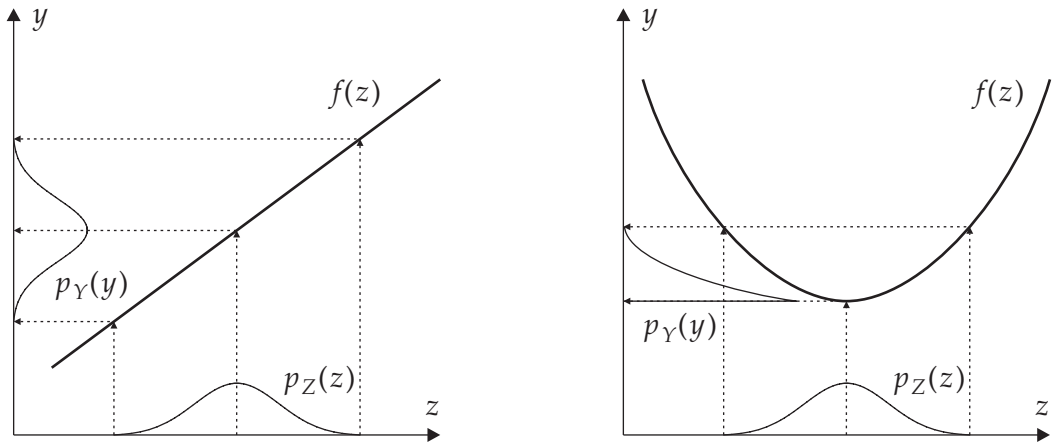

Figure 3.3: Influence of a random variable Z with probability distribution $p_Z(z)$ on the distribution $p_Y(y)$ of a response value Y.

After this decomposition, the system under consideration can be depicted schematically as in Figure 3.2. The design variables $\mathbf{x}$ are exclusively deterministic variables, and all random variables (commonly referred to as *noise parameters* or simply *noise*) are combined to a random vector $\mathbf{Z}$. The system constants $\mathbf{s}$ noted in the scheme represent all deterministic parameters that influence the system but are beyond control of the designer.

In optimization problems where noise parameters are present in the formulation of objective or constraints, Equations (2.6a-d) cannot be applied because the response values for f, g_j, and h_k are not deterministic values but also random values Y with corresponding probability distributions $p_Y(y)$, as illustrated in Figure 3.3. The figure depicts the case of a problem with one noise variable Z with the probability density function $p_Z(z)$. The distribution $p_Y(y)$ of the random response value Y is obtained by mapping Z onto the response by means of the corresponding governing equation. In general, the probability distribution of the response also depends on the settings of the design variables $\mathbf{x}$. In the case of Figure 3.3, the governing equation is $f(z)$. In a general optimization problem, objective f, and constraint functions g_j, and h_k, respectively, map the random input variables onto random response values. The shape of the resulting distribution density function $p_Y(y)$ will strongly depend on the form of the governing equation.

In order to solve the stochastic optimization problem with its random response values, a substitute optimization problem must be established in which all response values are deterministic. This is usually done by means of descriptive statistics, which extracts deterministic quantities from random response values. Many different possibilities exist to transform the original problem with stochastic response values into an optimization problem with deterministic output. Due to their different role in the optimization process, the stochastic objective function, equality, and inequality constraints are typically replaced by particular substitute formulations. In the present work, the discussion of possible approaches will be restricted to commonly used and reasonable formulations.

3.2.1 Equality Constraints Dependent on Random Variables

As soon as random variables influence the response values for equality constraints $h_k(\mathbf{x}, \mathbf{Z})$, the equality $h_k = 0$ cannot be fulfilled for all $\mathbf{z} \in \mathbf{\Omega}$. On this account, equality constraints should be avoided in the configuration of optimization problems with random variables. This can be accomplished by substituting the equality requirement into the formulation of objective and inequality constraints. This approach is proposed for all constitutive equality constraints such as the equilibrium condition in structural analyses [Das00]. If equality constraints depending on random variables cannot be evaded in the problem formulation, they are in general only fulfilled in a mean sense by substituting Equation (2.6c) by

$$\bar{h}_k(\mathbf{x}) = E\big(h_k(\mathbf{x}, \mathbf{Z})\big) = 0\,. \tag{3.19}$$

As another apparent alternative, the expected values for the random variables $\mathbf{Z}$ can be used to evaluate the equality constraints

$$h_k(\mathbf{x}, \bar{\mathbf{Z}}) = h_k\big(\mathbf{x}, E(\mathbf{Z})\big) = 0\,. \tag{3.20}$$

In either case, however, the equality will be violated for most events $\mathbf{z} \in \mathbf{\Omega}$, an inherent and unavoidable fact related to equality constraints that depend on random variables.

3.2.2 Inequality Constraints Dependent on Random Variables

In stochastic optimization, inequality constraints can be met with 100% probability i.e.

$$P\left\{g_j(\mathbf{x}, \mathbf{Z}) \leq 0\right\} = 1 \qquad \forall \quad \mathbf{z} \in \mathbf{\Omega} \quad ; \quad j = 1, \ldots, n_g \tag{3.21}$$

only in some special cases, for instance if the distributions of all random variables are bounded. In this case, the feasible design must back off the active constraints by a certain tolerance such that for all possible events $\mathbf{z} \in \mathbf{\Omega}$ the design $\mathbf{x}$ is always feasible. Consequently, the *worst case* of all $\mathbf{z} \in \mathbf{\Omega}$ with respect to the constraint functions defines the feasible domain.

$$g_j(\mathbf{x}, \mathbf{Z}) \leq 0 \qquad \forall \quad \mathbf{z} \in \mathbf{\Omega} \quad ; \quad j = 1, \ldots, n_g\,. \tag{3.22}$$

For a worst-case design, the probability distribution of the random variables within the bounds is of no importance, only the tolerance range influences the solution of the optimization problem. Hence, this formulation is often used if only vague (or even no) information on the probability distributions involved can be obtained and only tolerance ranges are dependably available.

In most engineering applications, there is no design $\mathbf{x} \in \mathbb{R}^n$ which meets all constraints with 100% probability. Thus, each design $\mathbf{x}$ will have a finite *probability of failure* P_F, which is defined by the probability of violating the constraints.

$$P_F = P\left\{g_j(\mathbf{x}, \mathbf{Z}) > 0\right\} \qquad \forall \quad \mathbf{z} \in \mathbf{\Omega} \quad ; \quad j = 1, \ldots, n_g \tag{3.23}$$

Accordingly, the probability of failure can be computed by the integral of the (joint) probability density function over the infeasible domain $\mathcal{U}$, as illustrated in Figure 3.4.

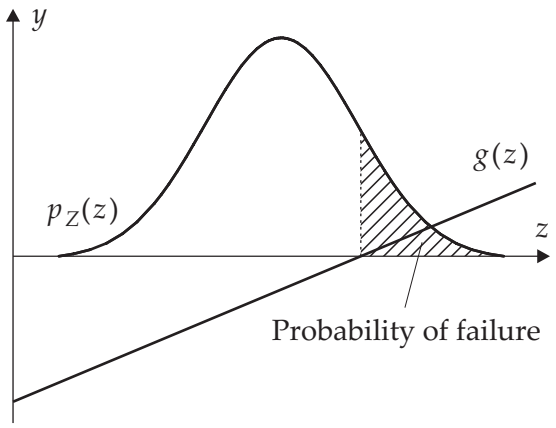

Figure 3.4: Probability of failure as integral of the probability density function over the infeasible domain for a 1D problem with one constraint.

$$P\left\{g_j(\mathbf{x},\mathbf{Z})>0\right\}=\int\limits_{\mathcal{U}} p_{\mathbf{Z}}(\mathbf{z})\,d\mathbf{z} \quad ; \quad j=1,\ldots,n_g \tag{3.24}$$

with

$$\mathcal{U}=\{\mathbf{z}\in\mathbf{\Omega}\mid g_j(\mathbf{x},\mathbf{Z})>0\} \tag{3.25}$$

The probability of failure can be used to reformulate the inequality constraints in Equation (2.6b) as

$$P\left\{g_j(\mathbf{x},\mathbf{Z})>0\right\}-P_{\max}\leq 0 \qquad \forall \quad \mathbf{z}\in\mathbf{\Omega} \quad ; \quad j=1,\ldots,n_g \tag{3.26}$$

using an additional optimization parameter $P_{\max}$, the maximum allowable probability of failure. The complement of the probability of failure is the *probability of safety* (also called *reliability*)

$$P_S=P\left\{g_j(\mathbf{x},\mathbf{Z})\leq 0\right\}=1-P_F \qquad \forall \quad \mathbf{z}\in\mathbf{\Omega} \quad ; \quad j=1,\ldots,n_g\,. \tag{3.27}$$

Derived from the level of reliability that is predefined by the designer, this formulation of the stochastic optimization problem is commonly termed *reliability-based design optimization (RBDO)*.

A more general approach to handle constraints subject to noise assigns an individual *cost function* $\gamma(y)$ to the possible violation of each constraint. Hence, the cost function $\gamma(y)$ assigns absolute costs to each possible state of the constraint $y=g(\mathbf{x},\mathbf{z})$. In view of the fact that an increasing violation of the constraint should be related to equal or higher costs, these cost functions should be monotonically non-decreasing i.e. $\gamma(a)\leq\gamma(b)$ for $a<b$. The expected cost for constraint violation can be restricted to a maximum allowable cost Γ by transforming the condition in Equation (2.6b) into

$$E\left(\gamma_j\left(g_j(\mathbf{x},\mathbf{Z})\right)\right)-\Gamma_j\leq 0 \quad \text{for each} \quad j=1,\ldots,n_g\,. \tag{3.28}$$

If the *HEAVISIDE function* (depicted in Figure 3.5 and sometimes also referred to as *saltus function*)

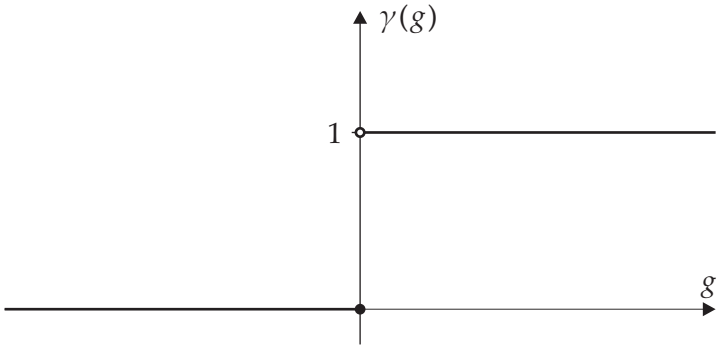

Figure 3.5: HEAVISIDE function.

$$\gamma(g) = \begin{cases} 0 & , \quad g \leq 0 \\ 1 & , \quad g > 0 \end{cases} \tag{3.29}$$

is used to represent the costs of each constraint violation, Equation (3.28) turns out to be equivalent to Equation (3.26).

$$E\left(\gamma\left(g_j(\mathbf{x},\mathbf{Z})\right)\right) = \int_{\mathbf{\Omega}} \gamma\left(g_j(\mathbf{x},\mathbf{z})\right)\, p_{\mathbf{Z}}(\mathbf{z})\, d\mathbf{z} = \int_{\mathcal{U}} p_{\mathbf{Z}}(\mathbf{z})\, d\mathbf{z} = P\left(g_j(\mathbf{x},\mathbf{Z}) > 0\right) \tag{3.30}$$

Each of the proposed approaches to handle inequality constraints in the stochastic optimization problem defines a new feasible domain $\mathcal{C}$ by means of Equations (3.22), (3.26), or (3.28), respectively.

3.2.3 Objective Function Dependent on Random Variables

Due to the randomness in $\mathbf{Z}$, the objective function $f(\mathbf{x},\mathbf{Z})$ in Equation (2.6a) must also be replaced by a deterministic substitute function $\rho(\mathbf{x})$ that provides some representative value for the random variable $Y = f(\mathbf{x},\mathbf{Z})$ to find a minimum. In stochastic optimization problems, a design $\mathbf{x}^*$ is considered as optimal if it fulfills the relationship

$$f(\mathbf{x}^*,\mathbf{Z}) \leq f(\mathbf{x},\mathbf{Z}) \qquad \forall\ \mathbf{x} \in \mathcal{C} \ \wedge\ \mathbf{z} \in \mathbf{\Omega} \tag{3.31}$$

i.e. if for this design the noise has no deteriorative (increasing) effect on the objective function and if there is no other design that results in a lower objective for any realization of $\mathbf{z} \in \mathbf{\Omega}$. A design $\mathbf{x}^*$ that fulfills the relation in Equation (3.31) is called *optimal robust design*. Figure 3.6 depicts a function $f(x,Z)$ where the range of possible variations Z around the design x^* has no influence on the response $y^* = f(x^*,Z)$. Under each circumstance $z \in \Omega$, the value for the objective function is always minimal. Accordingly, x^* is an optimal robust design.

In the context of stochastic optimization, the term *robustness* has a distinctive definition: *A system is called robust if the effect of a noisy input on the system response is minimal.* This notion is illustrated in Figure 3.7 where the objective function f is dependent on one random

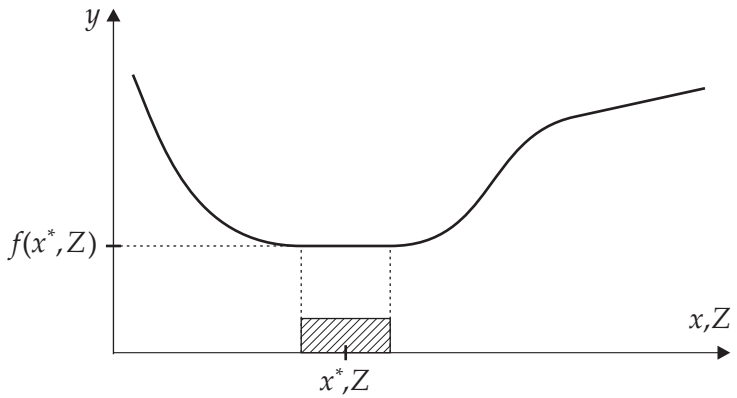

Figure 3.6: Optimal robust design x^*.

design variable X. This design variable is separable in a deterministic part x (the mean of X) and random variable Z with a normal distribution $p_Z(z)$ such that $X = x + Z$. The mean of Z is fixed to zero and the variance σ^2 is constant i.e. at every setting x, the probability distribution has the same spread. For each design x, the distribution of the noise $p_Z(z)$ is mapped onto the response by the functional relationship $Y = f(X) = f(x + Z)$ resulting in a distribution $p_Y(y)$ for the (random) response Y. In general, this distribution changes in position and shape dependent on the setting of the design variable. Hence, designs can be identified that result in a narrow distribution, others yield a larger variation in the response. Although design x_1 yields a lower value for the objective in the deterministic case, design x_2 is more robust in presence of noise because the variation of the resulting distribution $p_Y(y)$ is smaller. Thus, large deviations from the deterministic (or nominal) case are less likely to occur.

For most engineering problems, there are no optimal robust designs $\mathbf{x}^* \in \mathcal{C}$ which minimize $f(\mathbf{x}, \mathbf{Z})$ for each possible realization of $\mathbf{z} \in \mathbf{\Omega}$ (as for instance in the problem depicted in Figure 3.7). To identify the best possible approximation is the central problem in statistical decision theory [Fer67, Ber85, Lau05] which provides some effective substitute formulations. Based on the information available for the random variables, two different types of decision-theoretic approaches are distinguished [JZ72]:

Decisions under risk are made when probability densities for the random input variables $\mathbf{Z}$ are available, and hence, probability distributions $p_Y(y)$ for the response values can be obtained.

Decisions under uncertainty subsume cases where only the possible range of each noise variable is known. About the associated probability density, however, no information is readily available. As a result, the set of possible output realizations can be determined but no distribution density can be assigned.

Each substitute formulation gains a scalar value from the originally random output Y of the objective providing a deterministic measure to assess the merit of each design during optimization. The proper choice for this so-called *robustness criterion* ρ is strongly problem

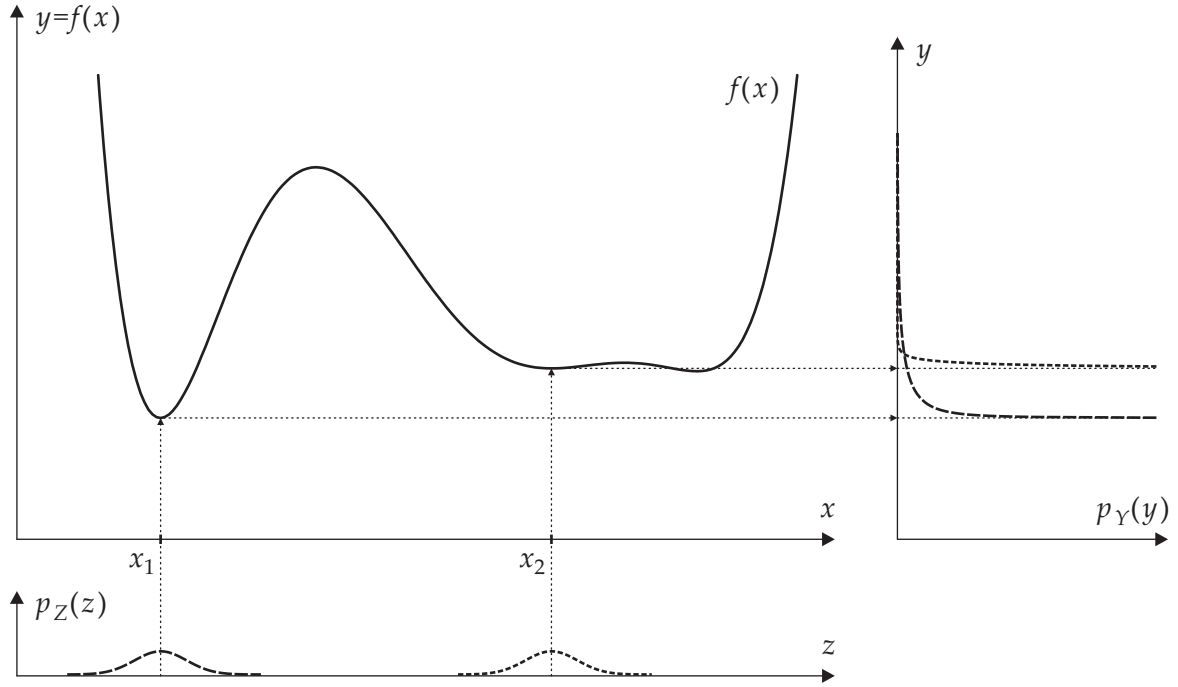

Figure 3.7: Robust vs. non-robust settings for a 1D problem with one random design variable X.

dependent and essentially an engineering decision. It should be noted that all formulations represent an approximation to the desired optimal robust case, and hence, imply some kind of compromise loosening the condition in Equation (3.31).

Example 2. To illustrate the different approaches and to facilitate a direct comparison, this example is used repeatedly for each robustness criterion. The objective function (see Figure 3.8)

$$f(x,z) = (2-x)\,(0.1-z-0.1\,x)+0.3$$

for this example depends on one (deterministic) design variable x and one noise variable Z. □

The discussion of commonly applied robustness criteria is started with *decisions under uncertainty*:

Minimax principle. For some optimization tasks, a *worst case scenario* could be of interest, which requires the random response to be bounded on $\boldsymbol{\Omega}$. In this case, the deterministic substitute formulation $\rho(\mathbf{x})$ for the stochastic objective function $f(\mathbf{x},\mathbf{Z})$ reads

$$\rho(\mathbf{x}) = \sup_{\mathbf{z}\in\boldsymbol{\Omega}} f(\mathbf{x},\mathbf{z})\,. \tag{3.32}$$

This formulation is also called *minimax principle* [vN28, Wal50]. For each setting of design variables $\mathbf{x}$, the effects of all possible events $\mathbf{z} \in \boldsymbol{\Omega}$ are scanned, and the outcome for the worst case is taken as decisive gage to assess the robustness of the current design. This

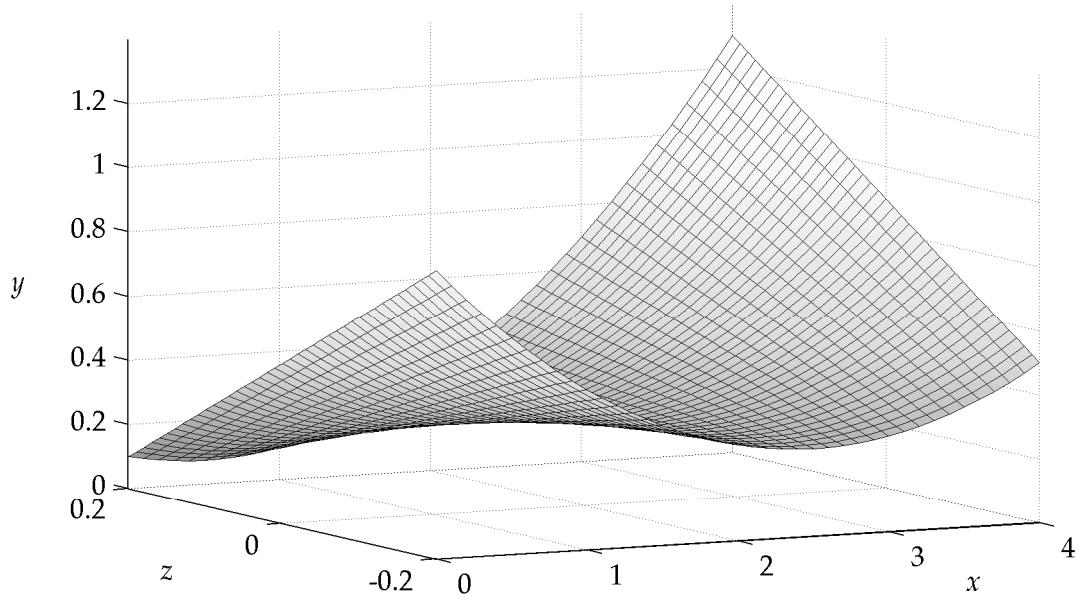

Figure 3.8: Objective function for Example 2 with one design variable x and one noise variable Z.

approach is also referred to as *maximin principle* for cases where the optimization problem is formulated as maximization task.

The minimax principle ignores the possible range in the output. Instead, it identifies the upper limit of the resulting range, and hence, it caps the deteriorative effects of the noise parameters. This robustness criterion leads to very conservative designs as it is based upon an extremely pessimistic attitude.

Example 2 [continued]. For the "decision under uncertainty" criteria, assume that the distribution of noise variable Z is unknown and only prescribed tolerances ± 0.2 delimit Z. Based on this assumption, the minimax principle in Equation (3.32) is applied to the above introduced example.

Figure 3.9 depicts a projection of the objective function onto the x-y plane. Hence, it shows the possible range of output realizations for each x and $z \in [-0.2, 0.2]$. The minimax principle allocates the upper limit of this range for each x as robustness criterion yielding the deterministic substitute function $\rho(x)$ depicted in Figure 3.10. The minimum of $\rho(x)$, which represents the optimal setting for the design variable resulting from the minimax principle, is located at $x^* = 2.0$. □

Minimax regret criterion. The *minimax regret criterion* focuses on minimizing the maximum *regret* that may result from making non-optimal decisions i.e. choosing a non-optimal design $\mathbf{x}$. SAVAGE [Sav51] and NIEHANS [Nie48] define regret as *opportunity loss* to the decision maker if design $\mathbf{x}$ is chosen and event $\mathbf{z} \in \mathbf{\Omega}$ happens to occur. The opportunity loss is

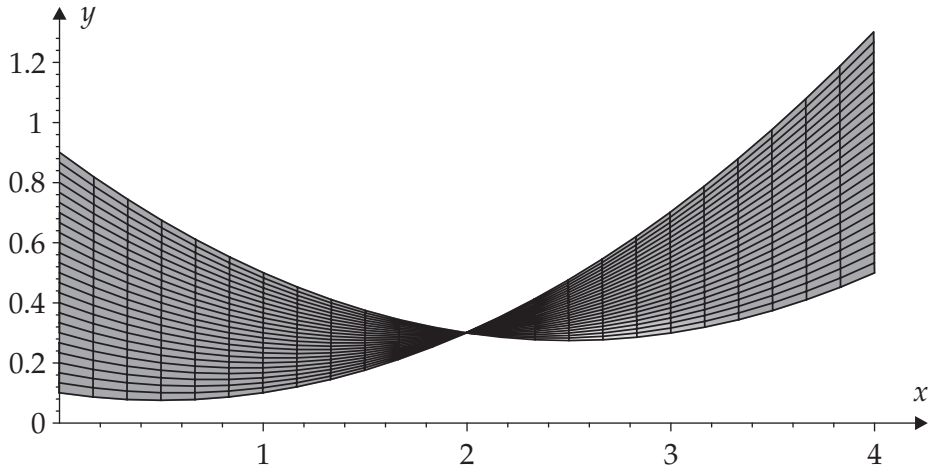

Figure 3.9: Projection of the objective function onto x-y plane.

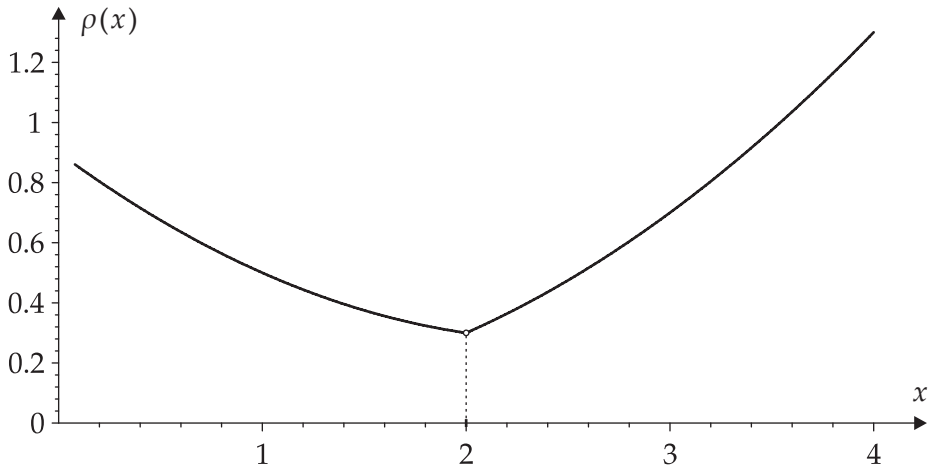

Figure 3.10: Surrogate function $\rho(x)$ resulting from Figure 3.8 for minimax principle.

the difference in the objective between the best obtainable response f^*

$$f^*(\mathbf{z}) = \inf_{\mathbf{x}\in\mathcal{C}} f(\mathbf{x}, \mathbf{z}) \tag{3.33}$$

for each possible event $\mathbf{z}$ and the actual outcome $f(\mathbf{x}, \mathbf{z})$ resulting from choosing $\mathbf{x}$

$$\rho(\mathbf{x}) = \sup_{\mathbf{z}\in\mathbf{\Omega}} \left(f(\mathbf{x}, \mathbf{z}) - f^*(\mathbf{z}) \right). \tag{3.34}$$

To obtain $f^*(\mathbf{z})$, all possible events are investigated separately, and the optimal decision $\mathbf{x}^*$ for each $\mathbf{z} \in \mathbf{\Omega}$ is evaluated assuming the underlying event occurs uniquely.

Another view at the minimax regret criterion would be that first, the best achievable response value for each event $\mathbf{z}$ is subtracted from $f(\mathbf{x}, \mathbf{z})$, then the worst case is determined as for the minimax criterion. As a result, the optimal design is identified as the one for which the worst case has a minimal deviation from the theoretical optimum f^*. Hence, the minimax regret criterion also takes into account the range of possible response values as opposed to the original minimax principle.

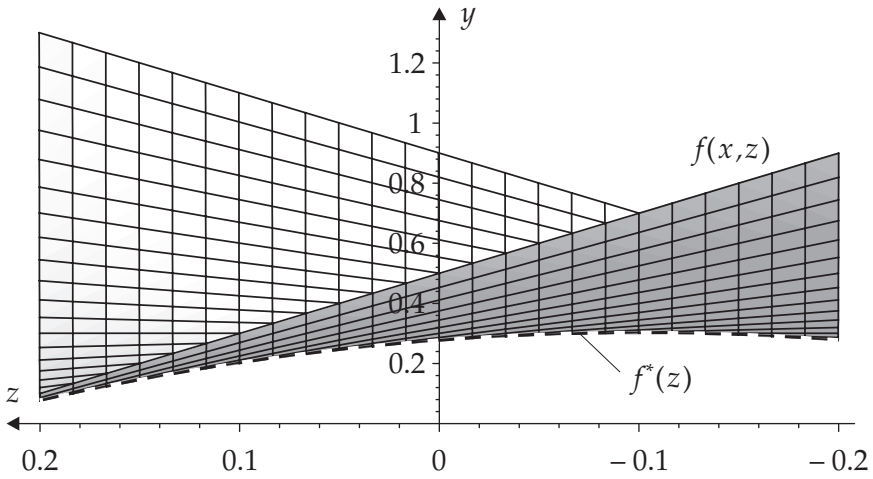

Figure 3.11: Projection of the objective function onto z-y plane.

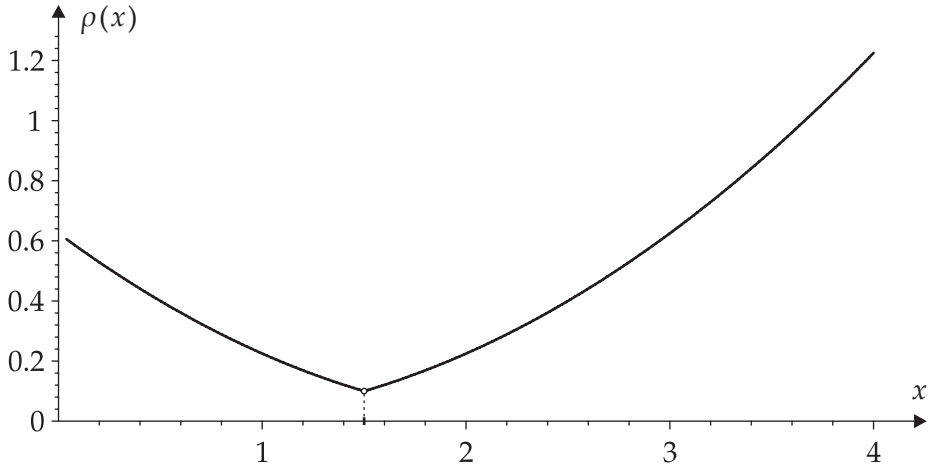

Figure 3.12: Surrogate function $\rho(x)$ resulting from Figure 3.8 for minimax regret criterion.

Example 2 [continued]. Referring to the assumption $z \in [-0.2, 0.2]$, the minimax regret criterion in Equation (3.34) can be evaluated for the established example. To find $f^*(z)$, the objective function is projected onto the z-y plane as depicted in Figure 3.11. The lower bound of the span (dashed line in Figure 3.11) represents $f^*(z)$. With $f^*(z)$, the opportunity loss $f(\mathbf{x}, \mathbf{z}) - f^*(\mathbf{z})$ is determined for each combination of decision x and event z. The minimax principle applied to the opportunity loss results in the deterministic substitute function $\rho(x)$ depicted in Figure 3.12. The optimal design characterized by this minimax regret criterion is located at $x^* = 1.5$. □

LAPLACE method. LAPLACE argues that for a serious assessment of a stochastic problem, the designer should allot a probability distribution $p_{\mathbf{Z}}(\mathbf{Z})$ to the noise. In absence of established probability information for the noise, he suggests the use of the *principle of insufficient reason* by BERNOULLI. It states that, if no probabilities have been assigned, there is insuf-

ficient reason to indicate that any state for $\mathbf{Z}$ is more or less likely to occur than any other state. Consequently, all events must be equally likely. Accordingly, a uniform distribution is assigned to the noise variables. This assumption turns the problem into a "decision under risk" problem. In this case, the assumed probability density function for the input allows for an estimation of the output distribution.

With information about the distribution of the random response at hand – either based on BERNOULLI's argument or derived from probability distributions known in advance – more detailed robustness criteria for the class of "decision under risk" problems can be formulated. The question on how to find this distribution of the response when the probability density of the noise parameters is known will be discussed in Section 3.3.

Quantile measures. Based on the probability density distribution of the output, a quantile q (e.g. 90% quantile) of the random objective function can be used as robustness criterion in analogy to the worst case.

$$\rho(\mathbf{x}) = C^{-1}(\mathbf{x}, q) \tag{3.35}$$

where C^{-1} denotes the inverse of the cumulative distribution function for the random objective $Y = f(\mathbf{x}, \mathbf{Z})$ as introduced in Equation (3.7). Here, C^{-1} is also a function of the design variables $\mathbf{x}$ because generally the probability density p_Y of the response also depends on the design variables.

For the resulting robust design $\mathbf{x}^*$, the respective percentage of possible realizations $\mathbf{z} \in \mathbf{\Omega}$ will yield a value for the objective $f(\mathbf{x}^*, \mathbf{Z})$ that is equal to or smaller than $\rho(\mathbf{x}^*)$. Similar to the worst case formulation, the quantile measure disregards the possible spread in the random response.

Example 2 [continued]. For the evaluation of "decision under risk" criteria, a probability distribution $p_Z(z)$ for the noise variable Z has to be specified. To illustrate the impact of the probability distribution on the resulting optimal design, two different cases are studied for this example:

- ◇ a uniform distribution according to Equation (3.12) with $a_Z = -0.2$ and $b_Z = 0.2$ and
- ◇ a normal distribution as defined in Equation (3.11) with $\mu_Z = 0.02$ and $\sigma_Z = 0.05$

as depicted in Figure 3.13.

Evaluating Equation (3.35) based on the aforementioned probability distributions for the noise variable Z and a 90% quantile results in the plots in Figure 3.14. The minimum for this criterion is located at $x^*_{\text{unif}} = 1.9$ and $x^*_{\text{norm}} = 1.72$ for the uniform distribution and the normal distribution, respectively.

If this criterion is evaluated for $q = 1$, the resulting substitute function $\rho(x)$ for the uniform distribution is equal to the minimax principle. For the normal distribution, no substitute function can be determined since the resulting distribution is essentially not bounded. Hence, the criterion yields infinite values for $\rho(x)$. □

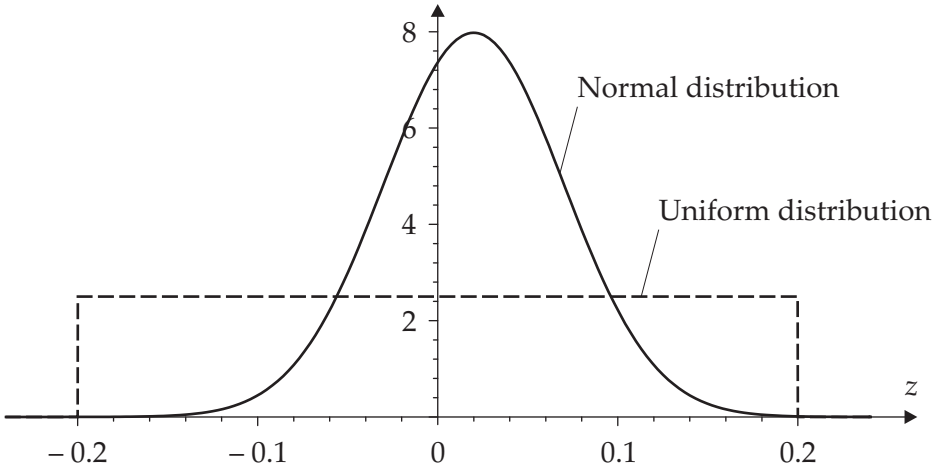

Figure 3.13: Probability distributions $p_Z(z)$ assumed for noise variable Z in Example 2.

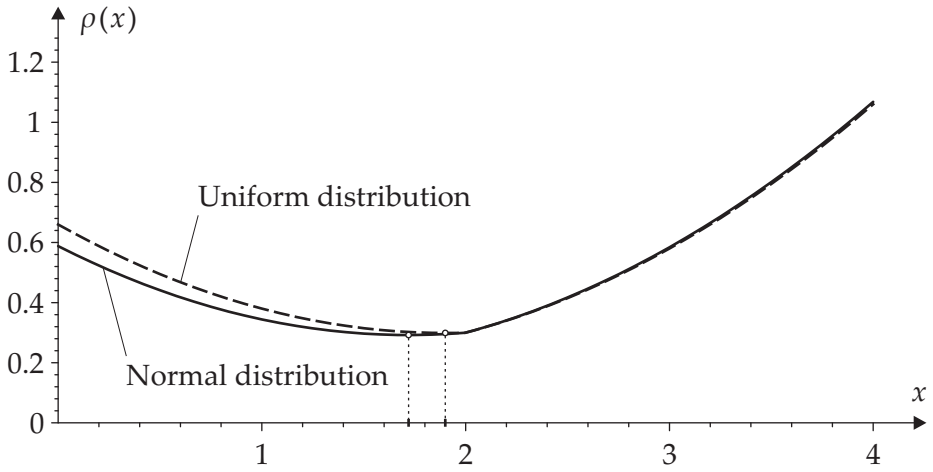

Figure 3.14: Surrogate functions $\rho(x)$ based on the quantile criterion with $q = 0.9$ applied to Example 2.

BAYES principle. For this criterion, the expected value for the random response $Y = f(\mathbf{x}, \mathbf{Z})$ is evaluated.

$$\rho(\mathbf{x}) = E\big(f(\mathbf{x}, \mathbf{Z})\big) = \mu_Y(\mathbf{x}) = \int_{\Omega} f(\mathbf{x}, \mathbf{z})\, p_{\mathbf{Z}}(\mathbf{z})\, d\mathbf{z} \tag{3.36}$$

Example 2 [continued]. The definition in Equation (3.36) constitutes the plots in Figure 3.15. The minimum mean value for the objective is obtained for designs $x^*_{\text{unif}} = 1.5$ and $x^*_{\text{norm}} = 1.4$, respectively. □

In general, taking into account only the mean value of the objective can result in a non-robust design because it disregards the spread of the distribution. In other words, this criterion makes no difference between a narrow response distribution $p_Y(y)$ and a wide spread

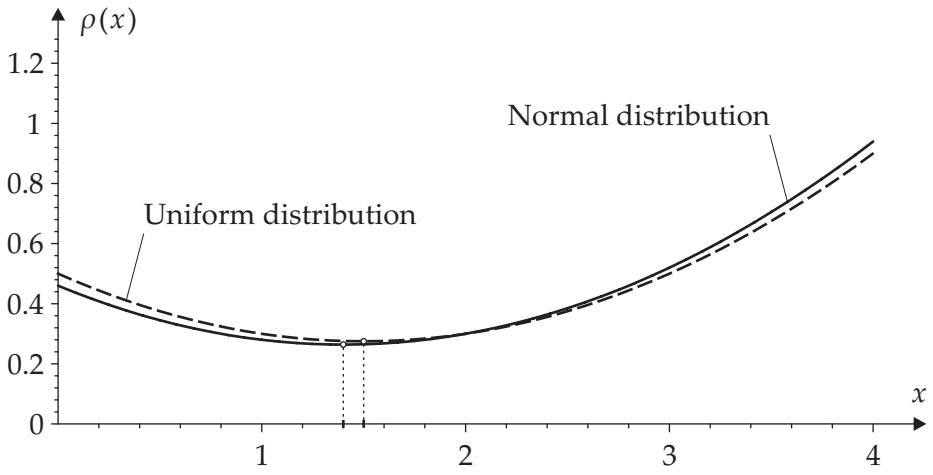

Figure 3.15: Surrogate functions $\rho(x)$ based on the BAYES principle applied to Example 2.

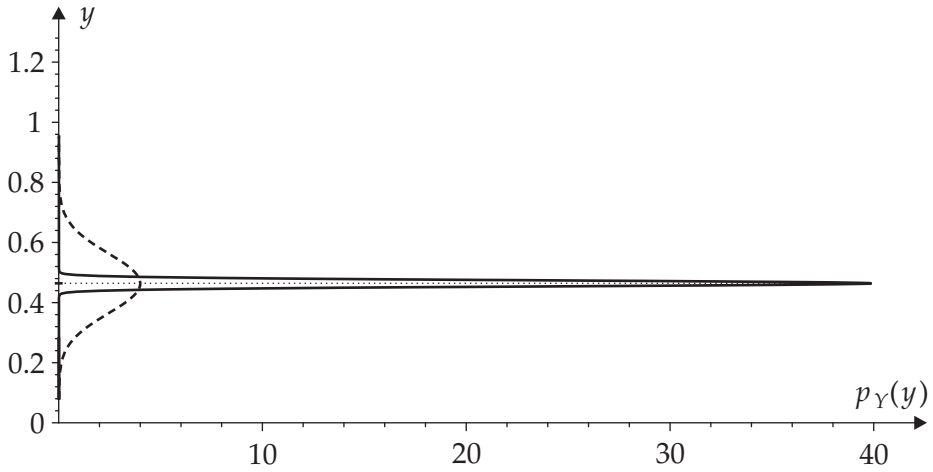

Figure 3.16: Probability distributions $p_Y(y)$ with identical mean but unequal standard deviation.

distribution if both have the same mean value as exemplified in Figure 3.16. Hence, the *average performance* of the design will be optimal but at the price of possibly large deviations from the mean performance. Consequently, the BAYES principle is used in cases where the good prospects of "beneficial deviations" due to noise balance the risks of "deteriorating effects" of noise variables. In many engineering problems, this approach is not appropriate, for instance a typical manufacturing process: beneficial deviations from the average performance of the product usually do not generate higher profit for the individual item whereas inferior goods surely entail additional costs for quality control and repair. In decision theory, a distinction is drawn between three different situations or attitudes:

1. A decision maker that places more emphasis on the chances of beneficial deviations. His behavior is called *risk-taking*.

2. A decision maker that ascribes equal weights to positive and negative deviations. His behavior is called *risk-neutral*.

3. A decision maker that lays stress on the deteriorative effects of variations. His behavior is called *risk-averse*.

In comparison with the BAYES principle – the preferred strategy for the risk-neutral designer – the substitute function of a risk-taker is smaller where significant variance exists. The risk-averse designer will augment the substitute function in comparison to the mean wherever the variance is large. The latter strategy leads to substitute functions $\rho(\mathbf{x})$ for robust design optimization that yield robust designs in terms of the above given definition – optimizing the overall performance while minimizing the variation due to noise.

Robustness criteria based on location and dispersion measures. Although all of the aforementioned strategies surely have their suitable applications, a minimal variation in the system performance proves to be beneficial for most stochastic optimization problems in structural engineering. In these cases, a multicriteria optimization with two objectives is necessary to characterize the optimum: to minimize the location and the dispersion of the random response, for instance the mean and the variance. As described in Section 2.1.4, several techniques are available to solve this multiobjective optimization problem.

If the *composite function approach* is used as introduced in Equation (2.2), the two objectives are combined to one robustness criterion by a weighted sum with user-specified weighting factors w_1 and w_2. Since the location of extrema does not change if a function is multiplied by a scalar (e.g. $1/w_1$), one weighting factor can be eliminated without changing the resulting optimum design (the response value at the optimum, however, is modified by this scalar multiplication). Here, the weighting factor for the mean is always fixed to 1.0 making the average performance of the system the gage which is adjusted by a multiple (weight w) of the dispersion measure. Hence, the response values of the resulting substitute functions have a plain meaning potentiating a straightforward comparison of different "robustness measures". In terms of decision theory, $w = 0$ corresponds to a risk-neutral designer, $w < 0$ describes the preference of a risk-taker, and $w > 0$ expresses risk-aversion. For the aim of robust design optimization (identifying a design $\mathbf{x}$ with minimal variance in the response) only values $w > 0$ make sense.

$$\begin{aligned} \rho(\mathbf{x}) &= E\big(f(\mathbf{x},\mathbf{Z})\big) + w\, V\big(f(\mathbf{x},\mathbf{Z})\big) \\ &= \mu_Y(\mathbf{x}) + w\big(\sigma_Y(\mathbf{x})\big)^2 \\ &= \mu_Y(\mathbf{x}) + w \int_{\Omega} \Big(f(\mathbf{x},\mathbf{z}) - \mu_Y(\mathbf{x})\Big)^2 p_{\mathbf{Z}}(\mathbf{z})\, d\mathbf{z}\,. \end{aligned} \tag{3.37}$$

To solve engineering problems, it is often more suitable to constitute the robustness criterion using the standard deviation instead of the variance. As a result, both the measure of central tendency and measure of dispersion and hence the resulting robustness criterion have the same unit as the original objective function.

$$\begin{aligned} \rho(\mathbf{x}) &= E\big(f(\mathbf{x},\mathbf{Z})\big) + w\,\sqrt{V\big(f(\mathbf{x},\mathbf{Z})\big)} \\ &= \mu_Y(\mathbf{x}) + w\,\sigma_Y(\mathbf{x}) \end{aligned} \tag{3.38}$$

The *signal to noise ratio (SNR)* as introduced by TAGUCHI [FC95] is also a robustness criterion based on the mean and the variance of a system response Y. Considering the case *the smaller – the better*, TAGUCHI assumed zero as the minimal possible response value. Accordingly, he formulated the following SNR as robustness criterion

$$\text{SNR} = 10 \log_{10} \left(\mu_Y^2 + \sigma_Y^2 \right) \ . \tag{3.39}$$

Since TAGUCHI performed a maximization of the SNR to find the optimum, his formulation of the SNR has the opposite sign. The operator "$10 \log_{10}$" does not change the location of the optimum, it simply transforms the magnitude of the robustness criterion into *decibel units* (dB). To make this robustness measure comparable to $\rho(\mathbf{x})$ in Equations (3.32) – (3.38), the SNR is altered as follows

$$\begin{aligned} \rho(\mathbf{x}) &= \big(\mu_Y(\mathbf{x})\big)^2 + \big(\sigma_Y(\mathbf{x})\big)^2 \\ &= \big(\mu_Y(\mathbf{x})\big)^2 + \int_{\boldsymbol{\Omega}} \Big(f(\mathbf{x},\mathbf{z}) - \mu_Y(\mathbf{x}) \Big)^2 p_{\mathbf{Z}}(\mathbf{z})\, d\mathbf{z} \\ &= \big(\mu_Y(\mathbf{x})\big)^2 + \int_{\boldsymbol{\Omega}} \big(f(\mathbf{x},\mathbf{z}) \big)^2 p_{\mathbf{Z}}(\mathbf{z})\, d\mathbf{z} - \big(\mu_Y(\mathbf{x})\big)^2 \\ &= \int_{\boldsymbol{\Omega}} \big(f(\mathbf{x},\mathbf{z}) \big)^2 p_{\mathbf{Z}}(\mathbf{z})\, d\mathbf{z} = E\left(\big(f(\mathbf{x},\mathbf{Z}) \big)^2 \right) \ . \end{aligned} \tag{3.40}$$

Since a monotonic transformation of a function does not change the position of its extrema but only the absolute value of the function (as the transformation $10 \log_{10}$ above), such a transformation can be applied to $\rho(\mathbf{x})$. For a positive argument $(\cdot)$, the positive root $\sqrt{\cdot}$ is a monotonic transformation. After taking the positive root of the formulation in Equation (3.40), the resulting robustness criterion has the same unit as the original objective function. Additionally, a weighting parameter w is introduced to allow for individual emphasis on the minimization of variations.

$$\rho(\mathbf{x}) = \sqrt{\big(\mu_Y(\mathbf{x})\big)^2 + \big(w\, \sigma_Y(\mathbf{x})\big)^2} \tag{3.41}$$

To compare the robustness criteria in Equations (3.37), (3.38), and Equation (3.41), so-called *indifference curves* are introduced. Originally developed for decision making in operations research, indifference curves are in fact contour lines of a function $\Psi(\mu, \sigma)$ combining the two objectives "mean" and "standard deviation" to one objective function. Each contour marks all combinations of μ and σ that the decision maker would equate in his personal preference i.e. between these μ-σ pairs, the decision maker is *indifferent*.

For a risk-neutral decision maker, the indifference curves are always parallel to the σ-axis. If a risk-averse criterion is chosen, the indifference curves are strictly decreasing with μ ($\partial\sigma/\partial\mu < 0$) while for risk-takers they are strictly increasing ($\partial\sigma/\partial\mu > 0$) as illustrated in Figure 3.17. Since in most operations research texts the aim of the optimization is the maximization of the original objective function, the assignments of positive and negative slope in the indifference curves to risk-taker and risk-averse decision maker are interchanged.

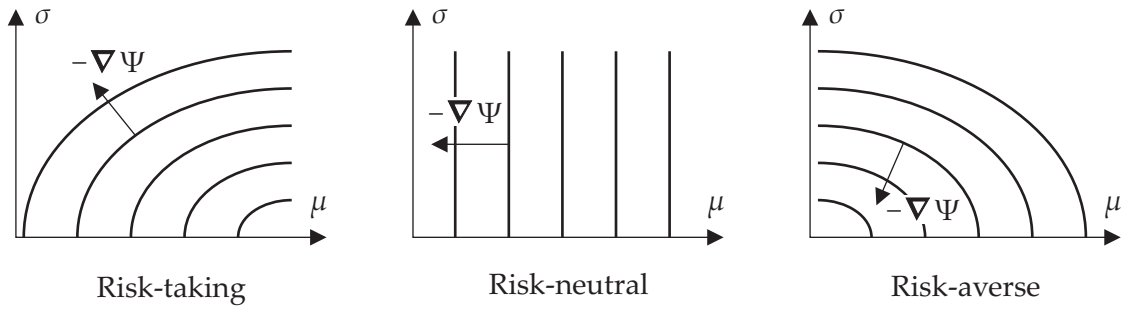

Figure 3.17: Indifference curves dependent on the attitude of the decision maker.

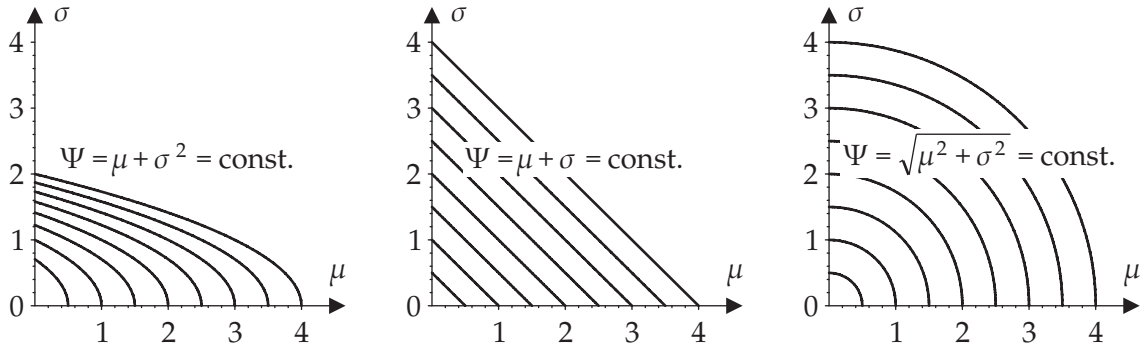

Figure 3.18: Indifference curves for robustness criteria in Equations (3.37), (3.38), and (3.41).

Based on the graphs in Figure 3.18 displaying Equations (3.37), (3.38), and (3.41) with $w = 1$, the difference between these robustness criteria can be evaluated. Compared to $\rho(\mathbf{x})$ in Equation (3.38), the robustness criterion in Equation (3.37) only slightly penalizes small standard deviations ($\sigma \ll 1$). This means that for exiguous variations ($\sigma \to 0$), the decision maker behaves almost risk-neutral ($\partial\sigma/\partial\mu \to -\infty$). In contrast, large standard deviations are severely penalized.

A special trait of Equation (3.41) is that with increasing mean the same standard deviation is regarded as less critical. For constant σ and increasing μ the slope of the indifference curves steepens. This can be useful in cases where the designer's assessment of variation is not fixed but relative to the absolute value of the mean. The main limitation of this formulation is that the mean value is restricted to be larger than or equal to zero by definition. Thus, this criterion can only be used if the objective function $f(\mathbf{x}, \mathbf{Z})$ cannot result in negative values.

Based on the definition of indifference curves, the decision maker may additionally establish different functions $\Psi(\sigma, \mu)$ and thus custom-made robustness criteria to account for an individual rating of different (μ, σ) pairs.

Example 2 [continued]. To illustrate the results of the composite function approach, the shape of the two components must be introduced first. The mean $\mu_Y(x)$ was introduced earlier and is depicted in Figure 3.15. The standard deviation $\sigma_Y(x)$ for both probability

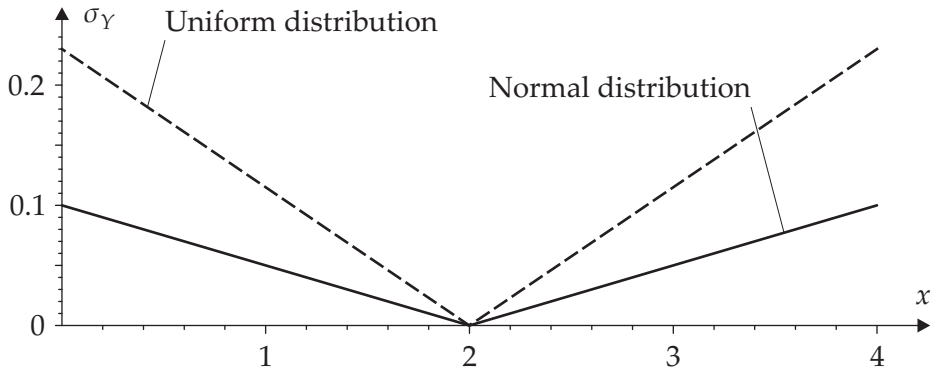

Figure 3.19: Standard deviation σ_Y of the resulting probability density $p_Y(y)$ for Example 2.

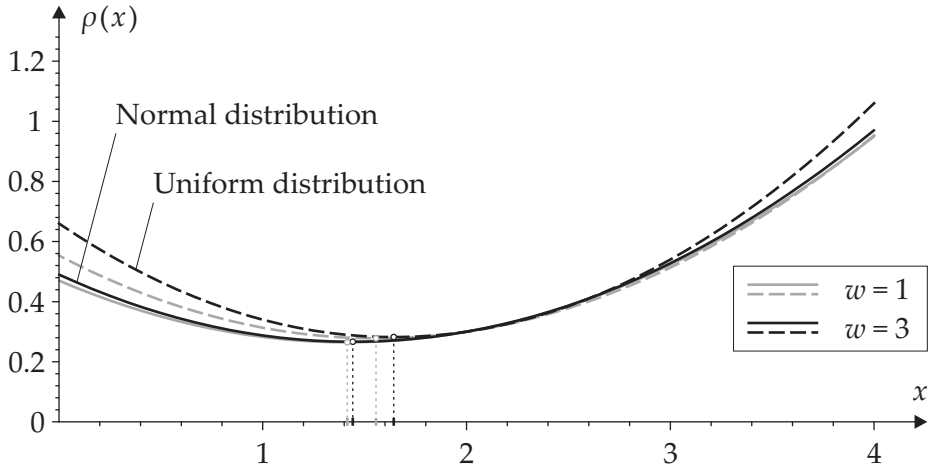

Figure 3.20: Surrogate functions $\rho(x)$ for composite robustness criterion in Equation (3.37) with varied weighting factor w.

distributions of this example is shown in Figure 3.19. Evaluating Equation (3.37) by choosing $w = 1$ and $w = 3$ yields the substitute functions depicted in Figure 3.20. Compared to the substitute function solely based on the mean, the composite function approach results in designs with lower variation in the response. For $w = 1$, the minima are represented by $x^*_{\text{unif}} = 1.559$ and $x^*_{\text{norm}} = 1.415$, respectively. If the designer's emphasis is on designs with lower variation in the objective, this intention can be expressed by increasing w. Accordingly, the optimum is shifted toward the minimum of the variance (located at $x = 2$). Choosing $w = 3$ for instance, relocates the minima to $x^*_{\text{unif}} = 1.643$ and $x^*_{\text{norm}} = 1.442$, respectively.

Figure 3.21 contains the graphs resulting from Equation (3.38). The optimal designs based on this robustness criterion with $w = 1$ are found at $x^*_{\text{unif}} = 2$ and $x^*_{\text{norm}} = 1.65$, respectively. Considering the case $w = 3$, the optimum for the uniform distribution remains unchanged because the standard deviation at $x = 2$ is equal to zero. Thus, a higher penalty factor on σ does not influence the optimum. For the normal distribution, the optimum is moved to the minimum in the standard deviation, thus constituting the minimum for $w = 3$

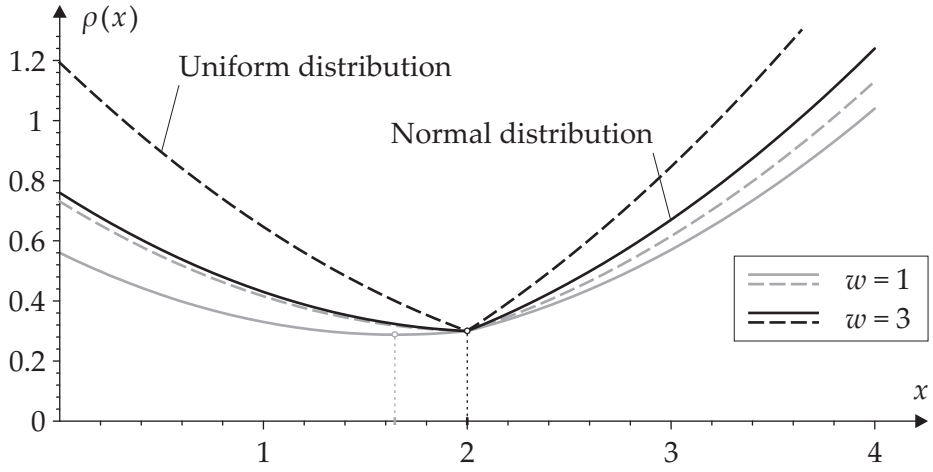

Figure 3.21: Surrogate functions $\rho(x)$ for composite robustness criterion in Equation (3.38) with varied weighting factor w.

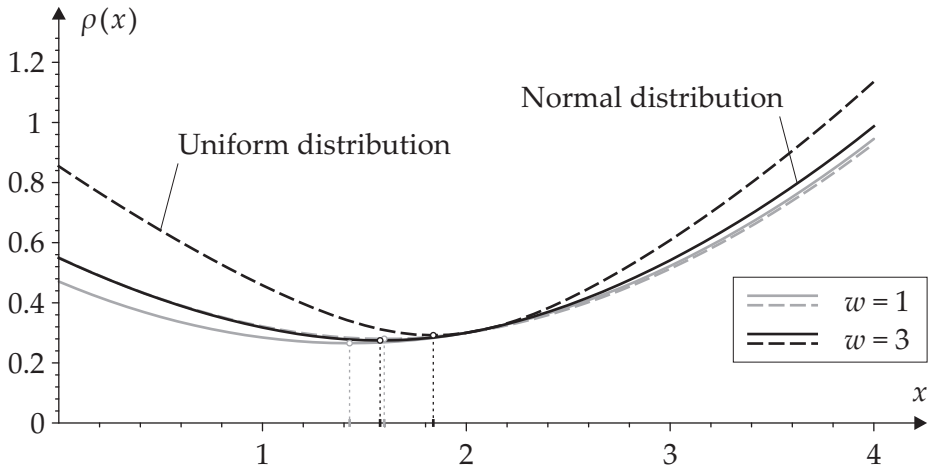

Figure 3.22: Surrogate functions $\rho(x)$ for composite robustness criterion in Equation (3.41) with varied weighting factor w.

at $x^*_{\text{norm}} = 2$.

The robustness criterion formulated in Equation (3.41) is also evaluated for the two alternative distribution functions and both weighting factor settings $w = 1$ and $w = 3$. In Figure 3.22, the corresponding substitute functions are plotted and the resulting optimal designs are indicated at $x^*_{\text{unif}} = 1.597$ and $x^*_{\text{norm}} = 1.427$ for $w = 1$, and $x^*_{\text{unif}} = 1.838$ and $x^*_{\text{norm}} = 1.578$ for $w = 3$, respectively. □

As an alternative solution procedure for the multicriteria optimization involving both mean and standard deviation as objective functions, the *preference function approach* can be applied as well. In this case, either component can be chosen as preference function (the actual objective function) while the other part is transformed into an additional constraint by imposing a maximum permissible value ($\sigma_{\max}$ or $\mu_{\max}$) on the respective quantity. According to Equation (2.1), the substitute formulation for the stochastic optimization problem then

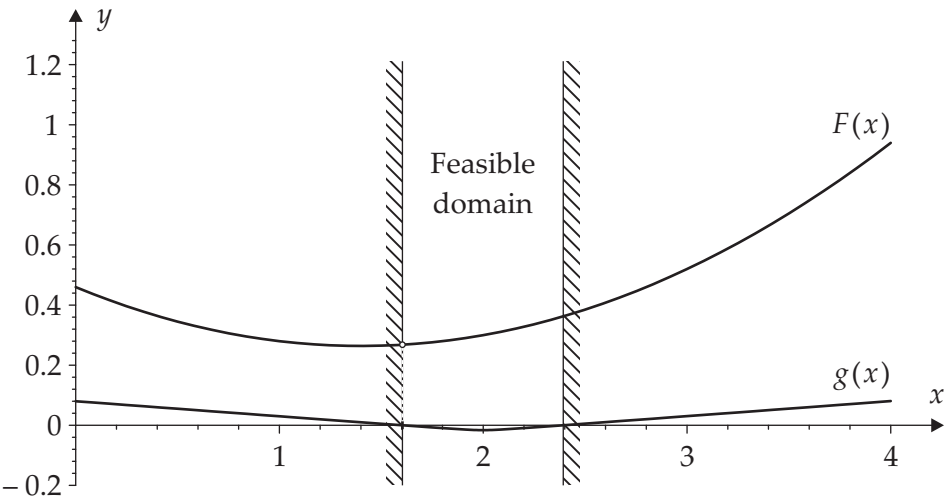

Figure 3.23: Robust design based on the preference function approach with upper limit on the standard deviation $\sigma_{\max} = 0.02$.

reads

$$F(\mathbf{x}) = \mu_Y(\mathbf{x}) \tag{3.42}$$
$$g(\mathbf{x}) = \sigma_Y(\mathbf{x}) - \sigma_{\max} \leq 0\,,$$

or alternatively,

$$F(\mathbf{x}) = \sigma_Y(\mathbf{x}) \tag{3.43}$$
$$g(\mathbf{x}) = \mu_Y(\mathbf{x}) - \mu_{\max} \leq 0\,.$$

Formulation (3.42) is used if the aim of the optimization is in fact not to obtain a "true" robust design (with minimal variance) but a design with optimal average performance for which the variance in the performance is not larger than a prescribed tolerance value $\sigma_{\max}$. The second approach might be the proper choice in cases where an optimization based on nominal values already exposed a design that would perform optimal in the deterministic case. Following the concept of Equation (3.43) would then allow to "back off" this theoretical optimum by a certain acceptable loss in average performance to minimize the variance due to the noise.

Example 2 [continued]. As an example for the preference function approach, emphasis is put on minimization of $\mu_Y(x)$, which is henceforth the actual objective $F(x)$. For the standard deviation $\sigma_Y(x)$, an upper bound is established by setting $\sigma_{\max} = 0.02$. Thus, the objective to minimize the variance is transformed into a constraint $g(x) = \sigma_Y(x) - 0.02$. In Figure 3.23, the new constraint $g(x)$ is plotted assuming the noise is normally distributed. Minimizing the preference function $F(x) = \mu_Y(x)$ on the feasible domain characterized by $g(x) \leq 0$ yields the optimal design at $x^*_{\text{norm}} = 1.605$. □

Cost function. Similar to the procedure for inequality constraints, cost functions $\gamma(y)$ can be introduced to find a substitute formulation $\rho(\mathbf{x})$ for robust design optimization. Since

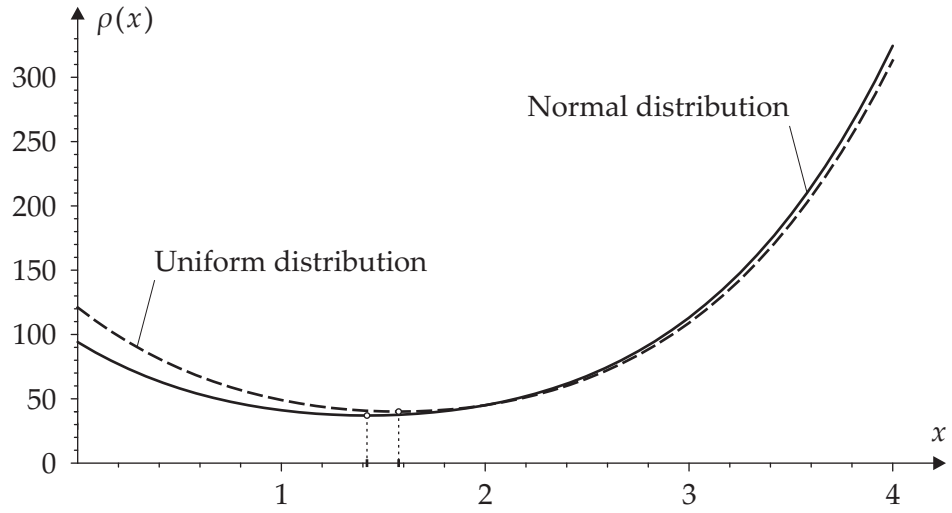

Figure 3.24: Robust design based on the cost function approach for Example 2.

particular costs are related to each possible response value y of $f(\mathbf{x}, \mathbf{z})$ and $y = g(\mathbf{x}, \mathbf{z})$, the expected overall costs for violation of constraints and variation in the objective can be optimized.

$$\begin{aligned} \rho(\mathbf{x}) &= E\left(\gamma_0\left(f(\mathbf{x}, \mathbf{Z})\right)\right) + \sum_{j=1}^{n_g} E\left(\gamma_j\left(g_j(\mathbf{x}, \mathbf{Z})\right)\right) \\ &= \int_{\Omega} \gamma_0\left(f(\mathbf{x}, \mathbf{Z})\right)\, p_{\mathbf{Z}}(\mathbf{z})\, d\mathbf{z} + \sum_{j=1}^{n_g} \left(\int_{\Omega} \gamma_j\left(g_j(\mathbf{x}, \mathbf{Z})\right)\, p_{\mathbf{Z}}(\mathbf{z})\, d\mathbf{z} \right) \end{aligned} \tag{3.44}$$

The advantage of the cost function approach is that the trade-off between the different elements of the stochastic optimization problem (violation of each constraint, mean and variance of the objective) is judged on a consistent basis, namely the individual cost (e.g. in terms of money or alternative measures such as the weight) contributed by each element of the optimization formulation. At the same time, the problem usually becomes an unconstrained optimization problem since all constraints are expressed in terms of their monetary equivalent and are summarized in the new objective function, the overall costs. The problem with this approach is to define appropriate and accurate cost functions for each possible contribution.

Example 2 [continued]. The quadratic cost function

$$\gamma_0(y) = 300\, y^2 + 60\, y$$

is supposed to describe the costs associated with a design x that produces the outcome $y = f(x)$. Since no constraints are formulated for this example, only the first expression in Equation (3.44) contributes to the substitute function $\rho(x)$. Figure 3.24 shows the evaluation of Equation (3.44) for the two probability density functions under investigation. The optimal designs based on minimum expected costs are $x^*_{\text{unif}} = 1.420$ and $x^*_{\text{norm}} = 1.575$, respectively. □

Concluding the Discussion of Introduced Robustness Criteria. A look at the substitute formulations applied to Example 2 reveals that each robustness criterion yields a distinct "robust design". It should be realized that for each formulation an engineering problem can be conceived which justifies and substantiates the eligibility of the corresponding criterion as an approximation to the (in most cases) unattainable goal of an optimal robust design. In general, one optimization problem can successfully be tackled via miscellaneous robustness criteria. For all intents and purposes, there is no better or worse robustness criterion; the proper choice for a suitable formulation is basically an engineer's decision. In fact, this conclusion was already suggested earlier by introducing decision-theoretic methods where the different criteria were derived depending on the preference of the decision maker. The individual choice should be made based on available information on the noise (probability density function or range) and the designer's demand on the system performance (main focus on good overall performance or more emphasis on minimal variance). Moreover, as revealed by the discussion of multicriteria optimization problems in Section 2.1.4, problems with more than one objective (in this case: location and dispersion of the probability distribution p_Y) do not have a unique solution but bring up a set of PARETO-optimal designs from which the designer has to pick his personal favorite.

3.2.4 Stochastic Optimization Terminology: Robustness versus Reliability

Many examples for stochastic optimization problems are described in the literature but, unfortunately, they are not always termed coherently. In this text, a consistent terminology is proposed that tries to combine the established terms from different communities.

Before the field of stochastic optimization can be addressed, *stochastic optimization procedures* and *stochastic optimization problems* must be distinguished. The first term summarizes all optimization algorithms that use stochastic sampling to find the solution of an optimization problem, for instance random search or evolutionary algorithms. The problem to be solved – as defined in Equations (2.6a-d) – does not have to be a stochastic optimization problem. Stochastic optimization procedures are also successfully applied to deterministic optimization problems i.e. where all parameters and variables involved are inherently deterministic. Correspondingly, *stochastic optimization problem* as a generic term subsumes the analysis of problems which comprise random variables in the problem formulation. To solve a stochastic optimization problem, it is not mandatory to choose a stochastic optimization procedure. Other solution techniques (as introduced in Section 2.3) can also be applied to this class of problems using substitute formulations presented earlier.

In many texts, the terms *robust design* (or *robustness*) *problem* and *reliability problem* are used to denote stochastic optimization problems. The matter which is actually labeled by these expressions, though, differs from author to author. Frequently, the entire field of problems with random variables is called "robust design optimization" [LP01, JL02]. In this text, any problem formulation containing functions of random variables is called a *general stochastic optimization problem*. Moreover, two special cases are distinguished depending on the functions affected by variations: objective function or constraints. If the objective is solely a function of deterministic variables and exclusively (inequality) constraints are affected by the random variables, one possible deterministic substitute formulation for this

problem reads

$$\begin{aligned}
&\text{minimize} && f(\mathbf{x}) \quad ; && \mathbf{x} \in \mathbb{R}^n && (3.45a)\\
&\text{such that} && P\left\{g_j(\mathbf{x},\mathbf{Z}) > 0\right\} - P_{\max} \leq 0 \quad ; && \mathbf{z} \in \boldsymbol{\Omega} \quad ; \quad j = 1,\ldots,n_g && (3.45b)\\
& && x_i^L \leq x_i \leq x_i^U \quad ; && i = 1,\ldots,n\,. && (3.45c)
\end{aligned}$$

The problem described by Equations (3.45a-c) is called a *reliability problem*. In other publications [PSP93, DC00], the term *feasibility robustness* is used to describe this problem. The methods used to solve reliability problems are summarized in the term *reliability-based design optimization (RBDO)*.

In case the noise variables merely affect the objective function $f(\mathbf{x},\mathbf{Z})$ (i.e. the constraints are deterministic or the problem is unconstrained), the problem is called a *robustness problem* or *robust design problem*. To solve this optimization task, the original stochastic problem is transformed into a deterministic form by applying a suitable robustness criterion $\rho(\mathbf{x})$ as described in Section 3.2.3. The solution of problems according to Equations (3.46a-d) is termed *robust design optimization*.

$$\begin{aligned}
&\text{minimize} && \rho(\mathbf{x}) \quad ; && \mathbf{x} \in \mathbb{R}^n && (3.46a)\\
&\text{such that} && g_j(\mathbf{x}) \leq 0 \quad ; && j = 1,\ldots,n_g && (3.46b)\\
& && h_k(\mathbf{x}) = 0 \quad ; && k = 1,\ldots,n_h && (3.46c)\\
& && x_i^L \leq x_i \leq x_i^U \quad ; && i = 1,\ldots,n && (3.46d)
\end{aligned}$$

This differentiation of the two special cases makes sense with respect to the methods needed to solve problems of each respective class. In robust design optimization, the mean and the variance play the most important roles in the formulation of the substitute function $\rho(\mathbf{x})$. To evaluate mean and variance adequately, a good representation of the probability distribution in areas with large probability is usually sufficient (e.g. the distribution in the area $\mu \pm 2\,\sigma$). On the other hand, to determine the relevant probability of failure (commonly $P_f \ll 1‰$ is chosen) in reliability problems, the "outer legs" (with low probabilities) of the probability density must be described accurately (often up to $\pm 6\,\sigma$ or more) [RB05]. Hence, the methods used to ascertain the resulting probability density p_Y by mapping the input density functions p_Z onto the response should accommodate the regions of main emphasis and their different accuracy requirements.

3.3 Methods to Solve Stochastic Optimization Problems

To solve stochastic optimization problems, the effect of randomness in input parameters on the crucial response values must be determined. Dependent on the substitute formulation transforming the stochastic problem into a deterministic form, the evaluation of the objective and/or constraints for one design involves

- ◇ a complete optimization run e.g. to determine the corresponding worst case,
- ◇ the calculation of the probability of failure P_F for reliability problems,

- ◇ the evaluation of integrals over the probability distribution p_Y to determine the expected value and the variance of the crucial response value for the robustness problem.

For both the minimax principle and the minimax regret principle, an optimization has to be performed to identify the worst case. Suitable optimization algorithms for different kinds of problems have been proposed and discussed in Section 2.3. An alternative approach to determine the robustness criterion ρ for these formulations is to examine only the vertices of the noise space assuming that the worst case will result from some extremal settings of the noise variables. This assumption typically holds whenever the effect of the noise variables is approximately linear, but not in general. Thus, applicability of this simplification should be examined carefully.

Suitable methods to determine the probability of failure as a prerequisite for reliability problems comprise

- ◇ First-order second moment approach (FOSM)
- ◇ First-order reliability method (FORM)
- ◇ Second-order reliability method (SORM)
- ◇ Monte Carlo sampling (MC)
- ◇ Importance sampling (IS)
- ◇ Directional sampling (DS)

and many other variants of sampling methods. Since the main issue of this work is rather to solve robustness than reliability problems, a presentation of methods which are specifically designed to estimate small probabilities will be omitted here. As a consequence of the large number of publications in this field, a list of references for reliability problems and solution techniques must be incomplete. The following list is meant to provide an excerpt of interesting contributions and reviews [TCB82, HR84, SBBO89, GS97, Roo02, RDKP01, OF02, Sav02, PG02, BM04]. A detailed review of reliability-based optimization techniques and applications is given in [FM03]. Illustrative examples for reliability problems and the successful application of the aforementioned techniques can be found e.g. in [TCM86, LYR02, GFO02, MF03, AM04, YCYG04].

In the following, several techniques to solve the robust design problem will be discussed. The aim of these approaches is either to find the probability distribution of the output variable p_Y or to compute directly its statistical measures (mean μ_Y, variance σ_Y^2). The resulting data are used as input for the robustness criterion which defines a deterministic substitute for the original problem.

As already derived in Equations (3.36), (3.37), and (3.40), substitute formulations that are based on mean and variance of the response involve the evaluation of integrals of the form

$$\int_{\Omega} \kappa(\mathbf{z})\, p_{\mathbf{Z}}(\mathbf{z})\, d\mathbf{z}\,. \tag{3.47}$$

To compute the mean $\mu_Y(\mathbf{x})$, the function κ takes the form $f(\mathbf{x}, \mathbf{z})$. For the calculation of the variance $\sigma_Y^2(\mathbf{x})$, κ either reads $(f(\mathbf{x}, \mathbf{z}))^2$ or $(f(\mathbf{x}, \mathbf{z}) - \mu_Y(\mathbf{x}))^2$ as derived in Equations (3.37) and (3.40). Since integration is only performed with respect to the noise variables $\mathbf{Z}$, dependency on $\mathbf{x}$ can be disregarded for the evaluation of the integral.

In most engineering applications, the functions f, g, and h are not known explicitly. Typically, the response values $\mathbf{y}$ can only be obtained pointwise as solution of a linear system of equations, for instance by means of the finite element method [ZT05]. Consequently, the integration has to be performed numerically. For the numerical computation of an integral, the basic idea is to approximate the original integrand by a function that is easy to integrate.

$$\int f(z)\, dz \approx \int \hat{f}(z)\, dz \tag{3.48}$$

These approximations are constructed by interpolating polynomials which are based on evaluations of the integrand at m sampling points. With prior knowledge about the class of polynomials to be used as approximation, the integration can be performed analytically yielding a weighted sum over the function evaluations at the sampling points.

$$\int f(z)\, dz \approx \int \hat{f}(z)\, dz = \sum_{l=1}^{m} w_l\, f(z_l) \tag{3.49}$$

The individual weights w_i have to be determined according to the class of polynomials used as approximation and the location of the sampling points. If these sampling points are equally-spaced, the resulting integration rules are called *NEWTON-COTES formulas*. A NEWTON-COTES formula can be constructed for any polynomial degree. The commonly used formulas of low degree are known by the names *rectangle rule* for constant approximations, *trapezoidal rule* for linear polynomials, and *SIMPSON's rule* for quadratic polynomials. To assure a good accuracy for the NEWTON-COTES formulas, the distance between the sampling points used for the integration needs to be small. For this reason, numerical integration is usually performed by splitting the original integration domain Ω into smaller subintervals, applying a NEWTON-COTES rule on each subdomain, and adding up the results. This procedure is called *composite rule*. A similar concept is used by the Gaussian quadrature rule. It is constructed to yield an exact result for polynomials of degree $2\,m - 1$ by a suitable choice of the m points and corresponding weights.

The quadrature rules discussed above are all designed to evaluate one-dimensional integrals. To compute the mean of response values that depend on multiple noise variables, multi-dimensional integrals have to be evaluated. One possibility to solve this problem is to formulate the multiple integral as nested one-dimensional integrals referring to FUBINI's theorem. This theorem necessitates some additional assumptions and reads

$$\int_{\mathbf{\Omega}} f(\mathbf{z})\, d\mathbf{z} = \int_{\Omega_1 \times \Omega_2 \times \cdots \times \Omega_n} f(\mathbf{z})\, d\mathbf{z} = \int_{\Omega_1} \int_{\Omega_2} \cdots \int_{\Omega_n} f(\mathbf{z})\, dz_n \cdots dz_2\, dz_1\,. \tag{3.50}$$

This approach requires the function evaluations to grow exponentially as the number of dimensions increases. Additionally, it only covers integration over a multi-dimensional domain $\mathbf{\Omega}$ that can be written as Cartesian product of one-dimensional domains $\Omega_1 \times \Omega_2 \times \cdots \times \Omega_n$.

Monte Carlo methods offer an alternative approach to compute multi-dimensional integrals. They may yield greater accuracy for the same number of function evaluations than repeated integrations using one-dimensional methods.

3.3.1 Plain Monte Carlo Method

Monte Carlo methods make use of the special form of the integral in Equation (3.47). This integral is solved based on m sampling points which are chosen with respect to the probability density of the noise variables $p_{\mathbf{Z}}$. After the function κ is evaluated at these sampling points, the solution of the integral can be approximated by

$$\int_{\Omega} \kappa(\mathbf{z})\, p_{\mathbf{Z}}(\mathbf{z})\, d\mathbf{z} \approx \sum_{l=1}^{m} w_l\, \kappa(\mathbf{z}^l)\ . \tag{3.51}$$

In *plain Monte Carlo simulations*, the sampling points are determined *randomly* in consistency with the probability density of the noise variables $p_{\mathbf{Z}}$. In consequence of the random sampling which is performed according to the probability distribution, the sampled response values are all weighted equally. In addition, the sum over all weights should add up to one in accordance with Equations (3.3) and (3.6), respectively.

$$\sum_{l=1}^{m} w_l = 1 \quad \wedge \quad w_l = \text{const.} \quad \Rightarrow \quad w_l = \frac{1}{m} \tag{3.52}$$

As an aside, this approach results in the equation for the *sample mean*. This formula is commonly used in descriptive statistics to estimate the mean of a random variable Y whose distribution p_Y is not known explicitly. Typically, the characteristics of a random variable can only be studied by means of sampling. In this case, the sample mean $\bar{y}$ provides an estimate for the mean μ_Y based on m random samples y_l.

$$\mu_Y \approx \bar{y} = \frac{1}{m} \sum_{l=1}^{m} y_l \tag{3.53}$$

Analogously, the *sample variance* s^2 is defined as an estimate for the variance of the underlying distribution. In minor inconsistency with Equation (3.52), it can be shown that for the sample variance choosing $w_l = 1/(m-1)$ yields an unbiased estimate for the variance σ_Y^2.

$$\sigma_Y^2 \approx s^2 = \frac{1}{m-1} \sum_{l=1}^{m} (y_l - \bar{y})^2\ . \tag{3.54}$$

3.3.2 Stratified Monte Carlo Method

By using random sampling, the allocation of sampling points is unsystematic and chances are that important subsets of the noise space are not taken into account. Especially, if there are regions with small probability but high impact on the investigated statistics, this influence might be ignored.

Stratified Monte Carlo sampling uses a partitioning of the entire noise space into disjoint subregions $\mathbf{\Omega}^l$, so-called *strata*, to ensure that from each subset samples are included. Typically, one sample is taken at random from each stratum and so the sample size m is equal to the number of strata. The weight, that is assigned to each particular sample, is given by the probability of the corresponding stratum.

$$w_l = P\{\mathbf{z} \in \mathbf{\Omega}^l\} = \int_{\mathbf{\Omega}^l} p_{\mathbf{Z}}(\mathbf{z})\, d\mathbf{z} \tag{3.55}$$

The strata are often – but not necessarily – selected to have equal probability. Accordingly, in stratified Monte Carlo, the individual samples can have different weights. If more than one sample is located in one stratum, the corresponding probability is divided by the number of samples per stratum to obtain their respective weight. Once the weights w_l and the response values y_l have been computed, Equation (3.52) can be used to compute mean and variance of the investigated random response Y.

Example 3. In this example, a stratified Monte Carlo sampling for eight sampling points in two dimensions is performed. Random variable Z_1 is normally distributed and Z_2 varies according to a uniform distribution as depicted in Figure 3.25. Despite the uniform distribution of Z_2, it is assumed that response values resulting from larger z_2 have to be examined more closely (e.g. because of a highly nonlinear behavior). Accordingly, the strata are chosen to emphasize sampling of the corresponding subregion. By contrast, the range of Z_1 is segmented into intervals of equal probability. Clearly, the weights of samples from the upper row of strata in Figure 3.25 have to be smaller than those from the lower row to avoid an erroneous evaluation of Equation (3.52). □

The big advantage of using stratified Monte Carlo is that the inclusion of specified subregions can be enforced. But then, two major questions have to be answered: how to define

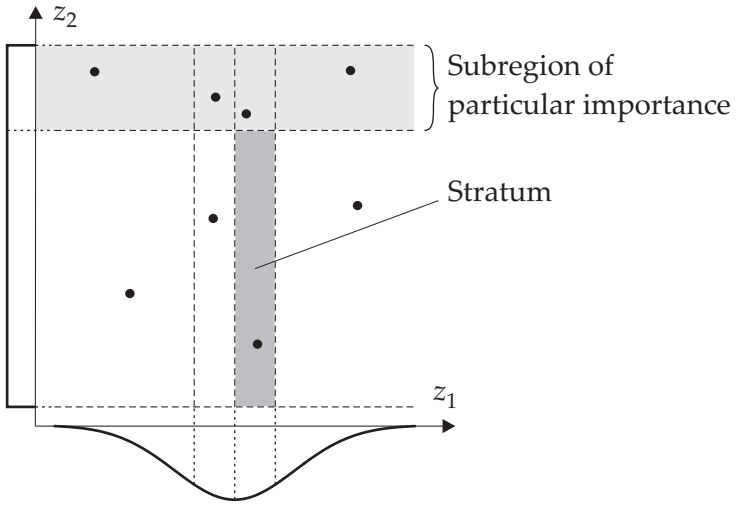

Figure 3.25: Stratified Monte Carlo sampling for a two-dimensional space with eight strata and one sampling point per stratum.

the strata and how to compute their probabilities? This can be a difficult task, especially for problems of high dimensionality.

3.3.3 Latin Hypercube Sampling

Latin hypercube sampling (LHS) also uses a segmentation of the integration domain. Hence, LHS is based on a similar basic idea as stratified Monte Carlo, but here the stratification is performed along each dimension. In a first step, the range Ω_i of each noise variable z_i is exhaustively subdivided into m intervals in consistency with the corresponding probability density i.e. the "width" of each interval is determined such that all intervals have equal probability, specifically $1/m$. In a second step, this segmentation is extruded to the entire domain thus defining m disjoint subregions along each coordinate direction. These subregions are also commonly termed *strata*. According to this procedure, the total number of strata is m^n where n determines the dimensionality of the integration domain. Obviously, those strata that emanate from the segmentation of one coordinate range are disjoint, strata arising from different coordinates are penetrating each other. Finally, the m sampling points have to be allocated in the segmented domain. To ensure that the samples are well distributed over each coordinate range, each stratum is designated to contain exactly one sample. To achieve this, one stratum along the first dimension z_1 is paired at random without replacement with one stratum that belongs to the second dimension z_2. Then a randomly selected stratum of the third dimension is appointed and combined with the pair. This procedure is continued until an n-tuple is defined. In a next step, the assembly of the n-tuple is repeated until each stratum along every dimension is addressed once. This procedure nominates m cells which are indicated by the n-tuples. From each of these cells, one sample is randomly chosen resulting in a Latin hypercube sampling with m samples [MBC79].

A prerequisite for the above described procedure for LHS is that all variables z_i are mutually independent. This implies that the joint probability density function can be described by Equation (3.17). For the case of correlated variables, IMAN and CONOVER presented a technique that is able to consider these correlations in Latin hypercube sampling [IC82].

Example 4. To illustrate this approach, a Latin hypercube sampling of eight points is exemplified. Figure 3.26 depicts the integration domain that is defined by random variables Z_1 (normal distribution) and Z_2 (uniform distribution), respectively. The range of each variable is split into eight intervals of equal probability. This results in strata of unequal width for variable Z_1. In the first step, strata 7 and 2 have been randomly drawn for Z_1 and Z_2, respectively. This pair nominates cell (7,2) for the first sampling point which is allocated at random within the cell. For the following steps, stratum 7 is removed from the set of strata available in the first dimension, and stratum 2 is canceled for the second dimension (sampling without replacement). This procedure is continued for the remaining seven sampling points, where cells (4,3), (3,7), (1,5), ... are nominated as depicted in Figure 3.26. □

Since all strata (and hence all cells) have equal probability by definition, each sampling point represents a domain of equal influence on the solution of the integral. Accordingly, the same reasons can be stated as for plain Monte Carlo to define the weights by $w_l = 1/m$.

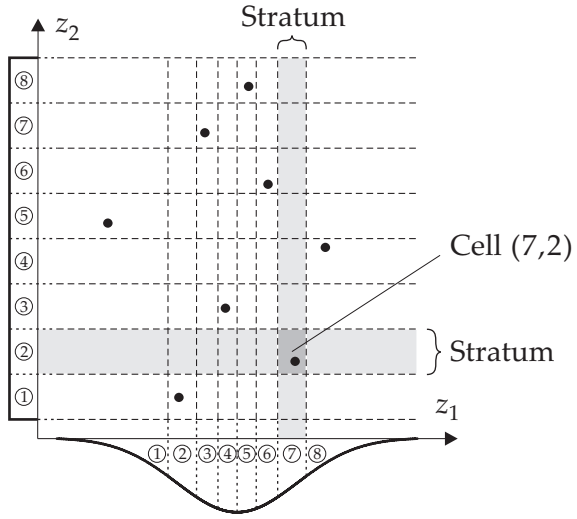

Figure 3.26: Latin hypercube sampling for a two-dimensional space with eight sampling points.

These weights together with the sampled response values y_l can be used in Equation (3.52) to compute the desired mean and variance, respectively.

3.3.4 TAYLOR Expansion for Robust Design Problems

For some special functions κ including linear and quadratic polynomials, the integral in Equation (3.47) can be solved analytically using exclusively simple statistics of the probability distribution $p_{\mathbf{Z}}(\mathbf{z})$. This characteristic trait is availed also for other functions when a TAYLOR series expansion is used to approximate the true functional relationship.

The simplest form is to use a linear Taylor expansion of $\kappa(\mathbf{z})$ based on the expansion point $\mathbf{z}'$

$$\hat{\kappa}(\mathbf{z}) = \kappa(\mathbf{z}') + \sum_{i=1}^{n} \left.\frac{\partial \kappa(\mathbf{z})}{\partial z_i}\right|_{\mathbf{z}'} (z_i - z_i') \tag{3.56}$$

Inserting this linear relation into Equation (3.47) yields

$$\begin{aligned}
\int_{\Omega} \hat{\kappa}(\mathbf{z})\, p_{\mathbf{Z}}(\mathbf{z})\, d\mathbf{z} &= \int_{\Omega} \kappa(\mathbf{z}')\, p_{\mathbf{Z}}(\mathbf{z})\, d\mathbf{z} + \int_{\Omega} \left(\sum_{i=1}^{n} \left.\frac{\partial \kappa(\mathbf{z})}{\partial z_i}\right|_{\mathbf{z}'} (z_i - z_i') \right) p_{\mathbf{Z}}(\mathbf{z})\, d\mathbf{z} \\
&= \kappa(\mathbf{z}') \int_{\Omega} p_{\mathbf{Z}}(\mathbf{z})\, d\mathbf{z} + \sum_{i=1}^{n} \left(\left.\frac{\partial \kappa(\mathbf{z})}{\partial z_i}\right|_{\mathbf{z}'} \int_{\Omega} (z_i - z_i')\, p_{\mathbf{Z}}(\mathbf{z})\, d\mathbf{z} \right) \\
&= \kappa(\mathbf{z}') + \sum_{i=1}^{n} \left(\left.\frac{\partial \kappa(\mathbf{z})}{\partial z_i}\right|_{\mathbf{z}'} \left(\int_{\Omega} z_i\, p_{\mathbf{Z}}(\mathbf{z})\, d\mathbf{z} - z_i' \right) \right)
\end{aligned} \tag{3.57}$$

If the expansion point is chosen to be the vector of mean values $\mathbf{z}' = \boldsymbol{\mu}_{\mathbf{Z}}$, the sum over i in

Equation (3.57) vanishes since by definition

$$\mu_{Z_i} = \int_{\Omega} z_i \, p_{\mathbf{Z}}(\mathbf{z}) \, d\mathbf{z} \, . \tag{3.58}$$

Consequently, the mean of the response $Y = f(\mathbf{x}, \mathbf{Z})$ can be approximated by

$$\mu_Y(\mathbf{x}) = \int_{\Omega} f(\mathbf{x}, \mathbf{Z}) \, p_{\mathbf{Z}}(\mathbf{z}) \, d\mathbf{z} \approx f(\mathbf{x}, \boldsymbol{\mu}_{\mathbf{Z}}) \tag{3.59}$$

if a linear Taylor expansion about $\mathbf{z}' = \boldsymbol{\mu}_{\mathbf{Z}}$ is a valid approximation of the original function. For a function $f(\mathbf{x}, \mathbf{z})$ that is linear in $\mathbf{z}$, Equation (3.59) is exactly satisfied.

Often, a linear approximation will not yield satisfactory results. In these cases, a second-order TAYLOR series

$$\hat{\kappa}(\mathbf{z}) = \kappa(\mathbf{z}') + \sum_{i=1}^{n} \left. \frac{\partial \kappa(\mathbf{z})}{\partial z_i} \right|_{\mathbf{z}'} (z_i - z_i') + \frac{1}{2} \sum_{i=1}^{n} \sum_{j=1}^{n} \left. \frac{\partial^2 \kappa(\mathbf{z})}{\partial z_i \, \partial z_j} \right|_{\mathbf{z}'} (z_i - z_i')(z_j - z_j') \tag{3.60}$$

may be used to improve the approximation. If this quadratic form is used in Equation (3.47), it can be written as

$$\begin{aligned} \int_{\Omega} \hat{\kappa}(\mathbf{z}) \, p_{\mathbf{Z}}(\mathbf{z}) \, d\mathbf{z} = \kappa(\mathbf{z}') &+ \sum_{i=1}^{n} \left(\left. \frac{\partial \kappa(\mathbf{z})}{\partial z_i} \right|_{\mathbf{z}'} \left(\int_{\Omega} z_i \, p_{\mathbf{Z}}(\mathbf{z}) \, d\mathbf{z} - z_i' \right) \right) \\ &+ \frac{1}{2} \sum_{i=1}^{n} \sum_{j=1}^{n} \left(\left. \frac{\partial^2 \kappa(\mathbf{z})}{\partial z_i \, \partial z_j} \right|_{\mathbf{z}'} \int_{\Omega} (z_i - z_i')(z_j - z_j') \, p_{\mathbf{Z}}(\mathbf{z}) \, d\mathbf{z} \right) \, . \end{aligned} \tag{3.61}$$

For mutually independent noise variables Z_i and the expansion point $\mathbf{z}' = \boldsymbol{\mu}_{\mathbf{Z}}$, the equation to compute the mean $\mu_Y(\mathbf{x})$ simplifies to

$$\mu_Y(\mathbf{x}) \approx f(\mathbf{x}, \boldsymbol{\mu}_{\mathbf{Z}}) + \frac{1}{2} \sum_{i=1}^{n} \left. \frac{\partial^2 f(\mathbf{x}, \mathbf{z})}{\partial z_i^2} \right|_{\mathbf{x}, \boldsymbol{\mu}_{\mathbf{Z}}} \sigma_{Z_i}^2 \, . \tag{3.62}$$

Obviously, this formula gives the exact result if $f(\mathbf{x}, \mathbf{z})$ at maximum contains terms which are of second order in $\mathbf{z}$.

In an analogous manner, an explicit functional relationship can be derived for the variance σ_Y^2 if a linear TAYLOR approximation is used. Again, the expansion point is chosen to be $\mathbf{z}' = \boldsymbol{\mu}_{\mathbf{Z}}$.

$$\sigma_Y^2(\mathbf{x}) \approx \sum_{i=1}^{n} \sum_{j=1}^{n} \left. \frac{\partial f(\mathbf{x}, \mathbf{z})}{\partial z_i} \right|_{\mathbf{x}, \boldsymbol{\mu}_{\mathbf{Z}}} \left. \frac{\partial f(\mathbf{x}, \mathbf{z})}{\partial z_j} \right|_{\mathbf{x}, \boldsymbol{\mu}_{\mathbf{Z}}} \mathrm{Cov}(Z_i, Z_j) \tag{3.63}$$

This formula is also known as *first-order second moment (FOSM)* approach, since second moment information of the noise parameter distribution (i.e. the covariance matrix) is mapped onto the second moment of the response (variance σ_Y^2) by means of first-order information $\partial f(\mathbf{x}, \mathbf{z}) / \partial \mathbf{z}$.

For uncorrelated variables Z_i, the off-diagonal elements of $\mathrm{Cov}(Z_i, Z_j)$ vanish and by definition $\mathrm{Cov}(Z_i, Z_i) = \sigma^2_{Z_i}$. Under this restriction, Equation (3.63) reads

$$\sigma^2_Y(\mathbf{x}) \approx \sum_{i=1}^{n} \left(\left. \frac{\partial f(\mathbf{x}, \mathbf{z})}{\partial z_i} \right|_{\mathbf{x}, \boldsymbol{\mu}_\mathbf{Z}} \right)^2 \sigma^2_{Z_i} \,. \tag{3.64}$$

For quadratic TAYLOR series approximations, the computation of the variance requires higher-order information e.g. the third central moments of $\mathbf{Z}$ and partial derivatives of higher-order. The corresponding equations can be found in [LLFSS98].

Due to the fact that a linear approximation has to be determined to compute mean and variance of the output distribution directly from the respective statistics of the noise parameters (without need for higher-order information), the application of this procedure is limited to a small number of problem types. They can typically be used if either the dispersion of $\mathbf{Z}$ is so small that a linear TAYLOR approximation is still valid in the respective region Ω ("narrow" probability distributions) or if the system behavior is known to be (approximately) linear at least over the range of variability ($\partial f(\mathbf{x}, \mathbf{z}) / \partial \mathbf{z} \approx$ const.).

The other solution techniques presented above, namely sampling methods and optimization algorithms, have in common that they require multiple evaluations of the original response to assess one design configuration i.e. to evaluate the deterministic substitute function ρ for a specific $\mathbf{x}$. Problems that can be studied in-depth (i.e. through many evaluations of the original model) the presented methods allow for an effective robust design optimization. For complex problems, however, the number of simulations needed to find a robust design may quickly become prohibitive. This problem arises frequently in engineering applications. Consequently, it will be addressed in the following chapter, where the metamodeling concept is introduced to reduce computational burden.

Chapter 4

Metamodels Replacing Computer Simulations

Today's engineering methods are strongly based on complex computer codes and numerical analyses (like nonlinear finite element analyses) which solely provide pointwise (discrete) information about the underlying relationship. Only in few applications, an analytic relationship can be established between input variables and output of a system under investigation. As a consequence, the solution of stochastic optimization problems requires many evaluations of the governing equations, for instance to compute the worst case or to evaluate the integral over the probability density. Especially for problems that can only be studied by means of time-consuming numerical analyses, stochastic optimization of the original problem becomes prohibitive. The permanent efforts in enhancing the underlying analysis codes and the increasing complexity of the structures under investigation countervail the steady enhancements in processor speed and computing power. Hence, it may not be expected that stochastic optimization problems will be easily manageable in the near future.

To reduce the computational burden, a solution method using global approximations (cf. Section 2.3.6) is presented. These global approximations are also termed *metamodels* or *surrogate models* since they are used as temporary substitution for the original code [Bar98]. A metamodel replaces the true functional relationship $f(\mathbf{x}, \mathbf{z})$ by a mathematical expression $\hat{f}(\mathbf{x}, \mathbf{z})$ that is much cheaper to evaluate. Usually, an individual metamodel is established for each single response value y. In general, the metamodel $\hat{f}$ can be set up to depend on selected inputs and noise variables only – omitting those variables with negligible or no impact on the selected response y. To shorten the notation, the two different types of input variables (design variables and noise variables) are assembled to one input vector $\mathbf{v}$.

$$\mathbf{v} = \begin{bmatrix} \mathbf{x} \\ \mathbf{z} \end{bmatrix} \tag{4.1}$$

The individual components of $\mathbf{v}$ are subsequently addressed by v_i with $i = 1 \ldots n$. Accordingly, the statement $\mathbf{y} = f(\mathbf{x}, \mathbf{z})$ is rewritten as $\mathbf{y} = f(\mathbf{v})$. The metamodel concept is illustrated in Figure 4.1.

For the generation of a metamodel, an appropriate number of sampling points is needed. These points can be selected via design of experiments (DoE) techniques to gain a maximum of information about the characteristics of the underlying relationship between input

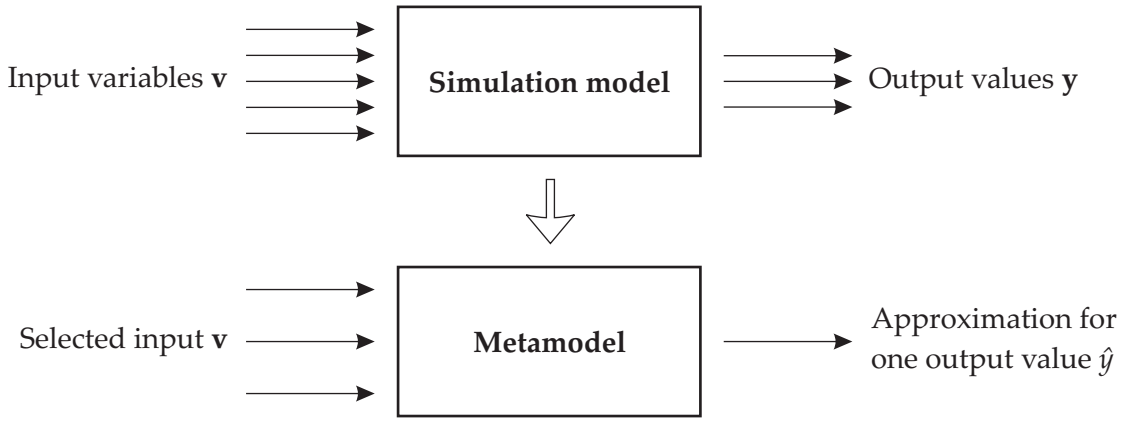

Figure 4.1: Metamodels replacing time-consuming computer simulations.

and output. A suitable DoE technique must be carefully chosen since each type of surrogate model has need of different attributes with respect to the distribution of the sampling points. Accordingly, diverse DoE techniques will be thoroughly discussed in Chapter 5. After selecting a compatible combination of global approximation method and DoE technique, the original simulation is performed for the designs appointed by the coordinates of the sampling points. With the information obtained from these *computer experiments*, the metamodel can be fit to provide an efficient estimate for the original function [KS97].

The main benefits of metamodels can be summarized as follows:

1. It is much cheaper to evaluate a metamodel than to perform a complex computer simulation. This yields a reduction in computational effort where many function evaluations are necessary (e.g. in optimization or stochastic analyses).

2. By use of metamodels, the designer can easily explore the entire design space to get a more profound understanding of the system under investigation.

3. Metamodels can be used to combine information gathered from different sources, for instance analysis codes for different disciplines (e.g. fluids, structures, or thermodynamical problems), or physical experiments and computer simulations.

4. Parallel computing is simple, since in general the individual sampling points are appointed simultaneously. Hence, the necessary computer experiments can be performed independently and in parallel.

5. Metamodels can be used to smooth response values if noise is present in the observations.

In the remainder of this chapter, a selection of prominent metamodeling approaches will be familiarized. The chapter concludes with a comparison of the different metamodel formulations.

4.1 Response Surface Models

The name *response surface model (RSM)* might be somewhat misleading, since all types of metamodels constitute a "surface" which enables the user to predict the response at untried points. Accordingly, the term RSM is used as synonym for metamodels in some other texts. However, the common use of RSM, which is also adopted here, is to address *polynomial regression models*.

The basic idea, which was originally intended for the analysis of physical experiments, is to establish an explicit functional relationship (response surface) between input variables $\mathbf{v}$ and output value y. This is done by fitting free parameters $\boldsymbol{\beta}$ of a function $\eta(\mathbf{v}, \boldsymbol{\beta})$ to the observed response values. In general, certain discrepancies between response surface and observations are acceptable since some inaccuracy ε cannot be precluded when performing physical experiments.

$$y = \eta(\mathbf{v}, \boldsymbol{\beta}) + \varepsilon \tag{4.2}$$

There is no restriction concerning the *regression function* η used for the response surface. Typically, a linear model is used, where the term "linear" addresses the linearity with respect to the coefficients $\boldsymbol{\beta}$ (termed *regression coefficients*)

$$\eta(\mathbf{v}, \boldsymbol{\beta}) = \sum_{j=1}^{n_\beta} \beta_j \, \eta_j(\mathbf{v}) = \hat{\boldsymbol{\beta}}^T \boldsymbol{\eta}(\mathbf{v}) \, . \tag{4.3}$$

In this case, the function $\eta(\mathbf{v}, \boldsymbol{\beta})$ is the sum over a user-determined set of n_β linearly independent functions $\eta_j(\mathbf{v})$ called *regressors*. Each regressor is multiplied by a scalar valued variable β_j. With regard to the use of matrix notation, the individual regressors are assembled into the vector $\boldsymbol{\eta}(\mathbf{v})$.

$$\boldsymbol{\eta}(\mathbf{v}) = \Big[\eta_1(\mathbf{v}),\, \eta_2(\mathbf{v}),\, \ldots,\, \eta_{n_\beta}(\mathbf{v})\Big]^T \tag{4.4}$$

The restriction to linear models constitutes a significant simplification for the estimation of the regression coefficients β_j.

With the vector $\tilde{\mathbf{y}}$ of size $m \times 1$ containing the response values of the original code gained at sampling points $\mathbf{v}^l$ (with $l = 1 \ldots m$), Equation (4.3) inserted in Equation (4.2) and evaluated at $\mathbf{v}^l$ reads

$$\tilde{\mathbf{y}} = \mathbf{F}\,\boldsymbol{\beta} + \mathbf{e} \, . \tag{4.5}$$

In Equation (4.5), the matrix $\mathbf{F}$ contains the individual regressors evaluated at the sampling points.

$$\mathbf{F} = \begin{bmatrix} \eta_1(\mathbf{v}^1) & \eta_2(\mathbf{v}^1) & \cdots & \eta_{n_\beta}(\mathbf{v}^1) \\ \eta_1(\mathbf{v}^2) & \eta_2(\mathbf{v}^2) & \cdots & \eta_{n_\beta}(\mathbf{v}^2) \\ \vdots & \vdots & & \vdots \\ \eta_1(\mathbf{v}^m) & \eta_2(\mathbf{v}^m) & \cdots & \eta_{n_\beta}(\mathbf{v}^m) \end{bmatrix} \tag{4.6}$$

The vector $\mathbf{e}$ of size $m \times 1$ denotes the differences between predicted response value $\eta(\mathbf{v}^l, \boldsymbol{\beta})$ and original observation $\tilde{y}_l$, which are called *residuals*.

$$e_l = \tilde{y}_l - \eta(\mathbf{v}^l, \boldsymbol{\beta}) \quad , \quad l = 1 \ldots m \tag{4.7}$$

Referring back to the application of analyzing physical experiments, it is assumed that the function $\eta(\mathbf{v}, \boldsymbol{\beta})$ describes the underlying system behavior correctly and the residuals $\mathbf{e}$ emerge exclusively from measurement errors or experimenter's mistakes. Consequently, the residuals can be assumed to be normally distributed with mean zero, having no correlation and constant variance σ^2. Based on this assumption, the least squares approach can be applied to calculate an estimation for the regression coefficients. This method is called *linear regression analysis*. The linear regression by means of least squares is thoroughly discussed in many statistical texts e.g. [BD87, MPV01, MM02].

The least squares approach identifies an estimation for the regression parameters $\hat{\boldsymbol{\beta}}$ by minimization of the sum of squared residuals

$$\sum_{l=1}^{m} \Big(\tilde{y}_l - \eta(\mathbf{v}^l, \boldsymbol{\beta}) \Big)^2 = \mathbf{e}^T \mathbf{e} \,. \tag{4.8}$$

Accordingly, Equation (4.5) is transformed yielding the formulation for the linear regression analysis

$$\min_{\boldsymbol{\beta}} \; (\tilde{\mathbf{y}} - \mathbf{F}\,\boldsymbol{\beta})^T (\tilde{\mathbf{y}} - \mathbf{F}\,\boldsymbol{\beta}) \,. \tag{4.9}$$

The minimization is performed analytically by use of the necessary condition at the minimum

$$\left. \frac{\partial \big((\tilde{\mathbf{y}} - \mathbf{F}\,\boldsymbol{\beta})^T (\tilde{\mathbf{y}} - \mathbf{F}\,\boldsymbol{\beta}) \big)}{\partial \boldsymbol{\beta}} \right|_{\hat{\boldsymbol{\beta}}} = 0 \,. \tag{4.10}$$

This turns the minimization problem into a linear system of equations

$$-\,2\,\mathbf{F}^T \tilde{\mathbf{y}} + 2\,\mathbf{F}^T \mathbf{F}\,\hat{\boldsymbol{\beta}} = 0 \tag{4.11}$$

which can be solved for $\hat{\boldsymbol{\beta}}$ if $\mathbf{F}^T\mathbf{F}$ is invertible, viz. if there are at least as many sampling points and corresponding response data as there are regression coefficients to be estimated.

$$\hat{\boldsymbol{\beta}} = (\mathbf{F}^T \mathbf{F})^{-1}\, \mathbf{F}^T \tilde{\mathbf{y}} \tag{4.12}$$

Together with the established functional relationship $\eta(\mathbf{v}, \boldsymbol{\beta})$, the coefficients $\hat{\boldsymbol{\beta}}$ define the global approximation

$$\hat{y} = \hat{f}(\mathbf{v}) = \eta(\mathbf{v}, \hat{\boldsymbol{\beta}}) = \sum_{j=1}^{n_\beta} \hat{\beta}_j \eta_j(\mathbf{v}) = \hat{\boldsymbol{\beta}}^T \boldsymbol{\eta}(\mathbf{v}) \,. \tag{4.13}$$

For a general engineering problem that was not examined yet, the main difficulty will be the proper specification of a suitable regression function $\eta(\mathbf{v}, \boldsymbol{\beta})$, which is capable of revealing the important characteristics of the original problem. To unravel this hitch, response surface models are often restricted to a delimited region including only a part of the design space. As a consequence, the optimization process has to be executed iteratively by sequentially fitting new RSM approximations on a subregion of the design space.

In analogy to the TAYLOR series expansion, it can be argued that any sufficiently smooth function can be approximated by a polynomial. The smaller the applicable subregion or

the higher the order of the polynomial, the better the prediction of the model. Typically, polynomials of first or second order are used for RSM approximations.

$$\eta(\mathbf{v}, \boldsymbol{\beta}) = \beta_0 + \sum_{i=1}^{n} \beta_i \, v_i \tag{4.14}$$

$$\eta(\mathbf{v}, \boldsymbol{\beta}) = \beta_0 + \sum_{i=1}^{n} \beta_i \, v_i + \sum_{i=1}^{n} \sum_{\substack{j=1 \\ j>i}}^{n} \beta_{ij} \, v_i \, v_j + \sum_{i=1}^{n} \beta_{ii} \, v_i^2 \tag{4.15}$$

For the sake of a handy notation, the subscripts of regression parameters β in Equations (4.14) and (4.15) differ from the syntax used before. Here, the regression parameters are indexed by zero (constant term), single subscripts i (first-order terms), and double subscripts ij (second-order terms), respectively. Nevertheless, they are assembled in one vector $\boldsymbol{\beta}$ when occurring in matrix notation.

A crucial point for the accuracy of the response surface is the intricate decision on a function η. To ensure that a proper choice was made for η, the *model adequacy* has to be checked. The main tool to assess the quality of the model is the analysis of the residuals

$$e_l = \tilde{y}_l - \hat{y}_l \tag{4.16}$$

of the fitted model.

Graphically, the model adequacy can be checked by plotting the residuals over the predicted response $\hat{y}_l = \hat{f}(\mathbf{v}^l)$ as illustrated in Figure 4.2. The plot should not exhibit any outstanding pattern (cf. Figure 4.2a). A distinct funnel structure indicates that assuming constant variance for the residuals may not be admissible. Obviously, the variance is varying with the absolute value of the response. Residual plots that reveal a clear trend as in Figure 4.2c&d expose an inappropriate choice for the regression function η. In these cases, other regressors should be used (for instance higher order polynomials or rational functions) or the subregion for the model should be scaled down.

In addition to the graphical method which is rather a qualitative analysis, quantitative measures can be established to assess model adequacy. One possible statistical quantity is the *coefficient of determination* R^2 which is defined as

$$R^2 = 1 - \frac{SS_e}{SS_t} \tag{4.17}$$

with the sum of squared residuals

$$SS_e = \sum_{l=1}^{m} (\tilde{y}_l - \hat{y}_l)^2 = \tilde{\mathbf{y}}^T \tilde{\mathbf{y}} - \hat{\boldsymbol{\beta}} \, \mathbf{F}^T \tilde{\mathbf{y}} \tag{4.18}$$

and the total sum of squares

$$SS_t = \sum_{l=1}^{m} (\tilde{y}_l - \bar{y})^2 = \tilde{\mathbf{y}}^T \tilde{\mathbf{y}} - m \, \bar{y}^2 \tag{4.19}$$

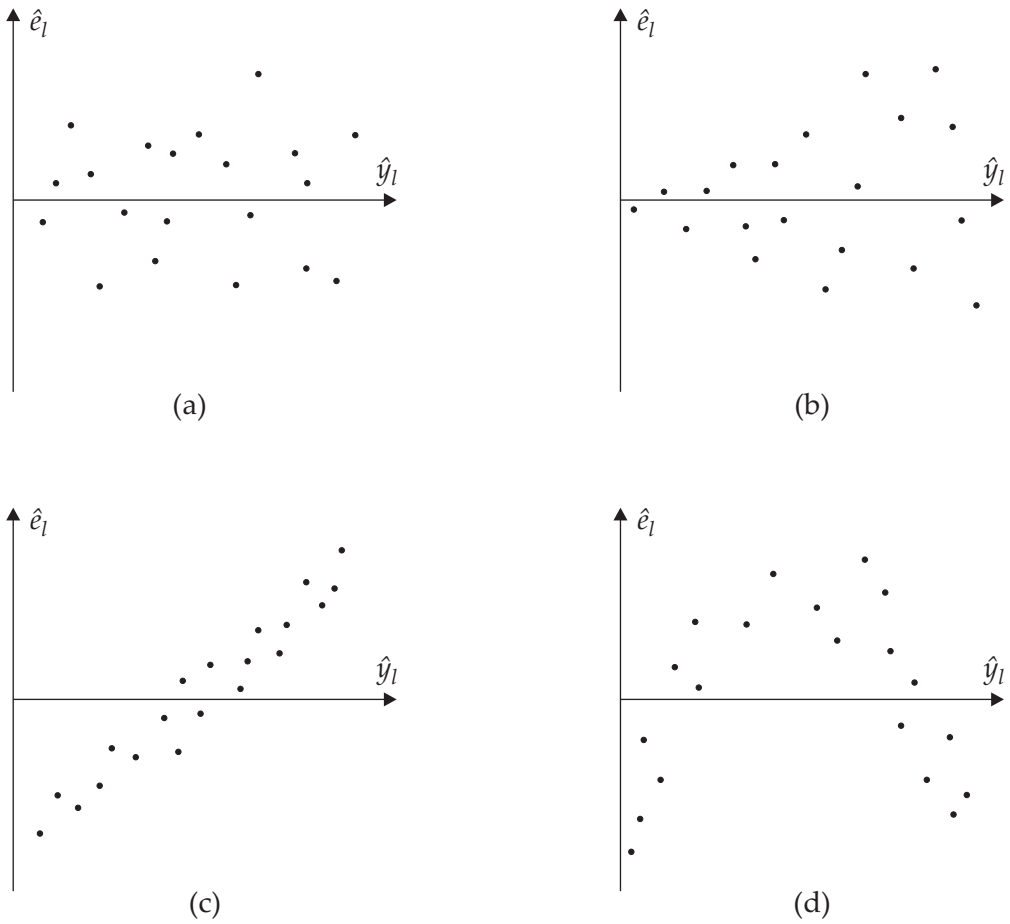

Figure 4.2: Typical patterns for residual plots: (a) no outstanding pattern, (b) funnel pattern, (c) linear pattern, and (d) nonlinear pattern.

where $\bar{y}$ denotes the mean of the sample response values. The measure R^2 can take values between 0 and 1. It can be interpreted as the amount of variance in the sample response explained by the fitted response surface. A value of $R^2 = 1$ suggests a perfect fit, where no residuals remain. However, this statistic must be handled with care. Augmenting the regression function by adding new regressors will result in an increase (or at least not a decrease) in the coefficient of determination regardless of the true benefit these terms provide for the predictive behavior of the model. Even a value of 1 can be easily obtained if the number of regressors is on par with the number of sampling points. In this case, the response values at the sampling points are interpolated and not approximated. For the applicability of the model in between the sampling points, however, no information is provided. The *adjusted coefficient of determination*

$$R^2_{\text{adj}} = 1 - \frac{m-1}{m-p}\left(1 - R^2\right) \tag{4.20}$$

can be used to avoid this trap. The scalar p denotes the size of the vector $\boldsymbol{\beta}$ i.e. the number of regressor terms in the model including the potentially existing constant term. The adjusted R^2 statistic does not necessarily increase as additional terms are included into the regression function. The value for R^2_{adj} will rather decrease as irrelevant terms are added to the model.

Finally, before the response surface model is used to approximate the original system at untested points, the fidelity of the model has to be tested. This can be accomplished via different *model validation* schemes. The simplest approach to validate the model is to sample fresh response values at additional points in order to compare these observations with the corresponding approximations. A prominent validation technique that circumvents the evaluation of the original system at additional coordinate settings and the accompanying computational effort is the so-called *cross validation*. It can be applied in cases where gathering of further information about the system is costly or even risky. To assess the predictive behavior of the model, the set of sampling points is split into two parts, one for the generation and another for the validation of the model. The first subset of data is called the *training data*, or *estimation data*, the other subset is termed *validation data*, or *test data*. The regression coefficients are estimated based on the training data, the fidelity of this approximation is judged based on the validation data.

Dependent on the nonlinearity of the problem under investigation, quadratic polynomials may not be adequate to reproduce the true relationship. Augmenting the polynomial order of the regression function is related to some pitfalls as for instance the rapidly increasing number of required sampling points or the tendency to oscillations in the prediction. Reducing the size of the subregion for the approximation is improper in certain cases, especially if stochastic problems have to be explored by global approximations. Here, the effects of all possible variations must be considered in one iteration step, and hence, the smallest admissible subregion must comprehend the entire range of variations. A transformation of the input variables $\mathbf{v}$ or the output value y can be used to enhance the predictive behavior of the model. As shown in [BD87] and [MPV01], a linear response surface with transformed variables often approximates the original code better than a model based on a quadratic regression function. In structural optimization, typical input variables (for instance geometric data or material properties) are often related to the response values (e.g. stress or displacements) by rational functions. Therefore, reciprocal transformations, that establish a polynomial model with respect to the inverse input variables, are especially useful for structural optimization problems.

It is important to note that response values collected at sampling points are in general only approximated by the response surface if the number of sampling points exceeds the number of regression coefficients. It was assumed that the established regression function correctly represents the true behavior of the original system. The residuals were accepted because of the assumed measurement inaccuracy in the data mining process. As a consequence, the occurring error is supposed to be normally distributed with $\varepsilon \sim N(0, \sigma^2)$ where σ^2 is constant. Based on this reasoning, the least squares method can be applied to fit the response surface. Due to the fact that computer experiments (numerical analyses) are typically deterministic in a sense that repeated calculations with the same parameter settings return the same values up to the accuracy of the numerical processor, this rationale cannot be sustained. It should be emphasized that computer experiments can also produce a noisy output if either the code explicitly contains random numbers or if so-called *numerical noise* occurs [TvKM95, GBH$^+$97]. In the latter case, it is questionable whether numerical noise is essentially comparable to random noise and legitimates the use of the standard least-squares technique. Despite this controversial issue, RSM techniques have been successfully applied

to compute a "global gradient" for use in gradient-based optimization algorithms – especially in cases when problems exhibit highly nonlinear (noisy) behavior constituting many local minima [GDN+94, NGV+95].

With regard to the case of deterministic computer experiments, the surrogate model is expected to hit each observation exactly i.e. the global approximation should interpolate the sampled response values. Obviously, as soon as residuals emerge from fitting a response surface to computer experiments, there is a systematic error in the model (called *bias*) which is rooted in an inadequate regression function. The two different types of errors can be written formally as:

$$\text{1. Random error:} \qquad \varepsilon_{\text{rand}} = y - E(y) \tag{4.21}$$

$$\text{2. Systematic error:} \qquad \varepsilon_{\text{bias}} = E(y) - \eta(\mathbf{v}, \boldsymbol{\beta}) \tag{4.22}$$

Summing up Equations (4.21) and (4.22) yields

$$y = \eta(\mathbf{v}, \boldsymbol{\beta}) + \varepsilon_{\text{rand}} + \varepsilon_{\text{bias}} \,, \tag{4.23}$$

a formula which details Equation (4.2). Since random effects are barred from computer experiments, the random part $\varepsilon_{\text{rand}}$ in Equation (4.23) does not exist. Consequently, the correct relationship between numerical analysis and response surface reads

$$y = \eta(\mathbf{v}, \boldsymbol{\beta}) + \varepsilon_{\text{bias}} \,. \tag{4.24}$$

The deterministic trait of $\varepsilon_{\text{bias}}$ is inconsistent with the assumptions made for the least squares regression. In fact, the residuals should vanish i.e. an appropriate response surface should interpolate the response values at the sampling points. SACKS et al. [SWMW89] compiled the following remarks on deterministic computer experiments as basis for response surface models:

- ◇ The error in a response surface approximation is solely governed by an inadequate regression function.
- ◇ The rationale underlying the three basic principles of experimental design [Mon01], which are replication, randomization, and blocking, is not supportable.
- ◇ The standard methods to determine confidence intervals or prediction intervals based on residuals of a least squares fit are not applicable.

According to the first observation, the (adjusted) coefficient of determination R^2 (or R^2_{adj}) can be used to assess the quality of the approximation, and hence, the usefulness of the prediction.

4.2 Moving-Least-Squares Models

The method of *moving-least-squares (MLS)* is an extension to the response surface method presented above. In the literature [LS86, MPV01], this concept is also termed *locally weighted*

regression or *weighted least squares*. To motivate the idea, it is recapitulated that random errors do not occur in deterministic computer experiments. Hence, the residuals of a good approximation are expected to vanish – a perfect model should interpolate the sampled response values.

The key idea of MLS is to focus on a good local fit around the point currently under investigation, the *prediction point*. According to this approach, it is preferred to have large residuals rather far away from the prediction point than close to it. This can be achieved by assigning individual weights w_l to the squared residuals e_l^2 before they are summed up

$$\sum_{l=1}^{m} w_l \left(\tilde{y}_l - \eta(\mathbf{v}^l, \boldsymbol{\beta}) \right)^2 = \mathbf{e}^T \mathbf{W}\, \mathbf{e} \tag{4.25}$$

with the *weighting matrix*

$$\mathbf{W} = \begin{bmatrix} w_1 & & & 0 \\ & w_2 & & \\ & & \ddots & \\ 0 & & & w_m \end{bmatrix} . \tag{4.26}$$

If the weights are all chosen to be equal to one, the weighting matrix reads $\mathbf{W} = \mathbf{I}$ and the MLS method simplifies to standard linear regression. To improve the local approximation resulting in small residuals around the prediction point or even an interpolation of the corresponding response values, the weights must be assigned unequally. Clearly, the residuals of sampling points that are closer to the current coordinates must be stressed more heavily than those further away. Accordingly, the individual weights are determined by means of a *weighting function* $\omega(d)$ which is a decreasing function of the distance d. The scalar Euclidean distance between two arbitrary points $\mathbf{v}^i$ and $\mathbf{v}^j$ is defined by

$$d_{ij} = \left\| \mathbf{v}^i - \mathbf{v}^j \right\| . \tag{4.27}$$

The particular distances

$$d_l = \left\| \mathbf{v} - \mathbf{v}^l \right\| \tag{4.28}$$

between prediction point $\mathbf{v}$ and the respective sampling points $\mathbf{v}^l$ give the corresponding weight w_l for each residual

$$w_l = \omega(d_l) . \tag{4.29}$$

So far, the weighting function is only restricted to decreasing functions. This allows for many different formulations [LS86] e.g. the class of reciprocally proportional functions where $w \propto 1/d$. One customary class of functions is defined through

$$\omega(d) = \frac{1}{1 + a\, d^b} \tag{4.30}$$

with $a > 0$ and b as user-specified constants. The effects of different choices for a and b are illustrated in Figure 4.3a. The formulation of Equation (4.30) results in values $w \in [0, 1]$. This prevents the weight from tending toward infinity for very small distances d, a possible

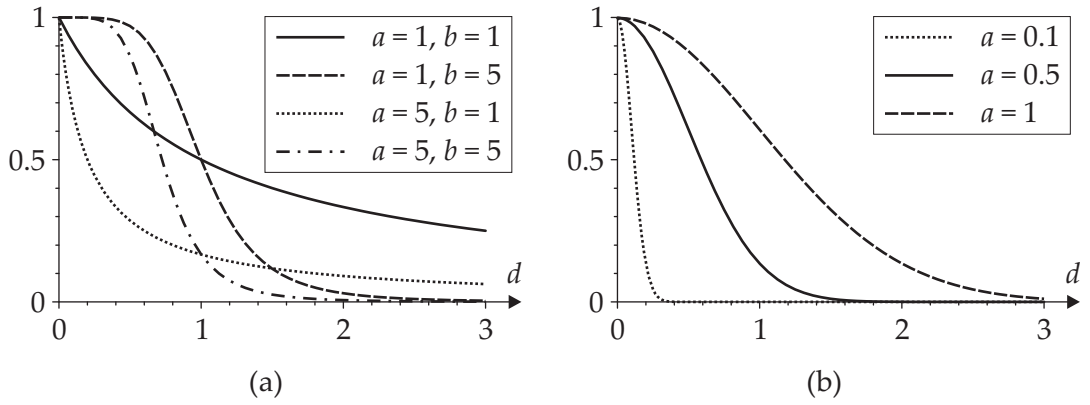

Figure 4.3: Illustration of different weighting functions for MLS: (a) Equation (4.30), and (b) Equation (4.31).

cause for numerical problems. For the same reason, it is often advisable to define a minimal allowable value for w. It is also common practice to restrict the weighting function to a *compact support* i.e. only in a distinct region (the support), the function takes values unequal to zero. However, an appropriate support size at any prediction point $\mathbf{v}$ is needed to avoid a singular matrix $\mathbf{F}$ caused by an insufficient number of considered sampling points (cf. Section 4.1).

An alternative weighting function can be derived in analogy to the probability density of a normal distribution. This weighting function reads

$$\omega(d) = \mathrm{e}^{-\frac{1}{2}\frac{d^2}{a^2}} \tag{4.31}$$

with $a > 0$. Here, the parameter a corresponds to the standard deviation of a probability density function. The smaller a is chosen, the narrower the maximum of the weighting function will be (as depicted in Figure 4.3b). For a better control of the respective free parameters a and b, and to avoid domination of the distance value by one dimension, it is often useful to normalize the input variables v_i for instance to the range $[-1, 1]$.

After the individual weights w_l have been computed, the weighting matrix $\mathbf{W}$ is defined and the least squares fit can be performed. With Equation (4.5) solved for $\mathbf{e}$, the weighted sum over squared residuals formulated in Equation (4.25) can be rewritten as

$$\left(\mathbf{y} - \mathbf{F}\,\hat{\boldsymbol{\beta}}\right)^T \mathbf{W} \left(\mathbf{y} - \mathbf{F}\,\hat{\boldsymbol{\beta}}\right) \tag{4.32}$$

The minimum of Equation (4.32) is found by means of the necessary condition for a minimum

$$\left.\frac{\partial\left(\left(\mathbf{y} - \mathbf{F}\,\hat{\boldsymbol{\beta}}\right)^T \mathbf{W} \left(\mathbf{y} - \mathbf{F}\,\hat{\boldsymbol{\beta}}\right)\right)}{\partial \boldsymbol{\beta}}\right|_{\hat{\boldsymbol{\beta}}} = 0 \tag{4.33}$$

which, in analogy to the standard regression introduced earlier, turns the minimization problem into a linear system of equations

$$-2\,\mathbf{F}^T\mathbf{W}\,\tilde{\mathbf{y}} + 2\,\mathbf{F}^T\mathbf{W}\,\mathbf{F}\,\hat{\boldsymbol{\beta}} = 0\,. \tag{4.34}$$

Solving Equation (4.34) for $\hat{\boldsymbol{\beta}}$ finally yields the regression coefficients

$$\hat{\boldsymbol{\beta}} = \left(\mathbf{F}^T \mathbf{W}\, \mathbf{F}\right)^{-1} \mathbf{F}^T \mathbf{W}\, \mathbf{y}\,. \tag{4.35}$$

Since the individual weight for each residual depends on the distance of the corresponding sampling point to the current prediction point, the weighting matrix $\mathbf{W}$ has to be recomputed for every new prediction point. This fact necessitates a separate regression analysis for each prediction point. Hence, the regression parameters $\hat{\boldsymbol{\beta}}$ now depend on the current coordinates of the prediction point $\mathbf{v}$.

$$\hat{\boldsymbol{\beta}}(\mathbf{v}) = \left(\mathbf{F}^T \mathbf{W}(\mathbf{v})\, \mathbf{F}\right)^{-1} \mathbf{F}^T \mathbf{W}(\mathbf{v})\, \mathbf{y} \tag{4.36}$$

Using these parameters for the MLS model, approximations $\hat{y} = \hat{f}(\mathbf{v})$ to the true response y at prediction point $\mathbf{v}$ are obtained by the *predictor*

$$\hat{y} = \hat{f}(\mathbf{v}) = \eta\left(\mathbf{v}, \hat{\boldsymbol{\beta}}(\mathbf{v})\right) = \sum_{j=1}^{n_\beta} \hat{\beta}_j(\mathbf{v}) \eta_j(\mathbf{v}) = \hat{\boldsymbol{\beta}}^T(\mathbf{v})\, \boldsymbol{\eta}(\mathbf{v})\,. \tag{4.37}$$

The weighted least squares regression can also be motivated by another point of view. In standard regression, one main postulate is the constant variance for the random error ε. Now, this fundamental assumption is dropped and the variance is allowed to vary throughout the investigated design space while maintaining the prerequisite of purely random error in the observed response values $\tilde{\mathbf{y}}$ (no systematic error). Figure 4.2b exemplifies the case where the variance of the residuals obviously increases with y. In such a case where the error variance depends on the point under investigation $\mathbf{v}$, the following definitions are used to characterize the error ε

$$E(\varepsilon) = \mathbf{0} \quad , \quad V(\varepsilon) = \sigma^2(\mathbf{v}) \tag{4.38}$$

Expressed in terms of the residuals at the sampling points, this spatial dependency can be expressed as

$$\mathrm{Cov}(e^l, e^k) = \sigma^2\, \mathbf{R} \tag{4.39}$$

where $\mathbf{R}$ is the correlation matrix of $\mathbf{e}$ with $\mathbf{R} \neq \mathbf{I}$. The (constant) global error variance σ^2 quantifies the overall error which is scaled by the correlation matrix. Since the correlation matrix must be non-singular and positive definite by definition, there exists a non-singular, symmetric matrix $\mathbf{K}$ of equal size with $\mathbf{K}^T\mathbf{K} = \mathbf{K}\,\mathbf{K} = \mathbf{R}$. By means of the matrix $\mathbf{K}$, the original observations $\tilde{\mathbf{y}}$ can be transformed into values with constant variance in accordance with the assumptions of standard regression [MPV01]. The transformed problem reads

$$\mathbf{K}^{-1}\, \tilde{\mathbf{y}} = \mathbf{K}^{-1}\, \mathbf{F}\, \boldsymbol{\beta} + \mathbf{K}^{-1}\, \mathbf{e}\,. \tag{4.40}$$

With the transformed residuals $\mathbf{K}^{-1}\, \mathbf{e}$, the standard procedure for least squares fit can be applied such that

$$\left(\mathbf{K}^{-1}\, \mathbf{e}\right)^T \mathbf{K}^{-1}\, \mathbf{e} = \mathbf{e}^T \mathbf{K}^{-T} \mathbf{K}^{-1}\, \mathbf{e} = \mathbf{e}^T \left(\mathbf{K}\,\mathbf{K}\right)^{-1} \mathbf{e} = \mathbf{e}^T \mathbf{R}^{-1}\, \mathbf{e}\,. \tag{4.41}$$

A comparison of this result with Equation (4.25) reveals that the latter approach leads to the same model as derived previously if the individual weights are assigned according to $\mathbf{W} = \mathbf{R}^{-1}$. Commonly, the residuals with unequal variance are assumed to be uncorrelated. This results in a diagonal structure of the correlation matrix which due to the relation $\mathbf{W} = \mathbf{R}^{-1}$ is related to the specific weights w_l by

$$\mathbf{R} = \begin{bmatrix} \frac{1}{w_1} & & & 0 \\ & \frac{1}{w_2} & & \\ & & \ddots & \\ 0 & & & \frac{1}{w_m} \end{bmatrix} \tag{4.42}$$

Conversely, a matrix $\mathbf{W}$ with non-zero off-diagonal terms corresponds to the assumption of correlated residuals.

Following the latter motivation for weighting the individual residuals in least squares regression, the specific weights w_l are assigned according to the assumed variance of the residuals which is in general a fixed value. In contrast, the MLS method presented above employs a user-specified weighting function to determine the weights dependent on the distance of the prediction point to the respective sampling point. Here, the weights for least squares regression are changing as the prediction point is "moving" through the design space – substantiating the name of the method.

4.3 Kriging Models

Based on the work of DANIEL G. KRIGE [Kri51] addressing problems in geostatistics [Cre93], *kriging models* are today a widespread global approximation technique. Their ability to exactly interpolate response values obtained at sampling points makes them particularly attractive for approximating deterministic simulations. SACKS et al. [SWMW89] were the first to use this approach to model deterministic output of computer codes. Referring to the title of their contribution "Design and analysis of computer experiments", this model type is also called *DACE model*. A kriging model approximates the original relationship by

$$y = \eta(\mathbf{v}, \boldsymbol{\beta}) + Z(\mathbf{v}) + \varepsilon \tag{4.43}$$

where $\eta(\mathbf{v}, \boldsymbol{\beta})$ is a polynomial with free parameters $\boldsymbol{\beta}$ as defined in Equation (4.3) for the response surface approach. $Z(\mathbf{v})$ represents the realization of a stationary, normally distributed Gaussian random process with mean zero, variance σ^2 and non-zero covariance. The term ε describes solely the approximation error (bias) since random errors are excluded in this formulation.

The expression $\eta(\mathbf{v}, \boldsymbol{\beta})$ provides a global trend for the system behavior as in the standard response surface approach. The general case, in which the choice of $\eta(\mathbf{v}, \boldsymbol{\beta})$ is not restricted, is called *universal kriging*. In many applications, the function η is introduced in the simplest possible way, namely $\eta(\mathbf{v}, \boldsymbol{\beta}) = \beta$ (often called *ordinary kriging*). The second part of the

formulation $Z(\mathbf{v})$ guarantees the interpolation of the observations $\tilde{\mathbf{y}}$ at the sampling points $\mathbf{v}^l$ as it creates a "localized deviation" from the polynomial part of the model. As a result, the output of the kriging model $\hat{y}_l$ at the m sampling points equals the original observations y_l i.e. the residuals at the sampling points vanish.

$$e_l = \tilde{y}_l - \hat{y}_l = 0 \quad ; \quad l = 1 \dots m \tag{4.44}$$

The Gaussian random process is characterized by the covariance matrix of $Z(\mathbf{v})$ defined as

$$\mathrm{Cov}\Big(Z(\mathbf{v}^k), Z(\mathbf{v}^l)\Big) = \sigma^2 \mathbf{R} \tag{4.45}$$

with the correlation matrix

$$\mathbf{R} = [R_{kl}] \quad ; \quad 1 \leq (k,l) \leq m \,. \tag{4.46}$$

The individual elements of the correlation matrix R_{kl} are defined by means of a correlation function R which takes each possible combination of sampling points as arguments.

$$R_{kl} = R(\mathbf{v}^k, \mathbf{v}^l) \quad ; \quad 1 \leq (k,l) \leq m \tag{4.47}$$

A correlation function has to fulfill the requirements $R(\mathbf{v}^k, \mathbf{v}^l) = R(\mathbf{v}^l, \mathbf{v}^k)$ and $R(\mathbf{v}^l, \mathbf{v}^l) = 1$, respectively, such that the resulting correlation matrix $\mathbf{R}$ is symmetric and its diagonal entries are all equal to one. Meeting these requirements, still many different formulations are feasible. In this text, only correlation functions of the form

$$R(\mathbf{v}^k, \mathbf{v}^l) = \prod_{i=1}^{n} R_i(v_i^k, v_i^l) \tag{4.48}$$

are considered i.e. products of n (size of vector $\mathbf{v}^l$) one-dimensional correlation functions $R_i(v_i^k, v_i^l)$. For kriging models, the predicted response values are assumed to be spatially correlated with the observations made at neighboring sampling points. Hence, the correlation function is expected to decrease with the distance to the sampling points (similar to the weighting functions used in MLS). Suitable one-dimensional correlation functions are e.g. the *Gaussian correlation function*

$$R(v^k, v^l) = \exp\Big(-\theta \left(v^k - v^l\right)^2\Big) \tag{4.49}$$

and the *linear correlation function*

$$R(v^k, v^l) = \max\Big\{0\,,\, 1 - \theta \left|v^k - v^l\right|\Big\} \tag{4.50}$$

The Gaussian correlation function constitutes a smooth model with an infinitely differentiable predictor while the linear correlation function establishes only C^0-continuous kriging models with piecewise linear interpolations. The parameter θ in Equations (4.49) and (4.50) is called *correlation parameter*. It controls the range of influence of the sampling points and has to fulfill the requirement $\theta > 0$. The formulation of Equation (4.48) offers great flexibility in selecting the correlation parameter θ independently for each dimension of the input

variables $\mathbf{v}$. The proper settings for θ_i will be discussed later in this section. So far, it will be treated as additional degree of freedom in the model description.

$$R(\boldsymbol{\theta}, \mathbf{v}^k, \mathbf{v}^l) = \prod_{i=1}^{n} R_i(\theta_i, v_i^k, v_i^l) \quad ; \quad \theta_i > 0 \tag{4.51}$$

Based on the assumption that deviations of the polynomial part of the model from observations $\tilde{\mathbf{y}}$ emerge as realizations of a stationary, normally distributed Gaussian random process with mean zero, variance σ^2 and covariance $\sigma^2\mathbf{R}$, the parameters of the process can be obtained by maximum likelihood estimation. The likelihood function for this Gaussian process given m correlated realizations $\tilde{y}_l$ is defined as

$$L\left[\boldsymbol{\beta}, \sigma^2, \boldsymbol{\theta} \,\middle|\, \tilde{\mathbf{y}}\right] = \frac{1}{\sigma^m \sqrt{|\mathbf{R}|\,(2\,\pi)^m}} \exp\left(-\frac{1}{2\,\sigma^2}\,(\tilde{\mathbf{y}} - \mathbf{F}\,\boldsymbol{\beta})^T\,\mathbf{R}^{-1}\,(\tilde{\mathbf{y}} - \mathbf{F}\,\boldsymbol{\beta})\right) \tag{4.52}$$

with the matrix $\mathbf{F}$ as introduced in Equation (4.6). The independent variables of the likelihood function are the regression parameters $\boldsymbol{\beta}$, the process variance σ^2, and the correlation parameters $\boldsymbol{\theta}$. To facilitate the maximization of Equation (4.52), the natural logarithm of the likelihood function is taken. The maximum likelihood estimates $\hat{\boldsymbol{\beta}}$, $\hat{\sigma}^2$ and $\hat{\boldsymbol{\theta}}$ for the model parameters can be obtained by means of the necessary condition for a maximum of L, namely by setting the partial derivative of $\ln(L)$ with respect to each independent variable equal to zero.

$$\left.\frac{\partial(\ln L)}{\partial \boldsymbol{\beta}}\right|_{\hat{\boldsymbol{\beta}}} = 0 \quad \Rightarrow \quad \hat{\boldsymbol{\beta}} = \left(\mathbf{F}^T\mathbf{R}^{-1}\mathbf{F}\right)^{-1}\mathbf{F}^T\mathbf{R}^{-1}\tilde{\mathbf{y}} \tag{4.53}$$

$$\left.\frac{\partial(\ln L)}{\partial \sigma^2}\right|_{\hat{\sigma}^2} = 0 \quad \Rightarrow \quad \hat{\sigma}^2 = \frac{1}{m}\left(\tilde{\mathbf{y}} - \mathbf{F}\,\hat{\boldsymbol{\beta}}\right)^T\mathbf{R}^{-1}\left(\tilde{\mathbf{y}} - \mathbf{F}\,\hat{\boldsymbol{\beta}}\right) \tag{4.54}$$

The partial derivative of L (or $\ln L$) with respect to $\boldsymbol{\theta}$ is hinged on the chosen correlation function. For many correlation formulations, an analytical solution does not exist, and hence, the maximum of L in $\boldsymbol{\theta}$ must be determined numerically. This means that the estimate $\hat{\boldsymbol{\theta}}$ has to be identified by use of an optimization algorithm adopting the results of Equations (4.53) and (4.54).

Using these optimal parameters for the kriging model, predictions $\hat{y}$ for the original system behavior at new coordinates $\mathbf{v}$ are available by means of the predictor

$$\hat{y} = \hat{f}(\mathbf{v}) = \hat{\boldsymbol{\beta}}^T\boldsymbol{\eta}(\mathbf{v}) + \mathbf{r}^T(\mathbf{v})\mathbf{R}^{-1}\left(\tilde{\mathbf{y}} - \mathbf{F}\,\hat{\boldsymbol{\beta}}\right) \tag{4.55}$$

with the *correlation vector*

$$\mathbf{r}(\mathbf{v}) = \left[R(\mathbf{v}, \mathbf{v}^1),\, R(\mathbf{v}, \mathbf{v}^2),\, \ldots,\, R(\mathbf{v}, \mathbf{v}^m)\right]^T \tag{4.56}$$

containing the individual correlations between the current prediction point $\mathbf{v}$ and each sampling point.

In the literature, many examples can be found where kriging models were successfully applied to structural optimization problems [SMKM98, SAM98, KWGS02, MS03].

4.4 Radial Basis Function Models

The *radial basis function model (RBF)* is a metamodel composed of a polynomial part $\eta(\mathbf{v}, \boldsymbol{\beta})$ and a sum over radial functions ψ whose independent variable is the Euclidean distance between prediction point and respective sampling point as defined in Equation (4.28).

$$y = \eta(\mathbf{v}, \boldsymbol{\beta}) + \sum_{l=1}^{m} \lambda_l \, \psi\big(d_l(\mathbf{v})\big) + \varepsilon \tag{4.57}$$

In this formulation, λ_l and $\boldsymbol{\beta}$ are the model parameters which have to be fitted to the sampled data. This metamodel type is constructed to interpolate the observations $\tilde{y}_l$ at the sampling points. Since the residuals will be zero by definition, the difference between approximation model and original system behavior (expressed by ε) is originating from model bias. Similar to the kriging method, the polynomial part of RBF models provides a global trend for the response whereas the radial functions ensure the interpolation property of the model. The radial function $\psi(r)$ can take many forms, for instance

- ◇ the linear function
$$\psi(r) = r \,, \tag{4.58}$$
- ◇ the cubic function
$$\psi(r) = r^3 \,, \tag{4.59}$$
- ◇ the *thin plate spline*
$$\psi(r) = r^2 \log r \,, \tag{4.60}$$
- ◇ the *multiquadric* function
$$\psi(r) = \begin{cases} \sqrt{r^2 + a^2} & , \quad r > 0 \,, \\ 0 & , \quad r = 0 \,, \end{cases} \tag{4.61}$$
- ◇ the Gaussian function
$$\psi(r) = \mathrm{e}^{-a\, r^2} \,, \tag{4.62}$$

with $r \geq 0$ and a constant parameter $a > 0$. After selecting a radial function type, the polynomial part of the model is chosen such that the number of regression parameters is not larger than the number of sampling points. The parameters $\hat{\boldsymbol{\lambda}}$ and $\hat{\boldsymbol{\beta}}$ that define the interpolating RBF model can be determined by solving the linear system of equations

$$\begin{bmatrix} \boldsymbol{\Psi} & \mathbf{F} \\ \mathbf{F}^T & 0 \end{bmatrix} \begin{bmatrix} \hat{\boldsymbol{\lambda}} \\ \hat{\boldsymbol{\beta}} \end{bmatrix} = \begin{bmatrix} \tilde{\mathbf{y}} \\ 0 \end{bmatrix} \tag{4.63}$$

where the matrix $\mathbf{F}$ is defined as in Equation (4.6). The matrix $\boldsymbol{\Psi}$ contains the evaluations of radial function ψ at all possible combinations of sampling points according to

$$\boldsymbol{\Psi} = [\Psi_{kl}] \quad ; \quad 1 \leq (k, l) \leq m \tag{4.64}$$

with

$$\Psi_{kl} = \psi\Big(\big\|\mathbf{v}^k - \mathbf{v}^l\big\|\Big) \quad ; \quad 1 \leq (k,l) \leq m\,. \tag{4.65}$$

To ensure that Equation (4.63) has a unique solution, the polynomial part of the model must include at minimum a constant term β_0 in case ψ is linear or multiquadric. For the cubic or thin plate spline case, a linear polynomial as introduced in Equation (4.14) is required. If ψ is the Gaussian function, the polynomial η is even allowed to vanish [Pow92].

Using the parameters $\hat{\boldsymbol{\lambda}}$ and $\hat{\boldsymbol{\beta}}$ in Equation (4.57), predictions $\hat{y}$ for the original response at new coordinates $\mathbf{v}$ can be evaluated by means of the RBF model

$$\hat{y} = \hat{f}(\mathbf{v}) = \eta(\mathbf{v}, \hat{\boldsymbol{\beta}}) + \sum_{l=1}^{m} \hat{\lambda}_l\, \psi(d_l(\mathbf{v})) \tag{4.66}$$

4.5 Artificial Neural Networks

Artificial neural networks (ANN) are motivated by the functionality of the human brain which consists of billions of *neurons* interconnected by *synapses*. Together they form a complex network which is capable of processing information, for instance storing data or reasoning [Hay99, Zel00]. The neuron is the fundamental structural component of the brain and actually the element which processes the given information. A human brain consists of up to 100 billion neurons where each neuron can cross-link with other neurons through about 10 000 synapses. Within the network, neurons are connected both in parallel and in series. This biological marvel inspired the development of artificial neural networks in digital data processing technology to model and study high-dimensional and highly nonlinear systems. Typically, ANNs are used for the prediction of response values or for recognition problems [CU93, And97].

Artificial neural networks are composed of *nodes* (also called *units*) which correspond to the neurons in human brain. The structure of ANNs is characterized by layers as exemplified in Figure 4.4. Each ANN has one input layer and one output layer whose nodes accept

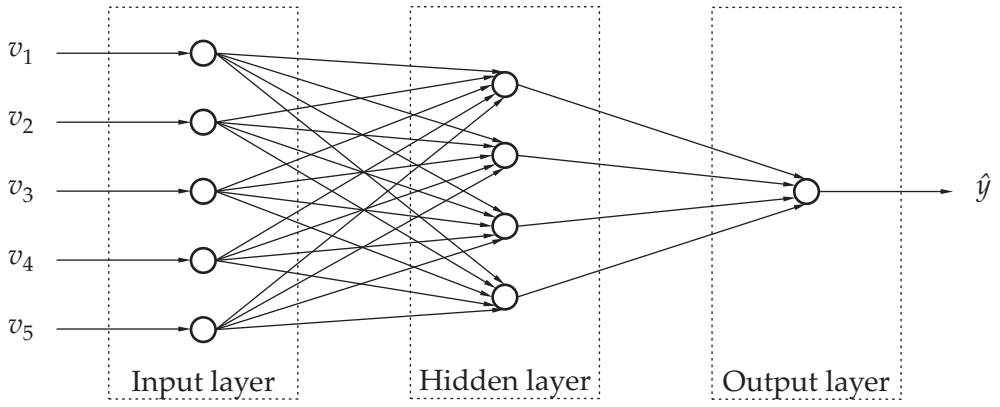

Figure 4.4: Structure of an artificial neural network with one hidden layer.

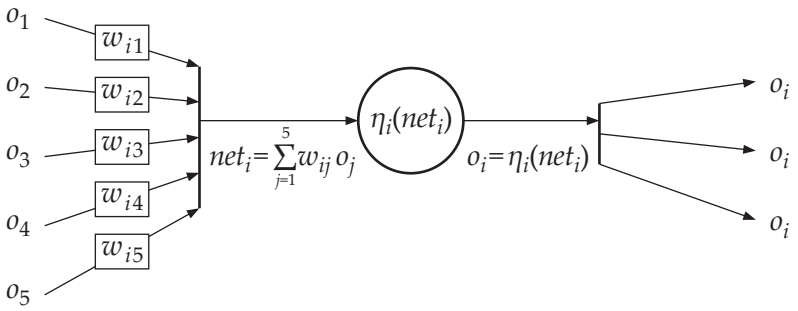

Figure 4.5: Data flow within an ANN at a single node i with anterior nodes $1-5$ and three posterior nodes.

input or produce output, respectively. Additionally, the ANN can have one or more hidden layers which contain intermediate variables.

To uniquely identify all components of the network, all nodes are continuously numbered across all layers (denoted by means of a single index i). The connections and their related quantities are addressed by doubly indexed values (index ij). In conformity with many texts in the field of ANNs, the first part i stands for the receiving unit. The second part j reveals the opposite end of the connection by the number of the emitting node. It should be noted that reverse order in the index can also be encountered in the literature. The set of nodes that are anterior to unit i define the set $A_i = \{j : \exists\, w_{ij}\}$, all nodes posterior to unit j are denoted by $P_j = \{i : \exists\, w_{ij}\}$.

The individual units i of an artificial neural network accept only one-dimensional input and transform it into nodal output o_i by the so-called *activation function* η_i. The scalar input value of a node i, which is termed *net input* and symbolized by net_i, is defined as weighted sum over output values o_j of all nodes j that are anterior and directly connected to unit i.

$$net_i = \sum_{j \in A_i} w_{ij}\, o_j \tag{4.67}$$

The individual weights w_{ij} used in Equation (4.67) are characteristic properties of the connections. The output value of node i, which is obtained from evaluation of the activation function $o_i = \eta_i(net_i)$, is passed on to all posterior nodes to contribute to their respective input. Figure 4.5 exemplifies this data flow within an artificial neural network at a representative node i. The output of units in the output layer finally represents the prediction for the response values $\hat{y}$. Hence, contrary to the statement in the introduction to the metamodeling concept, ANNs with multiple nodes in the output layer are able to approximate multidimensional response values.

As typical examples for the large variety of possible activation functions, only some representative formulations are introduced here (cf. Figure 4.6):

- the linear function

$$\eta(net) = net\ , \tag{4.68}$$

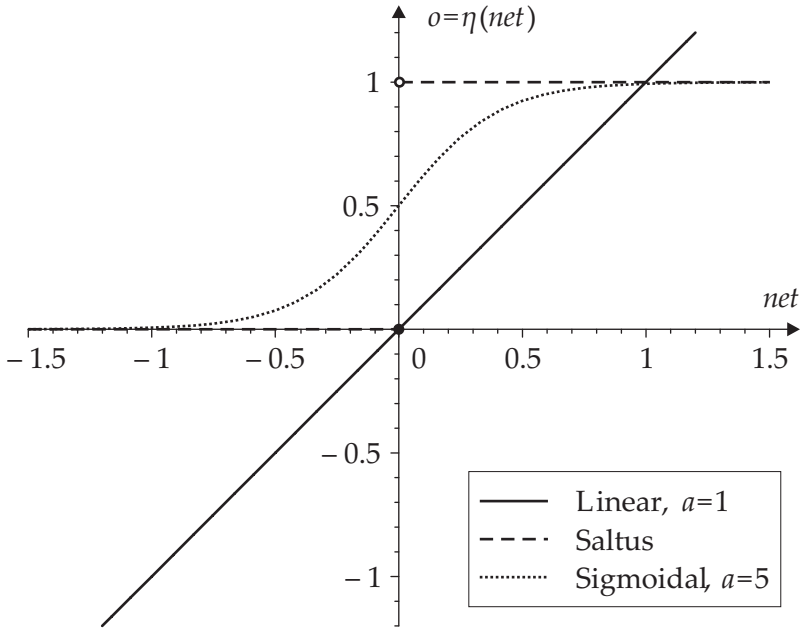

Figure 4.6: Illustration of activation functions commonly used in ANNs.

◇ the saltus function

$$\eta(net) = \begin{cases} 0 & , \quad net \leq 0 \\ & \\ 1 & , \quad net > 0 \end{cases} , \tag{4.69}$$

◇ the *sigmoidal function*

$$\eta(net) = \frac{1}{1 + \mathrm{e}^{-a\, net}} . \tag{4.70}$$

The parameter a governs the slope of the activation function. The sigmoidal activation function has two beneficial properties: First, as opposed to the linear function, the output is bounded and as a result the influence of every node is limited. This can prevent the ANN from being dominated by outliers in the training data. Second, the activation function is differentiable at any point, which is a necessary prerequisite for some methods to fit the ANN to given data.

Dependent on the configuration of the connections interlinking the individual units, two different types of ANNs are distinguished: *feedforward networks* and *recurrent networks*. In feedforward ANNs, the output of one node is only passed on to nodes in subsequent layers (cf. Figure 4.4), as opposed to recurrent ANNs, where the output of one node can also be used as input for nodes on the same layer or on preceding layers.

Before an artificial neural network can be used to approximate the behavior of a complex system, it must be fit to so-called *training data*. The training data consist of information obtained from the original problem viz. coordinates of m sampling points $\mathbf{v}^l$ together with corresponding observations $\hat{y}_l$ where $l = 1 \ldots m$. The fitting process is called *learning* (or *training*) in the context of ANNs. It is generally performed by adjusting the individual

weights of the connections (the actual degrees of freedom of an ANN). It can be seen as analog to the determination of the regression parameters $\boldsymbol{\beta}$ in RSM. Additionally, the learning phase may comprise a modification of the configuration which can either be achieved by changing the topology of the network (creation and deletion of nodes) or by varying the formulation of the activation function for particular nodes.

One of the most popular learning techniques, which can also handle network structures with hidden layers, is the *error backpropagation* method (also simply termed *backpropagation*). The description of this learning method will be derived exemplarily for feedforward networks with a one-dimensional output $\hat{y}$. A complete overview over all available techniques to train ANNs or for training of recurrent networks is beyond the scope of this text. Details on these methods can be found in the literature [And97, Hay99, Zel00].

The backpropagation method tries to minimize the prediction error E which is a function of the individual weights w_{ij}. It is defined by

$$E = \sum_{l=1}^{m} E_l \,, \tag{4.71}$$

where E_l denotes the prediction error evaluated for one element of the training set l according to

$$E_l = \frac{1}{2}(\tilde{y}_l - \hat{y}_l)^2 \,. \tag{4.72}$$

The value $\hat{y}_l$ is obtained by evaluating the ANN using $\mathbf{v}^l$ as input settings while $\tilde{y}_l$ denotes the original observation at $\mathbf{v}^l$. To identify the optimal settings for w_{ij}, a gradient-based optimization algorithm is applied to minimize the overall prediction error E. During each iteration step, the weights w_{ij} are altered by Δw_{ij}. This adjustment of the weights is carried out in direction of the negative gradient as described in Section 2.3.2

$$\Delta w_{ij} = -\alpha \, \nabla E \,, \tag{4.73}$$

where α governs the step size of the iteration steps. Expressing the gradient of E with respect to the individual weights w_{ij} in terms of E_l yields

$$\nabla E = \frac{\partial E}{\partial w_{ij}} = \frac{\partial}{\partial w_{ij}} \left(\sum_{l=1}^{m} E_l \right) = \sum_{l=1}^{m} \frac{\partial E_l}{\partial w_{ij}} = \sum_{l=1}^{m} \nabla E_l \,. \tag{4.74}$$

Hence, to compute the gradient ∇E, the partial derivatives of each E_l with respect to all w_{ij} have to be determined i.e. the m gradients ∇E_l. To reduce the number of subscripts in the following derivation, the index l denoting the currently evaluated training element is omitted for all interior variables of the ANN. To find an algorithm to compute ∇E_l, the gradient is expanded by use of the chain rule

$$\frac{\partial E_l}{\partial w_{ij}} = \frac{\partial E_l}{\partial net_i} \frac{\partial net_i}{\partial w_{ij}} \,. \tag{4.75}$$

The first factor of the expansion is called the *error signal* for unit j symbolized by δ_j. Using Equation (4.67), the second factor in Equation (4.75) can be simplified to

$$\frac{\partial net_i}{\partial w_{ij}} = \frac{\partial}{\partial w_{ij}} \left(\sum_{k \in A_i} w_{ik} \, o_k \right) = o_j \,. \tag{4.76}$$

Subsuming the definition of the error signal and Equation (4.76), Equation (4.75) can be rewritten as

$$\frac{\partial E_l}{\partial w_{ij}} = \delta_i \, o_j \; . \tag{4.77}$$

Accordingly, to determine the search direction for the descent algorithm, the output signal o and the error signal δ have to be computed for every relevant unit in the ANN. The output of all individual units o_i is obtained by propagating the input values $\mathbf{v}^l$ through the network, resulting in the approximation $\hat{y}_l$. To find the error signals of all relevant nodes, the residual $e_l = \tilde{y}_l - \hat{y}_l$ has to be propagated back through the ANN. The respective backpropagation formula can be derived from an expansion of the definition of δ_j by use of the chain rule

$$\delta_j = \frac{\partial E_l}{\partial net_j} = \frac{\partial E_l}{\partial o_j} \frac{\partial o_j}{\partial net_j} \tag{4.78}$$

The second factor of this expansion denotes the derivative of the activation function η_j with respect to its net input net_j.

$$\frac{\partial o_j}{\partial net_j} = \frac{\partial \eta_j(net_j)}{\partial net_j} = \eta_j'(net_j) \tag{4.79}$$

For the evaluation of the first factor, a distinction has to be made between units that belong to the output layer and all other units. If unit j is on the output layer, its output o_j equals the predicted response value $\hat{y}_l$. Accordingly, the derivative of E_l with respect to o_j can be found directly using Equation (4.72).

$$\frac{\partial E_l}{\partial o_j} = \tilde{y}_l - o_j \tag{4.80}$$

If unit j is not on the output layer, its error signal must be expressed in terms of its posterior nodes i. In this case, the chain rule is applied again resulting in

$$\frac{\partial E_l}{\partial o_j} = \sum_{k \in P_j} \frac{\partial E_l}{\partial net_k} \frac{\partial net_k}{\partial o_j} = \sum_{k \in P_j} \left(\delta_k \frac{\partial}{\partial o_j} \left(\sum_{j \in A_k} w_{kj} \, o_j \right) \right) = \sum_{k \in P_j} \delta_k \, w_{kj} \tag{4.81}$$

Resuming the results of Equations (4.79), (4.80), and (4.81), the individual error signals for all nodes can be computed by

$$\delta_j = \begin{cases} \eta_j'(net_j) \, (\tilde{y} - o_j) & , \quad \text{if } j \in \text{output layer} \; , \\ \eta_j'(net_j) \sum_{k \in P_j} \delta_k \, w_{kj} & , \quad \text{otherwise} \; . \end{cases} \tag{4.82}$$

With this relationship, the gradient ∇E_l in Equation (4.77) is clearly defined. To determine the gradient of the prediction error according to Equation (4.74), the process of propagating the input $\mathbf{v}^l$ through the ANN and the subsequent error backpropagation has to be performed for all m elements of the training data set.

With the gradient information available, the iteration step toward a minimal prediction error can be taken by adjusting the individual weights w_{ij} of the ANN according to

$$\Delta w_{ij} = -\alpha \sum_{l=1}^{m} \nabla E_l \; , \tag{4.83}$$

where α defines the step length of the gradient-based algorithm. It is often called *learning rate* in the context of ANNs. As presented in Section 2.3.2, the proper step length is found by a line search.

The backpropagation method introduced above is a so-called *off-line training* which means that all elements of the training set have to be evaluated before the weights are adjusted according to Equation (4.83). The additive characteristics of the update formula is often used to formulate an alternative approach, the *on-line training*. Here, the weights are modified after investigation of a single sampling point.

$$\Delta_l w_{ij} = -\alpha \, \nabla E_l \, , \tag{4.84}$$

Then, the other training points are considered one by one resulting in a consecutive tuning of the weights. This procedure is continued for all elements of the training set – and even repeated (several times) if the gradient ∇E_l is still not small enough. In this on-line training, the learning rate α is generally not determined by means of a line search but simply prescribed as a global parameter. The reason for this procedure is to save computation time. Since many other optimization steps will follow considering all other elements of the training set, it is usually sufficient to ensure a decrease in the error during each update in order to converge to a good overall fit of the ANN. In case α is a fixed parameter, a small value (for instance $\alpha \ll 1$) scales down the adjustment of weights and thus slows down the learning process. Choosing a larger value (e.g. $\alpha \geq 1$) bears the risk of overshooting the minimum in direction of $-\nabla E_l$. This overshooting may cause the error not to be reduced (or even increased) during the respective optimization step. Accordingly, it is common practice to start the backpropagation algorithm with reasonably large values for α and to lower the learning rate gradually during the training of the ANN.

The difficulties with using ANNs as surrogate models for time-consuming computer codes involve the large variety of possible layouts for the structure of ANNs and the complex implications on their predictive behavior. Moreover, the large number of parameters (weights w_{ij}) to be fit during the learning phase requires the evaluation of many sampling points to ensure a good fidelity of the model. This fact usually rules out ANNs as suitable surrogate models for problems that are expensive to analyze. Additionally, it should be noted that training of ANNs generally relies on gradient-based optimization algorithms, which only ensure convergence to local minima. Hence, the probability of finding the global minimum of the error function E can only be increased by initiating the learning phase from different starting points i.e. by varying the initial weights w_{ij}. As a consequence, establishing an ANN as useful and reliable surrogate model entails a significant computational effort in addition to the expense of evaluating the necessary sampling points.

4.6 Comparison of Metamodel Types for Stochastic Optimization Problems

In the previous sections, several metamodeling techniques have been introduced. This section offers a comparison of the individual characteristics for the presented metamodel types.

From the comparison of particular strengths and weaknesses of each formulation, a recommendation for the proper use in specific applications is derived.

In the literature, several comparative studies of metamodeling techniques have been published, for instance [BH93, CB93, Etm94, GW98, SMKM98, Alv00, JCS01, SPKA01, SLC01, Kri03, JDC03, SBG+04, FN05]. Most of these publications restrict themselves to few metamodel types and only one special application. Expectedly, these comparisons reveal that for each different kind of problem there is a distinct method that performs better than others. In [JCS01], the authors try to illuminate the predictive performance and accuracy of several metamodel formulations based on a whole set of test functions, which have been selected from [HS81]. Clearly, it is not possible to identify one class of metamodels that universally and perfectly fits any kind of function. However, several distinct statements can be formulated which can serve as a guideline for choosing the proper surrogate model for a particular problem.

RSM. Polynomial regression models are especially suitable in cases where the problem is known to be governed predominantly by low-order effects (linear or quadratic) and the number of input variables is limited ($n \leq 10$). Accordingly, these models are commonly applied in mid-range approximations. RSMs are also advantageous whenever the original response is not deterministic but exhibits significant noise (incl. numerical noise as discussed in Section 4.1). Here, the "smoothing" effect of RSMs typically causes these models to outperform all interpolating metamodel types. Example 6 on page 103 illustrates how the RSM approach smooths "noisy" observations.

When defining the setup of RSMs, the only free choice is in the regressors. On the one hand, this limited number of options makes RSM easy to handle, but on the other hand, it restricts the range of possible applications. In addition, an inadequate approximation quality of models with improper regressors cannot be improved by additional sampling points as outlined in Example 5 on page 102. Disregarding the fundamental assumption of random error, which is used to substantiate least-squares regression, induces possible pitfalls (cf. Section 4.1).

With regard to computational requirements, RSMs are very attractive. The fitting process is cheap and the effort to compute a prediction for the response is negligible – it simply requires an explicit function evaluation. Furthermore, for the solution of stochastic optimization problems, it can be advantageous to establish a linear or quadratic functional relationship between input and output. In this case, the statistical moments of the output distribution can be computed directly from statistics of the input analogously to the derivation in Section 3.3.4. RSMs also allow for a plain interpretation of the resulting model. When the model is fit on a normalized space, the regression parameters directly quantify the significance of each regressor.

MLS. The moving-least-squares approach makes use of regression techniques to define a global model based on a locally weighted polynomial approximation, which typically does not interpolate the observations. Accordingly, MLS models are favorable whenever RSMs cannot be established to be globally valid, but the function to be approximated is smooth enough such that in the proximity of the prediction point a polyno-

mial relationship can be accepted. In contrast to RSM, moving-least-squares approximations are capable of reflecting higher-order nonlinearities over the inspected region even with low-order polynomials (cf. Examples 5 and 6).

By means of the freely selectable weighting functions and their parameters, the MLS approach can be adapted to many different applications. Thus, the crucial problem is how to identify the proper weighting function and its parameters to control how fast the weight decays with the distance to sampling points.

The gain in approximation accuracy compared to RSM is countered by additional costs for the MLS prediction. For each single prediction, the individual weights for all residuals have to evaluated based on the distances between prediction point and respective sampling points. Afterwards, a separate regression analysis has to be performed for each prediction point.

Kriging. This type of metamodel is extremely flexible due to the large variety of feasible correlation formulations. If the function to be approximated is assumed to be smooth, the Gaussian correlation function is often a good choice. The combination of a polynomial model with a supplement $Z(\mathbf{v})$, which induces the interpolating nature of kriging models, allows for a more universal application. If the presumed polynomial order is not sufficient to capture the nonlinear effects of a problem, the add-on Gaussian process $Z(\mathbf{v})$ is able to make up for the deficiency. Thus, ordinary kriging (with a constant polynomial part) is often sufficient to obtain a adequate approximation as demonstrated in Example 5. Kriging models are typically very sensitive to noise because of the interpolating property. Hence, this model type should only be used if the underlying system provides reliable deterministic response values. Additionally, the accuracy of kriging models rapidly decreases if the correlation matrix becomes ill-conditioned. This effect emerges when individual sampling points are situated "too close" to each other – a problem that will be addressed again later in this text.

From a computational point of view, kriging models are less favorable. For the fitting process, an n-dimensional optimization is necessary to find the correlation parameters via maximum likelihood estimation. This usually restricts the applicability to problems with a number of input variables $n \leq 50$. Evaluating a kriging model is more time consuming than RSM since at each prediction point m distances have to be analyzed to compute $\mathbf{r}(\mathbf{v})$. Although the fitted kriging model does not provide a closed-form solution, the estimated correlation parameters $\hat{\boldsymbol{\theta}}$ enable the experienced user to roughly review the model fit. Small values for θ indicate a smooth approximation whereas large values imply highly nonlinear behavior of the prediction.

RBF. Radial basis function approximations are comparable to kriging models. Here, the flexibility to adapt to many different applications is due to the variety of radial basis functions. The accuracy of the obtained approximation is affected by the opted radial basis function and its free parameter. Similar to the problem of specifying the weighting functions for MLS approximations, there is no general rule how to find the best radial basis function for a problem. Since RBFs are constructed to interpolate the given observations, this issue is not that crucial as compared to MLS. RBFs generally yield good approximations even for highly nonlinear problems provided that enough train-

ing data have been collected at suitable sampling points. To ensure a unique solution of the fitting process, the minimum order of the polynomial part has to be observed.

In contrast to kriging, fitting an RBF model to the observations does not comprise an optimization procedure. This makes RBF approximations in general much cheaper to compute. Consequently, the restriction with respect to the number of input variables imposed on kriging models does not apply here. The time and effort required to evaluate the model at prediction points is of the same order as for kriging models and MLS approximations – in either case the distances between prediction point and all sampling points have to be evaluated. Other than MLS and kriging models, RBF approximations yield a closed form solution.

ANN. An artificial neural network is a nonlinear regression approach that is extremely versatile. One reason for this flexibility is the large diversity of possible network architectures (e.g. number of hidden layers and number of units in each respective layer). Additionally, the approximation quality can be controlled by the selection of appropriate activation functions. On the other hand, the wide range of alternatives encountered while setting up ANN approximations can pose a problem for the inexperienced user which often leads to a categorical rejection of this method. However, if employed properly, ANNs are a suitable approximation technique for high-dimensional and highly nonlinear problems.

The computational burden associated with the fitting process of ANNs is usually very high, since training consists of multiple optimization steps. To minimize the error function, it is often necessary to process the entire set of training data repeatedly. Hence, the use of ANNs can be efficient whenever the intended application involves many predictions. Due to the nested layout of ANNs, their conceivability is restricted to a graphical representation of the output. Validating model fit based on the resulting weights w_{ij} is virtually impossible.

Example 5. This example illustrates the effect of the number of sampling points and the polynomial order on the accuracy of the presented metamodels. In this comparison, ANNs are ignored because they do not base on a polynomial approximation. The original function, which is typically unknown, is assumed to have the form

$$f(v) = v^2 - 8\,v + 18\,.$$

For this function (solid gray line in Figure 4.7) approximations are fit based on response values gained at four and five sampling points (marked by circles), respectively. If the polynomial degree for the RSM approximation is chosen improperly, adding further sampling points does not improve the fidelity of the model. Figure 4.7a shows a linear RSM fitted to four sampling points. In Figure 4.7b, the same linear polynomial is fitted to five sampling points. Obviously, more points do not yield a significant improvement in accuracy. In such a case, the discrepancy between metamodel and original function is due to a systematic error, which will not vanish even for $m \to \infty$.

The MLS approximation is already better suited to reproduce the nonlinear behavior of the original function although the underlying polynomial is still linear. For the MLS models

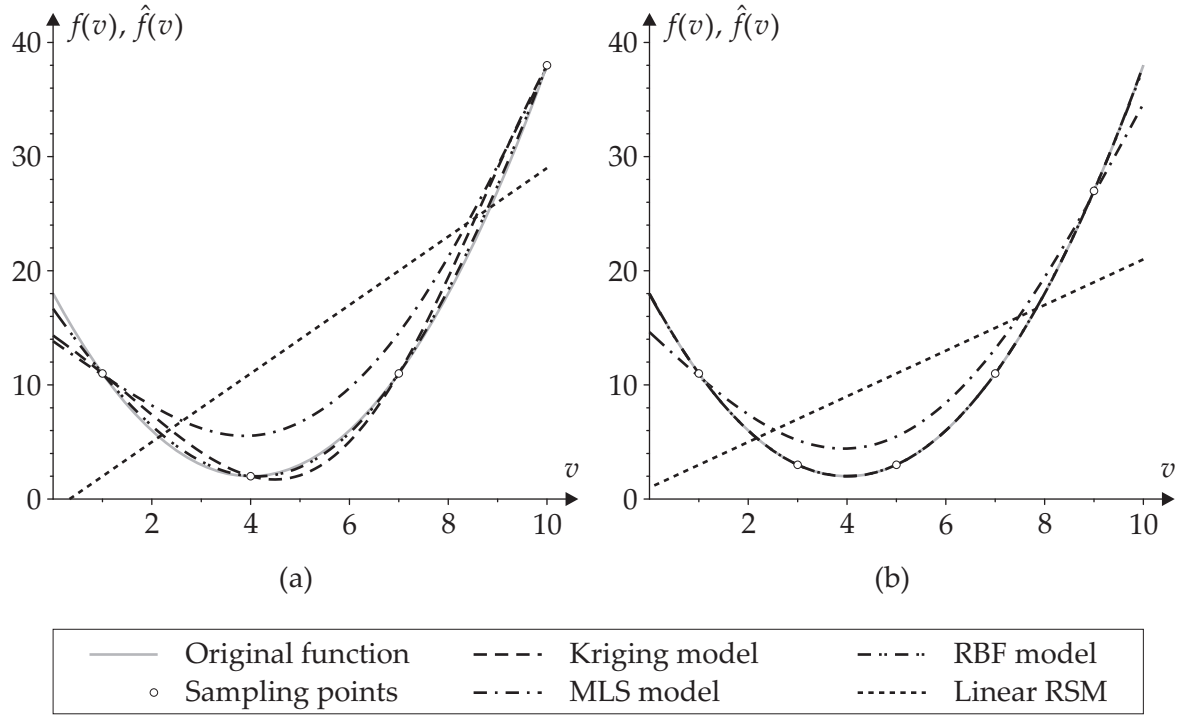

Figure 4.7: Effect of inapt polynomial order on different metamodel formulations: (a) approximation based on four sampling points and (b) approximation based on five sampling points.

depicted in Figure 4.7, Equation (4.31) is used as weighting function with $a = 0.5$. Clearly, the accuracy of the MLS approximation is improved by choosing more sampling points, but in general the observations are not interpolated.

The significance of both interpolating approximations (kriging and RBF) is much better even when based on only four sampling points. The accuracy increases further with the number of sampling points. Figures 4.7a & b show kriging models based on a zero-order polynomial (only a constant term β) and a Gaussian correlation function. Here, the spatial correlation part of the metamodel makes up for the deficiency of the polynomial part and a larger number of sampling points significantly improves the fidelity of the metamodel. Similarly, the radial basis functions enable a better predictive behavior of the RBF model. For the plotted RBF, $\psi(r)$ is a Gaussian function with $a = 0.1$. In the present case, the differences between original function and both kriging model and RBF each based on five sampling points are already so marginal that the plots are undistinguishable. Clearly, all model types would perfectly reproduce the original function, if a second-order polynomial η were used. In this case, the Gaussian random process $Z(v)$ of the kriging model vanishes with $\hat{\sigma}^2 \to 0$. For the RBF, the free parameters λ_l analogously tend to zero. □

Example 6. In Example 5 the predictive performance of different metamodeling approaches were compared in view of the approximation of a unimodal function. Here, a highly nonlinear function with many local minima is investigated, namely

$$f(v) = (v-4)^2 + 10\,\cos(2\,v)\,.$$

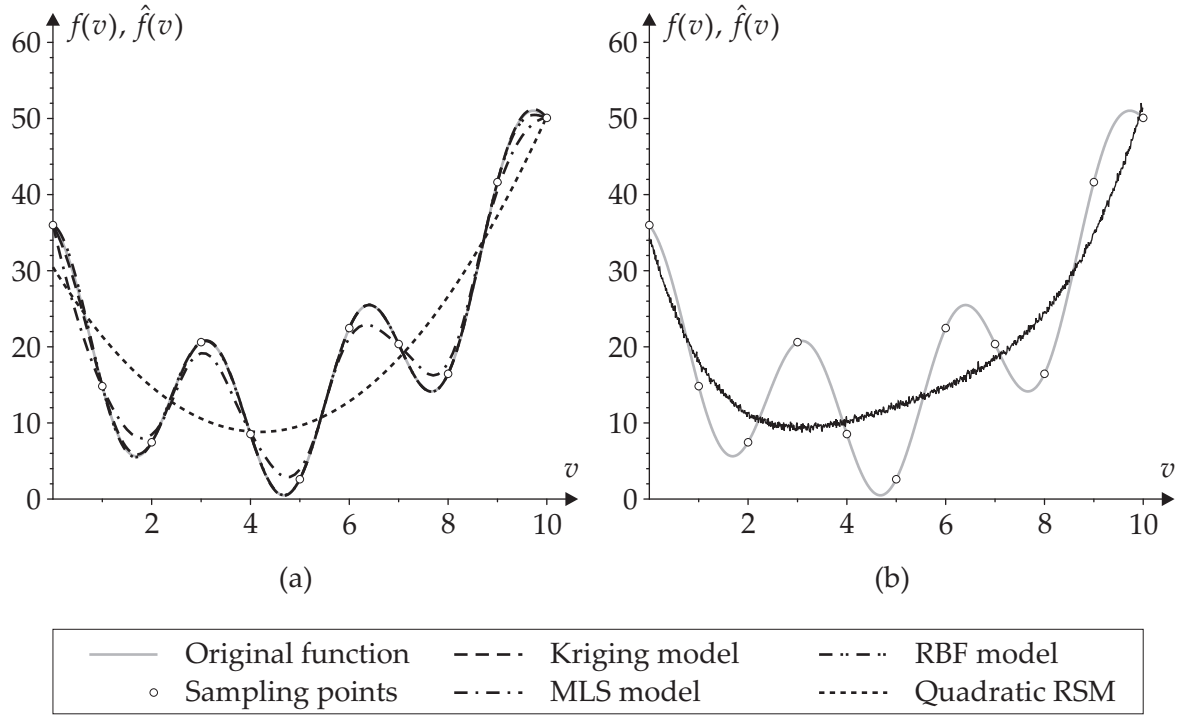

Figure 4.8: Approximation quality of different metamodel types: (a) approximation of a highly nonlinear function and (b) insufficient fit of a kriging model due to improper correlation parameter θ.

Figure 4.8a depicts the fitted approximations obtained by use of a quadratic RSM, an MLS model based on a quadratic polynomial and Gaussian weighting function ($a = 0.2$), an RBF approximation with Gaussian radial function ($a = 1$), and a kriging model. The polynomial part of both kriging and RBF model is set to a constant β. The correlation parameter of the kriging model was found by MLE to be optimal for $\theta = 5.04$. The conclusions that can be drawn from this example are similar to those for the unimodal function. The RSM approach is able to smooth the response. Here, the oscillating effect of the cosine function is either disregarded or compensated by the regression approach – depending on the purpose of the model. The MLS approach reproduces the main characteristics of the original function, however, it is not capable of retrieving the original observations at the sampling points. The approximations of kriging and RBF approach are both comparably good. During the set-up of the RBF model, a suitable setting for a has to be selected (manually), whereas the kriging model is fitted by means of the MLE approach resulting in computed correlation parameters. The optimization result of the maximum likelihood estimation should be observed carefully, since non-converged estimates can significantly disturb the approximation as illustrated in Figure 4.8b. In this case, bad initial values used for the optimization algorithm led to a diverged solution ($\theta = 0.01$). The resulting metamodel is clearly unfit as compared to the approximations in Figure 4.8a – especially in view of the high-frequency noise in the predicted response. □

In case no a-priori information at all is available about the problem characteristics, the findings of JIN et al. suggest that RBF approximations might be the most dependable

method [JCS01]. The fidelity of the resulting metamodel, however, can still be poor. Kriging models assist the user in that the MLE approach can be used to compute the optimal correlation parameters $\boldsymbol{\theta}$ at the expense of requiring an n-dimensional optimization run. In conclusion, both kriging and RBF models appear to be adequate for use in metamodel-based robust design optimization.

As already indicated earlier, the accuracy of all metamodel formulations presented above strongly depends on a qualified selection of sampling points. Consequently, the question is: How to determine coordinate settings of sampling points such that an optimal acquisition of information is achieved? This topic will be addressed in the next chapter.

Evidently, the list of metamodeling techniques presented in this chapter is not complete. The discussion of all formulations proposed in the literature could fill a voluminous textbook. Hence, only the most prominent and commonly used approaches have been discussed in the preceding sections. For more information on possible alternatives, it is referred to the survey papers of BARTON [Bar98] and SIMPSON et al. [SPKA01], as well as to the more recent textbook of FANG et al. [FLS05].

Chapter 5

Design of Experiments

The metamodeling techniques presented in Chapter 4 rely on training data which has to be collected at sampling points. The question on how to choose the coordinates for the sampling points in a best possible way is addressed by techniques called *design of experiments (DoE)*. On the one hand, it is advantageous to minimize the number of sampling points in order to reduce the experimental effort, but on the other hand, it is important to gather as much information as possible about the major characteristics of the system under investigation. Finally, the individual specification of the metamodel formulation intended for the approximation must be considered when selecting adequate coordinate settings of sampling points.

One of the pioneers of DoE methods was SIR RONALD A. FISHER, who worked in the agricultural field in the 1920s. Among other things, he studied the effects of different soil conditions and seed grades on the crop yield under varying environmental conditions. In his work, FISHER developed fundamental techniques for planning and analyzing physical experiments [Fis66]. These methods especially consider the stochastic property of experiments in presence of natural noise parameters (cf. Figure 3.2). Noise parameters, which may be obvious or unrecognized, disturb the analysis of the true fundamental relationship between controlled input and response values. To cancel the diverse effects of noise parameters, and hence, to increase the validity of conclusions drawn from physical experiments, statistical methods called *randomization*, *blocking*, and *replication* have been developed.

Randomization. Unrecognized noise parameters that affect the response values systematically may result in a misinterpretation of the true effects of input variables. To obviate this additional bias, the order in which the varied input settings are studied is randomized before evaluation. As a result, the additional error caused by the noise will be randomly distributed over all experiments. Thus, regression techniques will be able to smooth out the random error.

Blocking. Whenever deteriorating effects of prominent noise parameters are obvious or expected, blocking is used. In these cases, experiment settings are categorized in blocks that are expected to behave homogeneously within the respective group but differently compared to members of other groups. Typical examples for such prominent noise parameters are gender of subjects in clinical trials or weather conditions in outdoor experiments. Blocking allows for an individual assessment of the experiments independent of noise effects.

Replication. By means of replication, the experimental error can be estimated. Here, experiments with identical input settings are repeated several times. The sample variance for all replicates provides a measure for the expected error in the response. Additionally, the sample mean represents a more precise estimate for the expected response value than a single observation. It is important to distinguish *repeated measurements* and replicates. Multiple measurement of a response value investigating one and the same specimen solely reveals the *measurement error*, which, in general, constitutes only one part of the experimental error. In contrast, replicates allow for the estimation of the total random error associated with a physical experiment.

When applying DoE techniques, that were actually developed for the analysis of physical experiments, to the setup of *numerical experiments* (also termed *computer experiments*), there is one important aspect to be considered. Numerical experiments are inherently deterministic i.e. equal input yields the same response value up to floating point precision (unless programmed explicitly as stochastic code). Thus, the three strategies *replication*, *blocking* and *randomization* introduced to cancel random error and bias are dispensable in this context. Noise parameters that are expected to influence the response values are explicitly included in the problem formulation for the computational analysis. In this case, noise parameter settings become controllable during the engineering and design stage. This is an important prerequisite for robust design optimization, which strives for a design that is insensitive to noise during the operation period.

An *experimental design* represents a set of m experiments to be performed, expressed in terms of the n input variables v_i, which are called *factors* in the DoE context. In general, these factors contain the design variables of the problem and all controllable noise parameters. For each experiment, factor settings are fixed to specified values (called *levels*) constituting one sampling point $\mathbf{v}^l$. An experimental design is usually written in matrix form $\mathbf{X}$ (size $m \times n$) where the rows denote the individual sampling points and the columns refer to the particular factors v_i.

The proper choice for a particular DoE method depends on

- ◇ the intended utilization of the results. For instance, specific requirements relate to experimental designs used as basis for metamodels. Other prerequisites are relevant if the aim is to identify factor interdependencies or to perform a sensitivity analysis.
- ◇ prior knowledge of the type of problem to be analyzed. Pertinent characteristics comprise amongst others the nonlinearity and smoothness of the response and the identification of particularly interesting subregions in the design space vs. presumably non-relevant areas.
- ◇ additional restrictions, as for example a maximum number of acceptable sampling points, set by the effort related to their evaluation or a maximum number of levels to reduce the costs of producing physical specimens.

In the remainder of this chapter, different DoE methods are presented and their individual characteristics and areas of application together with possible restrictions are dis-

cussed. A more detailed description of standard DoE techniques can be found e.g. in [BB94, Tou94, DV97, Mon01, SWN03].

5.1 Full Factorial Designs

An experimental design is called *factorial design* if the n factors governing the system are varied only on a finite number of predefined levels l. A *full factorial design* contains all possible factor-level combinations. The total number of experiments to be performed results from the product of the respective number of discrete levels for each factor.

$$m = \prod_{i=1}^{n} l_i \tag{5.1}$$

The designation of all types of full factorial designs reflects this formation rule (cf. Figures 5.1 and 5.2): A full factorial design with n factors, each evaluated at l levels, is symbolized by l^n. Obviously, the design consists of l^n sampling points. To specify the individual settings for each sampling point, the two levels of 2^n designs are typically coded by -1 and 1, respectively (or simply $-/+$). Accordingly, -1, 0, and 1 are used to symbolize the different levels of 3^n designs. This syntax is especially helpful if the design space along each variable is normalized to the range $[-1, 1]$.

It should be pointed out that most publications on DoE denote the number of factors by k. Thus, in relevant literature, design classes are commonly termed 2^k or 3^k. The slight discrepancy compared to common notation is accepted for the sake of accordance with the rest of the text at hand.

Factorial designs are typically used for *screening experiments*. Here, the aim is to identify either especially significant factors or factors with negligible effect on the response. If factors with minor influence on the respective response value can be discovered, they can usually be excluded from further investigations. The dimensionality of a metamodel can be reduced accordingly, yielding a model formulation that is generally cheaper to fit and to evaluate.

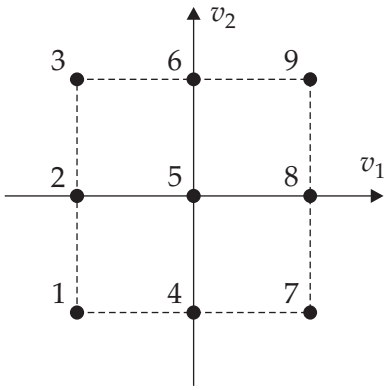

Figure 5.1: Full factorial design 3^2 – two factors varied on three levels.

Table 5.1: Setup of full factorial design 3^2.

Point No.	v_1	v_2
1	-1	-1
2	-1	0
3	-1	1
4	0	-1
5	0	0
6	0	1
7	1	-1
8	1	0
9	1	1

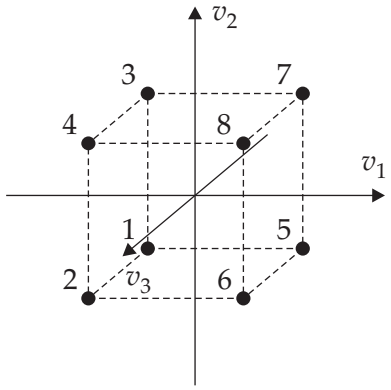

Figure 5.2: Full factorial design 2^3 – three factors varied on two levels.

Table 5.2: Setup of full factorial design 2^3.

Point No.	v_1	v_2	v_3
1	−1	−1	−1
2	−1	−1	1
3	−1	1	−1
4	−1	1	1
5	1	−1	−1
6	1	−1	1
7	1	1	−1
8	1	1	1

To assess the influence of input variables on the output, a linear model as introduced in Equation (4.3) is fit to the response values observed at the sampling points by means of least squares regression. The regressors are chosen to include all effects, the experimenter wants to assess. Each regression parameter characterizes one *effect* as it quantifies the impact of the corresponding regressor on the respective response value. The general form of a model to determine factor effects reads

$$\eta(\mathbf{v}, \boldsymbol{\beta}) = \beta_0 + \sum_{i=1}^{n} \beta_i v_i + \sum_{i=1}^{n} \sum_{\substack{j=1 \\ j \geq i}}^{n} \beta_{ij} v_i v_j + \sum_{i=1}^{n} \sum_{\substack{j=1 \\ j \geq i}}^{n} \sum_{\substack{k=1 \\ k \geq j}}^{n} \beta_{ijk} v_i v_j v_k + \dots \,. \tag{5.2}$$

In Equation (5.2), β_0 represents the mean response value. The model additionally includes *main effects* and *interaction effects*. Main effects are described by regression parameters whose corresponding regressor comprises only one factor (β_i, or $\beta_{ij\dots k}$ with identical subscripts $i = j = \dots = k$). Thus, main effect i quantifies the change in the response caused by a variation in v_i. If an effect of input variable v_i also depends on the setting of another input variable v_j, then this effect is an *interaction effect*. Interaction effects are specified by regression parameters with unequal subscripts. While 2^n designs allow only for the estimation of linear effects, 3^n designs already permit the quantification of quadratic effects. Generally speaking, to fit a polynomial of degree d, each factor has to be varied on at least $d + 1$ levels.

An increasing number of factors or levels rapidly raises the experimental effort. While a full factorial design for three factors and three levels constitutes $3^3 = 27$ sampling points, twice the number of factors (also evaluated on three levels) already yields $3^6 = 729$ experiments to be performed. One way to circumvent this problem is the use of fractional factorial designs.

5.2 Fractional Factorial Designs

A *fractional factorial design* consists of a subset of a full factorial design. These experimental designs are symbolized by l^{n-p}. As for full factorial designs, n factors are studied on l levels each. The nonnegative integer p defines the reduction compared to full factorial designs. As

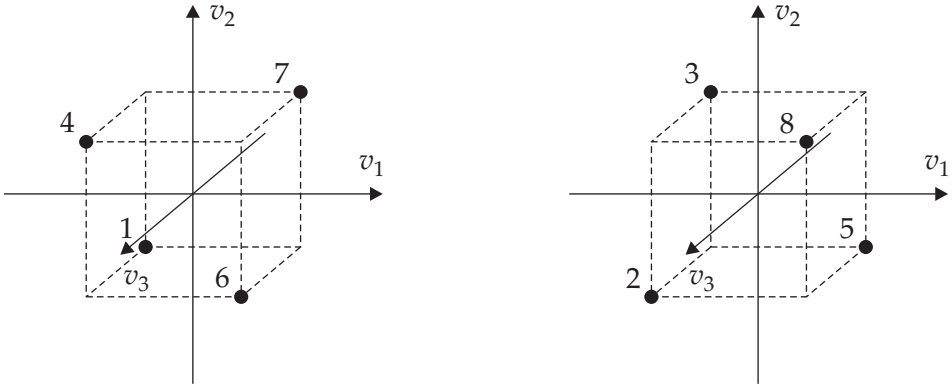

Figure 5.3: Two alternate fractional factorial designs of type 2^{3-1}.

indicated by this denomination, the total number of sampling points in a fractional factorial design is only a fraction of the corresponding full factorial design, where the fractional portion is $(1/l)^p$ of the full design. Accordingly, a 2^{3-1} design comprises half the number of experiments compared to the full factorial design ($2^{3-1} = 2^3/2^1 = 4$ sampling points). Both halves of a 2^3 design, which are both equitable choices for a fractional factorial design, are depicted in Figure 5.3. The coordinates of the respective sampling points are listed in Table 5.2.

As discussed in [Mon01], the use of fractional factorial designs is justified through

- ◇ the *sparsity of effects principle*. If a system depends on numerous input variables, it is most likely governed primarily by few main effects and low-order interactions. The disregard of higher-order interactions makes it possible to reduce the number of required sampling points.

- ◇ the *projection property of* 2^{n-p} *designs*. If p of the n factors are identified as insignificant and hence excluded from further investigations, the corresponding dimensions of the design space vanish. As a result, the sampling points are projected into the remaining $(n-p)$-dimensional subspace. With respect to the remaining $n-p$ factors, the originally fractional factorial design becomes a full factorial design (cf. Figure 5.4).

- ◇ *sequential experimentation*. Each fractional factorial design l^{n-p} represents a fragment of the underlying full factorial design l^n and this fragment is complementary to all alternative fractions (cf. Figure 5.3). Accordingly, a more significant and larger design (up to the full factorial design) can be assembled by sequentially sampling the l^p complementary fractions.

The composition of other fractional factorial designs is specified and illustrated in many reference books dealing with design of experiments e.g. [BB94, Mon01].

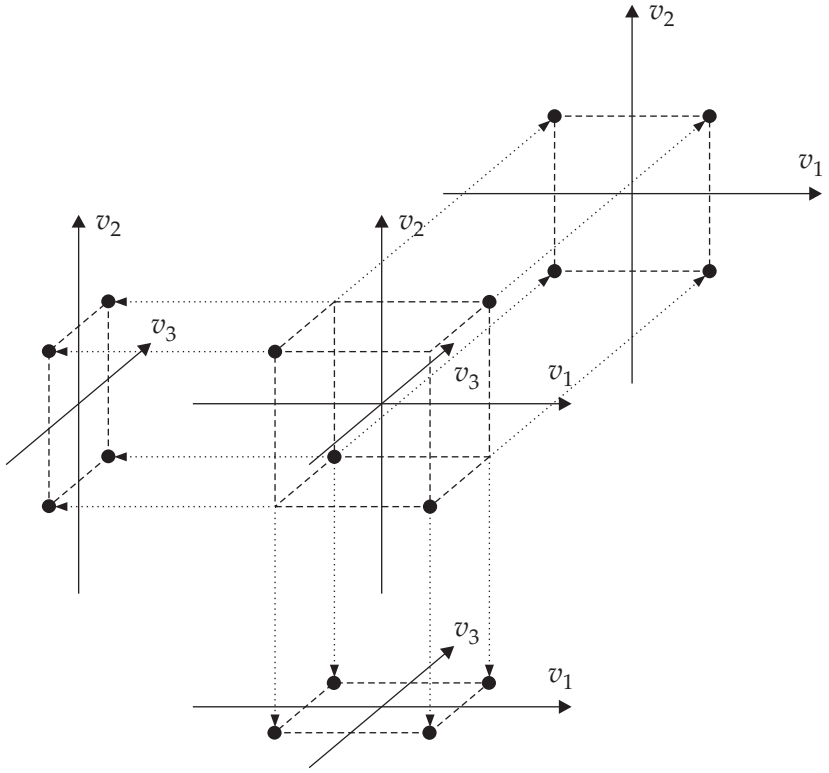

Figure 5.4: Projection of a 2^{3-1} design into three 2^2 designs.

5.3 Orthogonal Arrays

To describe orthogonal arrays, the definition of *orthogonality* in the DoE context has to be introduced first. An experimental design is *orthogonal* if the scalar product of any combination of its column vectors evaluates to zero. In other words, if a design is orthogonal, then $\mathbf{X}^T\mathbf{X}$ describes a diagonal matrix. This property assures a minimum variance in the parameters $\boldsymbol{\beta}$ when using linear regression. In fact, all full factorial designs of type 2^n and 3^n as well as all resultant fractional factorial designs 2^{n-p} and 3^{n-p} are orthogonal.

The *resolution R* is an important attribute of an experimental design [Mon01]. It explains to which extend main and interaction effects can be estimated independently. An experimental design has resolution R if no effect of p factors is confounded with any effect that includes less than $R - p$ factors. Resolution values are represented by Roman numerals. Most prominent resolutions are:

Resolution III. No main effect is confounded with any other main effect. Yet, main effects may be confounded with two-factor interactions, and interactions may be confounded among each other.

Resolution IV. Main effects are not confounded either with another main effect or with any two-factor interaction. Two-factor interactions may be confounded.

Table 5.3: Comparison of full factorial designs and orthogonal arrays with respect to their total number of sampling points.

Levels	Factors	Sampling Points Full Factorial Design			Sampling Points Orthogonal Array
2	3	2^3	=	8	4
2	7	2^7	=	128	8
2	15	2^{15}	=	32 768	16
3	4	3^4	=	81	9
3	13	3^{13}	=	1 594 323	27
4	5	4^5	=	1 024	16
4	21	4^{21}	=	4 398 046 511 104	64

Resolution V. Neither main effects nor two-factor interactions are confounded with any other main effect or two-factor interaction.

Based on the resolution of experimental designs and the definition of orthogonality, a special class of designs can be characterized. A full or fractional factorial design that is orthogonal and has resolution $R = \text{III}$ is termed *orthogonal array (OA)*. Supplementary to the previously introduced denomination, orthogonal arrays are commonly designated by l_{III}^{n-p}. Orthogonal arrays are focused on the assessment of main effects, whose number may be large. In case particular factor interactions are also of interest, these interactions have to be introduced explicitly as independent factors, for instance $v_3 = v_1 v_2$. As illustrated in Table 5.3, the number of sampling points in OAs are significantly smaller than in corresponding full factorial designs. This reduction and the saved effort is compensated by the limitation to consider only main effects. Before using OAs, it must be reviewed carefully whether main effects are sufficient to capture the distinctive behavior of the system under consideration. Prominent orthogonal arrays are listed e.g. in [Pha89].

5.4 PLACKETT-BURMAN Designs

PLACKETT and BURMAN introduced the construction of very economical designs. A *PLACKET-BURMAN design (PBD)* can be used efficiently in screening experiments when only main effects are of interest. A PBD with m experiments may be used for a problem containing up to $n = m - 1$ factors. These designs must be used very carefully though since all main effects are in general heavily confounded with two-factor interactions (resolution III). PBDs are defined for the case where the number of sampling points m is a multiple of four [PB46]. In case m is also a power of two, the resulting designs are identical with the respective 2^{n-p} fractional factorial designs. Still, PBDs can be an attractive choice for screening experiments in some special cases e.g. for $m = 12, 20, 24, 28,$ and 36. The layout for these designs is specified for instance in [MM02].

5.5 Experimental Designs for Fitting RSMs

Supplementary to DoE characteristics for screening experiments, experimental designs for response surface models based on computer simulations should offer the following features:

- ◇ assure a reasonable distribution of sampling points (and hence gained information) throughout the model space,
- ◇ allow designs of higher order to be built up sequentially,
- ◇ provide precise estimates of the model coefficients,
- ◇ limit the prediction variance of the metamodel,
- ◇ bring about a constant level of prediction variance throughout the model space,
- ◇ require a minimum number of runs.

In general, these attributes are conflicting. Hence, different aspects must be balanced to find a suitable experimental design for each particular application. As presented in Section 5.3, one important aspect is orthogonality.

Orthogonal designs to fit first-order polynomials include all full and fractional factorial designs of type 2^n and 2^{n-p}. Yet another first-order design is the *simplex design*. A simplex design contains the minimum number of experiments needed to fit a plain first-order polynomial, namely $n + 1$ sampling points. Figure 5.5a depicts the two-dimensional case where the simplex design is an equilateral triangle. All alternative configurations that arise from rotating the triangle around the origin are equitable. For $n = 3$, the simplex design is a regular tetrahedron which can also be rotated to find alternative designs. From Figure 5.5b it becomes obvious, that the three dimensional simplex design complies with the 2^{3-1} fractional factorial design depicted in Figure 5.3.

In many engineering applications, linear polynomials are not adequate to approximate the true functional relationship. In these cases, quadratic polynomials are typically used

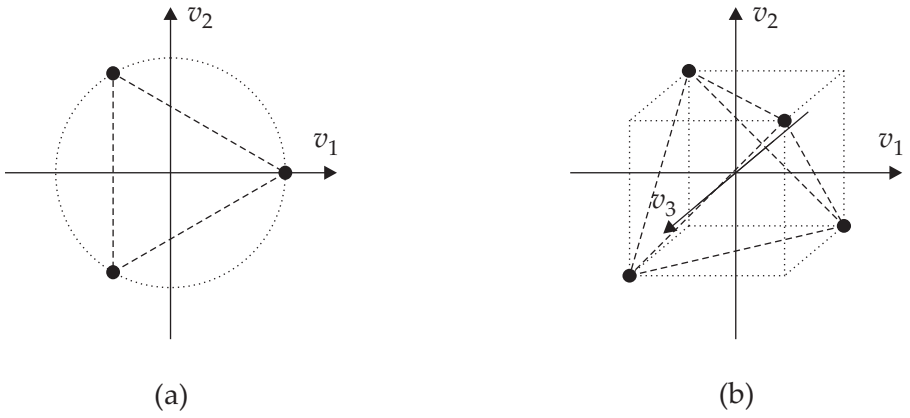

Figure 5.5: Simplex design (a) for two factors and (b) three factors.

to fit metamodels. Accordingly, experimental designs for quadratic response surfaces are discussed next. A 3^n factorial design provides three levels along each factor. Hence, it can be used to fit a quadratic polynomial. As already mentioned before, 3^n designs are also orthogonal, however, the resultant number of sampling points is often unacceptably large. Furthermore, they fail at another decisive criterion: *rotatability*. An experimental design is called *rotatable*, if the variance of the attained prediction

$$V(\hat{y}(\mathbf{v})) = \sigma^2 \, \boldsymbol{\eta}^T(\mathbf{v}) \left(\mathbf{F}^T\mathbf{F}\right)^{-1} \boldsymbol{\eta}(\mathbf{v}) \tag{5.3}$$

is only a function of the distance from the prediction point $\mathbf{v}$ to the center point of the factor space (in normalized space: $v_i = 0 \;\; \forall \;\; i = 1 \ldots n$) and not a function of the direction. To illustrate the idea, the case of a quadratic polynomial used as metamodel in an optimization procedure is considered. Taking the center point as starting point, it would be unfavorable to rely on a metamodel whose fidelity depends on the search direction since this could severely affect the optimization process. Further implications of using metamodels in an optimization procedure will be discussed in Chapter 6. While all two-level orthogonal designs are rotatable, the 3^n design and all its fractions are not rotatable, and hence, in general not an appropriate choice for response surface models.

5.5.1 Central Composite Designs

The most popular experimental design for fitting quadratic polynomials is the *central composite design (CCD)*. It is a combination of a two-level full factorial design (or a fractional factorial design of resolution V), one *center point*, and a set of so-called *star points*. The star points are situated on all coordinate axes with a distance α from the origin both in positive and negative direction. In case the analyzed system is not deterministic, the number of center points can be increased in order to create replicates. A typical three-dimensional CCD is depicted in Figure 5.6. By choosing the distance α appropriately, rotatability of the design can be retained [Mon01]. For

$$\alpha = \sqrt[4]{m_\mathrm{F}} \tag{5.4}$$

the resulting CCD is rotatable. Here, m_F denotes the number of sampling points in the factorial part of the design.

In fact, rotatability is one important criterion to control the prediction variance, but it is not the only one. Rotatability ensures that prediction variance is equal on spheres around the center point. Additionally, it would be desirable to have a prediction variance that is both constant and as small as possible throughout the entire model. Here, two typical shapes of investigated regions are distinguished: spherical and cuboidal regions, respectively.

Spherical Region. If the region under consideration is spherical, the CCD that has the most advantageous distribution of the prediction variance is obtained by choosing $\alpha = \sqrt{n}$. For the resulting design, all factorial and star points are situated on a (hyper)sphere with radius $\sqrt{n}$. Accordingly, this specific experimental design is called *spherical CCD*. The spherical CCD is not rotatable, but the deviation from perfect rotatability is compensated through a more consistent and small $V(\hat{y})$.

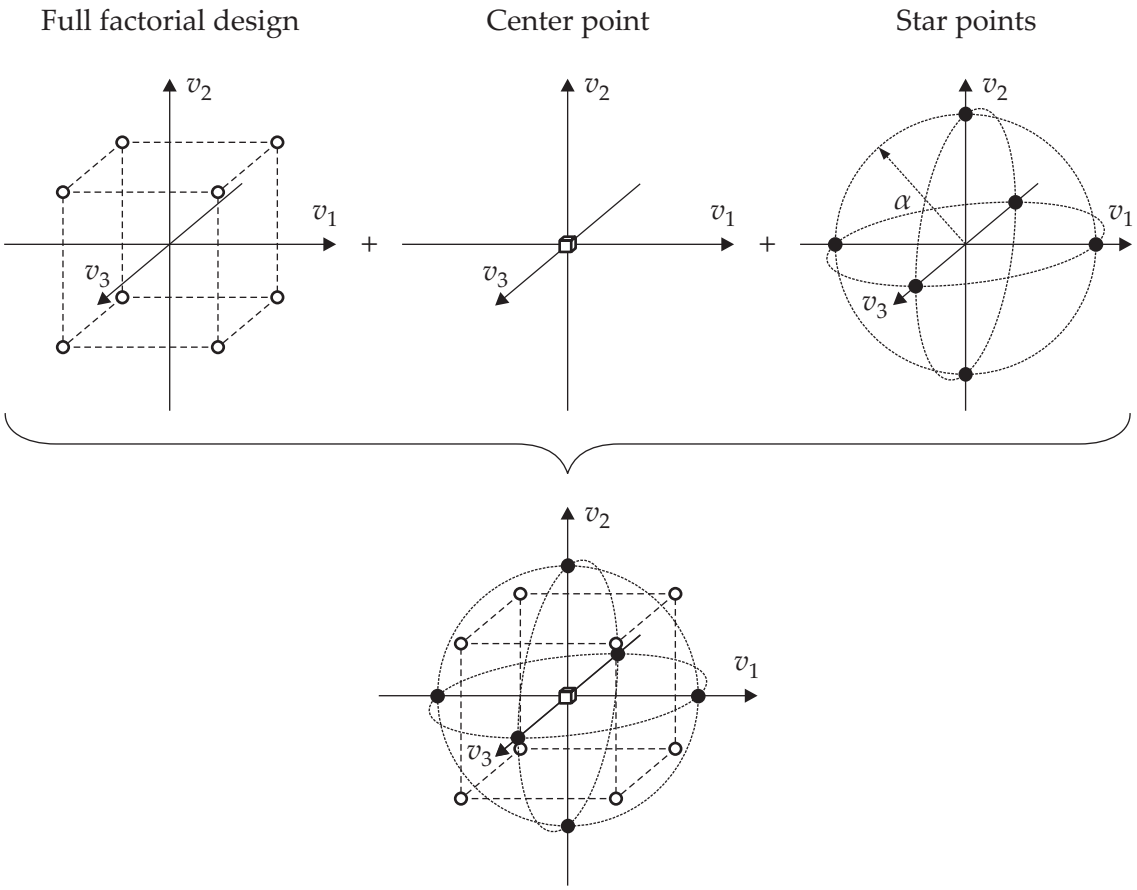

Figure 5.6: Assembly of a central composite design for three factors.

Cuboidal Region. Typically, the designing engineer specifies ranges for each factor which restrict the space of allowable factor settings to a cuboidal region. In these cases, the *face-centered central composite design (FCD)* defined by $\alpha = 1$ is a suitable choice. As indicated by the name and illustrated in Figure 5.7, the star points of an FCD are located at the centers of the faces defined by the factorial part. As a result, the prediction variance is relatively uniform over large parts of the investigated (cuboidal) region including the vertices. More details about the prediction variance can be found in [MM02].

Referring to the important features, which were listed at the beginning of Section 5.5, CCDs constitute an attractive class of experimental designs for response surface models. Their assembly allows naturally for sequential experimentation: First, a fractional factorial design is used, for instance for screening experiments. In a second step, a full factorial design is obtained either by excluding insignificant factors (using the projection property) or by sampling the missing complementary parts. Finally, to fit a second order polynomial and to achieve a uniform prediction variance, center and star points can be added.

Comparing CCDs to 3^n designs reveals, that CCDs are in general more efficient with respect to the number of sampling points (cf. Table 5.5). The 3^2 design is, in fact, equal to the two-level FCD. With increasing number of factors, however, the 3^n design rapidly reaches an immense number of experiments.

Table 5.4: Setup of CCD with three factors.

Point No.	v_1	v_2	v_3
1	-1	-1	-1
2	-1	-1	1
3	-1	1	-1
4	-1	1	1
5	1	-1	-1
6	1	-1	1
7	1	1	-1
8	1	1	1
9	$-\alpha$	0	0
10	α	0	0
11	0	$-\alpha$	0
12	0	α	0
13	0	0	$-\alpha$
14	0	0	α
15	0	0	0

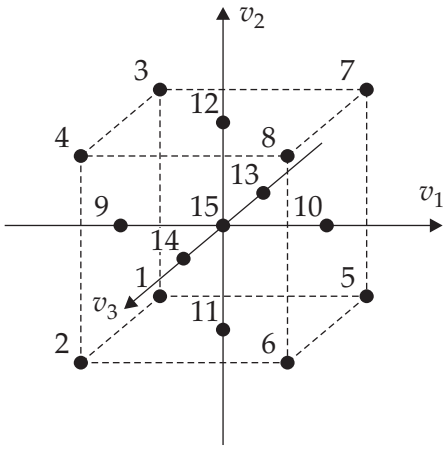

Figure 5.7: Face-centered central composite design ($\alpha = 1$) for three factors.

5.5.2 BOX-BEHNKEN Designs

Closely related to the CCD but avoiding extremal factor settings (vertices of the factor space) is the *BOX-BEHNKEN design (BBD)*, which is illustrated in Figure 5.8. The BBD is a spherical design, in which all points have the same distance to the center point (with the obvious exception of the center point itself). As a result, BBDs are rotatable or at least nearly rotatable. They are frequently used when the evaluation of extremal factor settings is related to excessive costs. Since no experiments are performed at extremal factor settings, a BBD is not suited for predicting response values at the vertices of the factor space.

For the case of three, four, or five factors, BBDs are constructed as follows. First, the

Table 5.5: Comparison of CCDs with one center point to 3^n full factorial designs.

Factors	Sampling Points CCD			Sampling Points 3^n Design
	m_F	Star Points	Total	Total
2	4	4	9	9
3	8	6	15	27
4	16	8	25	81
5	32	10	43	243
6	64	12	77	729

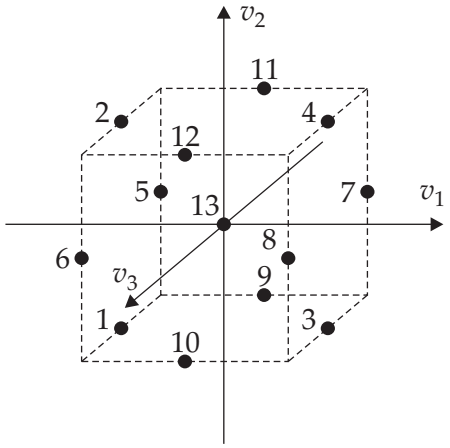

Figure 5.8: BOX-BEHNKEN design for three factors.

Table 5.6: Setup of BBD with three factors.

Point No.	v_1	v_2	v_3
1	−1	−1	0
2	−1	1	0
3	1	−1	0
4	1	1	0
5	−1	0	−1
6	−1	0	1
7	1	0	−1
8	1	0	1
9	0	−1	−1
10	0	−1	1
11	0	1	−1
12	0	1	1
13	0	0	0

factors are paired off in all possible combinations. Then, for each pair, a 2^2 full factorial design is established in which the remaining factors are set to zero. Finally, one center point is added. Again, if the system under inspection is not deterministic, the number of center points should be augmented to create replicates. In Table 5.6, sampling points 1 – 4 emerge from a 2^2 design for factors v_1 and v_2 with v_3 set to zero for all four experiments. Analogously, points 5 – 8 and 9 – 12 originate from combinations (v_1, v_3) and (v_2, v_3), respectively. Lastly, the single center point is listed on position 13. For $n \geq 6$, the approach is slightly different, as described in detail in [MM02].

5.5.3 Optimality Criteria Designs

Although the standard experimental designs discussed before are generally very efficient, there are situations where they are not suitable. Such situations include an irregular region of interest, which is not a (hyper)cube or (hyper)sphere, or nonstandard polynomial models i.e. models that consist of selected monomials only (in contrast to full linear or quadratic polynomials). In these cases, computer-generated experimental designs can be used, which are constructed using particular optimality criteria. These optimality criteria are based either on the prediction variance as introduced in Equation (5.3) or on information about the variance of the regression parameters described by the covariance matrix

$$\mathrm{Cov}(\boldsymbol{\beta}) = \sigma^2 \left(\mathbf{F}^T\mathbf{F}\right)^{-1} . \tag{5.5}$$

For a given set of regressors $\boldsymbol{\eta}$, the variance in the regression parameters and the prediction variance only depend on the experimental design. The sampling point coordinates affect the matrix $\mathbf{F}$ and hence $\left(\mathbf{F}^T\mathbf{F}\right)^{-1}$. To minimize $\mathrm{Cov}(\boldsymbol{\beta})$, a characteristic (scalar) value for the assessment of a matrix has to be chosen. Clearly, several qualified options exist:

D-Optimality. An experimental design is called *D-optimal* if the determinant of $\left(\mathbf{F}^T\mathbf{F}\right)^{-1}$ is minimized. This criterion can also be interpreted geometrically as minimizing the volume of the dispersion ellipsoid for $\boldsymbol{\beta}$ [BB94].

A-Optimality. An experimental design is called *A-optimal* if the trace of $\left(\mathbf{F}^T\mathbf{F}\right)^{-1}$ is minimized. The geometrical equivalent of this criterion is the mean length of the semi-axes of the dispersion ellipsoid for $\boldsymbol{\beta}$ to be minimal.

E-Optimality. An experimental design is called *E-optimal* if the largest eigenvalue of $\left(\mathbf{F}^T\mathbf{F}\right)^{-1}$ is minimized. Geometrically, this accords with a minimization of the largest semi-axis of the dispersion ellipsoid for $\boldsymbol{\beta}$.

G-Optimality. An experimental design is called *G-optimal* if the maximum prediction variance as defined in Equation (5.3) is minimized.

V-Optimality. An experimental design is called *V-optimal* if the average prediction variance is minimized.

Effective methods to determine an experimental design according to these criteria usually proceed as follows. First, a set of regressors is chosen for a specified region of interest. Second, a number of experiments to be performed is fixed. Then, an optimality criterion is picked. Finally, experimental designs are composed from a selected set of candidate points and compared with other design combinations. The restriction to a predefined set of sampling points to be considered (typically from a grid of points spaced over the feasible design region) significantly reduces the computational effort to find an "optimal" design. Clearly, the design which is found as a result of this procedure is in general not optimal in a global sense. Yet, it represents the best design which only relies on the selected set.

5.6 Experimental Designs for Interpolating Models

The essential features of experimental designs established in Section 5.5 for polynomial regression models similarly apply to all other surrogate models. For metamodel formulations that interpolate the observations at all sampling points, however, emphasis on individual aspects is perforce placed differently.

In fact, for all metamodels a minimal prediction variance, and hence, a minimal approximation error is deemed the most important criterion. In many cases, the prediction variance cannot be determined a priori. For instance, the prediction variance of the kriging predictor $\hat{y} = \hat{f}(\mathbf{v})$ is expressed by the *mean squared error (MSE)*

$$\mathrm{MSE}\left(\hat{f}(\mathbf{v})\right) = \sigma^2 \left(1 - \begin{bmatrix} \boldsymbol{\eta}^T(\mathbf{v}) & \mathbf{r}^T(\mathbf{v}) \end{bmatrix} \begin{bmatrix} \mathbf{0} & \mathbf{F}^T \\ \mathbf{F} & \mathbf{R} \end{bmatrix} \begin{bmatrix} \boldsymbol{\eta}(\mathbf{v}) \\ \mathbf{r}(\mathbf{v}) \end{bmatrix}\right) . \tag{5.6}$$

To evaluate the MSE, the correlation parameters $\boldsymbol{\theta}$ have to be known (cf. definition of $\mathbf{R}$ and $\mathbf{r}$). The estimation of $\boldsymbol{\theta}$, however, is part of the fitting process and yet depends on the sampled observations. Consequently, it is not possible to identify the optimal design with

respect to prediction variance, if the correlation parameters are not known in advance. Then again, it can be seen from Equation (5.6) that the distance between the current prediction point **v** and the surrounding sampling points play an important role for the fidelity of the metamodel. Intuitively, it makes sense that for an interpolating model, its approximation quality depends on the distance to the surrounding sampling points. Due to the interpolation property and the deterministic characteristics of the underlying observations, the error at any sampling point vanishes, hence, the prediction variance must be exactly zero at these points. If both the original function and the surrogate model are continuous functions, the possible approximation error will increase with the distance of the prediction point to the sampling point. As a consequence, the so-called *space-filling property* will be stressed in the context of interpolating metamodels. This feature ensures that the sampling points are evenly spread over the entire factor space. As a result, the distance to the nearest sampling points does not become too large for an arbitrary prediction point. Although it was already postulated for polynomial regression models that a reasonable distribution of the experiments throughout the factor space is desirable, this criterion was disregarded in favor of an explicit examination of prediction variance and variance of the regression parameters.

5.6.1 Space-Filling Designs

One possibility to create an even distribution of sampling points is to superimpose an n-dimensional equidistant grid on the factor space as illustrated in Figure 5.9a. Designs that are defined by means of a grid have two main drawbacks. First, the designer cannot arbitrarily choose the number of sampling points to be included. The total number of experiments is a result of the segmentation along each factor. Second, in case irrelevant factors are detected, a projection of the design onto a subspace with reduced dimensionality would yield many replicated points.

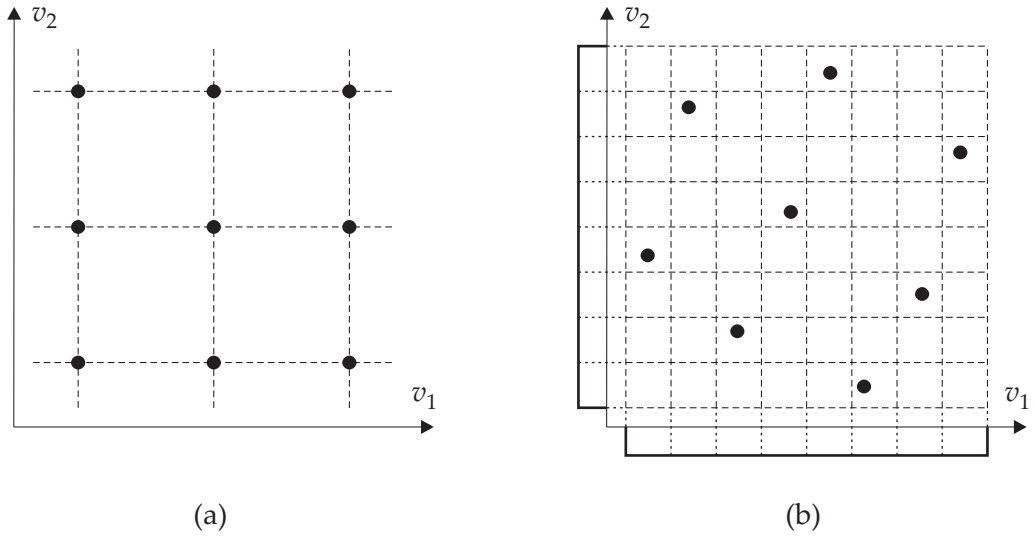

Figure 5.9: Examples for space-filling designs: (a) design based on an equidistant grid ($m = 3^2 = 9$), and (b) Latin hypercube design with $m = 8$.

As an alternative, a distance-based criterion can be applied to assure a space-filling property of the design [JMY90]. One possibility to define such a criterion is the minimum Euclidean distance between any two sampling points $\mathbf{v}^k$ and $\mathbf{v}^l$ pursuant to Equation (4.27). A design that maximizes this criterion is called *maximin distance design*. This criterion guarantees that no two points are "too close" to each other. An alternative criterion to assess the distribution of the experiments is to determine the maximum distance between an arbitrary prediction point to its closest sampling point. A design that minimizes this criterion is said to be a *minimax distance design*. Obviously, setting up an optimal experimental design solely based on the above mentioned distance criteria would be complex since an infinite number of designs would have to be studied. A commonly applied method to reduce this effort is to primarily restrict the number of candidate designs by a another criterion, which is cheap to evaluate, before the distance criterion is applied.

5.6.2 Latin Hypercube Designs

Latin hypercube sampling offers an attractive method to construct experimental designs that are unpretentious from a computational point of view. The setup of such a design, which is called *Latin hypercube design (LHD)*, is exemplified in Figure 5.9b. In a first step, the factor space is normalized i.e. each factor is scaled to have the range [0,1]. Under this condition, the dimensions (length, distances) will be comparable across different factors. As described in Section 3.3.3, the (normalized) factor space is segmented by dividing the range of each factor into m strata. Accordingly, the factor space is split into m^n cells. Since an even distribution of the sampling points is desired, the probability density function for each factor is assumed to be uniform. As a result, all individual strata have equal width. Then, a subset of m cells is selected at random such that each stratum is only addressed once. In each of the m subset cells, one sampling point is placed – typically in the center of the cell. Alternatively, the position of a sampling point within the cell can also be allocated by random sampling following a uniform distribution. The resulting LHD evenly spreads the m observations over the range of each individual factor. As a result, LHDs possess a beneficial projection property. The segmentation of the factor space into strata guarantees that no replicates are generated when the number of crucial factors is reduced after screening. In general, however, a Latin hypercube design does not have to be space-filling with respect to the entire factor space as illustrated in Figure 5.10a.

Since the construction of numerous LHDs requires only modest time and effort, they offer an attractive possibility to restrict the number of designs for which a distance criterion will be evaluated (cf. Section 5.6.1). Although the number of designs used to evaluate the distance criterion is reduced to a finite number of randomly generated LHDs, the computational effort to evaluate the minimax distance criterion, is still significantly larger compared to the maximin distance criterion. While for the latter, merely all possible combinations of two sampling points (resulting in $m(m-1)/2$ pairs) have to be evaluated per candidate design, the minimax distance criterion theoretically requires the analysis of an infinite number of prediction points to identify the decisive maximum distance. This makes the *minimax distance LHD*, although perfectly consistent with the originally postulated attribute for interpolating metamodels, inappropriate for most applications. A *maximin distance LHD* for

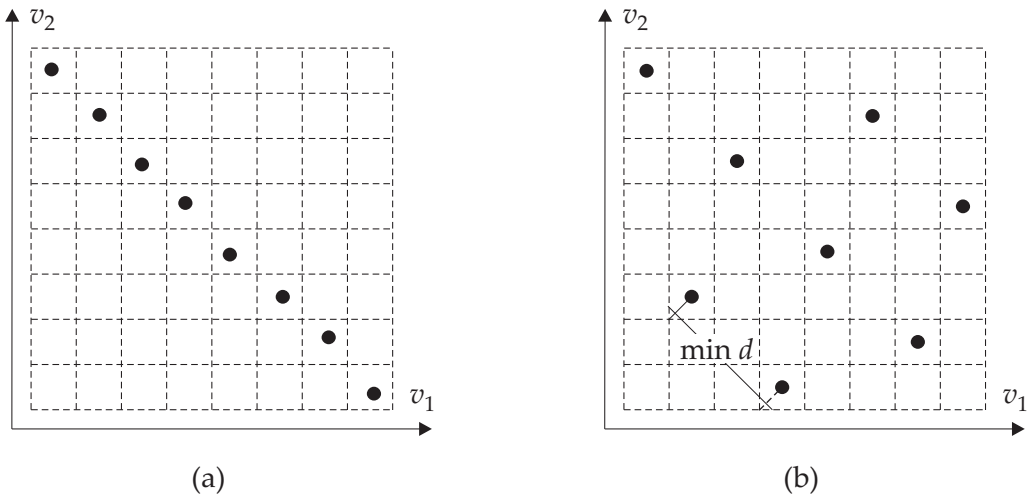

Figure 5.10: Space-filling property of Latin hypercube designs with $m = 8$ sampling points: (a) design with poor spatial distribution, and (b) maximin distance design.

two factors and $m = 8$ sampling points is depicted in Figure 5.10b.

OWEN introduced a further approach to generate space-filling designs which are developed from standard OAs. The resulting designs are called *randomized orthogonal arrays* [Owe92] which are, in fact, Latin hypercube designs. Randomized orthogonal arrays that are based on OAs with $m = l^2$ experiments where each factor is varied on l levels have the attractive feature that a projection onto any two-factor subspace will yield a regular $l \times l$ grid. Further comments on randomized orthogonal arrays can also be found in [Tan93]. The approach is also suitable for the application of the maximin distance criterion as shown in [Tan94].

The concept of space-filling *nested designs* is introduced in [Hus06]. A group of designs is called *nested* when it consists of N separate designs, which are constructed such that one design is a subset of another, namely $\mathbf{X}_1 \subseteq \mathbf{X}_2 \subseteq \ldots \subseteq \mathbf{X}_N$. Nested designs are helpful especially in the context of validating a metamodel. In this case, the number of designs is typically chosen as $N = 2$. Consequently, the set $\mathbf{X}_1$ can be used as a training set for fitting the metamodel, whereas the sampling points defined by $\mathbf{X}_2 \setminus \mathbf{X}_1$ are used for validating purpose. After validation, the entire experimental design $\mathbf{X}_2$ can be used with the validated model parameters. Due to the special construction of these nested designs, the space-filling property is maintained for the larger design $\mathbf{X}_2$. Furthermore, nested designs can be used for sequential sampling (cf. Chapter 6). In this case, an initial design $\mathbf{X}_1$ can be augmented by the sampling points in $\mathbf{X}_2 \setminus \mathbf{X}_1$ yielding the enlarged design $\mathbf{X}_2$.

The approach of AUDZE and EGLAIS [AE77] uses the physical analogy of the minimum potential energy to find optimal Latin hypercube designs with a uniform distribution over the factor space. In accordance with the formulation of LHDs, the factor space is divided into m strata with only one sampling point per stratum. The sampling points are assumed to have unit mass which is affected by repulsive forces. The magnitude of these forces is presumed to be inversely proportional to the squared distance between the points. This

yields the following expression for the potential Π to be minimized:

$$\Pi = \sum_{l=1}^{m} \sum_{\substack{k=1 \\ k \geq l}}^{m} \frac{1}{d_{kl}^2} \tag{5.7}$$

To find the specific arrangement of points in factor space that results in minimum potential energy is in fact a discrete problem. For a fixed number of experiments m and predefined number of factors n, only a finite number of combinations of cells has to be examined – more precisely $(m\,!)^n$ different combinations are possible. Obviously, even a moderate number of factors and sampling points results in an immense number of designs to be investigated, e.g. ten experiments arranged in a three-dimensional factor space offer $(10\,!)^3 \approx 4.8 \cdot 10^{19}$ different layouts. To handle the computational burden associated with these scores, genetic permutation algorithms have been successfully applied [BST04].

Due to the fact that the set of sampling points will be augmented during the optimization process as outlined in Section 6.2, the initial space-filling property is not crucial for a successful optimization process. As a consequence of the subsequent update procedure, it is typically sufficient to build an interpolating metamodel based on a maximin distance LHD which was selected from a limited number of LHDs. The resulting experimental design is not expected to be perfectly space-filling, but also not as unfit as illustrated in Figure 5.10a. A possibly poor space-filling property will improve gradually as further points are added to the set of sampling points. The model update is motivated and described in detail in the following chapter.

Chapter 6

Metamodels Used in Optimization Procedures

Whenever approximations are used as a surrogate for an original computer simulation, the potential prediction error between predicted and true response has to be borne in mind. Typically, these metamodels are used within an optimization process where the function evaluations during the iteration steps are obtained as predictions of the metamodel. As a result of the optimization process, a *predicted optimum* is obtained which can be seen as an estimate for the true optimum. It would be careless to trust this result and to take the prediction as final result. Clearly, the predicted optimum has to be validated for instance by a verification run at the predicted optimum which is performed with the original simulation model. In case the accuracy of the prediction is not appropriate, further steps have to follow. Typically, a sequential approach is chosen in which the significance of the metamodel is increased by an iterative update procedure.

Since problems with random variables in the problem formulations have to be treated differently to some extent, the standard procedures for the solution of purely deterministic optimization problems are described first. This means that all factors are assumed to be design variables.

6.1 Move Limit Strategy for Mid-Range Approximations

As outlined in Sections 4.1 and 4.6, the accuracy of polynomial regression models mainly depends on a proper selection of the polynomial degree used to formulate the approximation. Adding extra information in form of training data at further sampling points (at so-called *infill points*), in general does not improve the model fit. Following the reasoning of TAYLOR series expansions, however, even a low-order polynomial can be an adequate approximation for a sufficiently smooth function, if the area of validity is chosen small enough. Hence, the postulation can be deduced that the range of validity for the approximation must diminish to improve the fidelity of the metamodel.

An approach which is translates this idea into an update procedure for optimization in conjunction with polynomial regression models is the *move limit strategy*. Here, the true functional relationships for f, g, and h are replaced sequentially by explicit mid-range approximations symbolized by $\hat{f}$, $\hat{g}$, and $\hat{h}$, respectively. These approximations are not intended to

be valid over the entire factor space, but only on a subregion characterized by more stringent upper and lower bounds on the factors. These bounds are iteratively adapted as the optimization process advances, thus motivating their name: *move limits*. Together, the surrogate models and the current move limits define a *subproblem* of the form

$$\begin{aligned}
&\text{minimize} && \hat{f}^{(l)}(\mathbf{x}) \quad ; && \mathbf{x} \in \mathbb{R}^n && \text{(6.1a)}\\
&\text{such that} && \hat{g}_j^{(l)}(\mathbf{x}) \leq 0 \quad ; && j = 1, \ldots, n_g && \text{(6.1b)}\\
& && \hat{h}_k^{(l)}(\mathbf{x}) = 0 \quad ; && k = 1, \ldots, n_h && \text{(6.1c)}\\
& && x_i^{L,(l)} \leq x_i \leq x_i^{U,(l)} \quad ; && i = 1, \ldots, n && \text{(6.1d)}
\end{aligned}$$

Here, the superscript (l) denotes the current iteration. Accordingly, $x_i^{L,(l)}$ and $x_i^{U,(l)}$ symbolize the move limits for which

$$x_i^{L,(l)} \geq x_i^L \quad \wedge \quad x_i^{U,(l)} \leq x_i^U \tag{6.2}$$

must hold, i.e. the move limits must stay within the global side constraints (x_i^L and x_i^U, respectively).

In the setup of this multipoint approximation strategy, the key issues are how to move the limits, which define the current subregion. Several options have been proposed in the literature [TFP93, Etm97, KS99, KEMB02] on how to adapt the current subregion. The rationales behind the different methods differ only slightly. The common idea is to move the current subregion in the design space following the search directions of the optimization algorithm. To ensure a sufficient accuracy of $\hat{f}$, the size of the subregion is reduced whenever the approximations are not good enough.

A popular alternative to adjust size and position of the current subregion is the *successive response surface method (SRSM)*. According to the SRSM scheme, the optimization process begins with the selection of a starting design $\mathbf{x}^{(0)}$ representing the center point of the first region of interest (iteration number $l = 0$). The initial subregion is described by its upper and lower bounds which are determined individually for each design variable x_i based on the user-determined *range factors* $r_i^{(0)}$.

$$\begin{aligned}
x_i^{L,(l)} &= x_i^{(l)} - 0.5\, r_i^{(l)}\\
x_i^{U,(l)} &= x_i^{(l)} + 0.5\, r_i^{(l)}
\end{aligned} \tag{6.3}$$

Clearly, for the initial subregion, the iteration number is $l = 0$. Now, a subproblem according to Equation (6.1a) is established and solved – resulting in the optimum design $\mathbf{x}^{*,(l)}$. This optimum design will serve as center point for the next subproblem $\mathbf{x}^{(l+1)} = \mathbf{x}^{*,(l)}$. The bounds of the new subregion are calculated pursuant to Equation (6.3). The new range $r_i^{(l+1)}$ is obtained by

$$r_i^{(l+1)} = \lambda_i^{(l+1)}\, r_i^{(l)} \tag{6.4}$$

where $\lambda_i^{(l+1)}$ symbolizes the *contraction rate*. To formulate the contraction rate several other quantities have to be established. which are introduced next. The vector

$$\Delta\mathbf{x}^{(l+1)} = \mathbf{x}^{(l+1)} - \mathbf{x}^{(l)} \tag{6.5}$$

describes the moving direction of the subregion. The indicator value

$$d_i^{(l+1)} = 2\frac{\Delta x_i^{(l+1)}}{r^{(l)}} \tag{6.6}$$

quantifies the relative position of the new center point within the previous move limits. Specifically, this indicator value can only take values within the interval $[-1, 1]$ in which $d_i = -1$ indicates that the coordinate setting $x_i^{(l+1)}$ of the new center point lies on the lower move limit $x_i^{L,(l)}$ of the previous subregion. Analogously, $d_i = 1$ means that the respective coordinate of the new center point hits the upper move limit $x_i^{U,(l)}$ during the optimization, and $d_i = 0$ reveals that the position of the center point has not changed in terms of the ith design variable.

Two additional parameters are used in the formulation of the contraction rate.

$$\lambda_i^{(l+1)} = \eta + \left|d_i^{(l+1)}\right| (\gamma - \eta) \tag{6.7}$$

The zoom parameter η and the contraction parameter γ. Obviously, these parameters represent the extremal settings for λ_i. The contraction rate equals the zoom parameter in case $d_i = 0$. The other extremum $\lambda_i = \gamma$ is obtained for $|d_i| = 1$. Typically, $\eta = 0.5$ and $\gamma = 1$ are chosen. As a result, the subregion will rapidly diminish in size if the obtained optimum is close to the corresponding center point. As the distance of the optimum to the center increases, the size reduction is gradually retarded. If the current optimum is located on the move limits, the true optimum is expected to be outside the subregion. Thus, the new subregion does not change in size ($\lambda_i = 1$).

Using the above described procedure can result in severe oscillations between two subregions, especially if a linear approximation is chosen for the subproblem formulation. In this case, consecutive optima are typically found on opposite sides of the respective subregions once the current optimum is close to the true optimum. To prevent this troublesome behavior, the normalized oscillation indicator

$$\hat{c}_i^{(l+1)} = \sqrt{\left|c_i^{(l+1)}\right|}\,\mathrm{sign}\left(c_i^{(l+1)}\right) \quad \text{with} \quad c_i^{(l+1)} = d_i^{(l+1)}\, d_i^{(l)} \tag{6.8}$$

can be used to define a modified contraction parameter γ which makes for a diminution of the subregion as soon as oscillation occurs. The contraction parameter is then determined by

$$\gamma = \frac{\gamma_{\mathrm{pan}}\left(1 + \hat{c}_i^{(l+1)}\right) + \gamma_{\mathrm{osc}}\left(1 - \hat{c}_i^{(l+1)}\right)}{2} \tag{6.9}$$

where γ_{osc} introduces additional shrinkage to attenuate oscillation. Typical values for γ_{osc} are between 0.5 and 0.7. From Equation (6.9), it can be seen that $\gamma = \gamma_{\mathrm{pan}}$ results from $\hat{c}_i = 1$. This pure panning case arises when the current optimum hits the same (upper or lower) move limit in two sequent iterations.

Although the presented SRSM approach is rather heuristic, it has been successfully applied to many optimization problems, for instance in [SC02]. For the solution of stochastic optimization problems, this approach is not suited in the present form. To evaluate the

deterministic surrogate formulations based on the methods that have been introduced in Section 3.3, the entire noise space $\mathbf{\Omega}$ has to be examined in each iteration step – either to find the worst case of all possible realizations or to solve the integral in Equation (3.47). Accordingly, the approximations have to be global, at least with respect to the noise space. A successive partitioning of the entire factor space into subregions in order to increase the fidelity of the approximation would exclude possibly decisive parts of $\mathbf{\Omega}$. An appropriate adaptation of the SRSM approach to stochastic optimization problems is to restrict the update procedure to the factors v_i that correspond to design variables while the factor ranges of the noise variables remain unaffected i.e. each subproblem approximation covers the entire noise space; only the design space is zoomed in. The major drawback of this approach is that the behavior of the original system with respect to the noise variables has to be approximated globally by polynomials – whether this is satisfactory strongly depends on the problem under investigation.

6.2 Update Procedures for Global Approximations

Different scenarios can cause an insufficient accuracy of the predicted optimum when interpolating metamodels are used to approximate the true functional relationship. On the one hand, the predicted optimum can fall into a region where the prediction error is large. In other words, the predictive behavior of the surrogate model around the predicted optimum can be quite poor. According to this, the predicted value can significantly depart from the true functional response with the consequence that the true optimum is missed, as illustrated in Figure 6.1 a. This fault can easily be found by a *verification run*, i.e. the evaluation of the original function at the respective design. On the other hand, the location of the true optimum might not be predicted by the metamodel, if in the surroundings of the true minimum no points are sampled. This means that in a specific region of the design space, a (possibly decisive) minimum might remain undetected. A verification run potentially misses this deficiency since the predicted response might match the original response quite well around the predicted optimum design. Such a configuration is depicted in Figure 6.1 b. Furthermore, if the predicted optimum by chance coincides with a sampling point, a verification run even has no relevance at all. The interpolating trait assures that the metamodel exactly represents the original observations at the sampling points. Hence, a poor fidelity cannot be detected by simply comparing the response values of metamodel and original model at the predicted optimum. Accordingly, to avoid these possible pitfalls, special update procedures have been proposed for interpolating metamodels. Again, the different methods are first familiarized for the case of a deterministic optimization problem as presented in the literature. Then suitable enhancements are proposed to augment the range of application to stochastic optimization problems including noise variables.

All of these update procedures start with a small set of sample points to fit a first metamodel to the sampled data. Based on this metamodel, one or more additional sample points are determined sequentially where the original computer simulation will be evaluated. Taking into account the responses at these additional sample points, a new metamodel is built. Several different criteria are available to determine infill points, which are presented next.

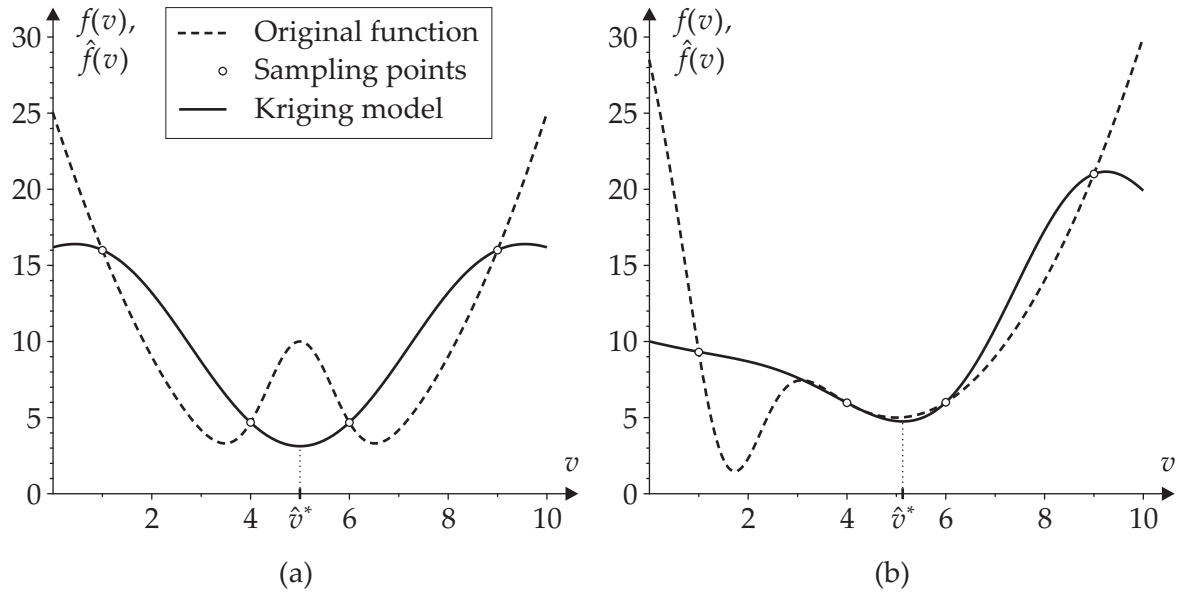

Figure 6.1: Pitfalls arising from the use of (interpolating) metamodels in optimization.

6.2.1 Strategies to Improve the Fidelity of the Metamodel

The first approach aims at improving the metamodel, i.e. infill points are placed where the prediction error of the model is large. Hence, the global fidelity of the surrogate model is sequentially augmented. In this context, the *integrated mean squared error (IMSE)* and the *maximum mean squared error (MMSE)* are two prominent criteria. They have originally been proposed as DoE techniques for the initial sampling of computer experiments as detailed in [SWMW89]. However, these criteria are also appropriate to the search for infill points. In this case, the evaluation of both criteria is straightforward, even the hurdles [Etm94] associated with the primary sampling are eliminated: The computational effort to find coordinate settings for one infill point is relatively small compared to the computation time needed to set up a complete experimental design. Furthermore, the necessary correlation parameters $\boldsymbol{\theta}$ do not have to be guessed as in the initial state. As soon as a search for infill points is conducted, the correlation parameters have already been estimated based on the existing set of samples. With these correlation parameters, the new points are positioned to minimize

$$\text{IMSE} = \int_{\mathcal{D}} \text{MSE}\left(\hat{f}(\mathbf{x})\right) d\mathbf{x} \tag{6.10}$$

or

$$\text{MMSE} = \max_{\mathbf{x}\in\mathcal{D}} \text{MSE}\left(\hat{f}(\mathbf{x})\right), \tag{6.11}$$

respectively. The mean squared error (MSE) of the prediction $\hat{f}$ is computed according to Equation (5.6) based on the updated set of sampling points (incl. the candidate point) whereas the correlation parameters of the metamodel are estimated from the current set of sampling points with the respective original response values.

A third criterion which only addresses model improvement is the *entropy criterion* presented in [CMMY88]. This approach can be reformulated to be equivalent to maximizing the

determinant of the correlation matrix $\mathbf{R}$ as defined in Equation (4.46). Again, the candidate point is added to the set of sampling points and the correlation matrix is established using the correlation parameters estimated from the existing set of samples. The candidate point yielding a minimal $\det(\mathbf{R})$ is taken as infill point for the updated model.

Computationally less expensive is the approach to identify the point with the largest prediction error of the existing metamodel. Since the MSE at this infill point is reduced to zero when it is added to the set of sampling points, the overall predictive behavior of the global approximation is sequentially increased [MS02]. It should be noted that the latter criterion is not identical to minimizing the MMSE criterion in Equation (6.11). Here, the location of maximum MSE of the current model is determined and added as infill point. In contrast, the MMSE criterion positions the infill point such that the MMSE of the *updated* metamodel is minimized under the assumption that the candidate point is added to the set of sampling points and that the current correlation parameters remain valid.

All of the criteria presented above gradually improve the overall fidelity of the metamodel. As a result, the sequentially updated metamodel has a balanced prediction error all over the model space. Information about regions with low response values including the predicted minimum determined by means of the existing metamodel is neglected during the selection of infill points. This procedure can be quite ineffective when numerous infill points are placed in regions with comparably large response values. The related computational effort might be better invested to refine the metamodels locally in the surroundings of the predicted optimum.

6.2.2 The Efficient Global Optimization Method

To achieve faster convergence to the global minimum, an approach called *efficient global optimization (EGO)* has been proposed by JONES et al. [JSW98]. This method performs a balanced global and local search based on metamodels which are sequentially updated during the optimization process. Here, two goals are weighed up during the search for infill points, namely a detailed investigation of the behavior around the estimated optimum (local search) and elimination of the possibility to miss the optimum due to a large prediction error (global search). The criterion used for the trade-off between global and local search is called *expected improvement criterion* [Sch97].

The expected improvement is computed as follows. The algorithm starts with an initial set of sampling points $\mathbf{x}^l$ (with $l = 1, \ldots, m$) for which the original model is evaluated. From the m (initial) observations y^l, the minimum feasible response value is determined. This response value $\tilde{y}^*$ represents the best tried and proven choice based on the information gathered so far. The *improvement* over $\tilde{y}^*$ related to an arbitrary y is defined by

$$I = \max\left\{0, (\tilde{y}^* - y)\right\} \ . \tag{6.12}$$

In case the improvement is evaluated with respect to a random variable Y, the improvement is also a random variable. Consequently, the expected improvement is defined as expected value of Equation (6.12).

$$E(I) = E\left(\max\left\{0, (\tilde{y}^* - Y)\right\}\right) \tag{6.13}$$

According to the definition of kriging models, the predictor $\hat{y}$ represents such a realization of a random stochastic process Y. The randomness is governed by the uncertainty about the true function value at untried $\mathbf{x}$. Hence, Y is characterized by $Y \sim N(\hat{y}, s^2)$. The corresponding probability density function of this normal distribution is symbolized by p_Y. The variance s^2 is the variance of the prediction error, which can be estimated by the MSE as defined in Equation (5.6). Since the model parameters $\hat{\boldsymbol{\theta}}$ and $\hat{\sigma}^2$ used to evaluate the MSE are typically not known in advance but only estimated from the observations, $\hat{s}^2 = \text{MSE}$ represents the estimated prediction variance. Using these estimates, the expected improvement for a kriging model prediction $\hat{y} = \hat{f}(\mathbf{x})$ can be expressed in closed form by

$$E(I) = \int_{-\infty}^{\tilde{y}^*} (\tilde{y}^* - y)\, p_Y(y)\, dy = (\tilde{y}^* - \hat{y})\, \Phi\left(\frac{\tilde{y}^* - \hat{y}}{\hat{s}}\right) + \hat{s}\, \phi\left(\frac{\tilde{y}^* - \hat{y}}{\hat{s}}\right) . \tag{6.14}$$

Since both $\hat{y}$ and $\hat{s}^2$ are dependent variables of $\mathbf{x}$, the expected improvement is also a function of $\mathbf{x}$. In agreement with standard literature in statistics, ϕ in Equation (6.14) denotes the probability density function of the standard normal distribution $N(0,1)$. Correspondingly, Φ represents the cumulative density function of the same distribution. A detailed derivation of Equation (6.14) can be found in Appendix A.1.

A closer look at the finding of Equation (6.14) reveals that the first addend becomes large if the prediction $\hat{y}$ constitutes an improvement with respect to $\tilde{y}^*$ and if this improvement is also reliable (i.e. $\hat{s}$ is small). The second addend is large wherever the estimated prediction error $\hat{s}$ is large. As a result, the expected improvement is large where $\hat{y}$ is presumably smaller than $\tilde{y}^*$ and/or where the prediction is possibly inaccurate. Clearly, the expected improvement tends to zero as the prediction point approaches a sampling point (at sampling points, $\tilde{y}^* - \hat{y} \leq 0$ by definition of $\tilde{y}^*$ and $\hat{s} \to 0$).

Figure 6.2 illustrates the expected improvement criterion. Here, $\tilde{y}^*$ represents the benchmark for the expected improvement over this value. Any realization y of the random process Y that is located left of this reference value is considered to be better, thus contributing to an expected improvement. The actual contribution amounts to the distance y to the reference value $\tilde{y}^*$ multiplied by the probability density of the individual realization. All values right of $\tilde{y}^*$ have an improvement of zero as formulated in Equation (6.12). Consequently, large $E(I)$ values are obtained when large parts of p_Y are located left (or rather below) of the benchmark $\tilde{y}^*$, as exemplified in Figure 6.2a. In contrast, Figure 6.2b depicts the case of a comparably small expected improvement.

In the search for infill points, the expected improvement is maximized and the corresponding location is added to the set of sampling points. With the additional observation at this infill point, the metamodel can be updated and the search for further infill points is repeated. This procedure is continued until the expected improvement is smaller than a user-defined lower threshold value, for instance 1%. It should be noted, that the expected improvement is not strictly decreasing with the model updates. Since the correlation parameters are re-estimated during each model update, the MSE can significantly vary – especially during an early stage of the update process. Thus, a suitable stopping criterion should ideally incorporate several successive $E(I)$ values, for instance the average over the last two or more iterations.

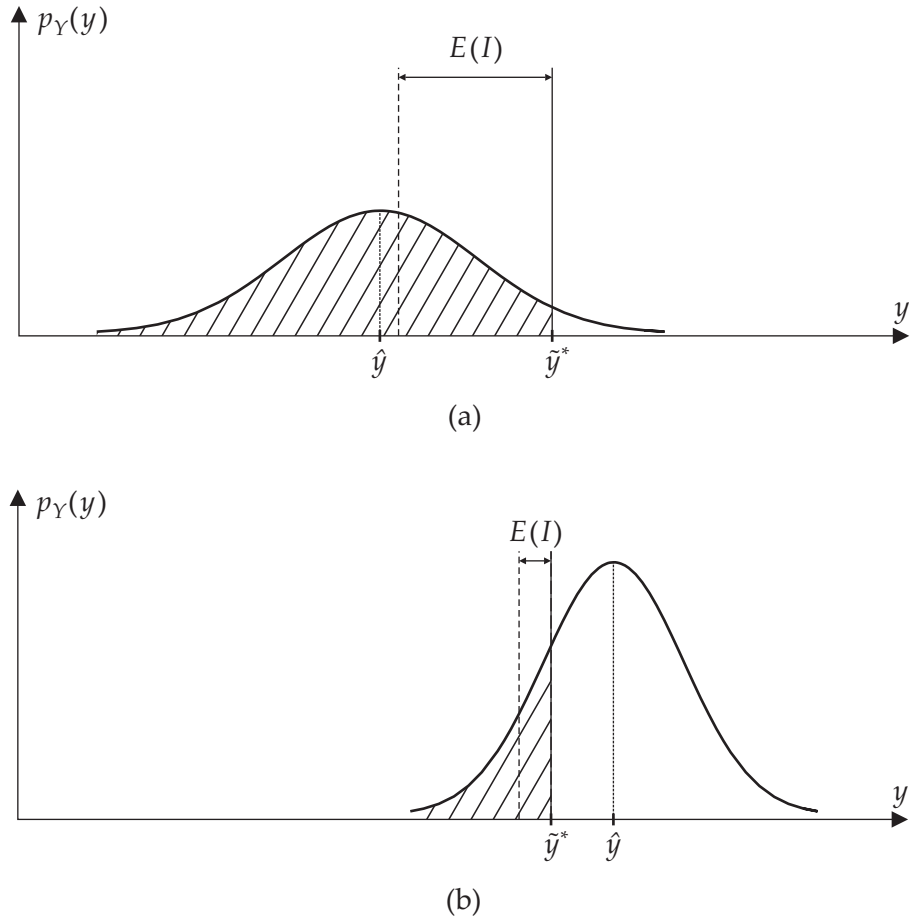

Figure 6.2: Expected improvement criterion for two different designs: (a) prediction $\hat{y}$ has a large $E(I)$ value, (b) the expected improvement of $\hat{y}$ is very small.

An approach which extends the expected improvement criterion to the constrained case is discussed in [SWJ98].

Example 7. To illustrate the EGO approach, the function

$$f(x) = (x-5)^2 - 15\ \mathrm{e}^{-(x-1.5)^2} + 5$$

is assumed to represent the original functional relationship. This function is approximated by a kriging model which is fitted to the four initial sampling points $\mathbf{X} = [1, 4, 6, 9]^T$. In Figure 6.3a, the original function and the fitted metamodel are plotted.

The characteristics of the expected improvement criterion are demonstrated in Figure 6.3b. The expected improvement criterion is highly multimodal. The different maxima identify promising candidates for infill points. For the first model update, the point $x' = 5.086$ has the largest $E(I)$. Hence, the original function is evaluated at x', and a new metamodel is fit to the set of five sampling points. Based on the updated metamodel (with updated MSE), the expected improvement is evaluated again, and the location with the largest expected improvement is taken as next infill point.

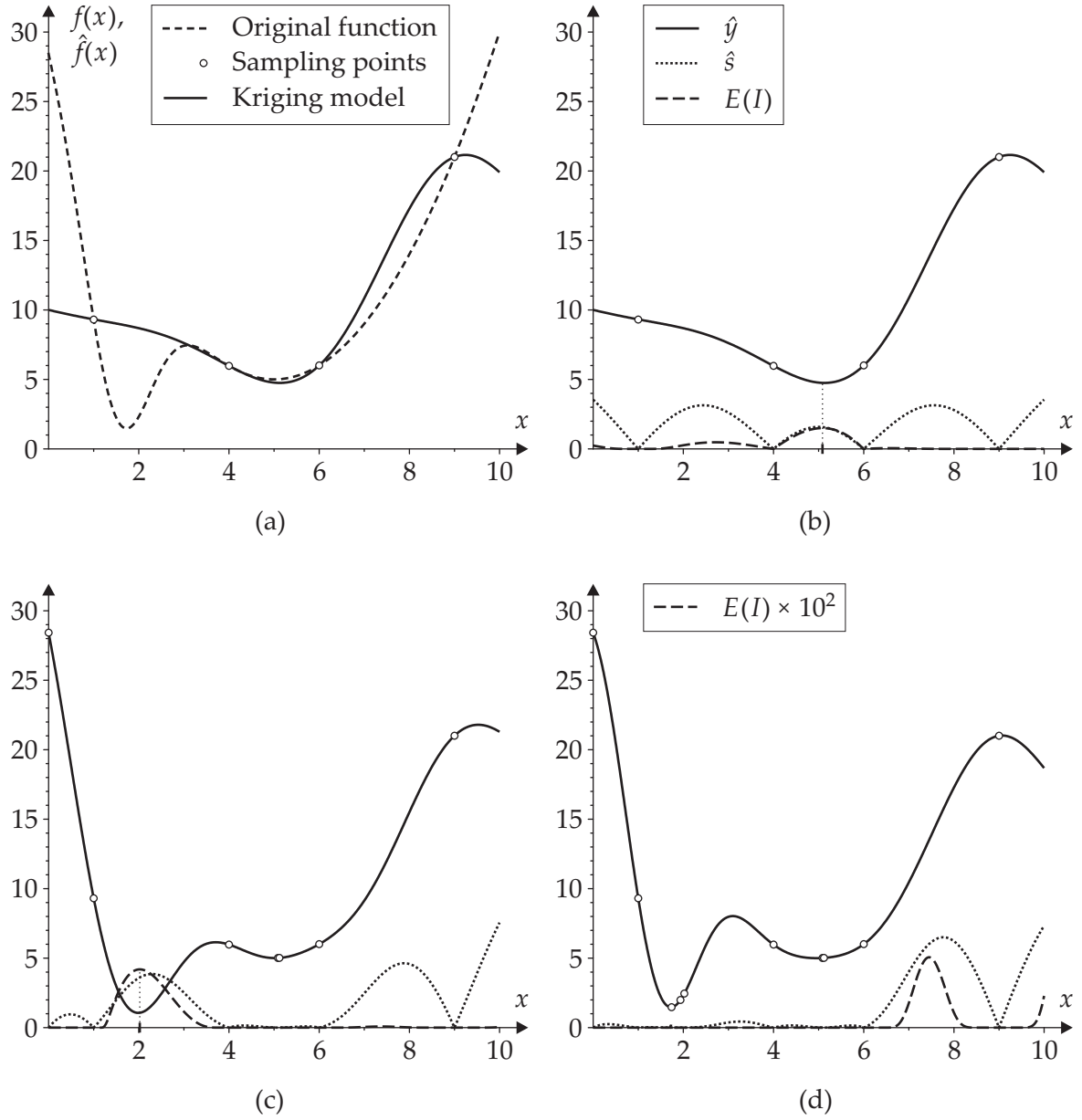

Figure 6.3: Efficient global optimization approach applied to Example 7: (a) Original function and initial metamodel, (b) expected improvement criterion and resulting infill point for first metamodel, (c) updated metamodel after addition of three infill points, (d) resulting metamodel after six updates.

Figure 6.3c depicts the state after three updates. After exploring the surroundings of the local minimum, the search is now conducted more globally. It can also be seen from this plot, that the expected improvement is not strictly decreasing with the model updates as discussed above.

After addition of six infill points, the maximum expected improvement is only around 0.05 (the expected improvement is scaled by 100 in Figure 6.3d). It can be seen from this figure that the metamodel reproduces the original function fairly well, especially in the rele-

vant neighborhood of the two minima. At this stage, the remaining error in the localization of the minimum is about 0.15%. After three more iterations, the global minimum is found to a precision of 10^{-5} and the expected improvement is reduced to the same order of magnitude. □

A typical problem that may occur especially in a later state of the EGO algorithm is ill-conditioning of the correlation matrix $\mathbf{R}$. Regarding the initial set of sampling points, the distances between particular points are approximately equal. During the update process, infill points are typically added either in rather large distance to existing sampling points (global search) or in close vicinity to existing points (local search). If, as a result, two points are very close to each other, the respective columns in $\mathbf{R}$ are nearly identical resulting in an ill-conditioned matrix.

A comparison of EGO with alternative criteria to select infill points (e.g. criteria presented in Section 6.2.1) is provided in [SPG02]. The approach has also been customized to work with RBF models instead of a kriging formulation as detailed in [SLK04]. An alternative approach which conducts the global part of the search by a simple maximin distance criterion has been suggested by REGIS and SHOEMAKER [RS05]. Their method follows the rationale used to establish the initial design of experiments for interpolating metamodels: With a view to increasing the fidelity of a metamodel, a suitable candidate for an infill point should augment the space-filling property of the original experimental design. Hence, the selection of the next point is accomplished by means of a minimization of the predicted response (based on the current metamodel) subject to a constraint on how close the infill point $\mathbf{x}'$ may be with respect to existing sampling points. Obviously, there is a largest possible distance restricted by the distribution of the existing m sampling points. This upper limit is given by

$$d_{\max} = \max_{\mathbf{x}' \in \mathcal{D}} \left(\min_{1 \le l \le m} \|\mathbf{x}' - \mathbf{x}^l\| \right) \tag{6.15}$$

To identify qualified candidates for infill points, the following constrained optimization problem has to be solved.

$$\begin{aligned} &\text{minimize} && \hat{f}(\mathbf{x}) \quad ; \quad \mathbf{x} \in \mathcal{D} && (6.16a) \\ &\text{such that} && \lambda\, d_{\max} - \|\mathbf{x} - \mathbf{x}^l\| \le 0 && (6.16b) \end{aligned}$$

Here, the user-determined parameter $\lambda \in [0, 1]$ controls whether the search is performed globally ($\lambda = 1$) or locally ($\lambda = 0$). Typically, large values (close to one) are preferred during the first update steps, and in a later stage a local search is allowed by choosing $\lambda = 0$.

So far, only deterministic optimization problems were treated in the context of update procedures for interpolating metamodels. For an efficient optimization of robust design problems, the approaches have to be extended to the case in which both design and noise variables are present.

6.2.3 Selection of Infill Points in Robust Design Optimization

A suitable modification of the standard EGO method to account for random variables in the problem description will be presented in this section. Obviously, it does not make sense to

treat random variables in the same way as design variables in the evaluation of the expected improvement. To evaluate the robustness criterion, noise variables settings which result in a better performance measure are typically irrelevant. The opposite is true: For a reliable assessment of the robustness criterion, the deteriorating effects of noise are of interest.

As a result and in contrast to the referenced literature, the search for infill points is split into two parts. First, the design space is explored to find those settings $\mathbf{x}'$ for the design variables that are most promising with respect to the robustness formulation $\rho(\mathbf{x})$. In a second step, the noise space is investigated and suitable noise variable settings $\mathbf{z}'$ are identified. Together, $\mathbf{x}'$ and $\mathbf{z}'$ form the desired infill point symbolized by $\mathbf{v}'$. For this infill point, a simulation run of the original model is performed and the metamodel can be updated.

Design Space Exploration. As a criterion to identify the design variable part $\mathbf{x}'$, the expected improvement according to Equation (6.13) is maximized. Since the aim of the robust design optimization is to find design variable settings $\mathbf{x}^*$ that are optimal with respect to the robustness criterion, the robustness value $y = \rho(\mathbf{x})$ replaces the response value $y = f(\mathbf{x})$ in the equation for the expected improvement. To obtain the vector $\tilde{\mathbf{y}}$, the robustness criterion is evaluated for all vectors $\mathbf{x}^l$ that are part of the set of sampling points $\mathbf{v}^l$. The resulting robustness values for $\mathbf{x}^l$ are all determined by means of the metamodel – either by an optimization to find the worst case or by a sampling method to evaluate the expectation integrals involved (cf. Section 3.3). Hence, the values $\tilde{y}_l = \rho(\mathbf{x}^l)$ are not evaluations of the original model but only predictions for the true robustness value at these points. Consequently, these values will in the following be denoted by $\hat{y}_l$ with the minimum value $\hat{y}^*$. The remaining uncertainty about the accuracy of $\hat{y}^*$ conflicts with the postulation of a "tried and proven" minimum $\tilde{y}^*$ to be used as a reference value for the computation of the expected improvement according to Equation (6.13). Since the robustness values y_l are evaluated on a kriging metamodel though, each of the predictions $\hat{y}_l$ including their minimum value $\hat{y}^*$ can also be seen as a realization of a random process with mean $\hat{y}_l$ and a corresponding prediction variance $\hat{s}^2$.

Details on how to compute $\hat{y}$ for robust design problems have been given in Chapter 3. Yet, a suitable estimate for the prediction error $\hat{s}$ at a specific design is not always straightforward to find. Specifically, in case of a robust design optimization, the prediction error related to the evaluation of the robustness criterion is required. The MSE, however, only quantifies the estimated prediction error between global approximation $\hat{f}$ and original code f. The crucial question is: How does the MSE associated with predictions of individual events $\mathbf{z} \in \mathbf{\Omega}$ influence the accuracy of the chosen robustness criterion? At this point, the two significantly different types of robustness criteria have to be distinguished: Either ρ is based on a minimax formulation or the formulation of ρ comprises an integral over the noise space.

For integral formulations of the form (3.47), the influence of each individual event on the robustness value is expressed by its probability density $p_{\mathbf{Z}}$, and hence, $\hat{s}^2$ can be estimated by

$$\hat{s}^2 = \int_{\mathbf{\Omega}} \mathrm{MSE}\,(\mathbf{x}, \mathbf{z})\; p_{\mathbf{Z}}(\mathbf{z})\; d\mathbf{z} \tag{6.17}$$

which is the mean of the MSE over the noise space. Equation (6.17) can be solved by the same sampling methods used to compute the robustness value itself (cf. Sections 3.3.1 through 3.3.3).

$$\hat{s}^2 \approx \sum_{L=1}^{M} w_L \,\mathrm{MSE}\left(\mathbf{x}, \mathbf{z}_L\right) \tag{6.18}$$

In Equation (6.18), M denotes the number of sampling points used to evaluate the expectation integral based on the metamodel. To distinguish these sampling points from the set of points which serve as training data for the metamodels, the respective subscripts are capitalized here. M can be a fairly large number since evaluations of the metamodel and its MSE are inexpensive to compute.

The problem with a minimax robustness criterion is that the influence of the MSE on the accuracy of the robustness value is not clear. A low MSE value at the location of the (currently estimated) worst case does not imply that this approximation is accurate enough. The true and decisive worst case – hidden in an area where the MSE is still large – might not be predicted by the model yet. Hence, the maximum prediction error defined by

$$\hat{s}^2 = \max_{\mathbf{z}\in\mathbf{\Omega}} \mathrm{MSE}\left(\mathbf{x}, \mathbf{z}\right) \tag{6.19}$$

is typically used as measure for the prediction error concerning a minimax-type robustness criterion. Using Equation (6.19) to estimate $\hat{s}$ implies that a large MSE value anywhere in the noise space (even within a possibly small range) governs the prediction accuracy of the robustness criterion. This approach is in line with the inherently pessimistic nature of the minimax criterion.

As already indicated above, in this configuration, the expected improvement has to be adapted to the special case where both the reference value and the evaluations of the candidate infill points are represented by random numbers denoted by Y^* and Y, respectively. This situation is illustrated in Figure 6.4. The random variables Y^* and Y are characterized by $Y^* \sim N(\hat{y}^*, \hat{s}^*)$ and $Y \sim N(\hat{y}, \hat{s})$, respectively. In this case, only those realizations y contribute to the expected improvement that are below the reference value $\hat{y}^*$ and have greater probability density p_Y than the corresponding probability density of the benchmark p_{Y^*}.

$$E(I) = E\left(\max\left\{0, (Y^* - Y)\right\}\right) = \int_a^b \left(\hat{y}^* - y\right)\left(p_Y(y) - p_{Y^*}(y)\right)\, dy \tag{6.20}$$

To compute the integral in Equation (6.20), the integration bounds a and b have to be known. These integration limits depend on the intersection points of the two probability density functions p_Y and p_{Y^*}. Contingent on their respective means and standard deviations (prediction errors), three cases can be differentiated: two normal distributions either have one or two intersections or both distributions are identical. In the latter case, they have an infinite number of points y that fulfill $p_Y(y) = p_{Y^*}(y)$.

If both prediction errors are equal, namely $\hat{s} = \hat{s}^*$, the probability density functions p_Y and p_{Y^*} intersect at exactly one point y_1.

$$y_1 = (\hat{y}^* + \hat{y})/2 \tag{6.21}$$

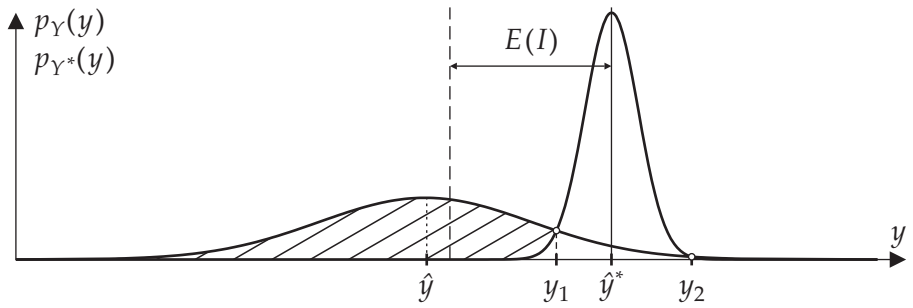

(a)

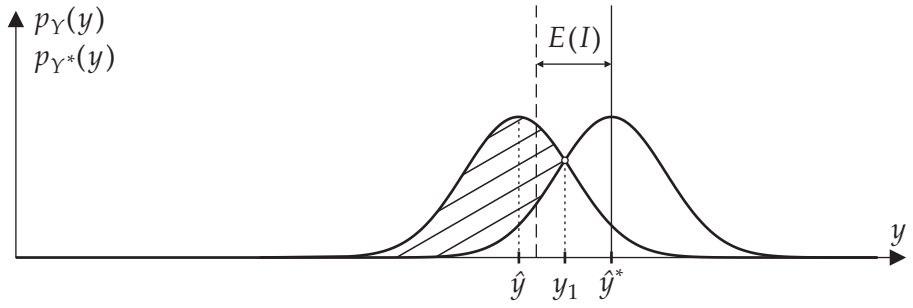

(b)

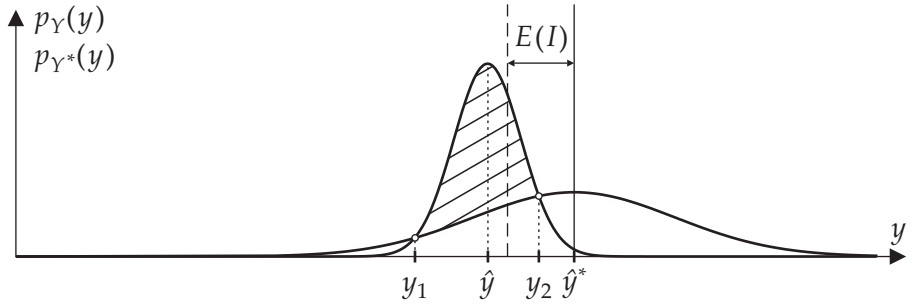

(c)

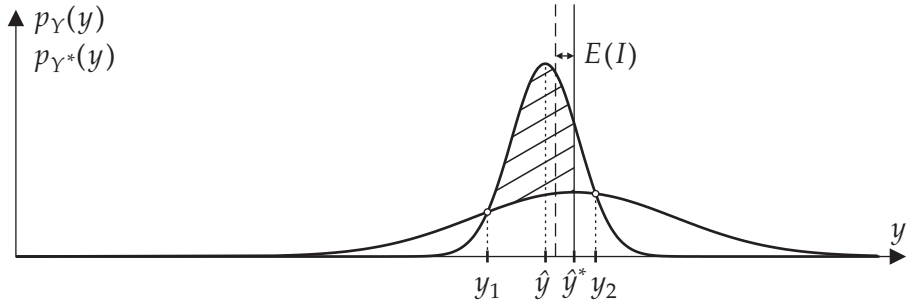

(d)

Figure 6.4: Expected improvement for the case of a random reference value.

In all other cases, the intersection points y_1 and y_2 can be determined by solving $p_Y(y) = p_{Y^*}(y)$ for y.

$$y_{1,2} = \frac{\hat{s}^2\,\hat{y}^* - (\hat{s}^*)^2\,\hat{y} \pm \hat{s}\,\hat{s}^* \sqrt{(\hat{y}-\hat{y}^*)^2 + 2\,\ln\left(\frac{\hat{s}}{\hat{s}^*}\right)\left(\hat{s}^2 - (\hat{s}^*)^2\right)}}{\hat{s}^2 - (\hat{s}^*)^2} \tag{6.22}$$

To achieve a consistent notation, the lower intersection point is always denoted by y_1, the upper point by y_2 i.e. such that $y_1 \leq y_2$ by definition.

To finally establish the integration limits, three different cases have to be distinguished:

1. If $\hat{s} > \hat{s}^*$, the probability density functions p_Y and p_{Y^*} intersect at two points. One intersection point is located below $\hat{y}^*$ (denoted by y_1), for the second intersection it holds that $y_2 > \hat{y}^*$. Accordingly, the lower and upper integration limits for the expected improvement are $a = -\infty$ and $b = y_1$, respectively. This situation is illustrated in Figure 6.4a. Evaluating Equation (6.20) with these integration limits yields

$$E(I) = (\hat{y}^* - \hat{y})\,\Phi\left(\frac{y_1 - \hat{y}}{\hat{s}}\right) + \hat{s}\,\phi\left(\frac{y_1 - \hat{y}}{\hat{s}}\right) - \hat{s}^*\,\phi\left(\frac{y_1 - \hat{y}^*}{\hat{s}^*}\right) \tag{6.23}$$

2. If $\hat{s} = \hat{s}^*$, the probability density functions p_Y and p_{Y^*} intersect at exactly one point. This point can be identified as $y_1 = (\hat{y}^* + \hat{y})/2$. An expected improvement larger than zero is only obtained if $\hat{y} < \hat{y}*$. In this case, the integration limits are $a = -\infty$ and $b = y_1$ as depicted in Figure 6.4b. Accordingly, Equation (6.20) also simplifies to Equation (6.23). The only difference compared to the first case is the definition of y_1.

3. If $\hat{s} < \hat{s}^*$, the probability density functions p_Y and p_{Y^*} also intersect at two points. Here again, three cases have to be distinguished:

   (i) If both intersection points are below the reference value $\hat{y}^*$, these intersection points are also the integration limits, namely $a = y_1$ and $b = y_2$ (cf. Figure 6.4c).

$$\begin{aligned} E(I) = {} & (\hat{y}^* - \hat{y})\left(\Phi\left(\frac{y_2 - \hat{y}}{\hat{s}}\right) - \Phi\left(\frac{y_1 - \hat{y}}{\hat{s}}\right)\right) \\ & + \hat{s}\left(\phi\left(\frac{y_2 - \hat{y}}{\hat{s}}\right) - \phi\left(\frac{y_1 - \hat{y}}{\hat{s}}\right)\right) - \hat{s}^*\left(\phi\left(\frac{y_2 - \hat{y}^*}{\hat{s}^*}\right) - \phi\left(\frac{y_1 - \hat{y}^*}{\hat{s}^*}\right)\right) \end{aligned} \tag{6.24}$$

   (ii) If $y_1 < \hat{y}^*$ and $y_2 > \hat{y}^*$, the integration limits are $a = y_1$ and $b = \hat{y}^*$ as depicted in Figure 6.4d.

$$\begin{aligned} E(I) = {} & (\hat{y}^* - \hat{y})\left(\Phi\left(\frac{\hat{y}^* - \hat{y}}{\hat{s}}\right) - \Phi\left(\frac{y_1 - \hat{y}}{\hat{s}}\right)\right) \\ & + \hat{s}\left(\phi\left(\frac{\hat{y}^* - \hat{y}}{\hat{s}}\right) - \phi\left(\frac{y_1 - \hat{y}}{\hat{s}}\right)\right) - \hat{s}^*\left(\frac{1}{\sqrt{2\pi}} - \phi\left(\frac{y_1 - \hat{y}^*}{\hat{s}^*}\right)\right) \end{aligned} \tag{6.25}$$

   (iii) If both intersection points are located above the reference value, the expected improvement is equal to zero.

The derivations of Equations (6.23) through (6.25) are presented in more detail in Appendix A.2.

In summary, to find promising design settings $\mathbf{x}'$, the expected improvement in Equation (6.20) can be maximized when the quantities $\hat{y}^*$, $\hat{s}^*$, $\hat{y}$, and $\hat{s}$ are known. In the search for the infill point, $\hat{y}^*$ and $\hat{s}^*$ are only determined once. To compute the respective expected improvement over $\hat{y}^*$, both the predicted robustness value $\hat{y}$ and the corresponding prediction error $\hat{s}$ have to be evaluated for each candidate point.

Noise Space Exploration. Once the most promising design variable settings $\mathbf{x}'$ for the infill point are determined, the noise space is examined to find matching noise settings $\mathbf{z}' \in \mathbf{\Omega}$. The rule or measure to identify $\mathbf{z}'$ will again depend on the type of robustness criterion ρ used to define the robust design problem.

In case ρ is of integral type, the infill point settings $\mathbf{z}'$ should ameliorate the predictive behavior of the model to obtain a more dependable evaluation of the integral. This can be achieved by placing the infill point where the prediction quality is still poor (i.e. where the MSE is large) and where in addition the individual prediction considerably influences the solution of the integral (locations with high probability density). Hence, a suitable criterion can be formulated by multiplication of both components

$$\mathbf{z}' = \arg\max_{\mathbf{z}\in\mathbf{\Omega}} \left(\mathrm{MSE}\left(\mathbf{x}', \mathbf{z}\right) p_{\mathbf{Z}}(\mathbf{z})\right) . \tag{6.26}$$

This criterion is in general more significant than simply maximizing the MSE because it potentially prefers regions with moderate MSE values but great importance for the solution of the integral over regions that exhibit large MSE values but have virtually no relevance for the evaluation of the expectation integral.

If ρ evaluates a worst case scenario, the rationale underlying the expected improvement formulation is applied to find settings for $\mathbf{z}'$. As opposed to the standard $E(I)$ formulation, the goal of the optimization at this stage is to find the *worst case* $y^{\#}$, or in other words, the maximum of the *deteriorating* noise effects. Hence, the objective for the search of promising noise variable settings $\mathbf{z}'$ should represent a trade-off between *worsening* of the objective and reducing the prediction error of the model in the noise space. The worsening associated with a response value y when compared to the reference value $y^{\#}$ is defined as

$$W = \max\left\{0, \left(y - y^{\#}\right)\right\} \tag{6.27}$$

For this worst case analysis within the noise space, the robustness criterion is formed by a single evaluation of the metamodel. Hence, the prediction error $\hat{s}$ at any point $\mathbf{z}$ can be computed directly from the MSE of the metamodel at point $(\mathbf{x}', \mathbf{z})$, namely $\hat{s} = \sqrt{\mathrm{MSE}\left(\mathbf{x}', \mathbf{z}\right)}$. Typically, there is no original sampling point with coordinates $(\mathbf{x}', \mathbf{z})$ even for arbitrary $\mathbf{z} \in \mathbf{\Omega}$. Hence, there exists no reference value $y^{\#}$ for which the prediction error vanishes and on this account both values have to be treated as realizations of a random process symbolized by random variables Y and $Y^{\#}$, respectively. As a replacement for a "tried and proven" observation $\tilde{y}^{\#}$, the prediction $\hat{y}^{\#}$ that has the smallest prediction error $\hat{s}^{\#}$ is chosen as reference value. Due to this choice, no distinction of cases as has been elaborated for the expected

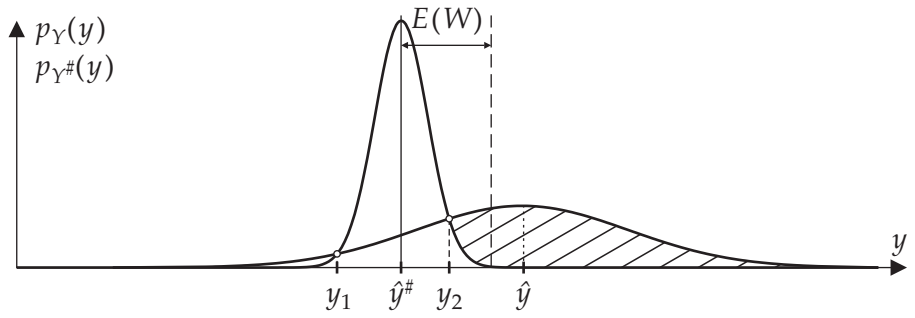

Figure 6.5: Expected worsening for the case of a random reference value.

improvement is needed; $\hat{s}^\# \leq \hat{s}$ holds by definition. Consequently, the integration interval is always from the upper intersection point y_2 to infinity. The intersection points $y_{1,2}$ of the two probability density functions p_Y and $p_{Y^\#}$ are defined analogously to Equation (6.22) with $y_1 \leq y_2$ (cf. Figure 6.5).

The *expected worsening* results from

$$\begin{aligned} E(W) &= E\left(\max\left\{0,(Y-Y^\#)\right\}\right) = \int_{y_2}^{\infty} \left(y-\hat{y}^\#\right)\left(p_Y(y)-p_{Y^\#}(y)\right)\,dy \\ &= \left(\hat{y}-\hat{y}^\#\right)\left(1-\Phi\left(\frac{y_2-\hat{y}}{\hat{s}}\right)\right) + \hat{s}\,\phi\left(\frac{y_2-\hat{y}}{\hat{s}}\right) - \hat{s}^\#\,\phi\left(\frac{y_2-\hat{y}^\#}{\hat{s}^\#}\right)\,. \end{aligned} \tag{6.28}$$

A detailed derivation of this Equation can be found in Appendix A.3.

In conclusion, the infill point settings for the noise variable part $\mathbf{z}'$ for integral-type robustness criteria are obtained according to Equation (6.26) while for minimax-type robustness criteria the expected worsening in Equation (6.28) is maximized. In both cases, the values for the design variables are fixed to $\mathbf{x}'$. Together the values for the design and the noise variables, $\mathbf{x}'$ and $\mathbf{z}'$, respectively, define the infill point $\mathbf{v}'$ according to Equation (4.1). For this infill point, a computer simulation will be performed next and the resulting response value will serve as additional information to update the metamodel.

This procedure can be continued, until either a lower bound on $E(I)$ of the design or a maximum number of runs is met. The complete process sequence is illustrated in a flowchart in Figure 6.6. The sequential update approach for interpolation metamodels in robust design optimization has been detailed for the case of a kriging metamodel formulation. However, the concept can identically be applied to RBF models by treating the RBF prediction as realization of a stochastic process. A discussion of this approach is given in [SLK04].

Since the expected improvement is highly multimodal, an extension of the sequential update procedure to parallel systems is straightforward. By choosing a global optimization algorithm that is able to detect and store local minima as well (e.g. a gradient-based optimizer with multiple starting points or an evolutionary strategy), a desired number of candidate infill points (typically equal to the number of processors available) can be identified within one update step. Analogously to the procedure described above, search for infill

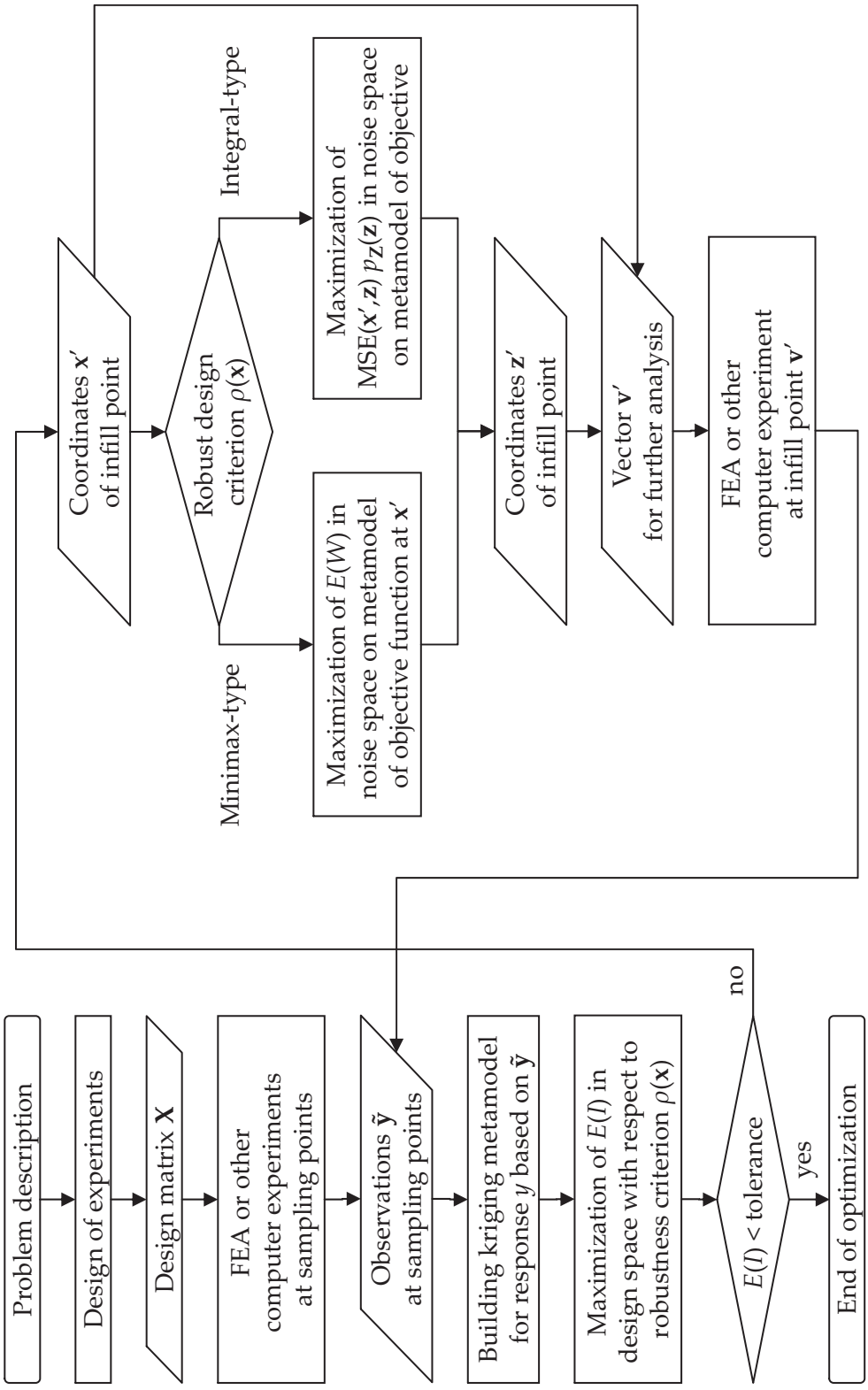

Figure 6.6: Enhanced sampling technique for robust design optimization.

points starts by investigating the design space. In this first step, several isolated maxima of Equation (6.20) are determined, for which in a second step corresponding noise variable settings are specified either by Equation (6.26) or from the maximum of Equation (6.28). The computer simulations defined by these input settings can then be evaluated in parallel. As a result, the metamodel gains more additional information during one update step yielding a better global approximation.

To increase numerical efficiency for kriging models even further, updating the estimated metamodel coefficients $\hat{\boldsymbol{\theta}}$ can be omitted for some iterations in the model update. This re-estimation of $\hat{\boldsymbol{\theta}}$ requires the solution of a multidimensional optimization problem as pointed out in Sections 4.3 and 4.6). The cost related to this refitting of the model parameters can reduce or even outweigh the benefit of a sequential update algorithm – especially if the number of variables and/or sampling points is large. Since the interpolating property of kriging metamodels does not depend on $\hat{\boldsymbol{\theta}}$, these correlation parameters do not necessarily have to be refit each time an infill point is included. In [GRMS06] a scheme is presented to determine whether the kriging model parameters should be updated.

In case the correlation parameters $\boldsymbol{\theta}$ are not re-estimated during the current model update, the position of the subsequent infill point will typically coincide with the location of the second best local maximum of $E(I)$ before the model update. In other words, the reason why the maximum expected improvement based on the updated model does in general not coincide with one of the local maxima of $E(I)$ identified for the previous model is that the correlation structure of the model changes due to the update in the model parameters.

Chapter 7

Numerical Examples

In this chapter, the procedure introduced in Figure 6.6 is tested on illustrative examples. To reveal the special behavior of the update procedure for metamodels in robust design optimization problems, three different mathematical test functions are investigated. The emphasis of these test examples is on a problem formulation that is on the one hand easy to understand and that on the other hand allows for a graphical representation of the progress in the optimization and update procedures. Hence, only functions with two input variables (one design variable and one noise parameter) are chosen, such that the response can still be shown in a 3D-plot.

The presentation of mathematical test functions is followed by an industrial application example of metamodel-based robust design optimization. The selected example deals with the robustness of a deep-drawing process and is rather typical for applications in the automotive industry. However, this illustration can only exemplify the range of possible applications. Examples from the field of civil engineering can be found in [JB05].

7.1 Quadratic Test Example

In the first example, the proposed procedure is tested on the function introduced in Example 2 on page 54ff.

$$f(x,z) = (2-x)\,(0.1-z-0.1\,x)+0.3$$

with the design space limited to $0 \leq x \leq 4$. For this robust design problem, the resulting probability distribution can be determined analytically, and hence exact results for the different robustness criteria are readily available (cf. results in Section 3.2.3). These analytical results serve as reference values for the robust design optima computed numerically.

The optimization is started by fitting a kriging metamodel (with Gaussian correlation function and constant polynomial part) to a training data set containing 10 sampling points. The necessary experimental design is obtained by means of the maximin distance LHD sampling technique i.e. a selection of 100 LHDs is sampled and the design with the largest minimum distance is chosen as basis for the initial sampling. A variety of 100 Latin hypercube designs can be obtained very quickly, however, the maximin distance design from this selection may still be far from being equally spread over the model space. Since further infill

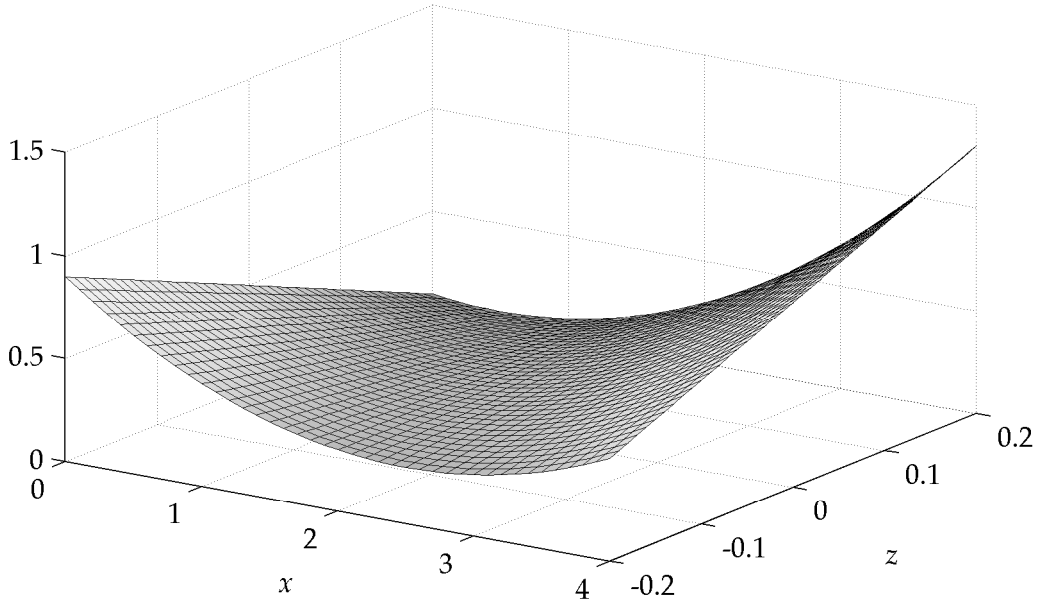

Figure 7.1: Quadratic test example.

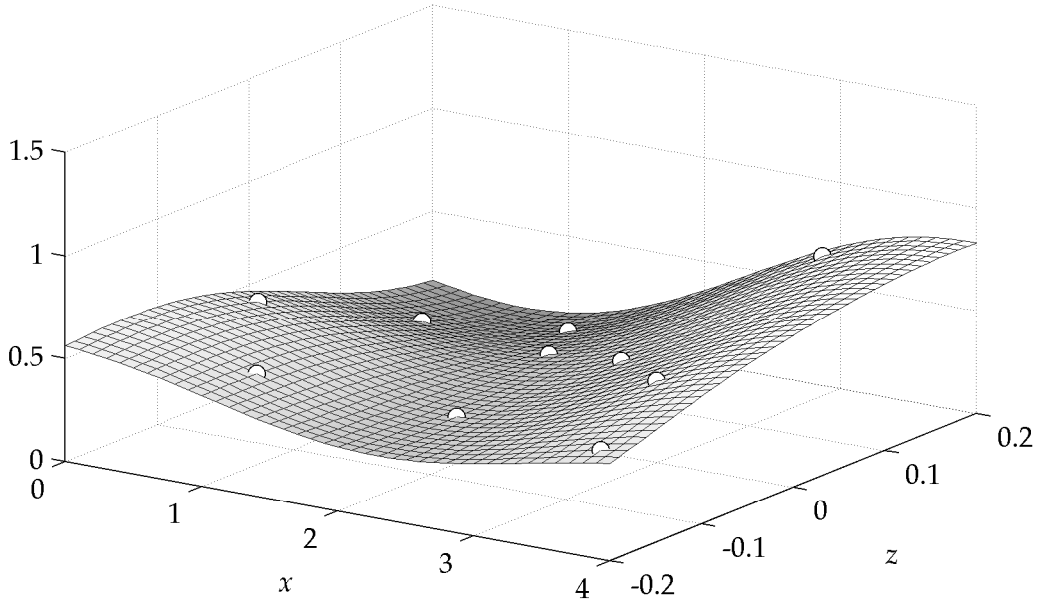

Figure 7.2: Initial kriging metamodel based on 10 samples.

points will be added during the optimization process, this shortcoming will be compensated steadily.

The original function f is evaluated for the initial sampling points and the first metamodel is fit to the resulting training data set. The original function is plotted in Figure 7.1 and Figure 7.2 depicts the initial model, where the sampling points are marked with white circles. Figure 7.3 depicts the estimated prediction variance (MSE) of the initial metamodel.

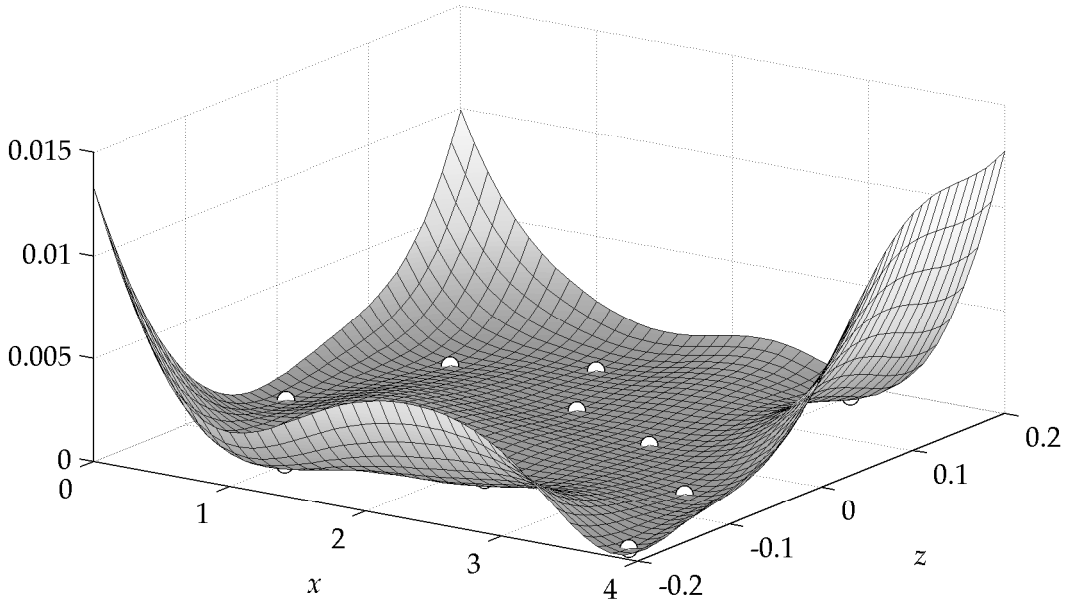

Figure 7.3: MSE of initial kriging metamodel.

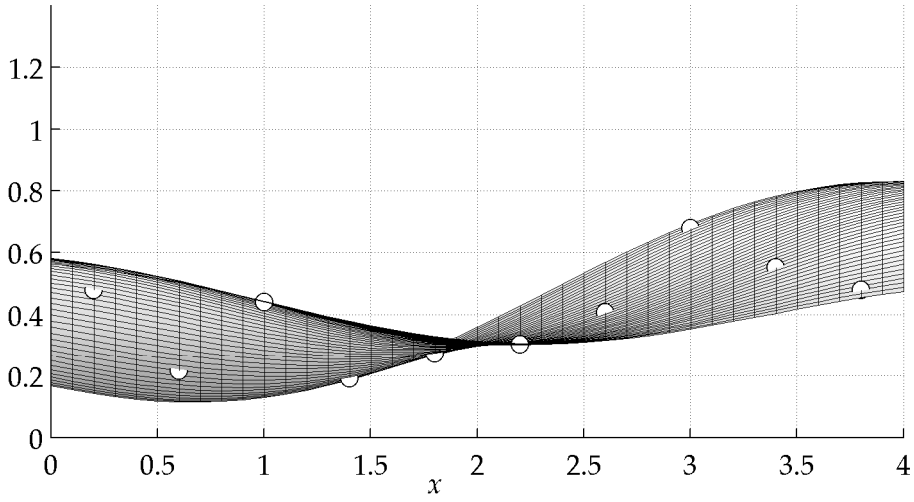

Figure 7.4: Projection of initial kriging metamodel onto design space (x-y-plane).

7.1.1 Worst-Case Robustness Criterion

In a first run, the robustness criterion is chosen to be of minimax-type. The noise variable Z is assumed to vary within the range $-0.2 \leq z \leq 0.2$. Hence, for each design x, the worst case of $z \in [-0.2, 0.2]$ represent the characteristic robustness value. Figure 7.4 shows the projection of the metamodel onto the design space (cf. Figure 3.11 for the same projection of the original function). As outlined in Section 3.2.3, the upper boundary of the displayed range corresponds to the worst-case robustness criterion.

The expected improvement criterion is evaluated for prediction $\hat{y}$ and prediction error

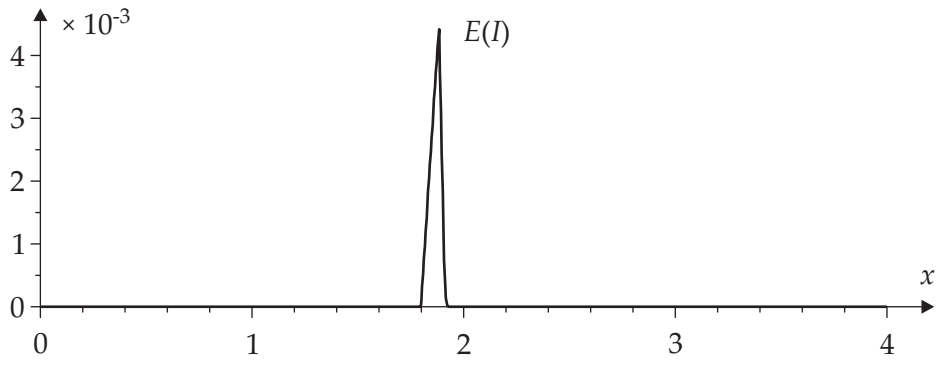

Figure 7.5: Expected improvement based on initial metamodel.

$\hat{s}$ of the initial metamodel. The maximum expected improvement is identified by means of the DiRect optimization algorithm. For the first model update, the design $x' = 1.885$ is found to be most promising (cf. Figure 7.5). For the candidate design variable setting x', the corresponding noise parameter setting is computed by maximizing Equation (6.28). This optimization task is also solved using the DiRect algorithm resulting in $z' = -0.2$. The infill point defined by (x', z') is added to the set of sampling points and the corresponding response is evaluated. Subsequently, a new metamodel is fit to the enlarged set of training data. The resulting metamodel is plotted in Figure 7.6, where the infill point is indicated by a black diamond.

Based on the new metamodel, the update procedure is repeated and this process is continued until the predefined stopping criterion is met. Typically, the update procedure is aborted when the expected improvement falls below a threshold value, which means that

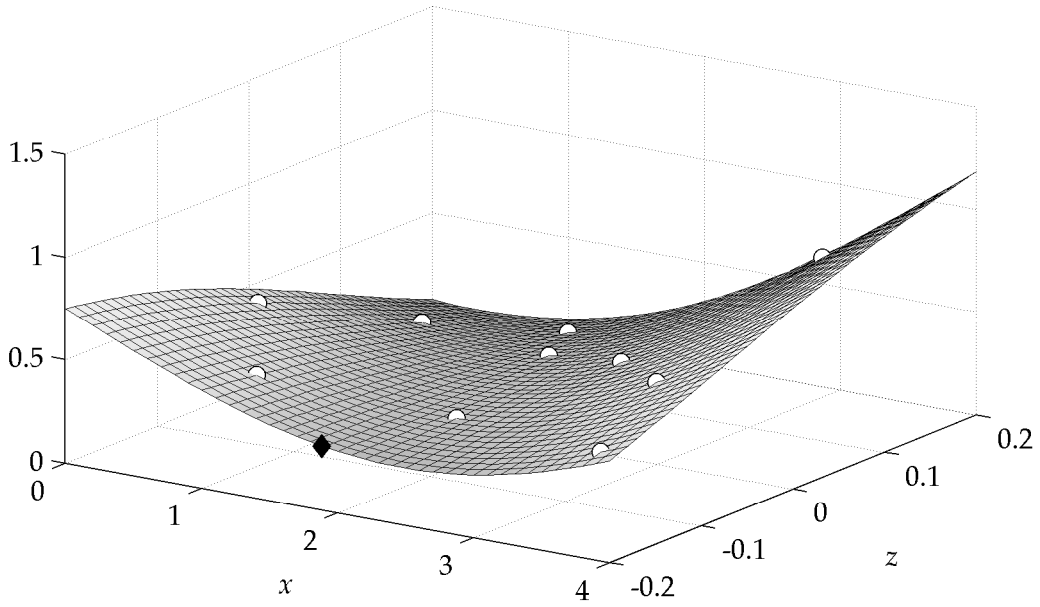

Figure 7.6: Updated kriging metamodel after inclusion of the first infill point.

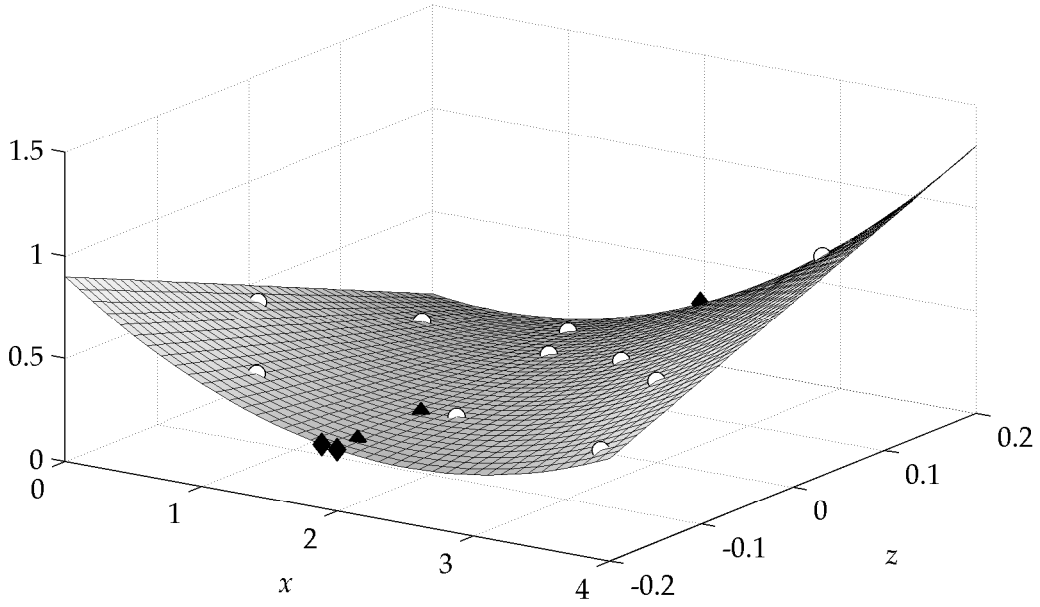

Figure 7.7: Final kriging metamodel after seven update sequences.

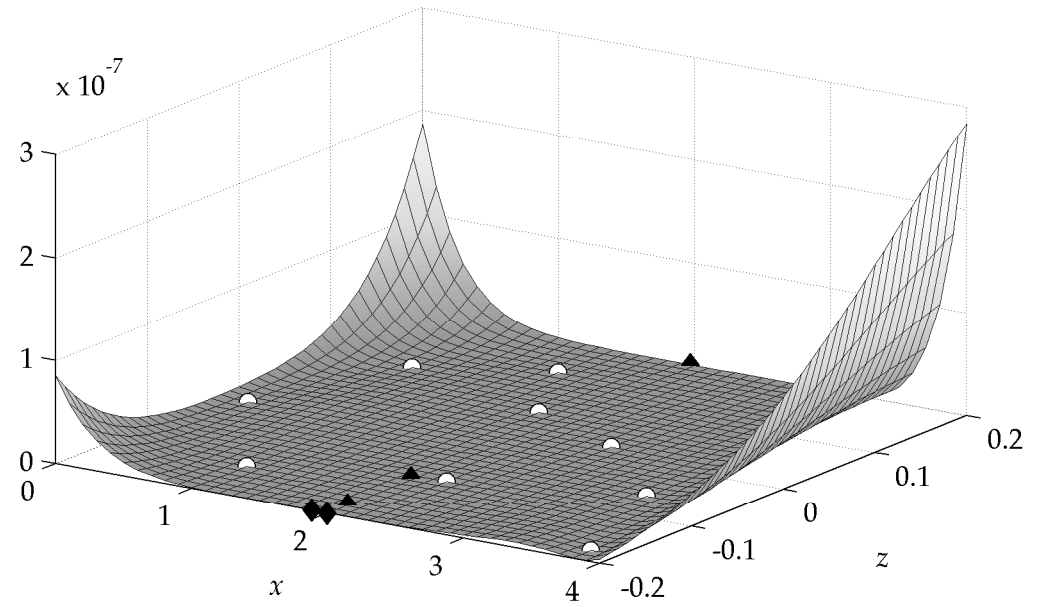

Figure 7.8: MSE of final kriging metamodel.

significant improvement cannot be expected for further model updates. Here, the model update is stopped as soon as the average of the three most recent expected improvement values undershoots 1‰ of the absolute robustness value i.e. the nominal value of the robustness criterion evaluated at the predicted minimum. This averaging accounts for the fact that the expected improvement is typically not monotonically decreasing. In the current test case, this lower limit is reached after five model updates.

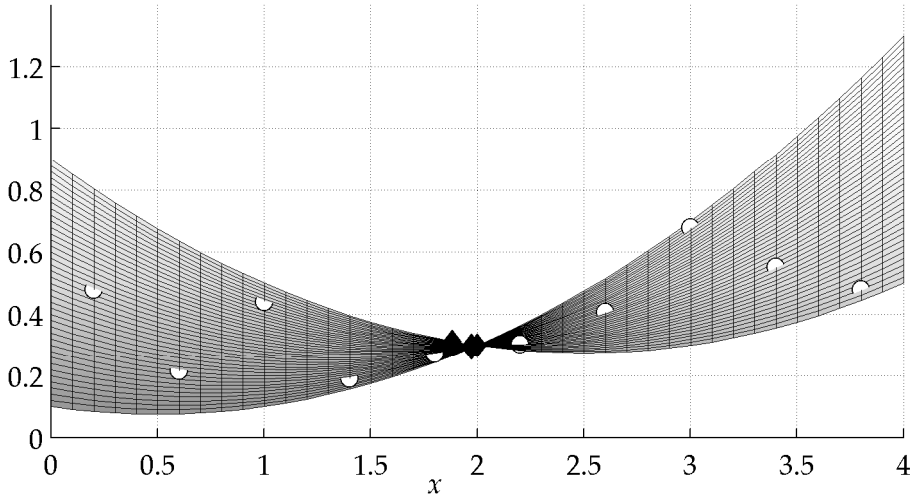

Figure 7.9: Projection of final kriging metamodel onto design space (x-y-plane).

Figure 7.7 shows how the infill points are placed: for all points, the design coordinate setting is around $x = 2$, which represents the true robust optimum. A closer investigation of the noise space reveals that for $x < 2$, the worst case is defined by $z = -0.2$ whereas for $x > 2$, the noise parameter setting $z = 0.2$ yields the worst case. The expected worsening criterion picked up both crucial locations to refine the metamodel approximation. As a result, the final metamodel predicts the robust optimum at the exact value of $\hat{x}^* = x^* = 2$.

7.1.2 Robustness Criterion Based on a Composite Function

For a second run, the robustness criterion is formulated as sum of the mean and the standard deviation of the response value – referring to Equation (3.38) with $w = 1$. The noise variable Z is described by a normal distribution with $\mu_Z = 0.02$ and $\sigma_Z = 0.05$. To evaluate the mean value and the standard deviation of the response, a plain Monte Carlo sampling with 1000 samples is performed on the metamodel.

The optimization is started with the same initial metamodel as in the previous run (Figure 7.2). The infill points, however, are determined according to the formulas for integral-type robustness criteria. In Figure 7.10, the expected improvement for the first model update is depicted. The sampling point at $x = 1.8$ and $z = 0.06$ causes the two local maxima in the expected improvement graph. At this point (as for all sampling points), the prediction error $\hat{s}$ vanishes and the expected improvement in the robustness criterion is small. The predicted robust design, however, is also located in this area. Thus, the expected improvement is rapidly increasing for designs smaller or greater than 1.8. For the design coordinate setting with the maximum expected improvement $x' = 1.733$, corresponding noise parameter settings are determined according to Equation (6.26) yielding $z' = -0.017$.

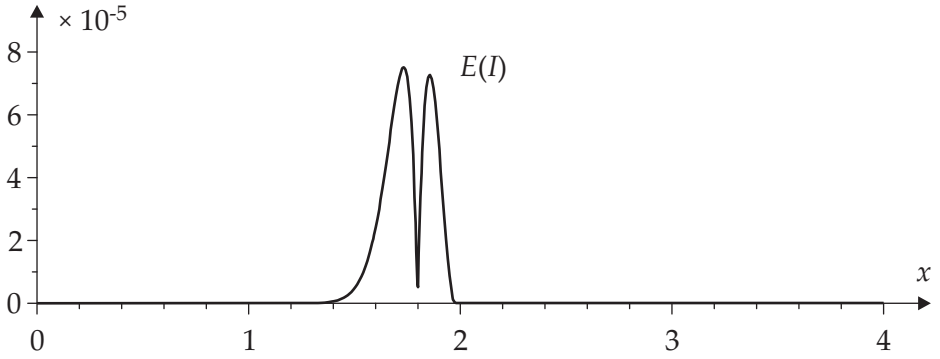

Figure 7.10: Expected improvement based on initial metamodel.

Following the update procedure, the point (x', z') is evaluated and added to the set of training data. Then, a new metamodel is fit and the update loop is repeated. Here again, the iteration is stopped when the average of the three most recent expected improvement values falls below 1‰ of the absolute robustness value. In the current example, the stopping criterion is met after five model updates.

As stated in Example 2, the analytical robust solution for this formulation is $x^* = 1.65$. The initial metamodel predicted the robust optimum at $\hat{x}^* = 1.721$. Using the final metamodel (depicted in Figure 7.11) to compute the robust optimum results in the prediction $\hat{x}^* = 1.646$. This result substantiates that the five infill points were chosen at qualified locations.

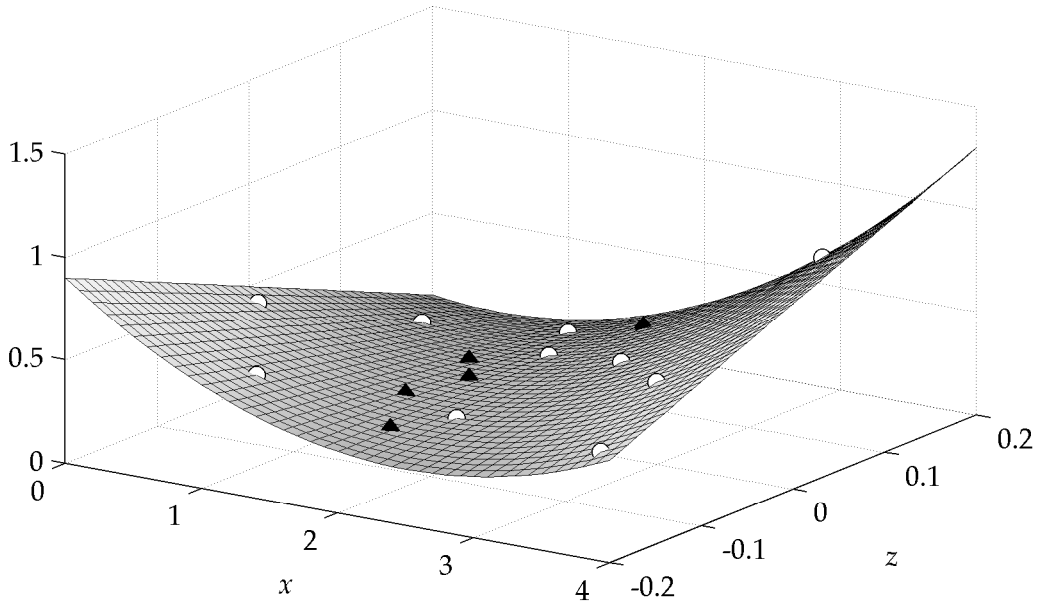

Figure 7.11: Final kriging metamodel after five update sequences.

7.2 BRANIN Function

The second numerical example is the well-known BRANIN function [Bra72, DS78]

$$f(x,z) = \left(z - \frac{5.1}{4\,\pi^2}\,x^2 + \frac{5}{\pi}\,x - 6\right)^2 + 10\left(1 - \frac{1}{8\,\pi}\right)\cos(x) + 10\,,$$

which is depicted in Figure 7.12. For this function, the design space limited to $-5 \leq x \leq 10$. The noise variable Z is assumed to vary according to a normal distribution with $\mu_Z = 5$ and $\sigma_Z = 2$. The robustness criterion is formulated as per Equation (3.38) with $w = 1$. The necessary statistics are evaluated as before – by means of a plain Monte Carlo sampling with 1000 samples.

The BRANIN function, which is typically used as test function for global optimization algorithms, is chosen for this example because it exhibits several local minima and is clearly multimodal along x. Accordingly, it can be assumed that several designs potentially qualify for a robust solution. Since function evaluations for this analytic equation are not expensive, the robustness criterion can also be evaluated on the original function. In Figure 7.13, the robustness criterion evaluated on the original function is plotted. It shows that two distinct designs represent local minima. The global minimum of the robustness criterion is located at $x^* = 10$.

In the initialization step, a kriging metamodel (again with Gaussian correlation function and constant polynomial part) is fit to training data consisting of 10 sampling points. The experimental design is obtained by the same maximin distance LHD sampling technique as in the previous example. The original function f is evaluated for the initial sampling points and the metamodel is fit to the resulting training data set. The resulting initial model is

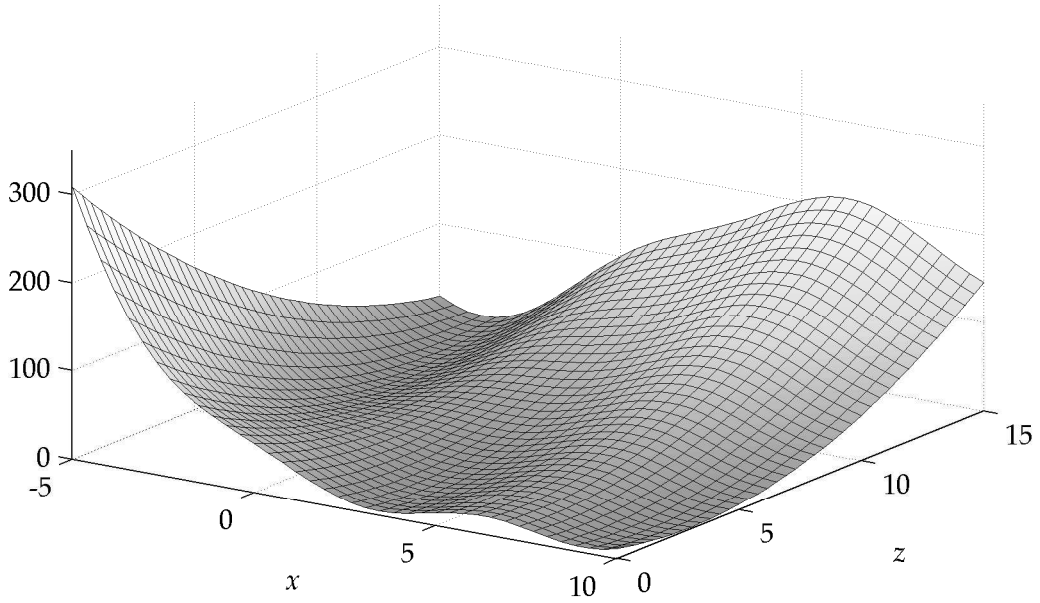

Figure 7.12: BRANIN function.

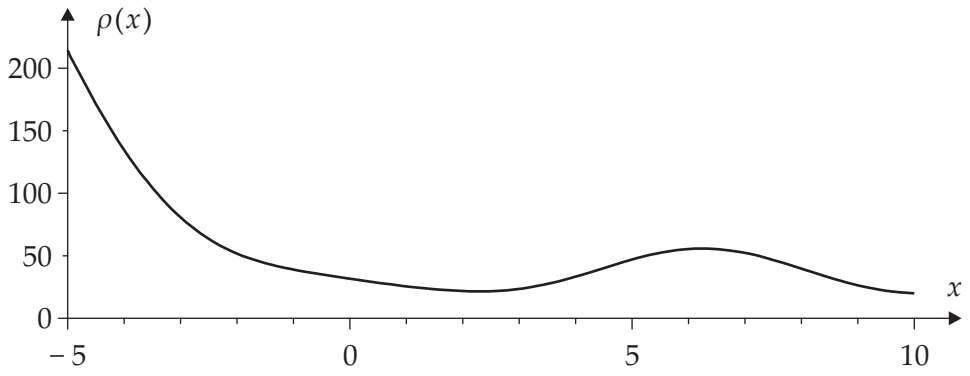

Figure 7.13: Robustness criterion for BRANIN function.

plotted in Figure 7.14. The corresponding prediction variance $\hat{s}^2$ is depicted in Figure 7.15.

The expected improvement criterion is evaluated for the initial metamodel and the maximum expected improvement is determined by means of the DiRect optimization algorithm. For the first model update, the design $x' = 10$ is identified as most promising infill point setting (cf. Figure 7.16). For the design variable coordinate x', the corresponding noise parameter setting is computed according to Equation (6.26) resulting in $z' = 3.474$. The located infill point is evaluated and added to the set of training data. Consequently, the metamodel is updated (as plotted in Figure 7.17) and the update loop is started over.

As in the previous examples, the model update is stopped as soon as the average of the three most recent expected improvement values undershoots 1‰ of the absolute robustness value. This lower limit is reached after seven model updates.

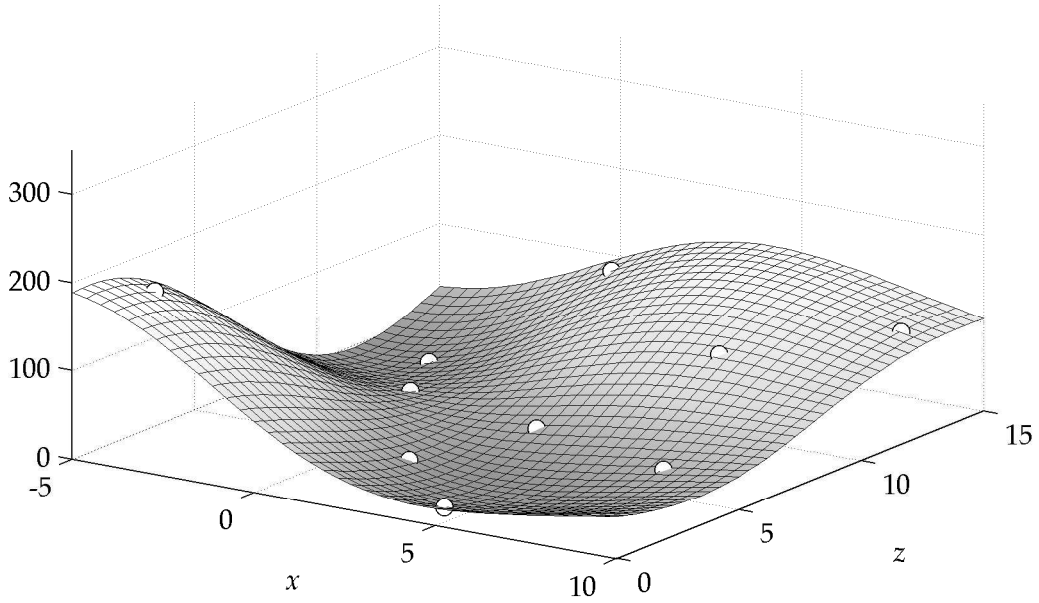

Figure 7.14: Initial kriging metamodel based on 10 samples.

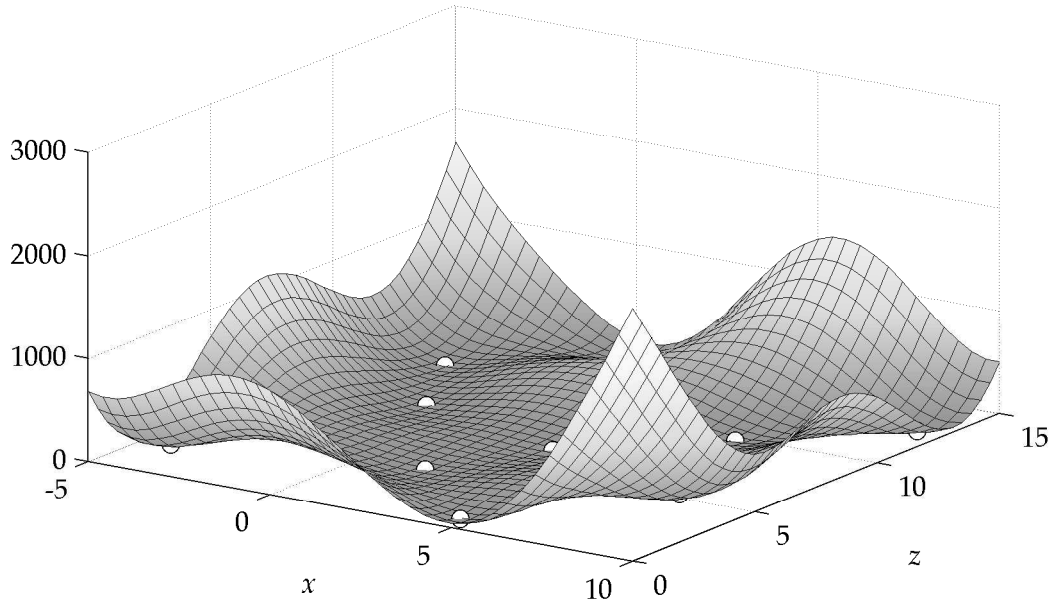

Figure 7.15: MSE of initial kriging metamodel.

As can be seen from Figure 7.18 depicting the final metamodel, the design settings of the infill points are clustered around two distinct values x both representing the (local) minima of the true robustness criterion. In the search for promising noise parameter settings, the prediction variance is weighted with the probability density of Z. This explains why the noise parameter settings of the infill points are only chosen from regions which significantly contribute to the robustness value, namely values around $\mu_Z = 5$.

It can be resumed that the proposed robust design optimization procedure picked up both candidates for a robust optimal design according to the chosen robustness criterion. The metamodel was refined in the vicinity of both design sites yielding the final prediction for the robust optimal design at the location of the true optimum $\hat{x}^* = x^* = 10.0$. Figure 7.19 shows that the estimated prediction variance of the final metamodel approximation vanishes for all important subregions of the model space. At the same time, the accuracy

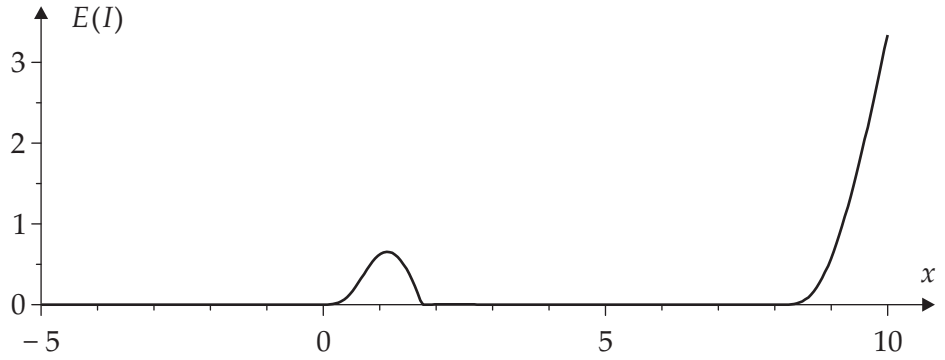

Figure 7.16: Expected improvement based on initial metamodel.

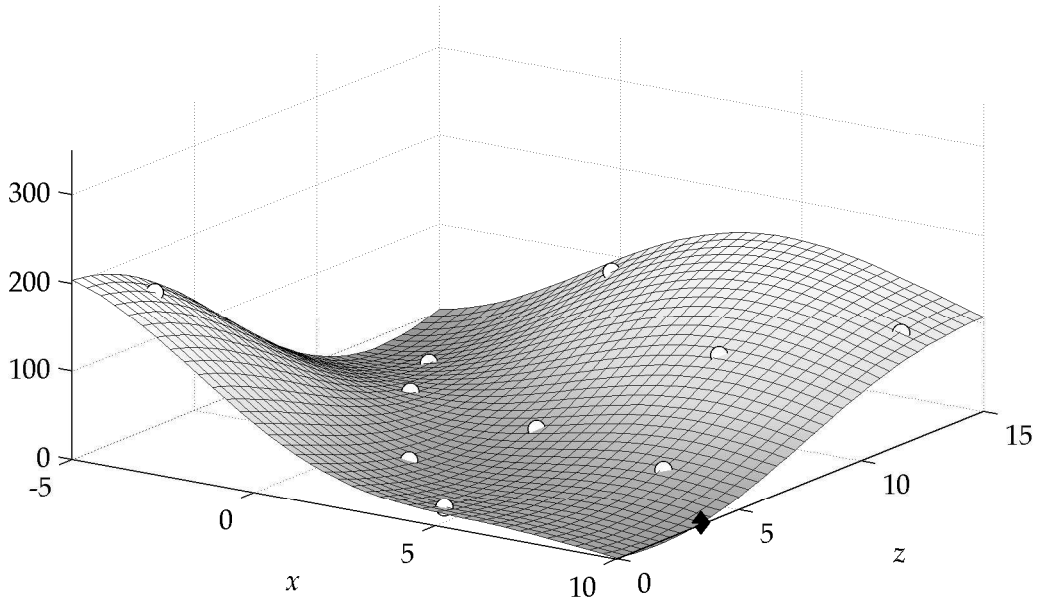

Figure 7.17: Updated kriging metamodel after inclusion of the first infill point.

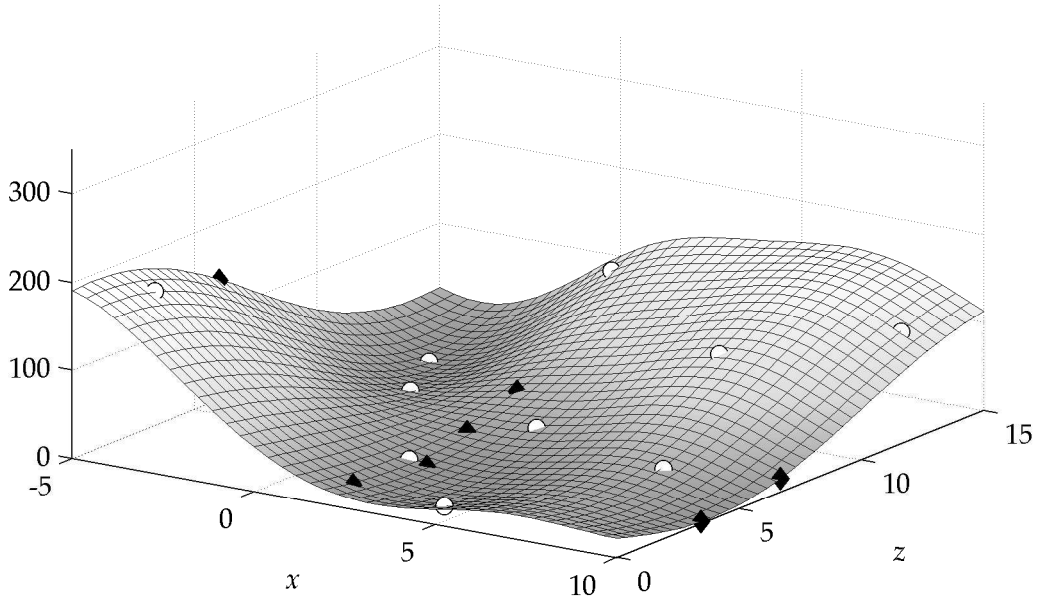

Figure 7.18: Final kriging metamodel after seven update sequences.

of the metamodel remains poor in regions which either do not contribute to the robustness criterion (negligible probability density p_Z for $z > 10$) or where the metamodel already predicts large robustness values i.e. for designs which are clearly non-optimal (in the present example $x < -2$).

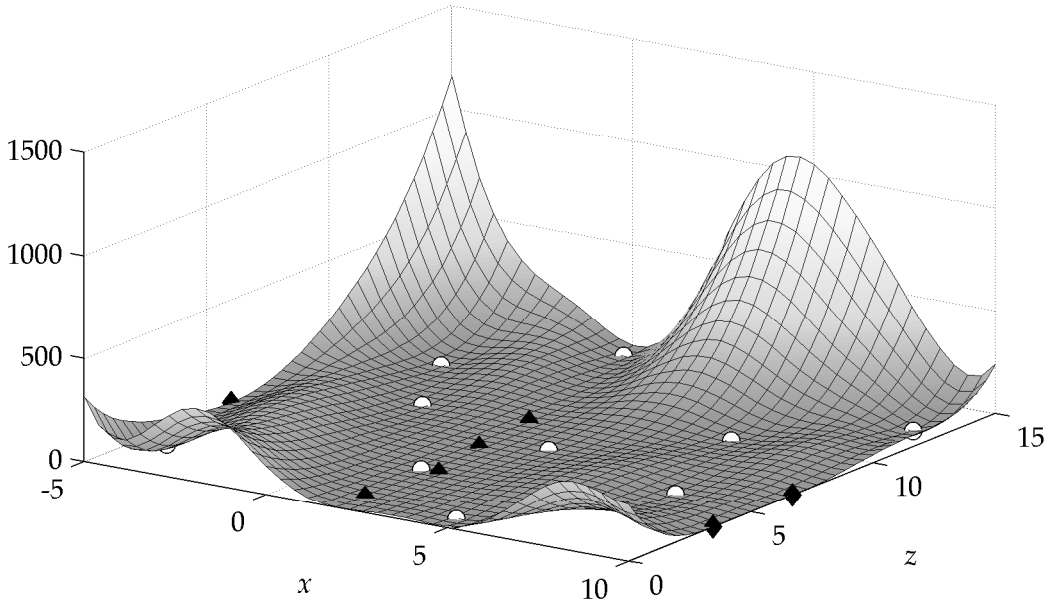

Figure 7.19: MSE of final kriging metamodel.

7.3 Six Hump Camel Back Function

The third numerical example is the so-called *six hump camel back function* [Bra72, DS75]

$$f(x,z) = 4\,x^2 - 2.1\,x^4 + \frac{1}{3}x^6 + x\,z - 4\,z^2 + 4\,z^4\ ,$$

which is depicted in Figure 7.20. The investigated design space is limited to $-2 \leq x \leq 2$. The noise variable Z is restricted to the range $-1 \leq x \leq 1$. The worst case within these tolerance bounds is taken as robustness criterion according to Equation (3.32). To evaluate the minimax robustness criterion, the DiRect optimization algorithm is applied.

The six hump camel back function was chosen for this example because it is well-suited to highlight the proposed method in the context of worst-case analysis. Since the function is highly multimodal, an accurate global approximation requires a large training data set (e.g. in [TSS$^+$05] 100 sampling points are used). Obviously, only one design $x = 0$ qualifies for a robust optimum. At this design, three different noise parameter settings are relevant, namely $z = -1$, $z = 0$, and $z = 1$. Hence, the update algorithm is expected to refine the metamodel mainly in these three subregions.

Again, a training data set of 10 sampling points (maximin distance LHD chosen from 100 LHDs) is evaluated and the same metamodel type as for the previous examples is fit to the data (Figure 7.21). Due to the comparably small set of sampling points, the initial model bears only little resemblance to the original function. The corresponding prediction variance $\hat{s}^2$ is depicted in Figure 7.22.

To determine the coordinate setting for the infill point, the design space is investigated first. Here, the maximization of the expected improvement yields the candidate $x' = 0.013$.

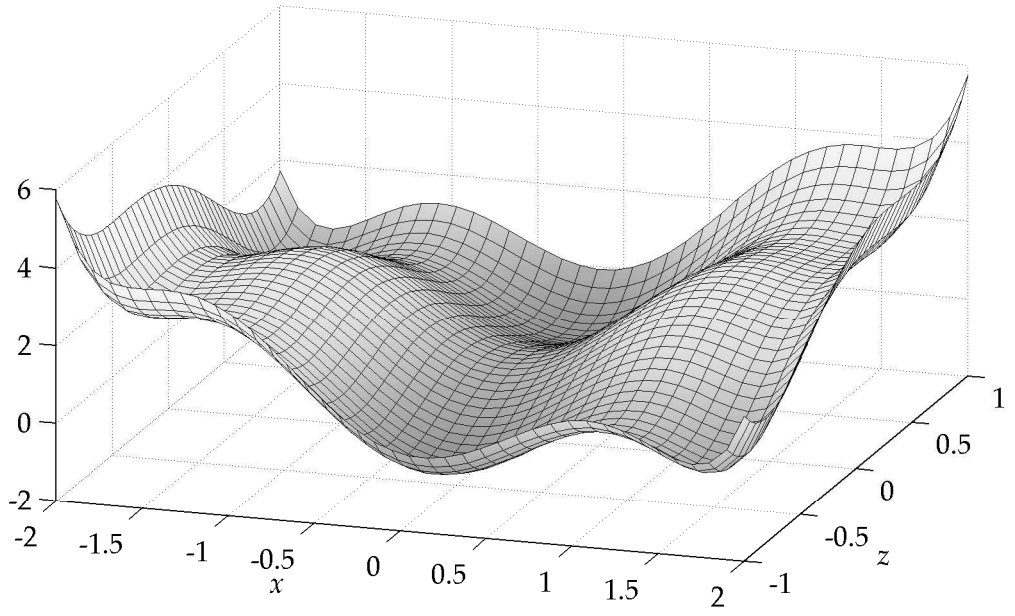

Figure 7.20: Six hump camel back function.

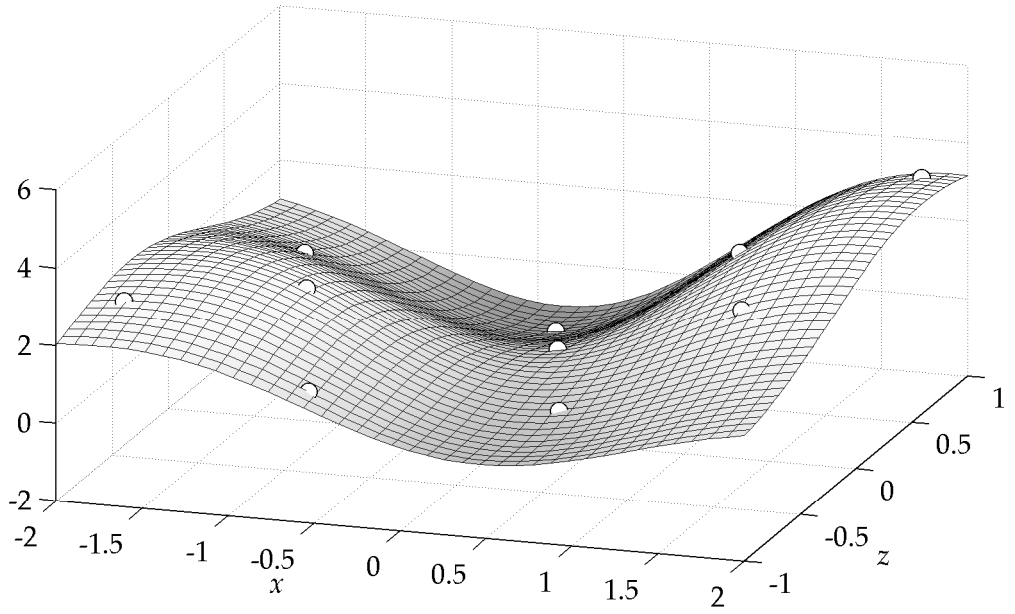

Figure 7.21: Initial kriging metamodel based on 10 samples.

For this design, a maximization of the expected worsening identifies the noise parameter setting for the infill point $z = -1$. The infill point (x', z') enlarges the set of training data for which a new metamodel is fit. The metamodel after inclusion of the first infill point is plotted in Figure 7.23.

For the updated metamodel, the expected improvement is maximized again and this procedure is continued until a stopping criterion is met. For this special example, the op-

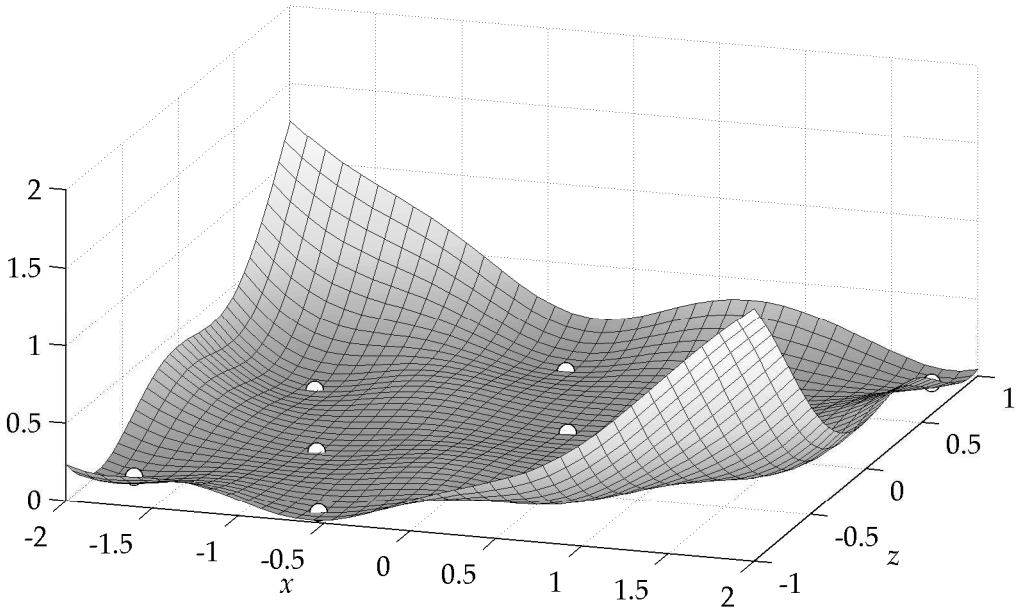

Figure 7.22: MSE of initial kriging metamodel.

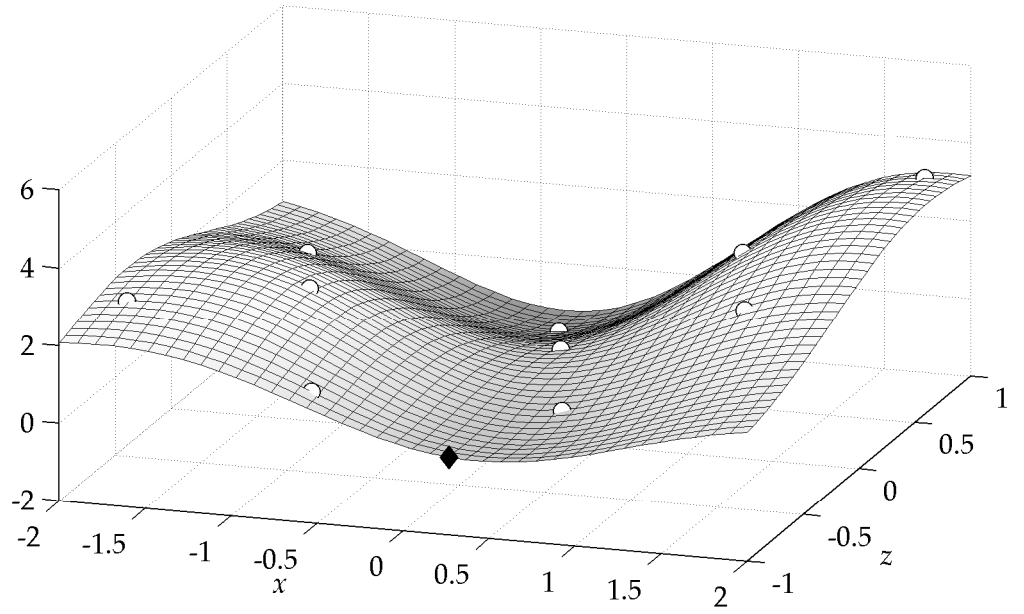

Figure 7.23: Updated kriging metamodel after inclusion of the first infill point.

timal robustness value is zero. Hence, it would not be reasonable to define the stopping criterion by means of a minimum expected improvement derived from a percentage of the robustness value. Consequently, the model update in this example is stopped as soon as the average of the three most recent expected improvement values undershoots the absolute value $\varepsilon = 0.001$ or when a maximum of 10 updates has been performed.

As illustrated by Figure 7.24, the first three infill points have been placed at the three

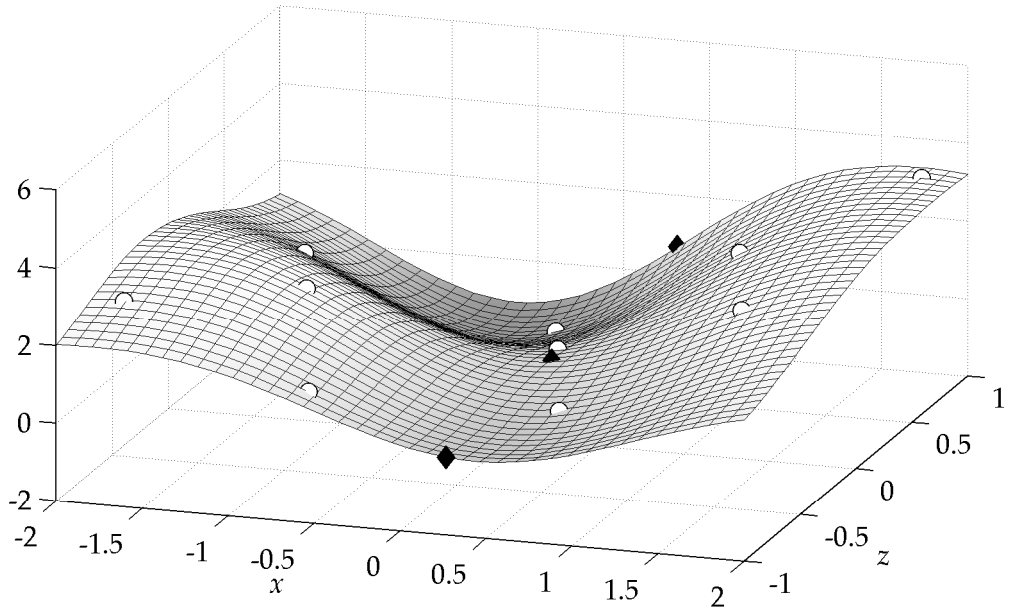

Figure 7.24: Kriging metamodel after three update steps.

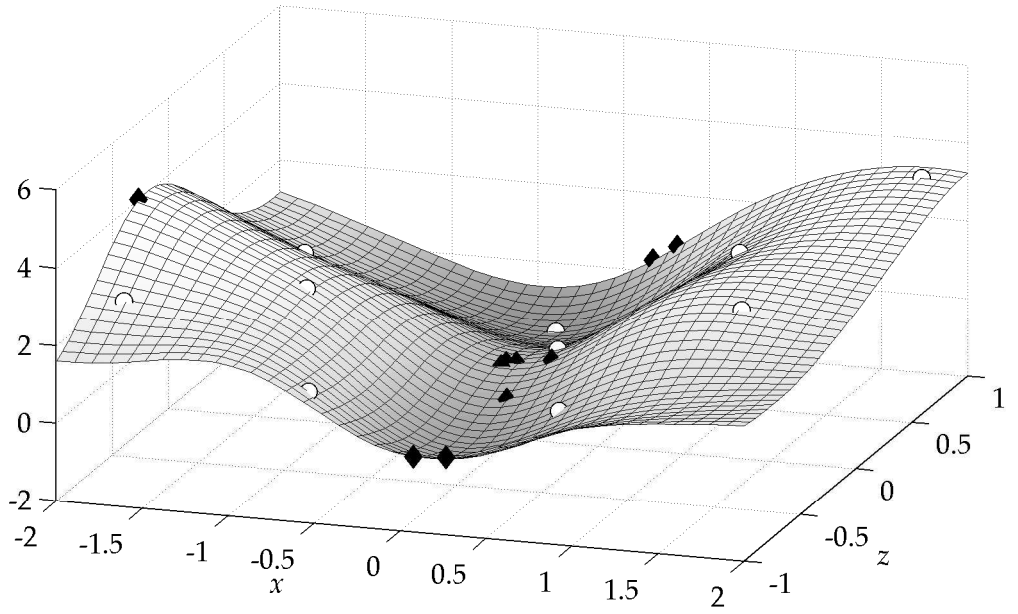

Figure 7.25: Final kriging metamodel after seven update sequences.

distinct locations which are most important for evaluation of the robustness criterion. After ten model updates (Figure 7.25), the infill points refined the crucial regions of the model such that the robust optimum is predicted accurately at $x = -0.534 \cdot 10^{-3}$ (true optimum at exactly $x^* = 0$). At this stage, the average of the three most recent $E(I)$ values is 0.003.

To illustrate how selective the update procedure focuses on the detection of the robust optimum, the projection of the original function onto the x-y-plane is contrasted with the

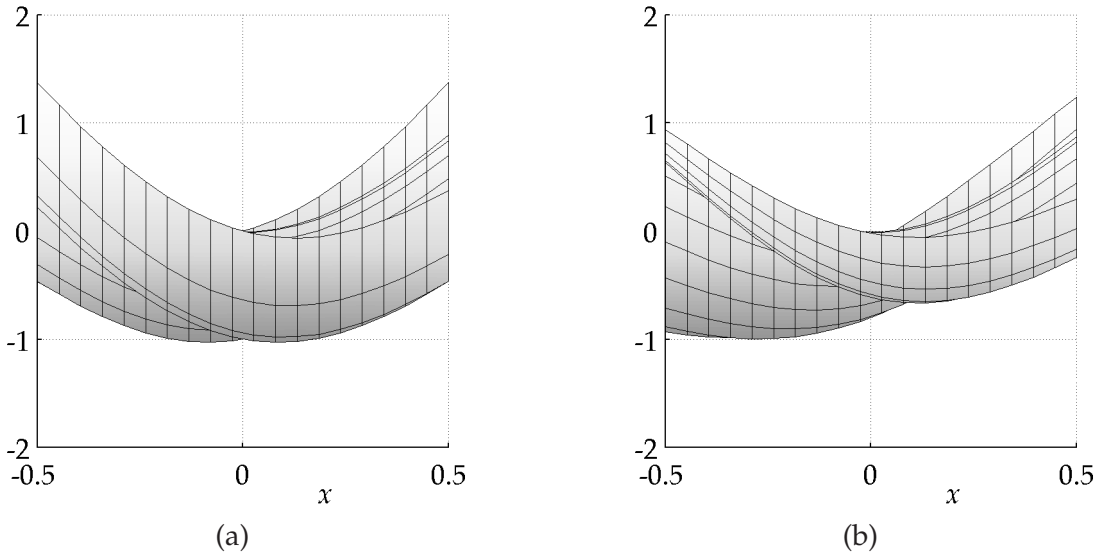

Figure 7.26: Comparison of (a) original function and (b) updated model in projection onto x-y-plane.

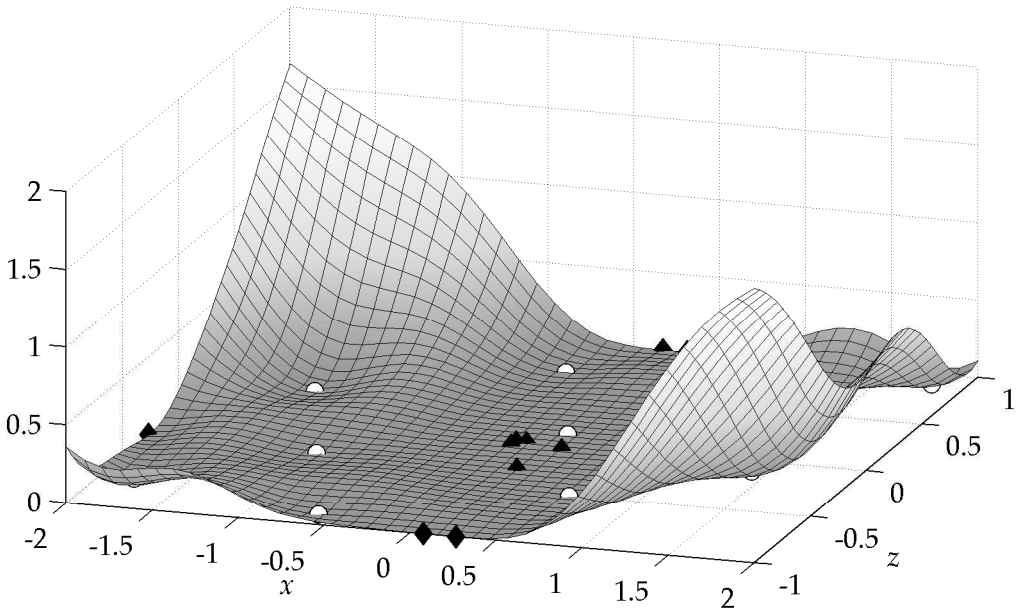

Figure 7.27: MSE of final kriging metamodel.

same projection of the final metamodel in Figure 7.26a&b. It can be seen, that the metamodel prediction only roughly estimates the true response values in large parts of the model space. However, the three decisive locations (at $x = 0$ with $z = -1$, $z = 0$, and $z = 1$) are approximated soundly. Finally, the prediction variance of the updated metamodel around the robust design $x = 0$ is close to zero over the entire range of possible noise variations (cf. Figure 7.27).

7.4 Robust Design Optimization of a Side Panel Frame in Sheet Metal Forming

As a final example, an industrial application is detailed in this section. The example shows the robust design optimization of a side panel frame which is produced by means of a deep drawing process. The design variables of this optimization problem comprise four geometric parameters, namely entry angle α_1, entry radius r, opening angle α_2, and frame depth h (cf. Figure 7.28). Simultaneously, two process variables are included into the set of design variables such that for each geometry to be studied, the best possible forming process setup is considered. Hence, the problem consists of six design variables in total. The most significant source of variation is the material, which is described by four parameters. These random variables are particularized by a joint probability density function derived from measurements of the sheet metal manufacturer.

In sheet metal forming, the quality of the designed part is typically assessed by means of the *forming limit diagram (FLD)* [MDH02, HT06]. The FLD is plotted in the space of the two principal strains $\varepsilon_{\text{major}}$ and $\varepsilon_{\text{minor}}$, respectively, which are both in-plain with the surface of the sheet metal. Accordingly, for each finite element of the analysis, its resulting principal strains are evaluated, and hence, each element is represented by a single point in the FLD. Depending on the position of this point in the diagram, different possible failure modes can be distinguished as presented in the schematic illustration of Figure 7.29.

The *forming limit curve (FLC)* represents the boundary between strain combinations producing localized necking and/or fracture (points above the FLC) and those that are permissible for the desired forming operation (points below the FLC). The FLC is material-

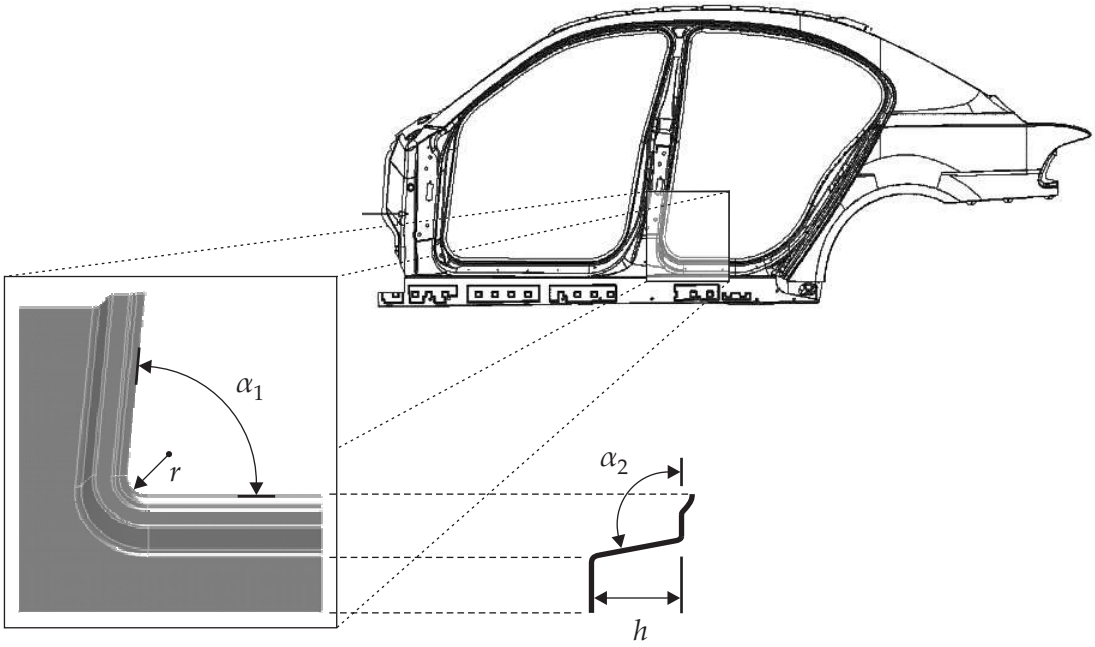

Figure 7.28: Geometric design variables of the problem.

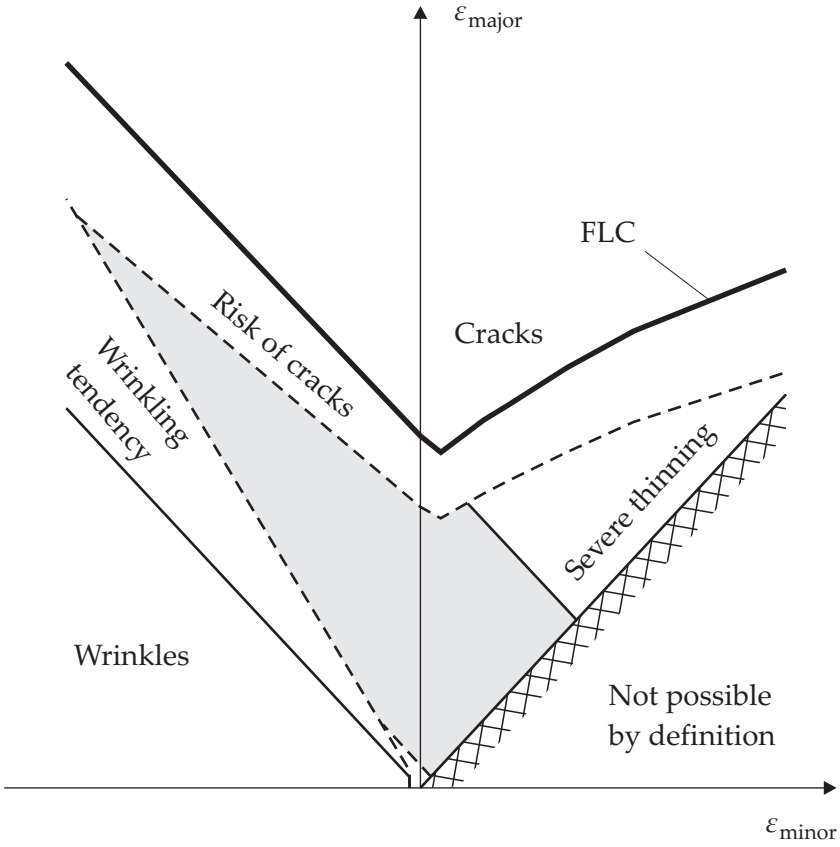

Figure 7.29: Schematic forming limit diagram (FLD).

dependent and is typically determined by means of physical experiments. Furthermore, the FLD identifies a region where wrinkling occurs, namely whenever $\varepsilon_{major} \leq -\varepsilon_{minor}$. Finally, specific combinations of major and minor principal strains can be identified which define states of excessive thinning. Typically, additional safety margins with respect to cracking and wrinkling are introduced as indicated by the dashed lines. Clearly, $\varepsilon_{major} \geq \varepsilon_{minor}$ holds by definition and thus there are no feasible points in the corresponding part of the FLD. Consequently, all points resulting from the respective finite element analyses should be inside the remaining area in the center of the FLD (highlighted in gray).

Before the optimization is started, the quality of the reference design is assessed. For this purpose, 200 Monte Carlo samples with varying material parameters are evaluated based on nonlinear finite element models. For each simulation run, the element with the highest risk of cracking is determined and only the corresponding point is plotted in the FLD. As a result, Figure 7.30a shows the FLD for the reference design containing 200 points. Each point represents the strain state of the most critical finite element for a specific combination of material parameters. It can be seen from Figure 7.31 that there are two particular locations on the blank sheet at which cracking can possibly occur. Due to this fact, the most critical elements also cluster in two distinct regions in the FLD.

The aim of the robust design optimization in this example is to reduce ε_{major} such that even in the worst case all elements are located within the optimal formability range. Con-

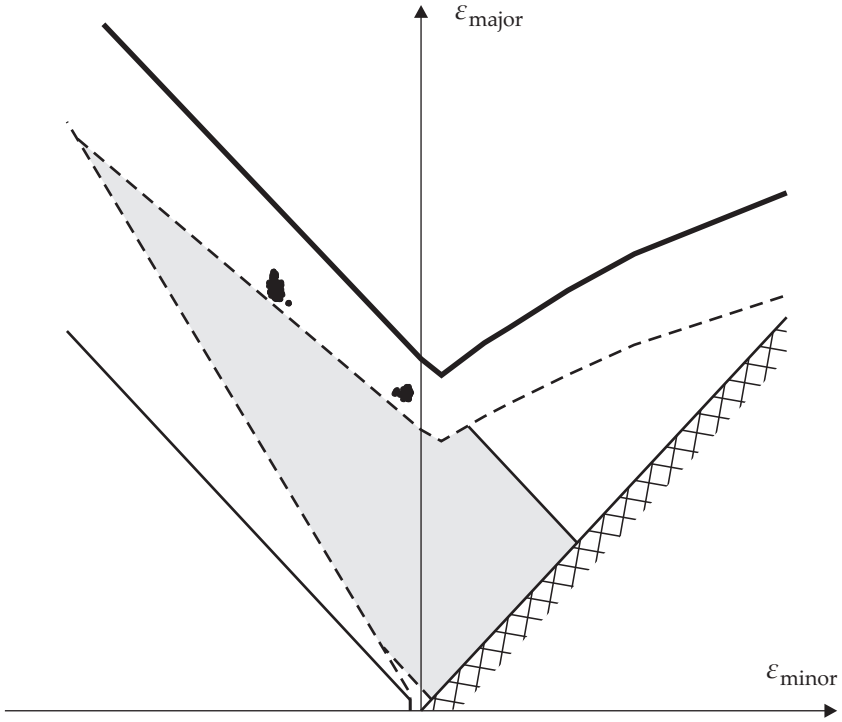

(a)

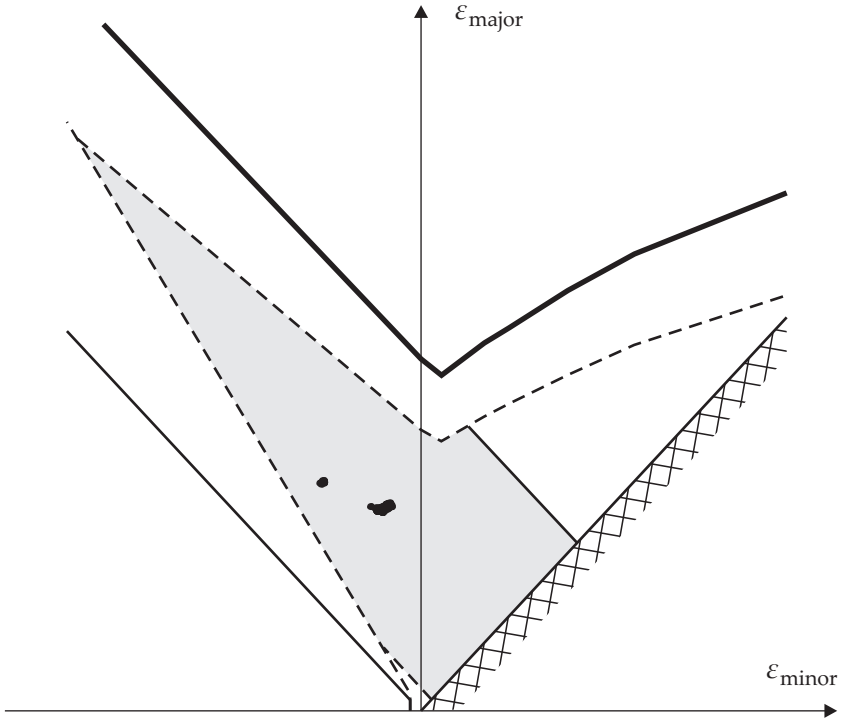

(b)

Figure 7.30: Forming limit diagrams comparing (a) reference design and (b) optimized design.

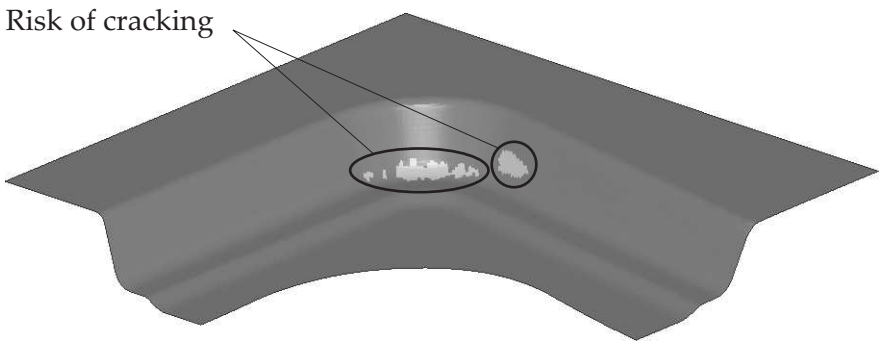

Figure 7.31: Two separate locations with pronounced risk of cracking in the reference design.

currently, the variation in this response value should be reduced to minimize the observable spread of points in the FLD. To achieve this goal, the objective function is composed according to Equation (3.38) with $w = 4$. The problem is tackled by using a maximin-distance Latin hypercube design with an initial size of 200 sampling points. For the resulting parameter settings, finite element analyses are performed to gain the required training data. Then, a first kriging metamodel with Gaussian correlation formulation is fitted and the proposed update procedure is repeated until the expected improvement averaged over the last three updates undershoots 0.1% of the robustness criterion evaluated at the estimated optimum. In this study, the $E(I)$ value falls below the given treshold after 12 model updates.

Finally, the obtained robust optimum is verified by means of another Monte Carlo sampling. Again, 200 analyses of the original finite element code are evaluated yielding the plot in Figure 7.30b. A comparison of the reference design with the optimized layout reveals that both criteria (mean and standard deviation) are significantly improved during the optimization. In general, the optimized design exhibits a more favorable formability and the variation is considerably reduced. To point out the smaller variance, a zoomed version of one of the scatter plots is depicted in Figure 7.32.

This industrial application proves both applicability and efficiency of the proposed

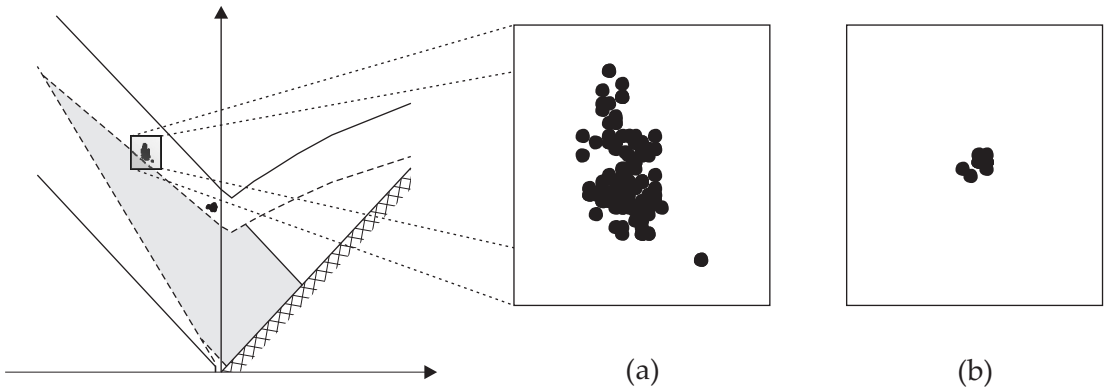

Figure 7.32: Zoomed scatter plots comparing (a) reference design and (b) optimized design.

method. Obviously, the two objectives i.e. to improve mean performance and to reduce the deteriorating effects caused by the variation in the material parameters are achieved during the optimization. The computational effort related to the complete robust design optimization (here: 212 FE simulations) is not much larger than what is typically spent to assess the robustness of one single design (in the present case: 200 simulations per design). Hence, with an average computation time of around 30 minutes per original analysis, the suggested approach is expensive, but still feasible for many applications.

Chapter 8

Conclusions and Outlook

In the present work, the concepts of robust design and reliability-based optimization were discussed – two special ways how to grasp and solve stochastic optimization problems. Stochastic optimization problems are characterized by the trait that some input parameters (so-called noise parameters) are not deterministic, but either uncertain or stochastic in nature. The challenge in solving this class of problems is to quantify the consequences of noise in the input parameters on some output value. In particular, respective tolerance ranges or probability distributions related to noise parameters have to be mapped onto ranges of fluctuation or probability densities of the observed response.

Once this information is obtained, the question arises how to assess and compare a probability distribution resulting from one design to an alternative design. For this purpose, suitable deterministic substitute formulations were compiled from different fields of research with a focus on robustness criteria derived from statistical decision theory. These substitute formulations were discussed in detail. On closer inspection, all robustness criteria could be classified into two groups: Robustness formulations based on statistics (for instance, mean value and standard deviation) or robustness criteria defined by extreme events (worst-case analysis).

In general, the presented formulations require a multitude of function evaluations to assess one single design. During an optimization process, where many alternative designs have to be considered, the number of required function evaluations rapidly becomes excessive. Especially in computational engineering, where analyses typically rely on nonlinear systems of equations (for instance, derived from a nonlinear finite element formulation), even pointwise solutions can be quite expensive to evaluate. To reduce the enormous numerical effort related to robustness analyses, metamodeling techniques were used in this thesis to replace the actual numerical analysis codes by a simpler formulation. Metamodels are fitted to each individual problem on the basis of training data i.e. response values of the original system obtained at a selection of sampling points. Different metamodeling techniques were introduced and compared in the present work. Special emphasis was placed on formulations that result in an interpolating model such that all training data points are exactly reproduced by the metamodel prediction.

To collect training data efficiently, the locations for sampling points have to be chosen systematically thus assuring a maximum gain in information with minimal effort. Various methods were proposed for this purpose, typically summarized under the notion of design

of experiments (DoE). Typically, a specific DoE method is most suitable in combination with each individual metamodel formulation. For interpolating models, experimental designs with space-filling property were introduced. This feature assures a balanced predictive performance of the approximation model throughout the investigated model space.

Finally, it was pointed out that optimization based on metamodels yields a prediction for the optimum. To guarantee for a reliable and accurate optimization result, a method to sequentially update the metamodel during the optimization process was proposed. In contrast to existing methods for sequential approximations in optimization, the update procedure is particularly tailored to solve robust design problems. In this context, the search for infill points is divided into two parts. The design and the noise space are explored successively using adapted search criteria. At this point, the proposed classification of robustness criteria was used to account for the individual requirements of each robustness formulation.

Three mathematical test functions and one industrial application were used to verify and illustrate the proposed method showing its applicability and efficiency. In reference to these examples, it should be noted that different optimization runs starting with random Latin hypercube designs will generally yield (at least slightly) different optimization results. Furthermore, by choosing too few sampling points, robust designs might remain undiscovered because the prediction error of the metamodel can dominate the "true variance" due to the noise.

Consecutive work will have to proof successful application of the proposed method to more industrial applications. As a possible application example from the field of civil engineering, the renewal of a historical wooden roof structure is envisioned. In this construction, actual state and condition of the aged wood and joints are uncertain.

The realization of such examples is still impeded by lacking or unavailable interfaces to link the optimization procedure to the respective analysis software. Here, the integration of the proposed concept in commercial optimization software, which typically feature interfaces to popular and well-established commercial solvers, would enable a broader range of applications.

In future research, the proposed method of sequentially updated metamodels for robust design problems could be augmented to include also reliability problems. In this case, care has to be taken that the metamodels for the constraints are updated in crucial subregions. Possible locations for infill points in constraint model update could include the *most probable point (MPP)* i.e. the point in the infeasible domain with the highest probability density.

Bibliography

[AE77] P. Audze and V. Eglais. New approach for planning out of experiments. *Problems of Dynamics and Strengths*, 35:104–107, 1977.

[AHH94] J. S. Arora, M. W. Huang, and C. C. Hsieh. Methods for optimization of nonlinear problems with discrete variables: A review. *Structural Optimization*, 8(2–3):69–85, 1994.

[Alv00] L. F. Alvarez. *Design Optimization Based On Genetic Programming*. PhD thesis, University of Bradford, UK, 2000.

[AM04] M. Allen and K. Maute. Reliability-based design optimization of aeroelastic structures. *Structural and Multidisciplinary Optimization*, 27(4):228–242, 2004.

[And97] J. A. Anderson. *An Introduction to Neural Networks*. MIT Press, Cambridge, MA, USA, 3rd print. edition, 1997.

[Aro89] J. S. Arora. *Introduction to Optimum Design*. McGraw-Hill Series in Mechanical Engineering. McGraw-Hill, New York, NY, USA, 1989.

[Bar98] R. R. Barton. Simulation metamodels. In *Proceedings of the 1998 Winter Simulation Conference*, pages 167–174, 1998.

[BB94] H. Bandemer and A. Bellmann. *Statistische Versuchsplanung*. B.G. Teubner Verlagsgesellschaft, Stuttgart, 4th edition, 1994.

[BD87] G. E. P. Box and N. R. Draper. *Empirical Model Building and Response Surfaces*. John Wiley & Sons, New York, NY, USA, 1987.

[BDF+99] A. J. Booker, J. E. Dennis Jr., P. D. Frank, D. B. Serafini, V. Torczon, and M. W. Trosset. A rigorous framework for optimization of expensive functions by surrogates. *Structural Optimization*, 17(1):1–13, 1999.

[Ber85] J. O. Berger. *Statistical Decision Theory and Bayesian Analysis*. Springer Series in Statistics. Springer-Verlag, New York, NY, USA, 2nd edition, 1985.

[BFM96] T. Bäck, D. B. Fogel, and Z. Michalewicz. *Handbook of Evolutionary Computation*. University Oxford Press, New York, NY, USA, 1996.

[BGLS97] J. F. Bonnans, J. C. Gilbert, C. Lemaréchal, and C. A. Sagastizábal. *Numerical Optimization. Theoretical and Practical Aspects*. Springer-Verlag, 1997.

[BH93] J. F. M. Barthelemy and R. Haftka. Approximations concepts for optimal structural design – a review. *Structural Optimization*, 5(3):129–144, 1993.

[Ble93] K.-U. Bletzinger. Extended method of moving asymptotes based on second-order information. *Structural Optimization*, 5(3):175–183, 1993.

[BM04] C. Bucher and M. Macke. Stochastic computational mechanics. In S. Jendo and K. Doliński, editors, *Reliability-Based Design and Optimisation*, number 16 in AMAS Lecture Notes, pages 99–156. Institute of Fundamental Technological Research, Polish Academy of Sciences, Warshaw, PL, 2004.

[Box80] J. Fisher Box. R. A. Fisher and the design of experiments, 1922-1926. *The American Statistician*, 34(1):1–7, 1980.

[Bra72] F. H. Branin Jr. Widely convergent method for finding multiple solutions of simultaneous nonlinear equations. *IBM Journal of Research and Development*, 16(5):504–522, 1972.

[Bro70] C. G. Broyden. The convergence of a class of double rank minimization algorithms. *Journal of the Institute of Mathematics and Applications*, 6:76–90, 1970.

[BS93] T. Bäck and H.-P. Schwefel. An overview of evolutionary algorithms for parameter optimization. *Evolutionary Computation*, 1(1):1–23, 1993.

[BSS93] M. S. Bazaraa, H. D. Sherali, and C. M. Shetty. *Nonlinear Programming. Theory and Algorithms.*, volume 2. John Wiley & Sons, 1993.

[BST04] S. J. Bates, J. Sienz, and V. V. Toropov. Formulation of the optimal Latin hypercube design of experiments using a permuation genetic algorithm. In *Proceedings of the 45th AIAA/ASME/ASCE/AHS/ASC Structures, Structural Dynamics & Materials Conference*, Palm Springs, CA, USA, April 2004.

[CB93] W. C. Carpenter and J.-F. M. Barthelemy. A comparison of polynomial approximations and artificial neural nets as response surfaces. *Structural Optimization*, 5(3):166–174, 1993.

[CMMY88] C. Currin, T. Mitchell, M. Morris, and D. Ylvisaker. A bayesian approach to the design and analysis of computer experiments. Technical Report ORNL–6498, Oak Ridge National Laboratory, Oak Ridge, TN, USA, September 1988.

[Cre93] N. A. C. Cressie. *Statistics for spatial data*. John Wiley & Sons, New York, NY, USA, rev. edition, 1993.

[CU93] A. Cichocki and R. Unbehauen. *Neural Networks for Optimization and Signal Processing*. Wiley, Chichester, UK, 1993.

[Dao05] F. Daoud. *Formoptimierung von Freiformschalen: Mathematische Algorithmen und Filtertechniken*. Schriftenreihe des Lehrstuhls für Statik TU München. Shaker Verlag, Aachen, 2005.

[Das97] I. Das. *Nonlinear Multicriteria Optimization and Robust Optimality*. PhD thesis, Rice University, Houston, TX, USA, April 1997.

[Das00] I. Das. Robust optimization for constrained, nonlinear programming problems. *Engineering Optimization*, 32(5):585–618, June 2000.

[Dav59] W. C. Davidon. Variable metric method for minimization. Technical report, Argonne National Laboratory, ANL-5990 Rev., Argonne, IL, USA, 1959.

[DC00] X. Du and W. Chen. Towards a better understanding of modeling feasibility robustness in engineering. *Transactions of ASME, Journal of Mechanical Design*, 122(4):385–394, 2000.

[Deb01] K. Deb. *Multi-Objective Optimization Using Evolutionary Algorithms*. John Wiley & Sons, Chichester, UK, 2001.

[DS75] L. C. W. Dixon and G. P. Szegö, editors. *Towards Global Optimisation*. North-Holland Publishing Company, Amsterdam, NL, 1975. Proceedings of a workshop at the University of Cagliari, IT, October 1974.

[DS78] L. C. W. Dixon and G. P. Szegö. The global optimization problem: an introduction. In L. C. W. Dixon and G. Szegö, editors, *Towards Global Optimisation 2*, pages 1–15. North-Holland Publishing Company, Amsterdam, NL, 1978.

[DV97] R. J. Del Vecchio. *Understanding Design of Experiments: A Primer for Technologists*. Hanser Understanding Books. Carl Hanser Verlag, Munich, 1997.

[EKO90] H. Eschenauer, J. Koski, and A. Osyczka, editors. *Multicriteria Design Optimization: Procedures and Applications*. Springer-Verlag, Berlin, 1990.

[Etm94] L. F. P. Etman. Design and analysis of computer experiments: The method of Sacks et al. Engineering Mechanics report WFW 94.098, Eindhoven University of Technology, NL, 1994.

[Etm97] L. F. P. Etman. *Optimization of Multibody Systems using Approximation Concepts*. PhD thesis, Eindhoven University of Technology, NL, 1997.

[Evt85] Y. G. Evtushenko. *Numerical Optimization Techniques*. Springer-Verlag, Berlin, 1985.

[FC95] W. Y. Fowlkes and C. M. Creveling. *Engineering Methods for Robust Product Design: Using Taguchi Methods in Technology and Product Development*. Addison-Wesley, Reading, MA, USA, 1995.

[Fer67] T. S. Ferguson. *Mathematical Statistics: A Decision Theoretic Approach*. Academic Press, New York, NY, USA, 1967.

[Fis66] R. A. Fisher. *The Design of Experiments*. Oliver & Boyd, Edinburgh, UK, 8th edition, 1966.

[Fle70] R. Fletcher. A new approach to variable metric algorithms. *The Computer Journal*, 13:317–322, 1970.

[Fle87] R. Fletcher. *Practical Methods of Optimization*, volume 2. John Wiley & Sons, 1987.

[FLS05] K.-T. Fang, R. Li, and A. Sudjianto. *Design and Modeling for Computer Experiments*. Computer Science and Data Analysis Series. Chapman & Hall/CRC, Boca Raton, FL, USA, 2005.

[FM03] D. M. Frangopol and K. Maute. Life-cycle reliability-based optimization of civil and aerospace structures. *Computers & Structures*, 81(7):397–410, 2003.

[FN05] J. Forsberg and L. Nilsson. On polynomial response surfaces and kriging for use in structural optimization of crashworthiness. *Structural and Multidisciplinary Optimization*, 29:232–243, 2005.

[FP63] R. Fletcher and M. J. D. Powell. A rapidly convergent descent method for minimization. *The Computer Journal*, 6:163–168, 1963.

[FR64] R. Fletcher and C. M. Reeves. Function minimization by conjugate gradients. *The Computer Journal*, 7(2):149–154, 1964.

[GBH+97] A. A. Giunta, V. Balabanov, D. Haim, B. Grossman, W. H. Mason, L. T. Watson, and R. T. Haftka. Multidisciplinary optimisation of a supersonic transport using design of experiments theory and response surface modelling. *Aeronautical Journal*, 101(1008):347–356, 1997.

[GDN+94] A. A. Giunta, J. M. Dudley, R. Narducci, B. Grossman, R. T. Haftka, W. H. Mason, and L. T. Watson. Noisy aerodynamic response and smooth approximations in HSCT design. In *Proceedings of the 5th AIAA/USAF/NASA/ISSMO Symposium on Multidisciplinary Analysis & Optimization, Technical Papers, Pt. 2*, pages 1117–1128, Panama City Beach, FL, USA, September 1994.

[GFO02] E. S. Gharaibeh, D. M. Frangopol, and T. Onoufriou. Reliability-based importance assessment of structural members with applications to complex structures. *Computers & Structures*, 80(12):1113–1131, 2002.

[Gol70] D. Goldfarb. A family of variable metric updates derived by variational means. *Mathematics of Computing*, 24:23–26, 1970.

[GRMS06] S. E. Gano, J. E. Renaud, J. D. Martin, and T. W. Simpson. Update strategies for kriging models used in variable fidelity optimization. *Structural and Multidisciplinary Optimization*, 32(4):287–298, 2006.

[GS97] M. Gasser and G. I. Schuëller. Reliability-based optimization of structural systems. *Mathematical Methods of Operations Research (ZOR)*, 46(3):287–307, 1997.

[Gut01] H.-M. Gutmann. A radial basis function method for global optimization. *Journal of Global Optimization*, 19(3):201–227, 2001.

[GW98] A. A. Giunta and L. T. Watson. A comparison of approximation modeling techniques: Polynomial versus interpolating models. In *Proceedings of the 7th AIAA/USAF/NASA/ISSMO Symposium on Multidisciplinary Analysis & Optimization, Collection of Technical Papers*, St. Louis, MO, USA, September 1998.

[Hay99] S. Haykin. *Neural Networks: A Comprehensive Foundation*. Prentice-Hall, Upper Saddle River, NJ, USA, 2nd edition, 1999.

[HG91] R. T. Haftka and Z. Gürdal. *Elements of Structural Optimization*. Kluwer Academic Publishers, Dordrecht, NL, 3rd & ext. edition, 1991.

[HK04] J. S. Han and B. M. Kwak. Robust optimization using a gradient index: MEMS applications. *Structural and Multidisciplinary Optimization*, 27(6):469–478, 2004.

[HL92] P. Hajela and C.-Y. Lin. Genetic search strategies in multicriterion optimal design. *Structural Optimization*, 4(2):99–107, 1992.

[HLP01] K.-H. Hwang, K.-W. Lee, and G.-J. Park. Robust optimization of an automobile rearview mirror for vibration reduction. *Structural and Multidisciplinary Optimization*, 21(4):300–308, 2001.

[HR84] M. Hohenbichler and R. Rackwitz. Mathematische Grundlagen der Zuverlässigkeitsmethoden erster Ordnung und einige Erweiterungen. Berichte zur Zuverlässigkeitstheorie der Bauwerke 72, Laboratorium für den konstruktiven Ingenieurbau (LKI), Technische Universität München, 1984.

[HS81] W. Hock and K. Schittkowski. *Test examples for nonlinear programming codes*. Springer-Verlag, Berlin, 1981.

[HT06] P. Hora and L. Tong. Prediction of forming limits in virtual sheet metal forming – yesterday, today and tomorrow. In *Proceedings of the FLC Zurich 2006*, IVP, ETH Zurich, CH, March 2006.

[Hus06] B. G. M. Husslage. *Maximin designs for computer experiments*. PhD thesis, Tilburg University, NL, 2006.

[IC82] R. L. Iman and W. J. Conover. A distribution-free approach to inducing rank correlation among input variables. *Communications in Statistics: Simulation and Computation*, B11(3):311–334, 1982.

[JB05] F. Jurecka and K.-U. Bletzinger. Numerische Methoden für eine lebenszyklusorientierte Statik. Schlussbericht zum BayFORREST Forschungsprojekt F253, Technische Universität München, December 2005.

[JCS01] R. Jin, W. Chen, and T. W. Simpson. Comparative studies of metamodelling techniques under multiple modelling criteria. *Structural and Multidisciplinary Optimization*, 23:1–13, 2001.

[JDC03] R. Jin, X. Du, and W. Chen. The use of metamodeling techniques for optimization under uncertainty. *Structural and Multidisciplinary Optimization*, 25(2):99–116, 2003.

[JGB04] F. Jurecka, M. Ganser, and K.-U. Bletzinger. Sampling techniques for sequential kriging metamodels in robust design optimisation. In B. H. V. Topping and C. A. Mota Soares, editors, *Proceedings of the Seventh International Conference on*

Computational StructuresTechnology, Stirling, UK, September 2004. Civil-Comp Press. paper 113.

[JHN05] J. Jakumeit, M. Herdy, and M. Nitsche. Parameter optimization of the sheet metal forming process using an iterative parallel Kriging algorithm. *Structural and Multidisciplinary Optimization*, 29(6):498–507, 2005.

[JL02] D. H. Jung and B. C. Lee. Development of a simple and efficient method for robust optimization. *International Journal for Numerical Methods in Engineering*, 53(9):2201–2215, 2002.

[JMY90] M. E. Johnson, L. M. Moore, and D. Ylvisaker. Minimax and maximin distance designs. *Journal of Statistical Planning and Inference*, 26:131–148, 1990.

[Jon01] D. R. Jones. The DIRECT global optimization algorithm. In *Encyclopedia of Optimization, Vol.1*, pages 431–440, Boston, MA, USA, 2001. Kluwer Academic.

[JPS93] D. R. Jones, C. D. Perttunen, and B. E. Stuckman. Lipschitzian optimization without the Lipschitz constant. *Journal of Optimization Theory and Applications*, 79(1):157–181, 1993.

[JSW98] D. R. Jones, M. Schonlau, and W. J. Welch. Efficient global optimization of expensive black-box functions. *Journal of Global Optimization*, 13(4):455–492, 1998.

[JZ72] W. Jurecka and H.-J. Zimmermann. *Operations Research im Bauwesen: Optimierung und Entscheidung von Ingenieurproblemen*. Springer-Verlag, Berlin, 1972.

[Kac85] R. N. Kackar. Off-line quality control, parameter design, and the Taguchi method. *Journal of Quality Technology*, 17(4):176–188, 1985.

[KEMB02] H. Kurtaran, A. Eskandarian, D. Marzougui, and N. Bedewi. Crashworthiness design optimization using successive response surface approximations. *Computational Mechanics*, 29:409–421, 2002.

[Kha96] R. Khattree. Robust parameter design: A response surface approach. *Journal of Quality Technology*, 28(2):187–198, 1996.

[Kim90] S. Kimmich. *Strukturoptimierung und Sensitivitätsanalyse mit finiten Elementen*. PhD thesis, Universität Stuttgart, 1990.

[Kir93] U. Kirsch. *Structural Optimization: Fundamentals and Applications*. Springer-Verlag, Berlin, 1993.

[KKB98] S. Kravanja, Z. Kravanja, and B. S. Bedenik. The MINLP optimization approach to structural synthesis. part I–III. *International Journal for Numerical Methods in Engineering*, 43(2):263–364, 1998.

[Koc02] P. N. Koch. Probabilistic design: Optimizing for six sigma quality. In *Proceedings of the 43rd AIAA//ASME//ASCE//AHS//ASC Structures, Structural Dynamics, and Materials Conference*, Denver, CO, USA, April 2002.

[Kri51] D. G. Krige. A statistical approach to some mine valuation and allied problems on the Witwatersrand. Master's thesis, University of the Witwatersrand, South Africa, 1951.

[Kri03] T. Krishnamurthy. Response surface approximation with augmented and compactly supported radial basis functions. In *Proceedings of the 44th AIAA/ASME/ASCE/AHS/ASC Structures, Structural Dynamics, and Materials Conference*, Norfolk, VA, USA, April 2003.

[KS86] R. N. Kackar and A. C. Shoemaker. Robust design: A cost effective method for improving manufacturing processes. *AT&T Technical Journal*, 65(2):39–50, 1986.

[KS97] J. P. C. Kleijnen and R. G. Sargent. A methodology for fitting and validating metamodels in simulation. Technical Report 97116, Department of Information Systems, Center for Economic Research, Tilburg University, 5000 LE Tilburg, NL, 1997.

[KS99] S. Kok and N. Stander. Optimization of a sheet metal forming process using successive multipoint approximations. *Structural Optimization*, 18(4):277–295, 1999.

[KWGS02] P. N. Koch, B. Wujek, O. Golovidov, and T. W. Simpson. Facilitating probabilistic multidisciplinary design optimization using kriging approximation models. In *Proceedings of the 9th AIAA/ISSMO Symposium on Multidisciplinary Analysis and Optimization*, Atlanta, GA, USA, September 2002.

[KYG04] P. N. Koch, R.-J. Yang, and L. Gu. Design for six sigma through robust optimization. *Structural and Multidisciplinary Optimization*, 26(3–4):235–248, 2004.

[Lau00] U. Lautenschlager. *Robuste Multikriterien-Strukturoptimierung mittels Verfahren der Statistischen Versuchsplanung*. FOMAAS, TIM-Bericht Nr. T16-05.00, Universität – GH Siegen, 2000.

[Lau05] H. Laux. *Entscheidungstheorie*. Springer-Verlag, Berlin, 6th (rev.) edition, 2005.

[LD60] A. H. Land and A. G. Doig. An automatic method for solving discrete programming problems. *Econometrica*, 28:497–520, 1960.

[LHP02] W. Li, L. Huyse, and S. Padula. Robust airfoil optimization to achieve drag reduction over a range of Mach numbers. *Structural and Multidisciplinary Optimization*, 24(1):38–50, 2002.

[LLFSS98] J. Lei, P. Lima-Filho, M. A. Styblinski, and C. Singh. Propagation of variance using a new approximation in system design of integrated circuits. In *Proceedings of the IEEE 1998 National Aerospace and Electronics Conference*, pages 242–246, July 1998.

[LP01] K.-H. Lee and G.-J. Park. Robust optimization considering tolerances of design variables. *Computers & Structures*, 79:77–86, 2001.

[LS86] P. Lancaster and K. Salkauskas. *Curve and Surface Fitting: An Introduction*. Academic Press, London, UK, 1986.

[LW66] E. L. Lawler and D. E. Wood. Branch-and-bound methods – a survey. *Operations Research*, 14:699–719, 1966.

[LYR02] J.-O. Lee, Y.-S. Yang, and W.-S. Ruy. A comparative study on reliability-index and target-performance-based probabilistic structural design optimization. *Computers & Structures*, 80:257–269, 2002.

[Mar02] K. Marti. Robust optimal design: a stochastic optimization problem. In K. Marti, editor, *Stochastic Optimization Techniques: Numerical Methods and Technical Applications*, volume 513 of *Lecture Notes in Economics and Mathematical Systems*, pages 35–55. Springer-Verlag, Berlin, 2002.

[MBC79] M. D. McKay, R. J. Beckmann, and W. J. Conover. A comparison of three methods for selecting values of input variables in the analysis of output from a computer code. *Technometrics*, 21(2):239–245, 1979.

[MDH02] Z. Marciniak, J. L. Duncan, and S. J. Hu. *Mechanics of sheet metal forming*. Butterworth-Heinemann, Oxford, UK, 2nd edition, 2002.

[MF03] K. Maute and D. M. Frangopol. Reliability-based design of MEMS mechanisms by topology optimization. *Computers & Structures*, 81:813–824, 2003.

[MH04] M. McDonald and M. Heller. Robust shape optimization of notches for fatigue-life extension. *Structural and Multidisciplinary Optimization*, 28(1):55–68, 2004.

[Min86] M. Minoux. *Mathematical Programming - Theory and Algorithms*. John Wiley & Sons, Chichester, NY, USA, 1986.

[MKV92] R. H. Myers, A. I. Khuri, and G. G. Vining. Response surface alternatives to the Taguchi robust parameter design approach. *The American Statistician*, 46(2):131–139, 1992.

[MM02] R. H. Myers and D. C. Montgomery. *Response Surface Methodology: Process and Product Optimization Using Designed Experiments*. John Wiley & Sons, New York, NY, USA, 2nd edition, 2002.

[Mon01] D. C. Montgomery. *Design and Analysis of Experiments*. John Wiley & Sons, New York, NY, USA, 5th edition, 2001.

[MPV01] D. C. Montgomery, E. A. Peck, and G. G. Vining. *Introduction to Linear Regression Analysis*. John Wiley & Sons, New York, NY, USA, 3rd edition, 2001.

[MR03] D. C. Montgomery and G. C. Runger. *Applied Statistics and Probability for Engineers*. John Wiley & Sons, New York, NY, USA, 3rd edition, 2003.

[MS02] J. D. Martin and T. W. Simpson. Use of adaptive metamodeling for design optimization. In *Proceedings of the 9th AIAA/ISSMO Symposium on Multidisciplinary Analysis and Optimization*, Atlanta, GA, USA, September 2002.

[MS03] J. D. Martin and T. W. Simpson. A study on the use of kriging models to approximate deterministic computer models. In *Proceedings of DETC 2003. ASME Design Engineering Technical Conferences and Computers and Information in Engineering Conference*, Chicago, IL, USA, 2003.

[Nai92] V. N. Nair. Taguchi's parameter design: A panel discussion. *Technometrics*, 34(2):127–161, 1992.

[NGV+95] R. Narducci, B. Grossman, M. Valorani, A. Dadone, and R. T. Haftka. Optimization methods for non-smooth or noisy objective functions in fluid design problems. In *Proceedings of the 12th AIAA Computational Fluid Dynamics Conference*, pages 21–32, San Diego, CA, USA, June 1995.

[Nie48] J. Niehans. Zur Preisbildung bei ungewissen Erwartungen. *Schweizer Zeitschrift für Volkswirtschaft und Statistik*, 84:433–456, 1948.

[NW99] J. Nocedal and S. J. Wright. *Numerical Optimization*. Springer series in operations research. Springer-Verlag, New York, NY, USA, 1999.

[OA96] I. G. Osio and C. H. Amon. An engineering design methodology with multistage bayesian surrogates and optimal sampling. *Research in Engineering Design*, 8:189–206, 1996.

[OF02] T. Onoufriou and D. M. Frangopol. Reliability-based inspection optimization of complex structures: A brief retrospective. *Computers & Structures*, 80:1133–1144, 2002.

[Owe92] A. B. Owen. Orthogonal arrays for computer experiments, integration and visualization. *Statistica Sinica*, 2:439–452, 1992.

[Par06] V. Pareto. *Manuale di Economia Politica*. Piccola Biblioteca Scientifica, Milan, IT, 1906. English translation by A. S. Schwier, *Manual of Political Economy*, MacMillan, London, UK, 1972.

[Par96] S. H. Park. *Robust Design and Analysis for Quality Engineering*. Chapman & Hall, London, UK, 1996.

[PB46] R. L. Plackett and J. P. Burman. The design of optimum multifactorial experiments. *Biometrika*, 33(4):305–325, 1946.

[PG02] R. C. Penmetsa and R. V. Grandhi. Efficient estimation of structural reliability for problems with uncertain intervals. *Computers & Structures*, 80:1103–1112, 2002.

[Pha89] M. S. Phadke. *Quality Engineering Using Robust Design: Robuste Prozesse durch Quality Engineering*. German translation: G. Liesegang. gfmt – Verlag, Munich, 1989.

[PLT98] M. Papadrakakis, N. D. Lagaros, and Y. Tsompanakis. Structural optimization using evolution strategies and neural networks. *Computer methods in applied mechanics and engineering*, 156(1–4):309–333, 1998.

[Pow92] M. J. D. Powell. The theory of radial basis function approximation in 1990. In W. Light, editor, *Advances in Numerical Analysis, Vol.2: Wavelets, Subdivision Algorithms and Radial Basis Functions*. Oxford University Press, Oxford, UK, 1992.

[PSP93] A. Parkinson, C. Sorensen, and N. Pourhassan. A general approach for robust optimal design. *Transactions of ASME, Journal of Mechanical Design*, 115:74–80, 1993.

[RB05] D. Roos and C. Bucher. Robust design and reliability-based design optimization. In *NAFEMS Seminar: Optimization in Structural Mechanics*, Wiesbaden, April 2005.

[RBM04] T. J. Robinson, C. M. Borror, and R. H. Myers. Robust parameter design: A review. *Quality and Reliability Engineering International*, 20(1):81–101, 2004.

[RDKP01] J. O. Royset, A. Der Kiureghian, and E. Polak. Reliability-based optimal structural design by the decoupling approach. *Reliability Engineering & System Safety*, 73:213–221, 2001.

[Rei97] J. Reinhart. *Stochastische Optimierung von Faserkunststoffverbundplatten. Adaptive stochastische Approximationsverfahren auf der Basis der Response-Surface-Methode*. PhD thesis, VDI Reihe 5 Nr. 463, VDI Verlag, Düsseldorf, 1997.

[RGN04] M. Redhe, M. Giger, and L. Nilsson. An investigation of structural optimization in crashworthiness design using a stochastic approach: A comparison of stochastic optimization and the response surface methodology. *Structural and Multidisciplinary Optimization*, 27(6):446–459, 2004.

[Roo02] D. Roos. *Approximation und Interpolation von Grenzzustandsfunktionen zur Sicherheitsbewertung*. PhD thesis, Bauhaus-Universität Weimar, January 2002.

[Ros87] S. M. Ross. *Introduction to Probability and Statistics for Engineers and Scientists*. Wiley Series in Probability and Mathematical Statistics. John Wiley & Sons, New York, NY, USA, 1987.

[Roy90] R. K. Roy. *A Primer on the Taguchi Method*. Competitive Manufacturing Series. Van Nostrand Reinhold, New York, NY, USA, 1990.

[RR96] B. Ramakrishnan and S. S. Rao. A general loss function based optimization procedure for robust design. *Engineering Optimization*, 25:255–276, 1996.

[RS05] R. G. Regis and C. A. Shoemaker. Constrained global optimization of expensive black box functions using radial basis functions. *Journal of Global Optimization*, 31(1):153–171, 2005.

[RSH98] W. J. Roux, N. Stander, and R. T. Haftka. Response surface approximations for structural optimization. *International Journal for Numerical Methods in Engineering*, 42(3):517–534, 1998.

[RSSH91] J. S. Ramberg, M. Sanchez, P. J. Sanchez, and L. J. Hollick. Designing simulation experiments: Taguchi methods and response surface metamodels. In B. L. Nelson, W. D. Kelton, and G. M. Clark, editors, *Proceedings of the 1991 Winter Simulation Conference*, pages 167–176, Phoenix, AZ, USA, 1991.

[Sac04] L. Sachs. *Angewandte Statistik: Anwendung statistischer Methoden*. Springer-Verlag, Berlin, 11th (rev. & upd.) edition, 2004.

[SAM98] T. W. Simpson, J. K. Allen, and F. Mistree. Spatial correlation metamodels for global approximation in structural design optimization. In *Proceedings of DETC '98 ASME Design Engineering Technical Conference*, pages 1–13, Atlanta, GA, USA, September 1998.

[Sav51] L. J. Savage. The theory of statistical decision. *Journal of the American Statistical Association*, 46:55–67, 1951.

[Sav02] M. Savoia. Structural reliability analysis through fuzzy number approach, with application to stability. *Computers & Structures*, 80:1087–1102, 2002.

[SBBO89] G. I. Schuëller, C. G. Bucher, U. Bourgund, and W. Ouypornprasert. On efficient computational schemes to calculate structural failure probabilities. *Probabilistic Engineering Mechanics*, 4(1):10–18, 1989.

[SBG+04] T. W. Simpson, A. J. Booker, D. Ghosh, A. A. Giunta, P. N. Koch, and R.-J. Yang. Approximation methods in multidisciplinary analysis and optimization: A panel discussion. *Structural and Multidisciplinary Optimization*, 27(5):302–313, 2004.

[SC02] N. Stander and K. J. Craig. On the robustness of a simple domain reduction scheme for simulation-based optimization. *Engineering Computations*, 19(4):431–450, 2002.

[Sch60] L. A. Schmit. Structural design by systematic synthesis. In *Proceedings of the Second ASCE Conference on Electronic Computation*, pages 105–122, New York, NY, USA, 1960.

[Sch81] L. A. Schmit. Structural synthesis – its genesis and development. *AIAA Journal*, 19(10):1249–1263, 1981.

[Sch97] M. Schonlau. *Computer Experiments and Global Optimization*. PhD thesis, University of Waterloo, CA, 1997.

[SCS00] A. Saltelli, K. Chan, and E. M. Scott, editors. *Sensitivity Analysis*. Wiley Series in Probability and Statistics. John Wiley & Sons, Chichester, UK, 2000.

[SF74] L. A. Schmit Jr. and B. Farshi. Some approximation concepts for structural synthesis. *AIAA Journal*, 12(5):692–699, 1974.

[Sha70] D. F. Shanno. Conditioning of quasi-Newton methods for function minimization. *Mathematics of Computing*, 24:647–656, 1970.

[SLC01] T. W. Simpson, D. K. J. Lin, and W. Chen. Sampling strategies for computer experiments: Design and analysis. *International Journal of Reliability and Applications*, 2(3):209–240, 2001.

[SLK04] A. Sóbester, S. J. Leary, and A. J. Keane. A parallel updating scheme for approximating and optimizing high fidelity computer simulations. *Structural and Multidisciplinary Optimization*, 27(5):371–383, 2004.

[SMKM98] T. W. Simpson, T. M. Mauery, J. J. Korte, and F. Mistree. Comparison of response surface and kriging models for multidisciplinary design optimization. In *Proceedings of the 7th AIAA/USAF/ISSMO Symposium on Multidisciplinary Analysis & Optimization*, pages 381–391, September 1998.

[SMKM01] T. W. Simpson, T. M. Mauery, J. J. Korte, and F. Mistree. Kriging models for global approximation in simulation-based multidisciplinary design optimization. *AIAA Journal*, 39(12):2233–2241, 2001.

[SPG02] M. J. Sasena, P. Papalambros, and P. Goovaerts. Exploration of metamodeling sampling criteria for constrained global optimization. *Engineering Optimization*, 34(3):263–278, 2002.

[SPKA97] T. W. Simpson, J. D. Peplinski, P. N. Koch, and J. K. Allen. On the use of statistics in design and the implications for deterministic computer experiments. In *Proceedings of DETC '97 ASME Design Engineering Technical Conferences*, Sacramento, CA, USA, September 1997.

[SPKA01] T. W. Simpson, J. D. Peplinski, P. N. Koch, and J. K. Allen. Metamodels for computer-based engineering design: Survey and recommendations. *Engineering with Computers*, 17:129–150, 2001.

[SSW89] J. Sacks, S. B. Schiller, and W. J. Welch. Designs for computer experiments. *Technometrics*, 31(1):41–47, 1989.

[Sva87] K. Svanberg. The method of moving asymptotes – a new method for stuctural optimization. *International Journal for Numerical Methods in Engineering*, 24(2):359–373, 1987.

[SWJ98] M. Schonlau, W. J. Welch, and D. R. Jones. Global versus local search in constrained optimization of computer models. Technical Report 83, NISS, www.niss.org, March 1998.

[SWMW89] J. Sacks, W. J. Welch, T. J. Mitchell, and H. P. Wynn. Design and analysis of computer experiments. *Statistical Science*, 4(4):409–435, 1989.

[SWN03] T. J. Santner, B. J. Williams, and W. I. Notz. *The Design and Analysis of Computer Experiments*. Springer Series in Statistics. Springer-Verlag, New York, NY, USA, 2003.

[Tag86] G. Taguchi. *Introduction to Quality Engineering*. Asian Productivity Organization, Tokyo, JP, 1986.

[Tan93] B. Tang. Orthogonal array-based Latin hypercubes. *Journal of the American Statistical Association*, 88:1392–1397, 1993.

[Tan94] B. Tang. A theorem for selecting OA-based Latin hypercubes using a distance criterion. *Communications in Statistics – Theory and Methods*, 23:2047–2058, 1994.

[TAW03] M. W. Trosset, N. M. Alexandrov, and L. T. Watson. New methods for robust design using computer simulation. In *Proceedings of the Section on Physical and Engineering Sciences*. American Statistical Association, 2003.

[TCB82] P. Thoft-Christensen and M. J. Baker. *Structural Reliability Theory and Its Applications*. Springer-Verlag, Heidelberg, 1982.

[TCM86] P. Thoft-Christensen and Y. Murotsu. *Application of Structural Systems Reliability Theory*. Springer-Verlag, Berlin, 1986.

[TFP93] V. V. Toropov, A. A. Filatov, and A. A. Polynkin. Multiparameter structural optimization using FEM and multipoint explicit approximations. *Structural Optimization*, 6:7–14, 1993.

[Tou94] H. Toutenburg. *Versuchsplanung und Modellwahl*. Physica-Verlag, Heidelberg, 1994.

[TSS+05] V. V. Toropov, U. Schramm, A. Sahai, R. D. Jones, and T. Zeguer. Design optimization and stochastic analysis based on the moving least squares method. In J. Herskovits, S. Mazorche, and A. Canelas, editors, *Proceedings of the 6th World Congress on Structural and Multidisciplinary Optimization (WCSMO6)*, Rio de Janeiro, BR, May 2005. ISSMO – International Society for Structural and Multidisciplinary Optimization, published on CD-Rom – paper 6412.

[TvKM95] V. V. Toropov, F. van Keulen, and V. L. Markine. Structural optimization in the presence of numerical noise. In *The First World Congress of Structural and Multidisciplinary Optimization (extended abstracts)*, Goslar, May 1995.

[USJ93] R. Unal, D. O. Stanley, and C. R. Joyner. Propulsion system design optimization using the Taguchi method. *IEEE Transactions on Engineering Management*, 40(3):315–322, 1993.

[Van82] G. N. Vanderplaats. Structural optimization - past, present and future. *AIAA Journal*, 20(7):992–1000, 1982.

[Van84] G. N. Vanderplaats. *Numerical Optimization Techniques for Engineering Design: with Applications*. McGraw-Hill, New York, NY, USA, 1984.

[Van06] G. N. Vanderplaats. Structural optimization for statics, dynamics and beyond. *Journal of the Brazilian Society of Mechanical Sciences and Engineering*, 28(3):316–322, 2006.

[Vie94] T. Vietor. *Optimale Auslegung von Strukturen aus spröden Werkstoffen*. FOMAAS, TIM-Bericht Nr. T04-02.94, Universität – GH Siegen, 1994.

[VM73] G. N. Vanderplaats and F. Moses. Structural optimization by methods of feasible directions. *Computers & Structures*, 3:739–755, 1973.

[VM90] G. G. Vining and R. H. Myers. Combining Taguchi and response surface philosophies: A dual response approach. *Journal of Quality Technology*, 22(1):38–45, 1990.

[vN28] J. von Neumann. Zur Theorie der Gesellschaftsspiele. *Mathematische Annalen*, 100:295–320, 1928.

[Wal50] A. Wald. *Statistical Decision Functions*. Wiley Publications in Statistics. John Wiley & Sons, New York, NY, USA, 1950.

[Yat64] F. Yates. Sir Ronald Fisher and the design of experiments. *Biometrics*, 20(2):307–321, 1964. In Memoriam: Ronald Aylmer Fisher, 1890-1962.

[YCYG04] B. D. Youn, K. K. Choi, R.-J. Yang, and L. Gu. Reliability-based design optimization for crashworthiness of vehicle side impact. *Structural and Multidisciplinary Optimization*, 26(3–4):272–283, 2004.

[Zel00] A. Zell. *Simulation neuronaler Netze*. Oldenbourg Verlag, Munich, 3rd (repr.) edition, 2000.

[ZFM05] C. Zang, M. I. Friswell, and J. E. Mottershead. A review of robust optimal design and its application in dynamics. *Computers & Structures*, 83(4–5):315–326, 2005.

[ZT05] O. C. Zienkiewicz and R. L. Taylor. *The Finite Element Method*. Butterworth-Heinemann, London, UK, 6th edition, 2005.

Appendix

Mathematical Derivations

This appendix provides detailed derivations and transformations that have been applied in the Equations addressed below. To keep the representation throughout the text as concise as possible, some rather lengthy intermediate steps in the derivations have been deferred to the appendix.

A.1 Derivation of the Standard Expected Improvement

In the following, the particular transformations that have been applied to find Equation (6.14) on page 131 are described in detail.

$$E(I) = \int_{-\infty}^{\tilde{y}^*} (\tilde{y}^* - y)\, p_Y(y)\, dy$$

Applying the substitution $y = t\,\hat{s} + \hat{y}$ and $\tilde{t}^* = \dfrac{\tilde{y}^* - \hat{y}}{\hat{s}}$

$$= \int_{-\infty}^{\tilde{t}^*} (\tilde{y}^* - t\,\hat{s} - \hat{y})\; p_Y(t\,\hat{s} + \hat{y})\; \frac{dy}{dt}\, dt$$

As a result of the substitution t has a standard normal distribution i.e. $t \sim N(0,1)$ and with $p_Y(t\,\hat{s} + \hat{y}) = \dfrac{1}{\hat{s}}\,\phi(t)$ (where ϕ symbolizes the probability density function of the standard normal distribution)

$$= \int_{-\infty}^{\tilde{t}^*} (\tilde{y}^* - t\,\hat{s} - \hat{y})\, \frac{1}{\hat{s}}\, \phi(t)\; \frac{dy}{dt}\, dt$$

With $\dfrac{dy}{dt} = \hat{s}$

$$= \int_{-\infty}^{\tilde{t}^*} (\tilde{y}^* - t\,\hat{s} - \hat{y})\, \phi(t)\, dt = (\tilde{y}^* - \hat{y}) \int_{-\infty}^{\tilde{t}^*} \phi(t)\, dt - \int_{-\infty}^{\tilde{t}^*} t\,\hat{s}\, \phi(t)\, dt$$

With the cumulative distribution function $\Phi(t) = \int \phi(t)\,dt$ of the standard normal distribution

$$= (\tilde{y}^* - \hat{y}) \left[\Phi(t)\right]_{-\infty}^{\tilde{t}^*} - \hat{s} \int_{-\infty}^{\tilde{t}^*} t\,\phi(t)\,dt = (\tilde{y}^* - \hat{y})\,\Phi(\tilde{t}^*) - \hat{s} \int_{-\infty}^{\tilde{t}^*} t\,\phi(t)\,dt$$

Making use of the properties of the exponential function in the formulation of ϕ, it can be shown that $d\phi(t)/dt = -t\,\phi(t)$ and hence $\int t\,\phi(t)\,dt = -\phi(t)$

$$= (\tilde{y}^* - \hat{y})\,\Phi(\tilde{t}^*) + \hat{s} \left[\phi(t)\right]_{-\infty}^{\tilde{t}^*} = (\tilde{y}^* - \hat{y})\,\Phi(\tilde{t}^*) + \hat{s}\,\phi(\tilde{t}^*)$$

Reversing the substitution for $\tilde{t}^*$ finally yields the formula given in Equation (6.14)

$$= (\tilde{y}^* - \hat{y})\,\Phi\left(\frac{\tilde{y}^* - \hat{y}}{\hat{s}}\right) + \hat{s}\,\phi\left(\frac{\tilde{y}^* - \hat{y}}{\hat{s}}\right)$$

A.2 Derivation of the Expected Improvement for Robust Design Problems

In this section, Equations (6.23) through (6.25) on page 138 are particularized.

$$\begin{aligned} E(I) &= \int_a^b (\hat{y}^* - y)\left(p_Y(y) - p_{Y^*}(y)\right) dy \\ &= \int_a^b (\hat{y}^* - y)\,p_Y(y)\,dy - \int_a^b (\hat{y}^* - y)\,p_{Y^*}(y)\,dy \end{aligned}$$

Making use of the results of Section A.1 and the substitution $y = t\,\hat{s} + \hat{y}$ for the first integral with $t_a = \dfrac{a - \hat{y}}{\hat{s}}$ and $t_b = \dfrac{b - \hat{y}}{\hat{s}}$ yields

$$= (\hat{y}^* - \hat{y}) \left[\Phi(t)\right]_{t_a}^{t_b} + \hat{s} \left[\phi(t)\right]_{t_a}^{t_b} - \int_a^b (\hat{y}^* - y)\,p_{Y^*}(y)\,dy$$

For the second integral the substitution $y = u\,\hat{s}^* + \hat{y}^*$ is used with $u_a = \dfrac{a - \hat{y}^*}{\hat{s}^*}$ and $u_b = \dfrac{b - \hat{y}^*}{\hat{s}^*}$

$$= (\hat{y}^* - \hat{y}) \left[\Phi(t)\right]_{t_a}^{t_b} + \hat{s} \left[\phi(t)\right]_{t_a}^{t_b} - \int_{u_a}^{u_b} (\hat{y}^* - u\,\hat{s}^* - \hat{y}^*)\,\frac{1}{\hat{s}^*}\,\phi(u)\,\frac{dy}{du}\,du$$

With $\frac{dy}{du} = \hat{s}^*$

$$= (\hat{y}^* - \hat{y}) \left[\Phi(t)\right]_{t_a}^{t_b} + \hat{s} \left[\phi(t)\right]_{t_a}^{t_b} + \hat{s}^* \int_{u_a}^{u_b} u\, \phi(u)\, du$$

Using the relation $\int u\, \phi(u)\, du = -\phi(u)$

$$= (\hat{y}^* - \hat{y}) \left[\Phi(t)\right]_{t_a}^{t_b} + \hat{s} \left[\phi(t)\right]_{t_a}^{t_b} - \hat{s}^* \left[\phi(u)\right]_{u_a}^{u_b}$$

To evaluate these terms, the integration limits have to be known. As introduced in Section 6.2.3, the integration limits a and b (and hence all derived quantities) depend on the intersection points of the probability density functions p_Y and p_{Y^*}.

For the first two cases, the integration limits are $a = -\infty$ and $b = y_1$. The substituted integration bounds are written as

$$t_a = -\infty\,,\; t_b = \frac{y_1 - \hat{y}}{\hat{s}}\,,\; u_a = -\infty\,, \text{ and } \; u_b = \frac{y_1 - \hat{y}^*}{\hat{s}^*}\,.$$

For these integration bounds, the formula for the expected improvement can be simplified to

$$E(I) = (\hat{y}^* - \hat{y})\, \Phi\left(\frac{y_1 - \hat{y}}{\hat{s}}\right) + \hat{s}\, \phi\left(\frac{y_1 - \hat{y}}{\hat{s}}\right) - \hat{s}^*\, \phi\left(\frac{y_1 - \hat{y}^*}{\hat{s}^*}\right)$$

For the third case with lower limit $a = y_1$ and upper limit $b = \hat{y}^*$, the integration bounds read

$$t_a = \frac{y_1 - \hat{y}}{\hat{s}}\,,\; t_b = \frac{\hat{y}^* - \hat{y}}{\hat{s}}\,,\; u_a = \frac{y_1 - \hat{y}^*}{\hat{s}^*}\,, \text{ and } \; u_b = \frac{\hat{y}^* - \hat{y}^*}{\hat{s}^*} = 0\,.$$

The expected improvement can be computed according to

$$\begin{aligned}
E(I) &= (\hat{y}^* - \hat{y}) \left[\Phi(t)\right]_{t_a}^{t_b} + \hat{s} \left[\phi(t)\right]_{t_a}^{t_b} - \hat{s}^* \left[\phi(u)\right]_{u_a}^{0} \\
&= (\hat{y}^* - \hat{y}) \Big(\Phi(t_b) - \Phi(t_a)\Big) + \hat{s} \Big(\phi(t_b) - \phi(t_a)\Big) - \hat{s}^* \left(\frac{1}{\sqrt{2\pi}} - \phi(u_a)\right) \\
&= (\hat{y}^* - \hat{y}) \left(\Phi\left(\frac{\hat{y}^* - \hat{y}}{\hat{s}}\right) - \Phi\left(\frac{y_1 - \hat{y}}{\hat{s}}\right)\right) \\
&\quad + \hat{s} \left(\phi\left(\frac{\hat{y}^* - \hat{y}}{\hat{s}}\right) - \phi\left(\frac{y_1 - \hat{y}}{\hat{s}}\right)\right) - \hat{s}^* \left(\frac{1}{\sqrt{2\pi}} - \phi\left(\frac{y_1 - \hat{y}^*}{\hat{s}^*}\right)\right)
\end{aligned}$$

In case the upper limit is specified by $b = y_2$, no simplifications are possible. The expected improvement has to be computed from

$$\begin{aligned}
E(I) &= (\hat{y}^* - \hat{y}) \left(\Phi\left(\frac{y_2 - \hat{y}}{\hat{s}}\right) - \Phi\left(\frac{y_1 - \hat{y}}{\hat{s}}\right)\right) \\
&\quad + \hat{s} \left(\phi\left(\frac{y_2 - \hat{y}}{\hat{s}}\right) - \phi\left(\frac{y_1 - \hat{y}}{\hat{s}}\right)\right) - \hat{s}^* \left(\phi\left(\frac{y_2 - \hat{y}^*}{\hat{s}^*}\right) - \phi\left(\frac{y_1 - \hat{y}^*}{\hat{s}^*}\right)\right)
\end{aligned}$$

A.3 Derivation of the Expected Worsening for Robust Design Problems

In this section, the derivation of Equation (6.28) on page 140 is presented in detail.

$$\begin{aligned} E(I) &= \int_{y_2}^{\infty} \left(y - \hat{y}^{\#}\right) \left(p_Y(y) - p_{Y^{\#}}(y)\right) \, dy \\ &= \int_{y_2}^{\infty} \left(y - \hat{y}^{\#}\right) p_Y(y) \, dy - \int_{y_2}^{\infty} \left(y - \hat{y}^{\#}\right) p_{Y^{\#}}(y) \, dy \end{aligned}$$

Making use of the results of Section A.1 and the substitution $y = t\,\hat{s} + \hat{y}$ for the first integral with the transformed integration limits $t_a = \dfrac{y_2 - \hat{y}}{\hat{s}}$ and $t_b = \infty$ yields

$$\begin{aligned} &= \left(\hat{y} - \hat{y}^{\#}\right) \Big[\Phi(t)\Big]_{t_a}^{\infty} - \hat{s} \Big[\phi(t)\Big]_{t_a}^{\infty} - \int_{y_2}^{\infty} \left(y - \hat{y}^{\#}\right) p_{Y^{\#}}(y) \, dy \\ &= \left(\hat{y} - \hat{y}^{\#}\right) \Big(1 - \Phi(t_a)\Big) + \hat{s}\,\phi(t_a) - \int_{y_2}^{\infty} \left(y - \hat{y}^{\#}\right) p_{Y^{\#}}(y) \, dy \end{aligned}$$

In analogy to Section A.2, the second integral is solved by the substitution $y = u\,\hat{s}^{\#} + \hat{y}^{\#}$ with $u_a = \dfrac{y_2 - \hat{y}^{\#}}{\hat{s}^{\#}}$ and $u_b = \infty$ yielding

$$\begin{aligned} &= \left(\hat{y} - \hat{y}^{\#}\right) \Big(1 - \Phi(t_a)\Big) + \hat{s}\,\phi(t_a) - \int_{u_a}^{\infty} \left(u\,\hat{s}^{\#} + \hat{y}^{\#} - \hat{y}^{\#}\right) \frac{1}{\hat{s}^{\#}}\,\phi(u)\,\frac{dy}{du}\,du \\ &= \left(\hat{y} - \hat{y}^{\#}\right) \Big(1 - \Phi(t_a)\Big) + \hat{s}\,\phi(t_a) - \hat{s}^{\#} \int_{u_a}^{\infty} u\,\phi(u)\,du \\ &= \left(\hat{y} - \hat{y}^{\#}\right) \Big(1 - \Phi(t_a)\Big) + \hat{s}\,\phi(t_a) + \hat{s}^{\#} \Big[\phi(u)\Big]_{u_a}^{\infty} \\ &= \left(\hat{y} - \hat{y}^{\#}\right) \Big(1 - \Phi(t_a)\Big) + \hat{s}\,\phi(t_a) - \hat{s}^{\#}\,\phi(u_a) \\ &= \left(\hat{y} - \hat{y}^{\#}\right) \left(1 - \Phi\left(\frac{y_2 - \hat{y}}{\hat{s}}\right)\right) + \hat{s}\,\phi\left(\frac{y_2 - \hat{y}}{\hat{s}}\right) - \hat{s}^{\#}\,\phi\left(\frac{y_2 - \hat{y}^{\#}}{\hat{s}^{\#}}\right) \end{aligned}$$